Dissertation zur Erlangung des Doktorgrades
der Fakultät für Chemie und Pharmazie
der Ludwig-Maximilians-Universität München

Identification of junctional adhesion molecule (JAM)-1 as a novel immunoglobulin superfamily ligand for lymphocyte function-associated antigen (LFA)-1

von

Georg Ostermann

aus

Cochem/Mosel

2002

Erklärung

Diese Dissertation wurde im Sinne von § 13 Abs. 3 bzw. 4 der Promotionsordung vom 29. Januar 1998 von Prof. Dr. Waldemar Kolanus betreut.

Ehrenwörtliche Versicherung

Diese Dissertation wurde selbständig, ohne unerlaubte Hilfsmittel erarbeitet.

München, den 15.11.2002

gez. Georg Ostermann

Dissertation eingereicht am	15.11.2002
1. Gutachter	Prof. Dr. Christian Weber
2. Gutachter	Prof. Dr. Waldemar Kolanus
Mündliche Prüfung am	17.12.2002

The present studies were performed from August 1998 to December 2001 under the supervision of Prof. Dr. Christian Weber at the Institute for Prevention of Cardiovascular Disease (IPEK), University Hospital, Ludwig-Maximilians University, Munich.

The results were in part published in:

Ostermann G., Weber K. S., Zernecke A., Schröder A., Weber C. (2002) **JAM-1 is a ligand of the β_2 integrin LFA-1 involved in transendothelial migration of leukocytes.** *Nature Immunol.* 3, 2, 151-158.

Acknowledgement

I am very grateful to Prof. Dr. Christian Weber for the possibility to prepare my studies in his research group, for allowing me to work on this interesting topic, and his invaluable supervision. He gave me great freedom in carrying out my work, but was also present when advice or support was needed.

I would like to thank Prof. Dr. Waldemar Kolanus for constant support during the preparation of this doctoral thesis and for agreeing to evaluate it, as well as for the scientific collaboration.

For further scientific collaboration and discussions I am very grateful to Dr. Kim Weber, not least for her introduction to various experimental techniques and her steady support, and to Dr. Jiri Neuzil.

I wish to thank Andreas Schröder, Nina Gellert and Dr. Gesche Heiss for the productive and friendly working atmosphere, mutual support and for critical scientific discussion. In addition, I wish to thank N.G. for her excellent technical assistance. Thanks also to Alma Zernecke.

I thank all my colleagues in the IPEK institute, both from the "gardenpavilon" and from the "Pettenkoferstraße headquarters" for the pleasant and friendly atmosphere, all the help and scientific discussion over the past four years. In particular I would like to mention Dr. Kristin Bauer, Dr. Christian Johannes, Dr. Markus (Alf) Bauer, Dr. Georg Draude, and Barbara Schell. Thanks also to Nada Vukorepa and Bernadette Breiden.

Last but not least special thanks to Dr. Nick Foulkes for critically reviewing this report with much patience.

Table of contents

Abbreviations and units

Abbreviations

β-Gal	β-galactosidase
Ab	antibody
AD	activating domain
AF-6	ALL-1 fusion partner from chromosome 6; S-afadin
AJ	adherens junction; *zonula adherens*
approx.	approximately
ATCC	American Type Culture Collection
BBB	blood-brain barrier
BSA	bovine serum albumin
CAM	cell adhesion molecule
CD	"cluster of differentiation" nomenclature
cDNA	complementary DNA
CHO cell	chinese hamster ovary cell
CHO-JAM	CHO cells expressing human JAM-1
CHO-vector	CHO cells transfected with the unmodified expression vector pcDNA3
CHO-WT	wild-type CHO cells
CIP	calcium and integrin-binding protein; calf intestine alkaline phosphatase
CTX family	cortical thymocyte *Xenopus* family
DBD	DNA-binding domain
DMSO	dimethylsulfoxide
DNA	deoxyribonucleic acid
dNTP	deoxyribonucleotide triphosphates
DTT	dithiothreitol
E. coli	*Escherichia coli*
EC	endothelial cell
ECM	extracellular matrix
EDTA	ethylenediaminetetraacetic acid
EGF	epidermal growth factor
ERK	extracellular signal-related kinase
F11R	F11 antigen (identical to JAM-1)
FAK	focal adhesion kinase
FCS	fetal calf serum
fig.	figure
GP	glycoprotein
HA epitope	hemagglutinin epitope
HEV	high endothelial venule
HUVEC	human umbilical vein endothelial cell
ICAM	intercellular adhesion molecule
IFN-γ	interferon-γ

Ig	immunoglobulin
IgSF	immunoglobulin superfamily
IL	interleukin
JAB1	Jun activation domain-binding protein 1
JAM	junctional adhesion molecule
LAD	leukocyte adhesion deficiency (LAD-I, LAD-II)
LFA-1	lymphocyte function-associated antigen-1; CD11a/CD18; $\alpha_L\beta_2$
LPS	lipopolysaccharide
mAb	monoclonal antibody
Mac-1	macrophage antigen-1; complement receptor type 3; CD11b/CD18; $\alpha_M\beta_2$
MAdCAM-1	mucosal addressin cell adhesion molecule-1
MCS	multiple cloning site
MHC	major histocompatibility complexes
MIDAS	metal ion-dependent adhesion site
mRNA	messenger RNA
NK cell	natural killer cell
OD_x	optical density at a wavelength of *x* nm
ORF	open reading frame
p	plasmid designation
PBMC	peripheral blood mononuclear cell
PBS	phosphate buffered saline
PCR	polymerase chain reaction
PDGF	platelet-derived growth factor
PDZ	PSD-95, disc large, ZO-1
PECAM-1	platelet endothelial cell adhesion molecule-1; CD31
PI3-kinase	phosphatidylinositol-3-OH kinase
PKC	protein kinase C
PLC	phospholipase C
PMA	phorbol-12-myristate-13-acetate
RNA	ribonucleic acid
rsJAM	recombinant soluble expressed extracellular domain of murine JAM-1
RT-PCR	reverse transcriptase polymerase chain reaction
s	plural designation
S. cerevisiae	*Saccharomyces cerevisiae*
s.d.	standard deviation
SDF-1α	stromal cell-derived factor-1α; CXCL12
SDS-PAGE	sodium dodecyl sulfate - polyacrylamide gel electrophoresis
sLe^X	sialyl Lewis X; CD15s
TCR	T-cell receptor
TJ	tight junction; *zonula occludens*
TNF-α	tumor necrosis factor-α
UTR	untranslated region
UV	ultraviolet
VCAM-1	vascular cell adhesion molecule-1; CD106
VE-JAM	human vascular endothelial junction-associated molecule (identical to JAM-2)
VLA-4	very late antigen-4; CD49d/CD29; $\alpha_4\beta_1$

vWF	von Willebrand factor
w/o	without
YTH system	yeast two-hybrid system
ZO	*zonula occludens* protein

Units

°C	degree Celsius
µF	micro Farad
µg	microgram
µl	microlitre
µm	micrometer
µM	micromolar
aa	amino acid
bp	base pair
cfu	colony forming units
cm	centimeter
dyn	dyne (= 10^5 Newton)
g	gram (weight) respective gravity (for centrifugation)
h	hour
kb	kilo base pairs
kDa	kilo Dalton
kV	kilo Volt
l	litre
M	molar (= mol/l)
mA	milliampere
mg	milligram
min	minute
ml	millilitre
mm	millimeter
mM	millimolar
mol	mole
N	normal
ng	nanogram
nm	nanometer
nt	nucleotide
O/N	overnight
pmol	picomole
rpm	revolutions per minute
s	second
U	unit
V	Volt
v/v	volume per volume
w/v	weight per volume
Ω	Ohm

1. Introduction

1.1. Transendothelial migration of leukocytes

Diapedesis of leukocytes, *i.e.* the transmigration through the vascular endothelium, is a highly regulated immunological process involved in leukocyte recruitment to sites of inflammation, and in lymphocyte homing[1].

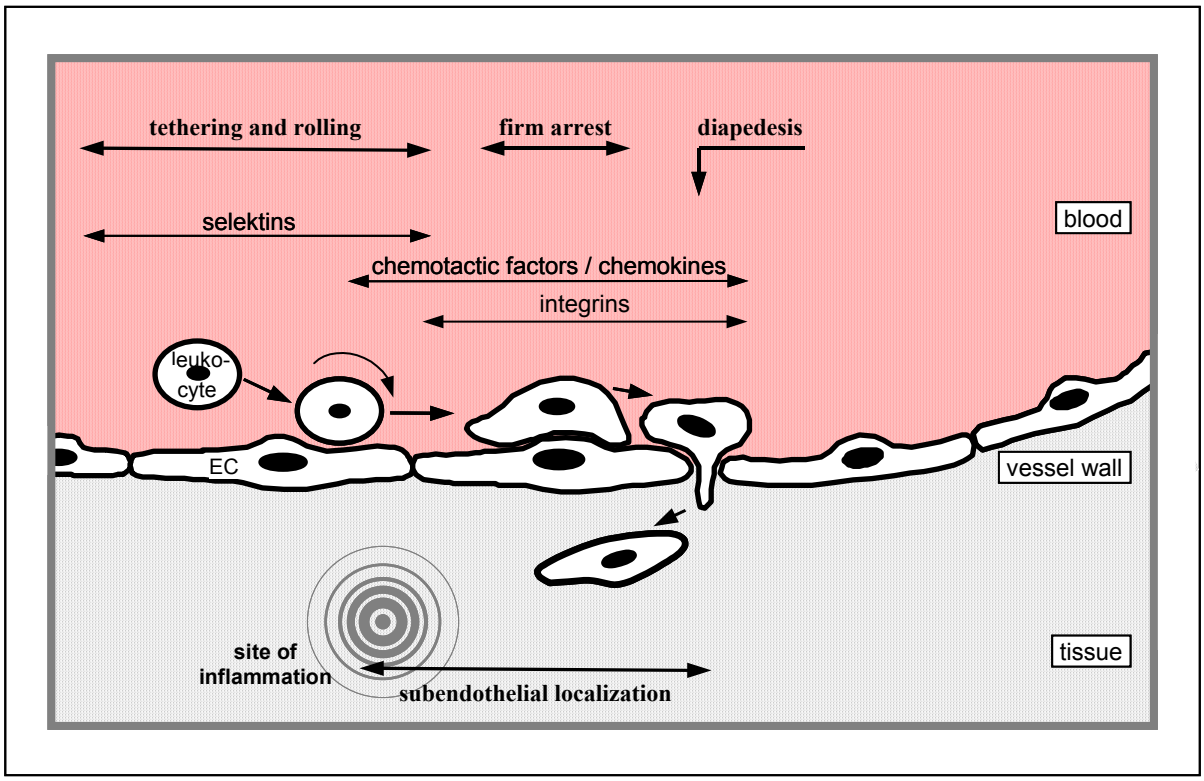

figure 1: Leukocyte recruitment and extravasation to sites of inflammation. Sequential steps involved in this process are **i)** tethering, **ii)** rolling and **iii)** firm arrest of the circulating leukocyte on the activated endothelium, followed by **iv)** diapedesis across the endothelial barrier and **v)** subendothelial migration. They are mainly mediated by selectin molecules, chemotactic factors and integrins and by their respective receptors or ligands, as indicated and described below.

During normal immune surveillance, lymphocytes recirculate in search of foreign antigens from the microvasculature into tissues, percolate through draining lymph nodes of the lymphatic system and finally return to the blood stream via the thoracic duct. Thereby naive lymphocytes preferentially home to and recirculate among peripheral lymph nodes through high endothelial venules (HEVs) that consist of endothelial cells (ECs) specialized for lymphocyte emigration. Memory T cells, on the contrary, preferentially extravasate through normal tissue endothelium

[1] The mechanisms of leukocyte diapedesis will be discussed hereinafter mainly for the process of transendothelial extravasation to sites of inflammation that corresponds in principle to mechanisms underlying transepithelial extravasation, e.g. through inflamed epithelia in case of mucosal infections, or lymphocyte homing.

of, for example, skin, lung and gut, and subsequently drain into their associated lymphoid tissues. This constitutive process of lymphocyte homing underlies similar principle mechanisms as inflammation-induced leukocyte diapedesis (Springer, 1994).

Injury or infections cause inflammatory responses that lead to the recruitment of granulocytes, monocytes and T cells to sites of inflammation. Leukocyte transmigration occurs in different sequential and in part, overlapping steps, *i.e.* tethering, rolling, firm arrest and finally extravasation (Butcher, 1991; Springer, 1994). At the molecular level these leukocyte-EC interactions are mainly mediated by selectins and their carbohydrate ligands, activating chemoattractants and their leukocytic receptors, and IgSF proteins in combination with their integrin receptors, respectively (**fig. 1**). Patrolling leukocytes undergo initial attachment (tethering) to the vessel wall mediated by selectins that are mainly expressed on the endothelium in response to inflammation. Due to the shear forces of the rapidly flowing blood stream (see **fig. 28**), reversible repetitive selectin-binding leads to leukocyte rolling on the blood vessel wall. The attracted cells are thus slowed down and enabled to sense the environment for endothelial inflammation signals provided by chemoattractants. Interaction with respective receptors leads to activation of the leukocytes that effects mainly the binding properties of their integrin surface receptors and results in high-affinity and high-avidity binding to their endothelial immunoglobulin superfamily (IgSF) counter-receptors. The major integrins implicated are lymphocyte function-associated antigen (LFA)-1, Mac-1 (macrophage antigen-1; complement receptor type 3), very late antigen (VLA)-4 and their ligands intercellular adhesion molecule (ICAM)-1 and vascular cell adhesion molecule (VCAM)-1. The adhesive molecular interactions amplify in a cascade-like manner and finally result in strong, sustained arrest and spreading of the leukocytes onto the endothelium under the given blood flow conditions.

Unlike the well-characterized molecular events involved in leukocyte rolling and their adhesion to activated endothelium, the mechanisms controlling the last step of their recruitment, *i.e.* the transendothelial extravasation, remains largely unknown (**fig. 1**) (Bianchi *et al.*, 1997). The intercellular junctions of the endothelium, in particular the apical tight junctions, have to open and close in a highly coordinated and reversible manner to allow leukocytes to reach inflammatory sites in the tissue and to coincidentally disable bleeding or an impairment of the functional permeability barrier.

Following transmigration into the tissue, leukocytes undergo directed migration through a concentration gradient of chemotactic cytokines (chemokines) to the site of inflammation (chemotaxis) (**fig. 1**). Depending on the type of leukocyte and its specialized function they release different inflammatory cytokines themselves. Thus they activate other white blood cells or enhance further leukocyte recruitment by stimulating the nearby endothelium to express additional adhesion molecules on its apical surface and to segregate chemokines. Moreover,

cytokine-activation influences the integrity of intercellular junctions and thus the paracellular permeability for additional recruited leukocytes across the endothelium (Shaw *et al.*, 2001c).

1.2. Intercellular junctions

Cell-cell contacts in tissues are characterized by specialized junctions. They ensure adjustable impermeability of cell layers for cellular and molecular components of the lumen (tight junctions) and provide adhesive contact sites for actin filaments (adherens junctions) or intermediate filaments (desmosomes), respectively. Moreover, they may provide cellular communication and regulated molecular interchange between adjacent cells (gap junctions).

Tight junctions (TJs) and adherens junctions (AJs) are formed by specific transmembrane proteins that promote homotypic cell adhesion (*i.e.* between cells of the same type) through their extracellular domains and anchor the cell-cell junctions to a complex network of cytoskeletal and signaling proteins by their cytoplasmic tails. In addition, transmembrane molecules such as junctional adhesion molecule (JAM)-1, platelet endothelial cell adhesion molecule (PECAM)-1 (Newman, 1997) and CD99 (Schenkel *et al.*, 2002) can concentrate at intercellular contacts (which for the latter two does not occur in direct association with TJs or AJs), and mediate cell adhesion by homophilic *trans*-interactions.

1.2.1. Tight junctions (*zonula occludens*)

TJs form a morphological and functional barrier between the apical and basolateral cell surface domains of endothelial or epithelial cell layers. They regulate selective diffusion of solutes and ions and the migration of immune cells along the paracellular space (barrier function). Moreover they constitute an intramembranous diffusion barrier restricting the intermix of apical and basolateral plasma membrane lipids and proteins (fence function), thus directly contributing to the maintenance of cell polarity (Schneeberger *et al.*, 1992; Nusrat *et al.*, 2000). TJs are particular well developed where permeability of endothelial or epithelial cell layers needs to be under strict control. A typical example is the impervious endothelial blood-brain barrier (BBB) where TJs are uniquely complex (Kniesel *et al.*, 2000). On the contrary, in high endothelial venules (HEVs) implicated in lymphocyte homing with high extravasation rates (Girard *et al.*, 1995), tight junctional complexes are frequently absent or present in only a primitive organization. TJs are generally located at the very apical site of epithelial cell layers. Endothelial TJs, however, can be less strictly localized and spatially intermingled with AJs at more basolateral sites (Anderson *et al.*, 1995).

The transmembrane constituents of TJs, all four membrane-spanning molecules, are the claudin proteins (Heiskala *et al.*, 2001) and occludin (Furuse *et al.*, 1993). They co-polymerize to heteropolymer TJ strands forming a continuous circumferential seal around the apical part of the cell and mediate adhesiveness to the TJ strands of the adjacent cells independently of extracellular Ca^{2+}. The members of the claudin family thereby appear to be the primary seal-forming proteins with the intrinsic ability to polymerize into continuous adhesive fibrils. They may mediate tissue-specific TJ properties by their respectively restricted expression and individual ability for homophilic (between identical molecules) and heterophilic (between different molecules) interactions *in cis* (both molecules anchored in the same cell membrane) and *in trans* (both molecules anchored in the membranes of separate, opposing cells) among themselves. Occludin exerts homophilic *trans*-interactions and can bind intracellularly actin filaments. Claudins and occludin bind each other and both can interact with the TJ proteins cingulin and, in a PDZ-dependent manner (see 1.7.5.), with the *zonula occludens* proteins ZO-1, ZO-2 and ZO-3. The latter are multi-domain proteins which interact with diverse cytoplasmic molecules mediating a direct link between the sealing proteins and the actin cytoskeleton (Lampugnani *et al.*, 1997; Tsukita *et al.*, 1999). Among them, ZO-1 may represent a cross-talking element between AJs and TJs since its membrane targeting may be regulated by binding initially to AJ components such as α- and β-catenins with subsequent segregation to TJs. Further interaction partners of ZO-1 are both ZO-2, ZO-3 and the PDZ domain-containing AF-6 (ALL-1 fusion partner from chromosome 6; S-afadin), a Ras substrate that is expressed at TJs as well as in AJs. Due to identical binding sites on AF-6, Ras can compete with ZO-1 for AF-6 binding which may provide a regulatory mechanism (Ebnet *et al.*, 2000). A third TJ-specific transmembrane protein is JAM-1 that may not constitute TJ strands *per se* but laterally associates with them. The protein interactions of JAM-1 with TJ components are discussed below.

The integrity of the TJs is dependent on the presence of extracellular Ca^{2+} that exerts its effects on AJs, in particular on cadherins, thus effecting TJs indirectly (Schneeberger *et al.*, 1992; Cereijido *et al.*, 2000). Therefore, the mechanisms of TJ assembly can be studied, besides in adenosine triphosphate (ATP) depletion-repletion experiments, in calcium-switch assays (Denker *et al.*, 1998). The degree of TJ tightness is dependent on their functional state and can be rapidly adapted to physiological needs. Assembly and barrier function are both influenced by intracellular signaling mediated e.g. by tyrosine kinases, intracellular Ca^{2+}, protein kinase C (PKC), (3',5')-cyclic adenosine monophosphate (cAMP) and phospholipase C (PLC) (Schneeberger *et al.*, 1992; Anderson *et al.*, 1995).

Moreover, TJ have to open and close in a highly coordinated and reversible manner to ensure transmigration of immune cells under physiological or pathological conditions of inflammation as well as during normal immune surveillance. Cytokines such as tumor necrosis factor (TNF)-α and interferon (IFN)-γ, which are released by transmigrated leukocytes at sites of inflammation,

directly influence the constitution of TJs and thus the paracellular permeability across endothelial and epithelial cells (Nusrat *et al.*, 2000). The molecular mechanisms of TJ regulation during leukocyte migration remain unclear.

1.2.2. Adherens junctions (*zonula adherens*)

AJs represent a ubiquitous and more basic type of organized intercellular contact structure. They are formed by clusters of transmembrane proteins belonging to the cadherin family, mainly VE-cadherin in vascular endothelial and E-cadherin in epithelial AJs (Yap *et al.*, 1997; Nagafuchi, 2001). Homophilic interactions *in trans* of cadherins are dependent of extracellular Ca^{2+}. In the cytosol they can directly link to the catenins β-catenin, plakoglobin and $p120^{CAS}$, the former which in turn binds to α-catenin. α-catenin interacts with vinculin, α-actinin, ZO-1 and actin, thus stabilizing the junctions. The cadherin-association with $p120^{CAS}$ leads to more mobile and dynamic AJs and dissociates after junction maturation (Lampugnani *et al.*, 1997). Like TJs, AJs are very dynamic and their composition can rapidly change according to the functional and maturational state of the cell. They are also involved in signal transduction, e.g. through β-catenin and plakoglobin-mediated signaling or through their recruitment of diverse signaling molecules to the sites of AJs.

1.3. Selectins

Selectins are adhesion molecules that mediate tethering and rolling of emigrating leukocytes on the endothelium (McEver *et al.*, 1995; Ebnet *et al.*, 1999). Their expression is strictly restricted to the leukocyte-vascular interaction system, and all three members, *i.e.* L-selectin, E-selectin and P-selectin, are critical involved in diapedesis during inflammation. The extracellular part of these type I transmembrane receptors consists of a N-terminal lectin-like carbohydrate recognition domain followed by an epidermal growth factor (EGF)-like domain and a varying number of short consensus repeats (SCRs). The main expression, regulation and molecular interaction features of the selectins are described below (**table 1**). For all three selectins the requirement for flow shear to mediate leukocyte rolling has been demonstrated (Lawrence *et al.*, 1997).

The ligands of selectin receptors are glycoproteins (**table 1**), most of which are mucin-like with *O*-glycosylated carbohydrate side chains, such as CD34, glycan-bearing cell adhesion molecule (GlyCAM)-1, P-selectin glycoprotein ligand (PSGL)-1 and mucosal addressin cell adhesion molecule (MAdCAM)-1 also involved in integrin $\alpha_4\beta_7$ binding (see 1.5.6.). The primary

recognition structure for selectins on the carbohydrate side chains of their ligands are terminally linked tetrasaccharides closely related to sialyl Lewis X (sLe^X; CD15s), an α(2→3)-sialylated and α(1→3)-fucosylated lactosamine. L-selectin on neutrophils, but not on T cells, also express sLe^X and thus serves as ligand for endothelial P- and L-selectin in neutrophil recruitment.

	L-selectin	E-selectin	P-selectin
CD nomenclature	CD62L	CD62E (ELAM-1)	CD62P
expression	leukocytes; constitutive	activated endothelium; transiently	endothelium and platelets; stored in granules
induced by	–	TNF-α, LPS, IL-1	TNF-α, LPS; histamine, thrombin
downregulation	surface-located protease	internalization and lysosomal degradation	internalization and recycling
main ligands	GlyCAM, CD34, MAdCAM-1, CLA-1	ESL-1, PSGL-1, L-selectin	PSGL-1, L-selectin

table 1: Expression, regulation and molecular interaction features of the selectin adhesion receptors. Abbreviations not further defined: ELAM-1 (endothelial leukocyte adhesion molecule-1), CLA-1 (cutaneous lymphocyte antigen-1), ESL-1 (E-selectin ligand-1). Note: P-selectin is stored in α-granules of platelets or in Weibel-Palade bodies of endothelial cells that are fused to the plasma membrane by stimulation of proinflammatory mediators such as histamine and thrombin.

The physiological importance of selectin-mediated interactions in leukocyte diapedesis is emphasized in type 2 leukocyte adhesion deficiency (LAD-II). This syndrome is characterized by an impaired fucose metabolism that causes the absence of fucose-containing sLe^X moieties in selectin ligands of affected patients (Etzioni *et al.*, 1992). The clinical picture includes recurrent bacterial infections mainly due to impaired neutrophil recruitment and thus is similar to that observed in LAD-I patients (see 1.5.5.5.).

1.4. Chemokines

The transition of transmigrating leukocytes from selectin-mediated activation-independent rolling to integrin-mediated activation-dependent firm arrest on the endothelium is induced by chemoattractants and their respective leukocytic receptors. Classical chemoattractants are the complement protein C5a, the lipid mediators leukotriene B4 (LTB_4) and platelet-activating factor (PAF), and bacterial N-formyl peptides (Springer, 1994). The majority of chemoattractants are however the chemokines (Ebnet *et al.*, 1999; Ward *et al.*, 1998), a family of small (6-14 kDa) chemotactic cytokines expressed and secreted by leukocytes and several tissue cells such as ECs, epithelial cells, smooth muscle cells (SMC) and fibroblasts. Endothelial chemokines, for

example, are induced by inflammatory cytokines such as interleukin (IL)-1 and TNF-α. They exert their function as soluble molecules as well as immobilized on the endothelium or the extracellular matrix (ECM) through binding with high avidity to heparin and heparan sulfate proteoglycans. Within inflamed tissues chemokines mediate the directed migration of extravasated leukocytes along a positive chemical concentration gradient (chemotaxis) to the site of inflammation, cells which can sense a concentration difference of 1 % across their diameter (Springer, 1994). Prior to this, they can mediate the firm arrest of rolling leukocytes on the endothelium at sites of inflammation by activating integrins via their respective chemokine receptors (Butcher, 1991; Springer, 1994). They also appear to be involved in mediating earlier stages of leukocyte extravasation and post-arrest events, *i.e.* rolling and chemotactic transendothelial migration (Weber *et al.*, 1996; Weber *et al.*, 1999b; Cinamon *et al.*, 2001a).

Chemokines are classified according to the position of the first two out of four conserved cysteine residues. The two main subfamilies are CXC chemokines with one intervening amino acid between the first two cysteines that effect mainly neutrophils, and CC chemokines where this conserved residues are adjacent and that effect mainly monocytes, lymphocytes and eosinophiles (Ward *et al.*, 1998). Notable representatives are the CC chemokines RANTES (regulated upon activation, normal T cell expressed and secreted; CCL5), monocyte chemoattractant protein-1 (MCP-1; CCL2), and macrophage inflammatory protein-1β (MIP-1β; CCL4) and the CXC chemokines IL-8 (CXCL8), growth-related oncogene-α (GRO-α; CXCL1) and stromal cell-derived factor (SDF)-1 (CXCL12)[2].

Chemokine receptors are seven transmembrane-spanning receptors expressed on leukocytes that are in general coupled to G proteins, in particular of the G_i class (Premack *et al.*, 1996; Mellado *et al.*, 2001). Thus the majority of chemokine receptor-mediated events are sensitive to *Bordetella pertussis* toxin (PTX). The signaling cascade of e.g. the IL-8–specific chemokine receptor CXCR1 leads to activation of PLC, PKC, small GTPases, Src-related tyrosine kinases and phosphatidylinositol-3-OH (PI3)-kinase, effecting processes involved in firm cell arrest and chemotaxis, such as activation of β_1 and β_2 integrin adhesion receptors and cytoskeletal rearrangements.

[2] Note: A new systematic chemokine nomenclature has been recently proposed based on the chemokine receptor nomenclature currently in use (Zlotnik *et al.*, 2000). Both classical and systematic names are stated.

1.5. Integrins

Integrins are evolutionary conserved surface adhesion receptors expressed by nearly all cell types, playing key roles in many cellular processes. Spanning the plasma membrane they are connected to the cellular environment, *i.e.* the extracellular matrix or neighboring cells, as well as to the cytoskeleton and the intracellular signal machinery. Thus integrins can function as environment sensor molecules transducing extracellular signals to the inner cell (termed outside-in signaling) or adapt their extracellular function in response to internally generated signals (termed inside-out signaling). Besides environmental recognition they mediate cellular migration and adhesion and thus are key players in physiological processes such as embryonic development, angiogenesis, wound healing, hemostasis, immune response and inflammation (Hynes, 1992; Horwitz, 1998). They provide survival signals to prevent programmed cell death (apoptosis) (Meredith *et al.*, 1993) but are also involved in pathological processes such as metastasis in cancer (Clezardin, 1998).

1.5.1. Molecular structure of integrins

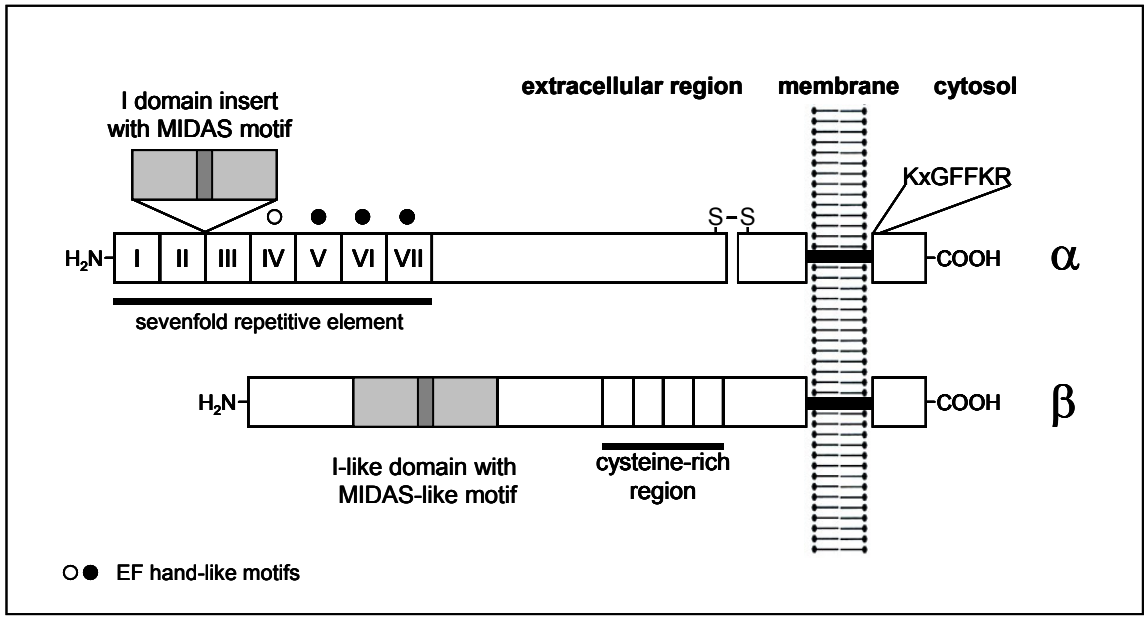

figure 2: Schematic representation of the domain structure of integrin αβ heterodimers. The seven homologous repeats of the α chain are designated by numbers (I-VII). The subunits α_L, α_M, α_X, α_D, α_1, α_2, α_{10}, and α_E contain an I domain between the repeat domains II and III. The MIDAS motif within the I domain is highlighted. I domain-containing integrins have three EF hand-like motifs ("●"; V-VII) whereas other integrins have four ("○●"; IV-VII) (Leitinger *et al.*, 2000). The sevenfold repetitive element is predicted to fold to form a β-propeller structure (Springer, 1997; Xiong *et al.*, 2001). In some cases, α subunits are cleaved at their membrane-proximal extracellular part via posttranslational proteolysis of the precursor molecule and linked there by a disulfide bond (Hynes, 1992). The integrin β chain contains a I-like domain with a MIDAS-like motif and a cysteine-rich region at the membrane-proximal part. Adapted from Leitinger *et al.*, 2000.

Cells can regulate their adhesive properties by cell type-dependent selective expression of different integrin molecules. To date, the integrin family consists of approximately 25 heterodimeric glycoprotein members. 19 α (120-180 kDa) and 9 β (90-110 kDa) subunits, all type I transmembrane proteins that have been identified, associate in a non-covalent manner to specific αβ complexes **(fig. 2)**. Both types of integrin subunits consist of large extracellular domains of 700-1100 aa that form a globular head structure at their N-terminal section containing the ligand binding regions (Humphries, 2000). By contrast their cytoplasmic tails of 30-50 aa are short, with exception of the β_4 intracellular tail formed by over 1000 residues (Hemler, 1990). Integrin α and β chains are assembled in the endoplasmic reticulum (ER), a requirement for their transport to the cell surface or, in some cases, to intracellular granules (Kishimoto *et al.*, 1989; Green *et al.*, 1998)

1.5.1.1. The integrin α chain

The N-terminus of integrin α chains contains a sevenfold repetitive element (I-VII) of about 60 aa (**fig. 2**). The last four repeats (IV-VII) resemble EF hand-like motifs with the consensus sequence DxDxDGxxD[3], characterized as divalent cation binding sites presumably for Ca^{2+} ions (Leitinger *et al.*, 2000). In I domain-containing α subunits, however, only the last three N-terminal repeats (V-VII) resemble EF hand-like motifs. The α chains of leukocyte β_2 integrins (*i.e.* α_L, α_M, α_X, and α_D) as well as the α_1, α_2, α_{10} and α_E chains contain this additional domain between the repeats II and III. The I domain is homologous to the von Willebrand factor (vWF) A domain and consists of approximately 200 aa residues. Within its sequence there is a highly conserved Mg^{2+}/Mn^{2+} binding motif termed metal ion-dependent adhesion site (MIDAS) that is implicated in the ligand binding of the respective integrins (Gahmberg *et al.*, 1997; Leitinger *et al.*, 2000). Previously the I domain allosteric site (IDAS), localized at a site spatially distinct from the MIDAS, was identified as a second domain involved in the ligand binding regulation of the β_2 integrin LFA-1 (Huth *et al.*, 2000; Lupher *et al.*, 2001).

The cytoplasmic tails of integrin α subunits exhibit only minor similarity between different family members, apart from the highly conserved membrane-flanking KxGFFKR motif that exerts an inhibitory effect on ligand binding in non-activated integrins. The deletion of the KxGFFKR sequence has been shown to result in the expression of constitutively active integrins, suggesting that this conserved motif functions in the maintenance of default low-affinity states in integrins (Williams *et al.*, 1994; Dedhar *et al.*, 1996).

---

[3] Single-letter amino acid code. Lowercase x represents any unspecified amino acid. Other lowercase letters correspond to residues conserved in at least three integrin subunits. Uppercase letters corresponds to near-invariant residues. Dashes represent non-conserved residues and/or gaps. Letters in brackets, separated by slashes, constitute mutual alternative amino acids at this sequence position.

1.5.1.2. The integrin β chain

The extracellular part of integrin β subunits exhibits two regions of homology. N-terminally there is a I domain-like motif with similarity to the α chain I domain, including the presence of a MIDAS-like metal binding motif. The membrane-proximal part is formed by a four-fold repeat of cysteine-rich, EGF-like domains of 40 aa residues (Green *et al.*, 1998; Humphries, 2000).

Conserved intracellular sequences of integrin β chains are the membrane-flanking sequence KLLv-ihDRRE and, with the exception of β_4, the NPx(Y/F) motif (Williams *et al.*, 1994; Liu *et al.*, 2000a).

1.5.2. Inside-out signaling

Many integrin receptors are normally in a low-affinity state and require activation to exert their adhesive function, especially integrins expressed in hematopoietic cells. Otherwise, circulation of patrolling blood cells in the vasculature or cell migration, accomplished by regulated cycles of attachment and de-attachment, would not be feasible due to firm cellular arrest mediated by integrin adhesion receptors locked in a sustained, constitutively active state. A rapid and highly regulated activation is ensured by signal transduction pathways affecting integrins inside-out signaling and thus their affinity and avidity state.

1.5.2.1. Affinity

The affinity of integrins for their extracellular ligands, in particular of those with an I domain (Liddington *et al.*, 2002), is regulated by conformational changes induced at the cytoplasmic tails of the heterodimer and transfered to its extracellular segment. For non-activated integrins the conserved membrane-flanking cytoplasmic motifs in both the α and the β chains are crucial for the maintenance of their low-affinity state. Mutations in or deletion of either the KxGFFKR or the KLLv-ihDRRE sequences, has been shown to result in a constitutive active state of integrins accompanied by high affinity binding to their ligands (Hughes *et al.*, 1998; van Kooyk *et al.*, 1999). Structural changes in activated integrins can be detected by specific monoclonal reporter antibodies (Shattil *et al.*, 1985; Dransfield *et al.*, 1989; Diamond *et al.*, 1994).

1.5.2.2. Avidity

The avidity of integrins can be regulated by their clustering on the membrane surface, e.g. at focal adhesion contacts. This alteration in surface distribution depends on the lateral mobility of

the integrins within the plasma membrane. This is thought to be enabled by a temporary disconnection from their cytoskeletal association (Lub *et al.*, 1997a; van Kooyk *et al.*, 2000; Leitinger *et al.*, 2000). Avidity-activated LFA-1 can be specifically detected by the reporter mAb NKI-L16 that recognizes a cluster-dependent epitope on the LFA-1 α_L chain (Keizer *et al.*, 1988; van Kooyk *et al.*, 1991).

1.5.2.3. Integrin activation

Different signaling pathways have been implicated in integrin inside-out signaling, although the precise nature of the direct molecular link to integrins remains largely unknown. For example, the small GTP binding protein R-Ras can activate integrins (Zhang *et al.*, 1996). On the contrary, the effect of H-Ras is more controversially discussed. H-Ras signaling to the Raf-1/ extracellular signal-related kinase (ERK) pathway suppresses integrin activation as shown for β_1 and β_3 integrins, whereas signal transduction via other pathways may lead to an integrin activation as demonstrated for β_1 and β_2 integrins (Hughes *et al.*, 1997; Shibayama *et al.*, 1999). For chemokine-triggered regulation of LFA-1 avidity in T cells, it appears that H-Ras is involved in both transient LFA-1 activation by signaling to PI3-kinase and in the subsequent down-regulation by activation of the Raf-1/ERK pathway, thus establishing a complex and bimodal involvement of H-Ras (Weber *et al.*, 2001a). Rho, another member of the Ras superfamily, exerts an influence on integrin activation by its regulatory function in cytoskeletal organization (Laudanna *et al.*, 1996).

Intracellular Ca^{2+} is also involved in inside-out signaling, e.g. by effecting clustering and adhesion properties of leukocyte integrins through activation of the Ca^{2+}-dependent protease calpain (Leitinger *et al.*, 2000). Furthermore, PI3-kinase (Hughes *et al.*, 1998) and PKC signal to integrins, the latter affecting integrin avidity but not affinity (Kolanus *et al.*, 1997; Gahmberg *et al.*, 1998). There are indications that cytoplasmic domains of integrins, which exhibit conserved serine, threonine and tyrosine residues, are phosphorylated in response to activators such as PKC. However, a significant role for phosphorylation in integrin activation has not yet been established (Hibbs *et al.*, 1991a; Hynes, 1992; Williams *et al.*, 1994; Gahmberg *et al.*, 1998).

Phorbol esters such as phorbol-12-myristate-13-acetate (PMA) efficiently activate leukocyte integrins in less than one hour via PKC (Gahmberg *et al.*, 1997). A more physiological stimulation compared to PMA is achieved e.g. by inflammatory cytokines like SDF-1α (CXCL12) (Campbell *et al.*, 1998; Weber *et al.*, 1999a). The G protein–coupled chemokine receptors are an example for the influence of outside-in signals from other surface receptors to integrin-activating signaling, as is the engagement of the T-cell receptor (TCR)/CD3 complex in LFA-1 activation (Dustin *et al.*, 1989).

Integrin inside-out signaling is also induced by direct interactions of intracellular regulatory and cytoskeletal proteins with integrin subunits. Additionally, lateral protein interactions *in cis* with adjacent membrane proteins can influence the activation state of integrins. Both aspects are described below. In addition to the effects of intracellular signaling, activation of integrins is also directed by extracellular signals. Since they represent metalloproteins, integrin function is dependent on extracellular divalent metal cations, *i.e.* Mg^{2+}, Mn^{2+} and Ca^{2+}, which influence their conformation and thus are important determinants of their affinity state. However, the role of Ca^{2+} appears to be more complex, since in some systems it revealed an inhibitory effect on integrin adhesiveness (Leitinger *et al.*, 2000; Humphries, 2000; Plow *et al.*, 2000).

1.5.3. Outside-in signaling

Beside their functional role as adhesion receptors, integrins are capable of delivering extracellular information to the interior of the cell. Integrin-triggered signal transduction cascades (outside-in signaling) lead to diverse cellular responses regulating gene expression, cell growth, migration, differentiation and survival (Hynes, 1992; Miranti *et al.*, 2002).

Outside-in signaling of integrins occurs frequently at focal contacts, where clusters of ligand-bound integrins complex with cytoskeletal, signaling and adaptor molecules. Importantly, integrin-initiated signals mediate the tyrosine phosphorylation of a number of cellular proteins, including Src and Fyn tyrosine kinases as well as the autophosphorylation of focal adhesion kinase (FAK). Activated FAK in turn phosphorylates paxillin and CAS that serve as scaffolds for the recruitment of various adapters and signaling molecules. Further signal transduction can lead to the activation of elements of the ERK/mitogen-activated protein kinase (MAPK) pathway (Howe *et al.*, 1998; Giancotti, 2000). However, integrins transduce their outside-in signals to many other downstream pathways, affecting regulatory proteins such as PI3-kinase, PLC and the small GTPases Rho, Rac and Cdc42 (Howe *et al.*, 1998; Longhurst *et al.*, 1998; Boudreau *et al.*, 1999; Schoenwaelder *et al.*, 1999; Dib *et al.*, 2000). Subsequent events include the modulation of cytoplasmic Ca^{2+} concentrations (Schwartz, 1993), PKC activity (Vuori *et al.*, 1993) and the Na^{+}/H^{+} antiporter activity accompanied by changes in intracellular pH values (Schwartz *et al.*, 1991).

Integrins, which posses no intrinsic catalytic activity, signal not only in a direct but also in a collaborative manner. In the latter case they take advantage of the downstream signaling pathways of other surface receptors described below by *trans*-activation (receptor cross-talk) to transduce specific signals to the cell interior. Moreover, outside-in signaling of integrins can regulate the function of other integrins. For example, ligand-bound exogenous $\alpha_{IIb}\beta_3$ has been shown to suppress the adhesive function of the endogenous integrin $\alpha_5\beta_1$ in the same cells

(*trans*-dominant inhibition) due to a blockade of $\alpha_{IIb}\beta_3$ signaling to the suppressed target integrin (Díaz-González *et al.*, 1996).

1.5.4. Integrin-interacting proteins

1.5.4.1. Integrin ligands: ECM proteins and counter-receptors

The majority of integrins bind extracellularly to ECM proteins. At least eight bind to fibronectin ($\alpha_4\beta_1$, $\alpha_5\beta_1$, $\alpha_V\beta_1$, $\alpha_V\beta_3$, $\alpha_{IIb}\beta_3$, $\alpha_V\beta_6$, $\alpha_4\beta_7$) and five to laminin ($\alpha_1\beta_1$, $\alpha_2\beta_1$, $\alpha_3\beta_1$, $\alpha_6\beta_1$, $\alpha_6\beta_4$). Other ECM ligands include collagen IV and vitronectin. A key recognition sequence for integrins on some ECM proteins is the tripeptide motif RGD that is for example involved in the binding of fibronectin to its integrin receptor $\alpha_5\beta_1$. Other integrins recognize different motifs (Hynes, 1992; Plow *et al.*, 2000). Due to their binding specificities, ECM proteins exert fundamental influence on many cellular processes with regard to their outside-in signal transduction and cytoskeletal connection mediated by their respective integrin receptor(s).

However, certain integrins interact with counter-receptors on other cells or in soluble plasma. One important example is the binding of $\alpha_{IIb}\beta_3$ on activated platelets to soluble fibrinogen or vWF in the process of wound healing (Hynes, 1992; Clemetson *et al.*, 1998). The leukocyte-specific integrin $\alpha_E\beta_7$ has been shown to bind epithelial expressed E-cadherin (Cepek *et al.*, 1994) that is involved in the formation of interepithelial AJs. Some integrin ligands belong to the family of IgSF proteins and contribute to endothelial adhesion or diapedesis of leukocytes. Beside the interaction of ICAMs with β_2 integrins (see below) this includes the interaction of $\alpha_4\beta_1$ (VLA-4) with VCAM-1 (CD106), $\alpha_4\beta_7$ with MAdCAM-1 and $\alpha_V\beta_3$ with PECAM-1 (CD31) (Elices *et al.*, 1990; Berlin *et al.*, 1993; Piali *et al.*, 1995; Elices *et al.*, 1990; Berlin *et al.*, 1993; Piali *et al.*, 1995).

1.5.4.2. Cytoskeletal integrin connections

The connection of integrins to the actin cytoskeleton is mainly formed via their β tails through the association with the actin binding proteins talin and filamin as well as the actin bundling protein α-actinin (Calderwood *et al.*, 2000; Critchley, 2000). Talin interacts with both vinculin and paxillin, the latter binding FAK that further phosphorylates signaling and adaptor molecules as described. Concerning the α subunit, paxillin has been shown to bind directly α_4 but not other integrin α tails, reducing focal adhesion and stress fibre formation and thus enhancing cell migration (Liu *et al.*, 1999; Giancotti, 2000).

Interactions of integrins with the cytoskeleton are thought to occur mainly as a consequence of integrin-ligand engagement (outside-in signaling). This contributes to cytoskeleton-reorganization, formation of focal adhesion complexes and to integrin activation (Hughes *et al.*, 1998; Schoenwaelder *et al.*, 1999). On the other hand, cytoskeletal association is required for integrin inside-out signaling. Thereby active receptor conformations may be stabilized (affinity), and transient disconnection during cytoskeletal reorganization allows lateral motility required for integrin clustering (avidity). Thus, extracellular integrin interactions can directly influence the state of cytoskeleton organization and *vice versa*.

1.5.4.3. Direct cytoplasmic interaction partners

The majority of protein interactions between integrins and cytoplasmic proteins described so far are specific for the β tail (Liu *et al.*, 2000a). Integrin-linked kinase (ILK), a serine/threonine kinase involved in cell adhesion, anchorage-dependent cell growth and fibronectin matrix assembly, binds to β_1, β_2 and β_3 cytoplasmic tails and may regulate integrin affinity (Hannigan *et al.*, 1996). A link between integrins and PKC is provided by the Trp-Asp (WD) repeat protein Rack-1. This receptor for activated PKC binds *in vivo* with its C-terminal three WD motifs to the membrane-proximal region of β_1, β_2 and β_5 tails following stimulation with phorbol ester (Liliental *et al.*, 1998). More specifically, the WD repeat protein WAIT-1 interacts with the leukocyte integrins $\alpha_4\beta_7$ and $\alpha_E\beta_7$ (Rietzler *et al.*, 1998). The integrin cytoplasmic domain-associated protein (ICAP)-1 interacts specifically with the highly conserved NPxY sequence of β_1 tails and is phosphorylated upon β_1 integrin-mediated cell-matrix adhesion (Chang *et al.*, 1997). Differently, β_3-endonexin recognizes a unique membrane-distal NITY motif found on integrin β_3 tails (Shattil *et al.*, 1995; Eigenthaler *et al.*, 1997) and thereby can increase $\alpha_{IIb}\beta_3$ affinity and fibrinogen-dependent platelet aggregation (Kashiwagi *et al.*, 1997).

The β_2 integrin LFA-1, described in detail below, interacts via its β subunit with the Jun activation domain-binding protein 1 (JAB1), a coactivator of the transcription factor c-Jun. This interaction results in an enhanced activity of the transcription factor activator protein (AP)-1 (Bianchi *et al.*, 2000), indicating a role of LFA-1 in the regulation of gene expression. A functional regulator of LFA-1 avidity is given by cytohesin-1, a cytosolic guanine nucleotide exchange factor (GEF) for ADP ribosylation factor (ARF)-GTPases that is predominantly expressed in hematopoietic cells (Kolanus *et al.*, 1996). Cytohesin-1 binds specifically with its N-terminal SEC7 domain to the membrane-proximal residues in the β_2 tail (Geiger *et al.*, 2000). By this interaction cytohesin-1 has a functional role in the activation of LFA-1–mediated T cell adhesion and spreading on the LFA-1 ligand ICAM-1 (Kolanus *et al.*, 1996) as well as in chemokine-induced T cell arrest on cytokine-activated endothelium with subsequent transendothelial migration under flow conditions (Weber *et al.*, 2001b). Plasma membrane

recruitment of cytohesin-1 is mediated by the PI3-kinase product phosphatidylinositol-(3,4,5)-triphosphate (PIP_3). PIP_3 specifically binds the pleckstrin homology (PH) domain of cytohesin-1 (Nagel *et al.*, 1998a; Nagel *et al.*, 1998b). In this way cytohesin-1 takes part in the linkage of phospholipid signaling via PI3-kinase to LFA-1 activation. Similarly the general receptor of phosphoinositides 1 (GRP1; cytohesin-3) but not the ARF nucleotide binding site opener (ARNO; cytohesin-2) interacts with CD18 and induces LFA-1–mediated lymphocyte adhesion to ICAM-1 (Korthäuer *et al.*, 2000).

Surprisingly in contrast to the integrin β subunit, only few direct interaction partners have been identified for the cytosolic part of integrin α subunits. The interaction with WAIT-1 described above is one example. Calcium and integrin-binding protein (CIP) binds to α_{IIb} and may be a candidate regulatory protein for $\alpha_{IIb}\beta_3$ (GPIIb/IIIa) in platelets (Naik *et al.*, 1997). Most importantly, the ubiquitously expressed Ca^{2+}-binding protein calreticulin binds to the highly conserved and functionally important KxGFFKR motif in integrin α tails (Rojiani *et al.*, 1991). It has been hypothesized that by this interaction, calreticulin disrupts the native default inactive state of integrins that is normally mediated by the KxGFFKR motif and thus activates integrin function (Dedhar, 1994). Its physiological role is demonstrated by calreticulin-null embryonic stem cells that have a severe defect in integrin-mediated cell adhesion (Coppolino *et al.*, 1997).

1.5.4.4. Lateral receptor interactions of integrins

Besides extracellular and cytosolic protein interactions, integrin receptors also cooperate in direct lateral association with other plasma membrane receptors (*trans*-activation). They are thus able to signal to different pathways (Boudreau *et al.*, 1999; Schwartz *et al.*, 2002). For example, β_1 integrins were shown to activate platelet-derived growth factor (PDGF) β-receptor independently of the presence of the PDGF ligand (Sundberg *et al.*, 1996). Transmembrane-4 superfamily (TM4SF) proteins (tetraspans) such as CD9, CD63, CD81 and CD151 can associate directly with certain integrins. Some of them recruit signaling enzymes such as PI4-kinase and PKC into complexes with integrins, linking them to phospholipid signaling and enabling PKC-dependent phosphorylation, e.g. of the α_3 or the α_6 cytoplasmic domain (Hemler, 1998; Longhurst *et al.*, 1998; Giancotti, 2000). Another integrin cross-talk partner is the five membrane-spanning integrin-associated protein (IAP; CD47) associated with the ubiquitous expressed $\alpha_V\beta_3$ and the platelet-restricted $\alpha_{IIb}\beta_3$. Several $\alpha_v\beta_3$-dependent neutrophil functions are strongly influenced by anti-CD47 treatment and IAP knock-out mice suggest a central role in leukocyte migration (Porter *et al.*, 1998). Contrary to these receptors, uPAR (urokinase-type plasminogen activator receptor; CD87) is an example of a cell surface receptor that lacks intracellular domains and thus has to signal through membrane-spanning lateral interaction partners such as the β_1, β_2 and β_3 integrins (Ossowski *et al.*, 2000).

1.5.5. Leukocyte-specific β_2 integrins

Approximately half of the known integrins are expressed by lymphocytes, monocytes and granulocytes. Cell-cell contacts mediated by β_2 integrins contribute to processes such as antigen presentation, cytotoxicity, phagocytosis and extravasation. Besides the β_7 group ($\alpha_4\beta_7$, $\alpha_E\beta_7$), β_2 integrins are presented exclusively on leukocytes. Presently four different α chains, *i.e.* the I domain-containing α_L, α_M, α_x and α_D, are known to associate with the β_2 (CD18) chain. The genes that encode them are located on chromosome 16, whereas the gene for CD18 is located on chromosome 21 (Gahmberg *et al.*, 1998).

1.5.5.1. LFA-1

One of the most abundant leukocyte integrins is the lymphocyte-function associated antigen-1 (LFA-1; $\alpha_L\beta_2$; CD11a/CD18). LFA-1 is predominantly expressed in lymphocytes and neutrophils and consists of the 180-kDa α_L chain associated with the 95-kDa β_2 chain common to all CD11/CD18-integrins. As a cell-adhesion receptor, LFA-1 is involved in a broad range of immunologic processes including B lymphocyte responses, antigen-induced T cell proliferation, T cell-mediated cytotoxicity, and natural killer (NK) cell activity (Dustin *et al.*, 1989; Arnaout, 1990; Springer, 1990). Furthermore, LFA-1 is a key player in the highly regulated process of lymphocyte homing and leukocyte extravasation to sites of inflammation, mediating firm arrest on the endothelium and subsequent transmigration (Butcher, 1991; Springer, 1994). Additionally LFA-1 appears to participate in the initial step of slowing-down the velocity of rolling leukocytes (Sigal *et al.*, 2000; Henderson *et al.*, 2001; Dunne *et al.*, 2002).

Without stimulation LFA-1 surface expression is generally not sufficient for adhesion thus allowing unresisted leukocyte circulation and highly specific regulation of its adhesive properties. Activation of LFA-1 is mainly achieved by inside-out signaling triggered, for example, by TCR signals (Dustin *et al.*, 1989), cytokines such as IL-12 (Mukai *et al.*, 2001), chemokines such as SDF-1 (Peled *et al.*, 1999) and other inflammation mediators. LFA-1 avidity can be rapidly induced with PKC-activating phorbol esters such as PMA (Dustin *et al.*, 1989) leading to the phosphorylation of S756 in the β_2 tail. However, mutational analysis has not revealed a significant role for phosphorylated S756 in LFA-1–mediated adhesion (Hibbs *et al.*, 1991a). The adjacent T758-T759-T760 motif does appear to be critical for this process, since mutation of one of these residues leads to decreased adhesion (Hibbs *et al.*, 1991a; Gahmberg *et al.*, 1998). The crucial role of intracellular partners or extracellular divalent cations in LFA-1 function has already been discussed.

Extracellularly, LFA-1 binds to ICAMs, a subfamily of type I membrane glycoproteins within the IgSF (Simmons, 1995; Gahmberg *et al.*, 1997). The main ligand is ICAM-1 (CD54) that is present on leukocytes, ECs and many other tissues although at low expression levels (Marlin *et al.*, 1987). On resting ECs it is rapidly inducible by inflammatory cytokines such as TNF-α, IFN-γ and IL-1. Truncation of the β_2 but not that of the α_L cytoplasmic domain eliminates LFA-1–binding to ICAM-1 (Hibbs *et al.*, 1991b), revealing the importance of integrin inside-out signaling in ligand binding. However, complete deletion of the β_2 cytoplasmic domain results in a constitutively active and LFA-1–clustering mutant that binds strongly to ICAM-1 (Lub *et al.*, 1997b). An important aspect of ICAM-1 binding to LFA-1 is its dimerization at the cell surface (Jun *et al.*, 2001). In addition to ICAM-1, LFA-1 binds to ICAM-2 (CD102) on ECs, leukocytes and platelets, to ICAM-3 (CD50) on lymphocytes, to the Landsteiner-Wiener blood group antigen ICAM-4 (LW) exclusively expressed on red cells and finally to the brain-specific telencephalin (TLN; ICAM-5) (Gahmberg *et al.*, 1997; Gahmberg *et al.*, 1998).

1.5.5.2. Mac-1

Mac-1 ($\alpha_M\beta_2$; CD11b/CD18; complement receptor type 3, CR3; macrophage antigen-1) recognizes a wide spectrum of ligands, which include ICAM-1 (Diamond *et al.*, 1991), the platelet glycoprotein (GP) Ibα (Simon *et al.*, 2000), the blood coagulation factors fibrinogen and factor X, and the complement fragment iC3b. It is exclusively expressed on monocytes, macrophages, neutrophils and NK cells. The levels of Mac-1 at the cell surface but not that of LFA-1 can be rapidly increased in response to chemotactic factors due to its storage in intracellular pools. Mac-1 plays an important role in phagocytosis of microorganisms and is involved in ICAM-1–mediated leukocyte attachment (Kishimoto *et al.*, 1989; Arnaout, 1990). Knock-out mice experiments have revealed a dominant role for LFA-1 compared to Mac-1 in the relative contribution to neutrophil adhesion and extravasation (Lu *et al.*, 1997; Ding *et al.*, 1999). Moreover, both β_2 integrins display different kinetics of activation in lymphocytes upon chemokine stimulation, *i.e.* transient avidity for LFA-1 and sustained avidity for Mac-1, a function of their respective cytoplasmic α tails (Weber *et al.*, 1999a).

1.5.5.3. p150,95

The expression of p150,95 ($\alpha_x\beta_2$; CD11c/CD18; CR4) is mainly restricted to myeloid cells. Like Mac-1 it is stored in intracellular granules and can also function as receptor for iC3b and fibrinogen (Dickeson *et al.*, 1998). Additionally, p150,95 represents beside CD14 the second monocyte receptor for endotoxin (Ingalls *et al.*, 1995).

1.5.5.4. $\alpha_D\beta_2$

$\alpha_D\beta_2$ (CD11d/CD18) is the most recently identified β_2 integrin (Danilenko *et al.*, 1995; van der Vieren *et al.*, 1995) and is mainly found in macrophages and granulocytes of the splenic red pulp. $\alpha_D\beta_2$ preferentially binds to ICAM-3.

1.5.5.5. Leukocyte adhesion deficiency type 1 (LAD-I)

The physiological importance of β_2 integrin adhesion molecules is revealed by the inherited autosomal recessive disorder LAD-I in which defects in the β_2 (CD18) gene cause a deficiency or loss in expression of all β_2 (CD11/CD18) integrins (Anderson *et al.*, 1987; Kishimoto *et al.*, 1989). This disease is characterized by recurrent severe and life-threatening bacterial infections and impaired wound healing with clinical similarities to LAD-II (see 1.3.). Concerned patients show abnormalities in many adhesion-dependent leukocyte functions including endothelial arrest, aggregation, chemotaxis, phagocytosis and cytotoxicity. The severity is directly related to the degree of β_2 integrin deficiency and may lead in severe cases to death during infancy. The molecular basis of this disease is a defective biosynthesis of CD18 due to mutations mainly localized around the MIDAS-like motif in the I-like domain (Leitinger *et al.*, 2000). These mutations impair heterodimer formation of the β_2 precursor with the respective α chain precursor, a process essential for subsequent carbohydrate processing and surface expression of the mature integrin (Anderson *et al.*, 1987; Arnaout, 1990). Thus, the surface expression of CD18 but as well that of the unaffected CD11 subunits is deficient in the leukocytes of LAD-I patients. Differently mutated β_2 subunits vary in their ability to complex with the α subunit, which leads to the heterogeneity of the clinical phenotype of LAD-I and offers insights into the structural basis of the integrin $\alpha\beta$ heterodimer formation (Shaw *et al.*, 2001a). LAD-I patients can be cured by bone marrow transplantation that restores leukocyte function.

1.5.6. α_4 integrins

The VLA-4/VCAM-1 interaction (Elices *et al.*, 1990) provides a second lymphocyte-EC adhesion mechanism distinct from the LFA-1/ICAM-1 interaction (Ronald *et al.*, 2001). Very late antigen (VLA)-4 ($\alpha_4\beta_1$; CD49d/CD29) is an atypical member of the ECM (fibronectin, laminin, collagen) receptor family of β_1 integrins (Hemler, 1990) with expression restricted to lymphocytes, monocytes and eosinophils. VLA-4 and the lymphocytic $\alpha_4\beta_7$ functions both as a matrix (fibrinogen) and cell receptor. In the case of the latter, they bind to VCAM-1 (CD106) (Elices *et al.*, 1990; Berlin *et al.*, 1993). Similar to ICAM-1, this IgSF member is expressed on the endothelium in response to inflammatory induction e.g. by TNF-α, IL-1 or LPS (Springer,

1995). In addition to VCAM-1, $\alpha_4\beta_7$ also interacts specifically with the IgSF protein MAdCAM-1 expressed by mucosal venules (Berlin *et al.*, 1993). In contrast to the β_2 integrins, VLA-4 and $\alpha_4\beta_7$ are able to support not only firm arrest and transmigration but also rolling of non-neutrophilic leukocytes on activated endothelium (Stewart *et al.*, 1995). LFA-1 and VLA-4 appear to exert distinct functions in the process of extravasation. In the case of monocytes, VLA-4 preferentially mediates cell arrest and subsequent lateral migration along the endothelium to the site of interendothelial junctions, where in turn LFA-1 is more crucial for diapedesis itself (Weber *et al.*, 1998).

1.6. Immunoglobulin superfamily

The immunoglobulin superfamily (IgSF) (Williams *et al.*, 1988) consists of proteins that contain modular domains with homology in sequence and tertiary structure to the variable (type V) and the constant (type C1 and C2) domain of antibodies (Bork *et al.*, 1994; Holness *et al.*, 1994; Vaughn *et al.*, 1996). Immunoglobulin (Ig)-like domains are constituted by 70 – 110 aa that form two β-sheets in a sandwich-like structure with seven to nine antiparallel β-strands. Two cysteine residues at a distance of 55 to 75 aa form an intramolecular disulfide bond within the Ig-like loop. Most IgSF members are integral transmembrane proteins with extracellular Ig-like domain(s) and divergent cytoplasmic tails. Despite the conserved folding of the Ig-like domains there is great diversity in the function of IgSF proteins as recognition and binding molecules, undergoing homophilic or heterophilic interactions both *in cis* and *in trans*. Noted members of the IgSF are TCR, class I and class II major histocompatibility complexes (MHC), CD4, CD8, FcγRII, the PDGF receptor, and integrin ligands such as ICAM-1, VCAM-1 and PECAM-1. On leukocytes, approximately 50 % of the surface proteins are IgSF molecules. Considering the dynamic process of cell-cell adhesion, the binding of a single IgSF molecule to its interaction partner may be very weak but can lead to significant adhesive strength by multivalent presentation as occurs in particular on activated cell surfaces.

1.7. Junctional adhesion molecule (JAM)-1

The type I transmembrane protein JAM-1 is a novel member of the IgSF family that was first characterized in the mouse (Martìn-Padura *et al.*, 1998) and found to be identical to murine antigen 106 (Malergue *et al.*, 1998). Due to its predominant expression at intercellular junctions between endothelial and epithelial cells and data from Chinese hamster ovary (CHO) cell

transfectants suggesting a role in cell-cell interaction, this surface protein was termed junctional adhesion molecule (Martìn-Padura *et al.*, 1998). Identification of the human homologue (Ozaki *et al.*, 1999; Williams *et al.*, 1999) revealed similarity with the partially sequenced platelet surface glycoprotein F11 antigen (F11R) (Kornecki *et al.*, 1990; Naik *et al.*, 1995). The subsequent determination of the complete sequence of F11R revealed its identity with human JAM-1 (Sobocka *et al.*, 2000; Gupta *et al.*, 2000).

1.7.1. Expression, localization and function of JAM-1

JAM-1 is expressed in the tissue of most major organ systems, such as heart, liver, lung, pancreas and kidney (Gupta *et al.*, 2000; Liang *et al.*, 2000; Naik *et al.*, 2001). Northern blot analysis revealed the expression of JAM-1 at the mRNA level as a single 2-kb transcript in mice (Martìn-Padura *et al.*, 1998; Malergue *et al.*, 1998), whereas human JAM-1 is transcribed into multiple mRNA molecules of 4.0, 2.4 and 1.9 kb resulting from differences in the size of the 3'-UTR (Williams *et al.*, 1999; Naik *et al.*, 2001).

JAM-1 is predominantly expressed in endothelial and epithelial cells. Immunofluorescence and immunoelectron microscopy as well as immunohistochemistry has localized JAM-1 expression specifically at apical tight junctional structures. Here it colocalizes with typical TJ markers such as ZO-1, occludin and cingulin, but not with AJ-associated molecules like β-catenin or E-cadherin (Martìn-Padura *et al.*, 1998). In epithelial cells JAM-1 was also found to localize subapically to TJs at more basolateral areas of intercellular contacts (Liang *et al.*, 2000; Liu *et al.*, 2000b). The junctional localization can be influenced by proinflammatory cytokines. A combined treatment of human umbilical vein endothelial cell (HUVEC) monolayers with TNF-α and IFN-γ causes JAM-1 to redistribute from the intercellular junctions over the cell surface, implicating a functional role in inflammatory processes (Ozaki *et al.*, 1999; Shaw *et al.*, 2001c). Its specific localization and data from resealing experiments of disrupted TJs (Liu *et al.*, 2000b; Liang *et al.*, 2000) suggest a functional role in generation and/or maintenance of TJs and the formation of cell polarity. The expression of JAM-1 in hematopoietic cells is discussed elsewhere within this report.

1.7.2. Molecular structure

Located on chromosome 1q21.1-21.3 (Naik *et al.*, 2001), the human *JAM-1* gene encodes a protein of 299 aa (see **fig. 17**) with an N-terminal signal sequence (27 aa), a large extracellular domain (211 aa), a single transmembrane domain (17 aa) and a short (44 aa) cytoplasmic tail (Liu *et al.*, 2000b). The extracellular part contains two Ig-like loops each flanked by two cysteine

residues (C50 and C109, C153 and C212) forming a disulfide bond. Thus JAM-1 belongs to the IgSF family and resembles structurally other cell adhesion molecules (CAMs). Whether the Ig-like domains are of type V or type C2 is still controversial (Naik *et al.*, 2001; Aurrand-Lions *et al.*, 2001b). JAM-1 exhibits two *N*-glycosylation sites, N185 and N191, that are both located in the membrane-proximal Ig-like domain 2. They lead in some cells to heterogeneous expression of JAM-1 due to differential glycosylation. Here, JAM-1 appears as ~40 kDa and ~37 kDa proteins in western blot analysis, and enzymatic deglycosylation reveals a core protein with a molecular mass of ~35 kDa (Naik *et al.*, 1995; Liang *et al.*, 2000). The cytoplasmic tail of JAM-1 is highly charged, contains several putative phosphorylation sites for PKC and other protein kinases and is distinguished by the PDZ domain-binding motif FLV at the C-terminal end.

JAM-1 is highly conserved among mammals, with murine, bovine and human JAM-1 displaying approximately 70 % overall identity at the amino acid level (Ozaki *et al.*, 1999). The high degree of conservation within the cytoplasmic tail with more than 80 % identity suggests similar intracellular function and/or regulation.

1.7.3. Extracellular homophilic interactions *in cis* and *in trans*

Analytical ultracentrifugation of rsJAM, the recombinant soluble expressed extracellular domain of murine JAM-1, reveals 89 % associates as dimers while 11 % forms tetramers but none appear as monomers. This demonstrates, in addition to the results of other *in vitro* studies, the capacity for dimerization and oligomerization (Bazzoni *et al.*, 2000a; Liang *et al.*, 2000). The presence of JAM-1 dimers on the cell surface, *i.e.* homophilic JAM-1 interactions *in cis*, was demonstrated in transfected CHO cells using a membrane-impermeable protein cross-linker (Bazzoni *et al.*, 2000a). Such homophilic interactions *in cis* are meditated by the N-terminal Ig-like domain 1 of JAM-1, forming an U-shaped dimer formation (see **fig. 29**) as revealed from the crystal structure of rsJAM (Kostrewa *et al.*, 2001).

Endothelial and epithelial JAM-1 exerts adhesive properties at intercellular junctions by homophilic binding *in trans* (between JAM-1 molecules of opposing cells) and thus participates in the arrangement of TJs and more basolateral junctional structures. Exogenously expressed in confluent CHO cells, JAM-1 is specifically concentrated at cell-cell contacts and decreases the paracellular permeability of the cell monolayer. If the CHO cells, which do not exert organized TJs, are only partially transfected, JAM-1 is solely concentrated at cell-cell contacts if the adjacent neighboring cell is also transfected (Martìn-Padura *et al.*, 1998; Naik *et al.*, 2001). *Trans*-homophilic interactions seems thus to mediate the recruitment of JAM-1 to intercellular junctions. Notably, soluble JAM-1–Fc chimera or monoclonal antibodies (mAbs) raised against JAM-1 inhibit or significantly slow down the resealing of disrupted intercellular junctions

between epithelial cells (Liang *et al.*, 2000; Liu *et al.*, 2000b), displaying the importance of *trans*-homophilic adhesive JAM-1 binding for the integrity of the cell monolayer. The X-ray structure of crystallized rsJAM revealed that pairs of *cis*-dimers contact each other *in trans* at their respective N-terminal Ig-like domain 1 (Kostrewa *et al.*, 2001), suggesting that this domain mediates most likely both *cis*- and *trans*-homophilic JAM-1 interactions.

1.7.4. Extracellular heterophilic interactions

JAM-1 was shown to function as a reovirus receptor (Barton *et al.*, 2001). The cell surface protein is recognized with high affinity by the globular head of the viral attachment protein σ1. JAM-1 is sufficient for virus attachment and endocytosis but it may not necessarily mediated these processes. However, the activation of nuclear factor (NF)-κB and apoptosis accompanying reovirus infection fully depends on the binding of reovirus to cellular JAM-1 via σ1. Furthermore, the extracellular binding of the JAM-1 mAb F11 to human platelet JAM-1 (F11R) has been shown to induce platelet activation and aggregation by cross-linking JAM-1 with FcγRII *in cis* (Kornecki *et al.*, 1990; Naik *et al.*, 1995; Sobocka *et al.*, 2000).

1.7.5. Intracellular interactions

The most striking element in the cytoplasmic domain of JAM-1 is its C-terminal PDZ domain-binding motif FLV. Nearly all intracellular proteins described so far that interact with JAM-1 contain PDZ domains, protein-binding domains of 80 – 90 aa in size recognized initially as sequence repeats in the mammalian postsynaptic density protein PSD-95, the *Drosophila* disc large tumor suppressor Dlg, and the mammalian tight junction protein ZO-1 (PDZ). PDZ proteins are predominantly localized at or involved in the formation of intercellular junctions, in particular of TJs, beneath the plasma membrane. They often express multiple copies of PDZ domains within their sequence, each of which can exert specificity to different PDZ-binding motif-containing interacting proteins. Thus they are able to function as scaffolding proteins at appropriate plasma membranes. Thereby they can form transmembrane-associated heterogeneous protein complexes with linkage to signal transduction pathways or to the actin cytoskeleton (Pawson *et al.*, 1997; Fanning *et al.*, 1999). Association of JAM-1 with these binding partners at junction compartments has been shown to generally depend on the C-terminal PDZ domain-binding motif of JAM-1. Whereas the extracellular JAM-1/JAM-1 interactions *in trans* appear to be sufficient to localize JAM-1 at the site of cell-cell boarders, intracellular JAM-1 interactions with PDZ domain-containing proteins might be necessary for the correct junctional localization and, in turn, enable JAM-1 to recruit and integrate such interacting partners into specific junctional structures.

The junctional *zonula occludens* protein (ZO)-1 binds directly JAM-1 with its PDZ domain(s) 2 and/or 3 and thus may link JAM-1 to PDZ domain 1-bound occludin and the actin filament system (Bazzoni *et al.*, 2000b; Ebnet *et al.*, 2000; Itoh *et al.*, 2001). The PDZ domain-mediated interaction of JAM-1 with AF-6 links JAM-1 to the cytoskeleton (Ebnet *et al.*, 2000), and may also mediate intracellular signaling since AF-6 can alternatively bind ZO-1 or the small GTPase Ras which has been reported to perturb cell-cell contacts and to decrease AF-6 and ZO-1 surface expression (Yamamoto *et al.*, 1997). AF-6 can recruit JAM-1 to TJs independent of its homophilic extracellular *trans*-interactions (Ebnet *et al.*, 2000). The AF-6/JAM-1 binding occurs only in recently confluent monolayers, suggesting a dynamic regulatory function of this interaction in the formation rather than in the maintenance of cell junctions. A third cytoskeleton linker may exist with the calmodulin-dependent serine protein kinase (CASK) that colocalizes in a PDZ domain-dependent manner with epithelial JAM-1 at both tight and basolateral junctions (Martínez-Estrada *et al.*, 2001). The multi-PDZ domain protein 1 (MUPP1) is localized at epithelial TJs and may act as multivalent scaffold protein organizing various proteins beneath the plasma membrane of TJs. It interacts with claudin by its PDZ domain 10 and with JAM-1 by its PDZ domain 9 (Hamazaki *et al.*, 2002). ASIP (atypical PKC isotype-specific interacting protein), the vertebrate homologue of the *Caenorhabditis elegans* polarity protein PAR-3, is also localized at epithelial TJs (Izumi *et al.*, 1998). ASIP forms a complex with the mammalian homologue of PAR-6, atypical PKC (aPKC) and the small GTPases Cdc42 and Rac-1. JAM-1 directly associates with the first PDZ domain of ASIP and might be able to recruit this signaling complex to TJs (Ebnet *et al.*, 2001; Itoh *et al.*, 2001). A cytoplasmic association of JAM-1 in a PDZ domain-independent manner has been demonstrated with the TJ protein cingulin (Bazzoni *et al.*, 2000b).

The exemplified large number of interactions with TJ proteins suggests an important role for JAM-1 in the organization of this intercellular contact structure. The dependence of JAM-1 on a single PDZ domain binding motif implicates a complex regulation of its interactions that may, among other factors, be dependent on the junctional maturation state (Martínez-Estrada *et al.*, 2001). The sequence and organization of TJ assembly and sealing, the functional role of the documented JAM-1–protein interactions and their influence and reliance on intracellular signaling, however, remains unclear.

With respect to intracellular signaling, JAM-1 has been reported to be phosphorylated by PKC upon platelet activation at Ser284 (Naik *et al.*, 1995; Ozaki *et al.*, 2000). Interestingly, the cytoplasmic tail of JAM-1 has sequence homology with that of occludin, suggesting a similar down-stream signaling pathway (Liu *et al.*, 2000b).

1.7.6. JAM-2 and JAM-3: co-founders of the JAM subfamily

During the last 2 years, the junctional adhesion molecule (F11R, JAM-1, antigen 106) emerged as prototype of a distinct JAM subfamily within the IgSF family. Additional members that have since been identified are human JAM-2 (Cunningham *et al.*, 2000) identical to human vascular endothelial junction-associated molecule (VE-JAM) (Palmeri *et al.*, 2000), murine JAM-2 (Aurrand-Lions *et al.*, 2000; Aurrand-Lions *et al.*, 2001a), human JAM-3 (Arrate *et al.*, 2001) and murine JAM-3 (Aurrand-Lions *et al.*, 2000) identical to murine VE-JAM (Palmeri *et al.*, 2000). Since human JAM-2 is homologous to murine JAM-3 but not to murine JAM-2, and since human JAM-3 is homologous to murine JAM-2 but not to murine JAM-3, this nomenclature requires some adjustment. To avoid ambiguity, hereinafter the JAM family member identified by Palmeri (designated human VE-JAM) and Cunningham and co-workers (Palmeri *et al.*, 2000; Cunningham *et al.*, 2000) is referred to as human JAM-2, and thus murine VE-JAM and the identical protein identified by Aurrand-Lions and co-workers (designated murine JAM-3) (Palmeri *et al.*, 2000; Aurrand-Lions *et al.*, 2000) is referred to as murine JAM-2. The designation of human JAM-3 by Arrate and co-workers (Arrate *et al.*, 2001) is retained and thus the murine homologue reported by Aurrand-Lions and co-workers (designated murine JAM-2) (Aurrand-Lions *et al.*, 2000; Aurrand-Lions *et al.*, 2001a) is referred to as murine JAM-3.

The close relationship between the three JAM family members JAM-1, -2, and -3 (with there human chromosomal localization 1q21.1-21.3 (Naik *et al.*, 2001), 21q21.2 (Palmeri *et al.*, 2000) and 11q25 (Arrate *et al.*, 2001), respectively), is revealed by the high degree of sequence identity amounting to 31-36 % and a similarity of approximately 50 % at the amino acid level. The two extracellular Ig-like domains of JAM-2 and JAM-3 exhibit a V-C2 structure, with an extra pair of cysteines in their membrane-proximal C2 loops not present in JAM-1. These structural properties are characteristic for the cortical thymocyte *Xenopus* (CTX) family (Chrétien *et al.*, 1998), thus the JAM members form a subgroup within the group of CTX family proteins (Aurrand-Lions *et al.*, 2001b). Different to JAM-1, the two *N*-glycosylation sites in JAM-2 and JAM-3 are distributed over both Ig-like loops in humans. The homology of the JAM family members concerns the overall sequence as well as the cytoplasmic tails. Here they exhibit two almost identical regions, A(Y/Q)(S/R)(R/K)GYF in the membrane-proximal part and C-terminally the PDZ-binding motif-containing sequence E(G/N)(D/E)F(K/R)(H/Q)(T/K)(S/K)-SF(L/V/I)(V/I). This suggests similar cytoplasmic functions and/or regulation of JAM-1, -2, and -3.

In contrast to JAM-1, the human JAM-2 and murine JAM-3 (not investigated so far for murine JAM-2 and human JAM-3) are restricted to endothelial expression and were not detected in epithelia. Interestingly, murine JAM proteins show heterogeneity in their subcellular localization at cell-cell contacts in transfected Madin-Darby canine kidney (MDCK) cells. JAM-3 is specifically expressed at the apical TJs, similar to JAM-1 that is however also localized at more

basolateral junctional areas in epithelial cells. On the contrary, JAM-2 is expressed only diffusely over the lateral site of intercellular junctions (Aurrand-Lions *et al.*, 2001b). Additional functional features of the JAM subfamily members are discussed elsewhere within this report.

2. Aim

In a search for specific interaction partners of the integrin α_L (CD11a) subunit using the yeast-two hybrid (YTH) system, a powerful genetic-based assay for the investigation of protein-protein interactions *in vivo,* the IgSF protein human JAM-1 was identified as a candidate binding partner of the β_2 integrin LFA-1 ($\alpha_L\beta_2$).

Subsequently, this protein-protein interaction and its specificity were to be verified in independent experiments and its functional implications at the molecular and cellular levels to be analyzed. Furthermore, the localization of the LFA-1–binding region within the JAM-1 sequence and redundancy with other β_2 integrin receptors was to be investigated. Establishment of a polyclonal antibody against human JAM-1 and a CHO cell line expressing heterotopic JAM-1 enabled the testing of the relevance of this novel interaction between these members of the integrin and JAM family in the cell-cell attachment of leukocytes. Cellular adhesion and transmigration assays performed both under static and laminar flow conditions using cells isolated from the human vasculature were employed to investigate the functional role of the LFA-1/JAM-1 interaction in the recruitment of leukocytes to sites of inflammation under more physiological conditions.

3. Materials and methods

Protocols were adapted from standard methods (Sambrook *et al.*, 1989; Ausubel *et al.*, 1995), unless referred to otherwise.

All solutions and media were prepared with ultra-pure water (Milli-Q Plus ultrapure purification pak, Milli-RO Plus purification pak; Millipore, Molsheim, France).

Reagents were from Sigma (St. Louis, MO) and Merck (Darmstadt, Germany), unless stated otherwise. Biochemicals, biomaterials, solutions, assays and small equipment for life science research were mainly from Amersham (Uppsala, Sweden), Bio-Rad (Hercules, CA), Boehringer Mannheim (Mannheim, Germany), Clontech (Palo Alto, CA), Difco Laboratories (Detroit, MI), GibcoBRL (Life Technologies; Paisley, Scotland), New England Biolabs (Frankfurt, Germany), Qiagen (Hilden, Germany), Roche Diagnostics (Mannheim, Germany), Santa Cruz Biotechnology (Santa Cruz, CA) and, if not stated otherwise, from Sigma.

3.1. General equipment

autoclave	autoclave type 23; MELAG Medizintechnik (Berlin, Germany)
centrifuges	Biofuge pico; Heraeus (Osterode, Germany) Omnifuge 2.OR; Heraeus (Osterode, Germany)
centrifuges, refrigerated	Biofuge pico; Heraeus (Osterode, Germany) Centrikon H-401, with rotors A8.24 and A6.9; Kontron-Hermle (Gosheim, Germany)
freezer, -70°C	ULT1706; Revco Scientific (Asheville, NC)
incubator	WTB binder (Tuttlingen, Germany)
liquid nitrogen tank	BT40; L'air liquide (Champigny, France)
magnetic stirrer	MR3001; Heidolph (Kelheim, Germany)
micor-pipettes	P20, P200, P1000; Gilson (Middleton, WI)
microscope	IX50; Olympus Optical GmbH (Hamburg, Germany)
pH meter	model 765 Calimatic; Knick (Berlin, Germany)
scales	model BP 2100S; Sartorius (Göttingen, Germany) model RI60P; Sartorius (Göttingen, Germany)
spectrophotometer	UVICON 930; Kontron instruments (Echingen, Germany)
thermomixer	Thermomixer compact; Eppendorf (Hamburg, Germany)
vortexer	REAX top; Heidolph (Kelheim, Germany)

3.2. General solutions

HBSS, 10x	Hanks' balanced salt solution	
HEPES	*N*-(2-hydroxyethyl)-piperazine-*N*′-(2-ethanesulfonic acid)	
HHMC	HBSS	1x
	HEPES	10 mM
	$MgCl_2$	1 mM
	$CaCl_2$	1 mM
	BSA	0.5% (w/v) (bovine serum albumin)
PBS	Dulbecco's phosphate buffered saline, w/o calium and magnesium; PAA Laboratories (Linz, Austria)	

3.3. Mammalian cell culture procedures

3.3.1. General

Cell culture work was performed under sterile conditions under a laminar flow hood using sterile disposable plastic ware.

3.3.2. Media and cell culture solutions

Media and cell culture solutions were from PAA (PAA Laboratories, Linz, Austria), GibcoBRL and, if not stated otherwise, from Sigma.

Unless purchased sterile, all media, solutions and supplements used in cell culture work were sterilized with a vacuum-driven 0.2-µm filter membrane filtration system or a 0.2-µm syringe filter. They were stored at 4°C and prewarmed to 37°C prior to use.

3.3.3. Culturing

Cell lines were placed in polystyrene culture flasks provided with 0.2-µm hydrophobic vent caps and maintained in a humidified 5 % CO_2 atmosphere in an incubator at 37°C. All culture media were supplemented to complete media with 10 % (v/v) fetal calf serum (FCS) and 50 mg/l of the antibiotic gentamicin to avoid bacterial contamination. Before use, FCS was treated for 30 min at 70°C to inactivate complement and stored at –20°C. Unless specified otherwise, cells were propagated in RPMI 1640 medium.

3.3.4. Cell harvest and subcultering

In general, adherent cells were grown to confluence and then detached by trypsinization (see below), whereas suspension cells were cultured to a density of approx. 10^6 cells/ml. They were harvested by centrifugation at 1,200 rpm for 5 min at room temperature. The supernatant was removed and cells were washed by resuspension in phosphate buffered saline (PBS) with subsequent recentrifugation. For subculturing, cells were resuspended in fresh medium and replaced in culture flasks at a density of approx. $2 \cdot 10^5$ cells/ml.

3.3.5. Trypsinization of adherent cell monolayers

Monolayers of adherent cell lines (CHO, HeLa, HUVEC) were dispersed by trypsin/EDTA-treatment (4 ml per 75-cm^2 culture flask) for 1-2 min. After incubation, the cell suspension was diluted with 1 volume of complete medium, washed, and then split (subcultivation ratio 1:6 - 1:10) or harvested by centrifugation.

3.3.6. Cell number determination

If cell density was to be determined, 50 µl of the cell suspension was mixed with 50 µl 0.4 % trypan blue solution to visualize non-viable cells. The cell numbers in four 0.1-mm^3 volumes were counted in a Neubauer hemacytometer under a binocular microscope and used to determine the mean cell density.

3.3.7. Freezing and thawing of mammalian cells

Cell lines were stored in 2-ml cryovials in a liquid nitrogen storage freezer. Cells were harvested at a concentration of 10^6 - 10^7 cells/ml, washed with PBS and resuspended in 2 ml freezing medium. The freezing medium consisted of complete culture medium supplemented to 10 % with the cryo-protective agent dimethylsulfoxide (DMSO). The cryovials were placed in a –70°C freezer O/N and transferred to liquid nitrogen for long-time storage.

Cryopreserved cells were thawed rapidly in a 37°C water bath, transferred in 5 volumes of prewarmed medium and centrifuged. The DMSO-containing supernatant was discarded and cells were seeded at high density in culture flasks.

3.3.8. Materials

cell culture incubator	Steri-Cult Incubator; Forma Scientific (Mariette; OH)
CO_2	carbon dioxide 3.0; Linde Gas (Höllriegelskreuth, Germany)
culture flask	Corning Inc. (Corning, NY)
filtration system, 0.2 µm	Stericup; Millipore (Bedford, MA)
gentamicin	GibcoBRL
laminar flow hood	BDK Luft- und Reinraumtechnik, Sonnenbühl-Genkingen, Germany)
RPMI 1640 medium	PAA
syring filter, 0.2 µm	Acrodisc; Pall (Ann Arbor, MI)
trypsin/EDTA solution (1x)	porcine trypsin (0.5 g/l) and EDTA·Na_4 (0.2 g/l) in HBSS

3.4. Immortalized cell lines

3.4.1. Chinese hamster ovary (CHO) cells

The epithelial CHO cell line (obtained from L.B. Klickstein, Harvard Medical School, Boston, MA) is derived from the ovary of a Chinese hamster (*Cricetulus griseus*). The adherent cells were cultured in DMEM/F12 medium.

3.4.2. HeLa cells

HeLa cells are adherent epithelial-like cells established from a patient with adenocarinoma and were obtained from ATCC (American Type Culture Collection, Manassas, VA). They were cultured in RPMI 1640 medium.

3.4.3. Jurkat T lymphocytes and related J-β_2.7, J-β_2.7/α_L and J-β_2.7/α_M cells

Jurkat cells are human T lymphocyte cells established from the peripheral blood of a patient with acute lymphoblastic leukemia. They were obtained from ATCC and cultured in RPMI 1640 medium.

J-β_2.7 cells are Jurkat cells that completely lack cell surface LFA-1 due to the lack of α_L expression effectuated by chemical mutagenesis (Weber *et al.*, 1997b). J-β_2.7 cell lines with

reconstituted LFA-1 surface expression (J-β_2.7/α_L) and heterotopic Mac-1 expression (J-β_2.7/α_M), respectively, were generated by transfection with α_L (CD11a) or α_M (CD11b) encoding cDNA (Weber *et al.*, 1997b; Weber *et al.*, 1999a). The Jurkat-related cell lines were provided by Dr. Kim Weber and maintained in normal RPMI 1640 culture medium with G418 supplementation (see 3.5.) in case of the transfectants J-β_2.7/α_L and J-β_2.7/α_M.

3.4.4. HL-60 cells

HL-60 is a promyelocytic cell line. These leukocytes were established from the peripheral blood of a patient with acute promyelocytic leukemia. They were obtained from ATCC and cultured in RPMI 1640 medium.

3.4.5. Mono Mac 6 cells

Mono Mac 6 is a monocytic cell line that was established from the peripheral blood of a patient with acute monocytic leukemia and was obtained from H.W. Ziegler-Heitbrock (Institut für Inhalationsbiologie, GSF, Gauting, Germany). The cells were maintained in 24-well plates with 2 ml MM6 medium per well. They were seeded at a density of $2 \cdot 10^5$ cells/ml and cultured 3-4 days before being subcultured or used in experiments. To subculture Mono Mac 6 cells they were pooled without discarding the medium and diluted to the initial concentration by adding fresh MM6 medium. For harvesting, cells were centrifuged at 800 rpm for 5 min at 25°C.

Materials

MM6 medium

RPMI 1640	1x
FCS (added after ultrafiltration; see below)	10 %
penicillin	0.1 U/l
streptomycin	100 µg/ml
MEM non-essential amino acid solution (100x)	1x
insulin, in phosphate-free buffer (0.9 mg/ml)	9 µg/ml
oxalacetat	1 mM
pyruvate	1 mM

The MM6 medium was ultrafiltered with a 20-kD cut off column (Ultrafilter U2000; Gambro Dialysatoren GmbH, Hechingen, Germany) to avoid LPS contamination which results in cell clumping, maturation and retarded growth. Subsequently the solution was supplemented with heat-inactivated FCS of low LPS content and sterilized by 0.2-µm filtration.

phosphate-free buffer

The phosphate-free buffer consisted of Puck's saline A solution (137 mM NaCl, 5.4 mM KCl, 4.2 mM $NaHCO_3$, 5.0 mM glucose, pH 6) and 7.5 % sodium bicarbonate solution at a ratio of 5:6.

3.4.6. THP-1 cells

THP-1 is a monocytic cell line established from the peripheral blood of a patient with acute monocytic leukemia. The cells were obtained from ATCC and maintained in RPMI 1640 medium.

3.5. Establishing of stable transfected CHO cell lines

CHO cell lines expressing recombinant proteins were generated by stable transfection of wild-type CHO cells (CHO-WT). Therefore the protein-encoding cDNA sequence was subcloned into the multiple cloning site (MCS) of the mammalian expression vector pcDNA3. CHO-WT cells were electroporated with the plasmid to express the recombinant protein under the control of the cytomegalovirus (CMV) promotor. Selection of successfully transfected cells was performed with the antibiotic G418 sulfate (geneticin) against which pcDNA3 provides resistance. To ensure homogeneity in the genetic subset, selected cells were singularized and screened for expression of the recombinant protein.

10^7 CHO-WT cells were resuspended in 1 ml ice-cold PBS, placed into an electroporation cuvette with a 0.4-cm electrode gap and mixed with 25-30 µg plasmid DNA. After 5 min of incubation on ice the cells were subjected to a high-voltage electric pulse of 270 V, 960 µF with a pulse control of 200 Ω. They were allowed to recover on ice for 5 min and then cultured for 2 days in non-selection medium. The medium was then replaced by selective medium containing 0.1 % (w/v) G418 sulfate. Non-transfected cells lost adhesive properties by death within 1-2 weeks and were removed by medium exchange. Outlived transfected cells were cultured to confluence under selection conditions.

After the selection phase cells were seeded into 96-well plates at a calculated density of 0.5 cell/well. Propagation of colonies derived from single cells was ensured for each well by microscopy. Upon reaching an appropriate cell density the clones were screened for recombinant protein expression by flow cytometry, western blotting and RT-PCR. A stable transfected cell

line was established by culturing of one of the generated clones showing the required expression profile.

Materials

electroporation cuvette	0.4 cm; Gene Pulser cuvette; Bio-Rad
electroporator	Gene Pulser II; Bio-Rad
G418 sulfate (geneticin)	Calbiochem (Schwalbach, Germany)
pcDNA3 vector	Invitrogen (Groningen, Netherlands)

3.6. Isolation of cells from the human vascular system

3.6.1. $CD4^+CD45RO^+$ T cell isolation

Peripheral blood mononuclear cells (PBMCs) were prepared by dextran-sedimentation and subsequent Ficoll-hypaque density gradient centrifugation from citrate anti-coagulated human blood. $CD4^+CD45RO^+$ memory T cells were isolated from the PBMC preparation by negative selection using magnetic cell separation.

A sample of 50 ml venous blood from a healthy volunteer was taken in a syringe filled with 6 ml 0.1 M sodium citrate and 5 ml 6 % (w/v) dextran in PBS. After 30-45 min of erythrocyte sedimentation the plasma supernatant was stratified over 12.5 ml Ficoll solution and centrifuged at 2,000 rpm for 20 min at 25°C (w/o brake). The pellet of granulocytes and residual erythrocytes was discarded (or subjected to neutrophil isolation; see below) and the supernatant was diluted 1:1 with RPMI 1640 medium/2 mM EDTA. Mononuclear cells were harvested as pellet from a second centrifugation at 1,000 rpm for 5 min at 25°C and resuspended in 50 ml buffer. Cells were washed by an additional resuspension-centrifugation step. Viability of the cells was determined by trypan blue exclusion.

For magnetic cell sorting, the freshly isolated PBMCs were resuspended in buffer (80 µl per 10^7 cells), mixed with a cocktail of hapten-conjugated antibodies[4] (20 µl per 10^7 cells) and incubated for 10 min at 8°C. The cells were washed with 10 ml buffer, centrifuged at 1,000 rpm for 5 min at 25°C and mixed with paramagnetic anti-hapten and anti-CD45RA microbeads (each 20 µl per 10^7 cells). Cells were incubated at 8°C for 15 min, washed, centrifuged, resuspended in buffer

[4] B cells, monocytes, NK cells, cytotoxic T cells, dendritic cells, early erythroid cells and platelets from PBMCs were labeled by a cocktail of hapten-conjugated CD8, CD11b, CD16, CD19, CD36 and CD56 antibodies for subsequent positive selection in a magnetic field.

(500 µl per 10^8 cells) and passed through an equilibrated separation column placed in a magnetic field. Magnetically labeled non-T helper cells and $CD4^+CD45RA^+$ cells were retard on the column, whereas non-labeled $CD4^+CD45RO^+$ T cells were recovered in the eluate for immediate experimental application.

Materials

antibodies, beads, columns	MACS $CD4^+$ T cell isolation kit, MACS CD45RA MicroBeads; Miltenyi Biotec (Bergisch Gladbach, Germany)
buffer	ice-cold PBS, 0.5 % (w/v) BSA, 2 mM EDTA
Ficoll solution	Biocoll Seperating Solution; Biochrom KG (Berlin, Germany)
sodium citrate, sterile	tri-sodium citrate dihydrate for erythrocyte sedimentation; Apotheke Klinikum Innenstadt (University Munich)

3.6.2. Isolation of polymorphonuclear neutrophils (PMNs)

Citrate anti-coagulated venous blood from a normal donor was subjected to erythrocyte sedimentation and subsequent plasma centrifugation over Ficoll-hypaque as described above. The pellet was resuspended in distilled water for hypotonic lysis of residual erythrocytes. After 30 s of incubation 0.1 volume 10x HHMC lacking calcium and magnesium were added and cells were centrifuged at 1,000 rpm for 5 min at 20°C. The neutrophil pellet was finally resuspended in 1x HHMC. Trypan blue exclusion showed greater then 95 % viability of the cells.

3.6.3. Human umbilical vein endothelial cells (HUVECs) – umbilical cord preparation

3.6.3.1. Isolation

Human ECs were isolated from the veins of umbilical cords according to Jaffe *et al.*, 1973. From each end of the freshly obtained umbilical cord 1 cm was cut off and the cord was hung up vertical. The upper end of the umbilical vein was cannulated and than sealed with artery clips. The vein was perfused with sterile PBS to wash out blood and sealed at the remaining end. Approx. 5 ml 0.1 % (w/v) α-chymotrypsin in PBS was infused to slight flatulence in order to detach the HUVECs from the interior vein wall. After 20 min of incubation at 37°C and a short cord massage the solution was flushed from the vein by perfusion with 10 ml PBS into 2 ml FCS that neutralizes α-chymotrypsin activity.

HUVECs were harvested by centrifugation at 800 rpm for 8 min at 25°C, resuspended in 24 ml EGM medium, divided into 2 collagen-coated 75-cm^2 flasks and cultured at 37°C as described

below. After 3 h the medium was renewed and blood residuents were removed from adherent cells by washing with PBS. The medium was changed after 24 h and cells were grown to confluence (passage 0) and then subcultured.

3.6.3.2. Culturing

HUVECs were cultured to confluence at 37°C under 5 % CO_2 in EGM medium with medium being changed twice a week. Adherent cells were detached by trypsinization. The cell suspension was diluted 1:2 with EGM medium, centrifuged with 800 rpm at 25°C for 8 min and reseeded at a concentration of approx. $5 \cdot 10^4$ cells/ml. HUVECs of passage 2-5 were used for experiments.

3.6.3.3. Collagenization

For adhesive growth, all cell culture flasks, petri dishes, 96-well plates and transwell-filter membranes subjected to HUVEC monolayer seeding were collagen-coated by incubation with a sterile collagen G solution of final 75 µg/ml in PBS for 15 min at room temperature.

3.6.3.4. Materials

collagen G solution	3 mg/ml collagen from calf skin in 12 mM HCl; Biochrom KG (Berlin, Germany)
EGM medium	Endothelial cell Growth Medium (low serum); PromoCell (Heidelberg, Germany)
umbilical cords	Frauenklinik vom Roten Kreuz (Munich)

3.7. Cell adhesion and transmigration applications

3.7.1. Static cell adhesion assay

Static adhesion assays for cells in suspension onto adherent cell monolayers or immobilized proteins as adhesion targets were carried out in 96-well plates. Cells in suspension were labeled with the fluorescent dye BCECF/AM and incubated with the respective adhesion target covering the base of the well. Cells lacking adhesive properties during the experimental procedure were removed by repeated steps of flick washes. Remaining cells with established adhesive cell interactions were evaluated by fluorescence spectrometry.

CHO cells or HUVECs were resuspended in complete culture medium, seeded into flat-bottom wells of 96-well tissue culture plates and cultured to confluence within 2-3 days. HUVEC monolayers were seeded in collagenized wells and stimulated with TNF-α (100 U/ml) plus IFN-γ (200 U/ml) O/N at 37°C where appropriate. Non-specific adhesion was blocked by incubation of the cell monolayers for 2 h at 37°C with 200 µl medium containing 0.5 % BSA. The monolayers were then preincubated for 30 min at room temperature with anti–JAM-1, ICAM-1 mAb or ICAM-1 Fab and, for control purpose, with preimmunization serum or IgG_1 isotype control, as indicated.

Cells in suspension tested for adhesion (*i.e.* Jurkat, J-β_2.7, J-β_2.7/α_L, J-β_2.7/α_M, HL-60, $CD4^+CD45RO^+$ and CHO cells) were fluorescence labeled by resuspension at a density of 10^6 cells/ml in HHMC that was supplemented with BCECF/AM at a final concentration of 1.6 µM. They were incubated for 30 min at 37°C, washed with PBS and resuspended in HHMC at a density of $2 \cdot 10^6$ cells/ml. Some cells were pretreated for 30 min at room temperature with TS1/22 mAb, TS1/18 mAb or IgG_1 isotype control, as indicated. $CD4^+CD45RO^+$ T cells subjected to cytokine-stimulated HUVEC monolayers were additionally preincubated with anti–VLA-4. The cell suspension was added at 10^5 cells/50 µl/well into the microtiter plate after supplementing with either PMA (100 ng/ml) or SDF-1α (1 µg/ml), as indicated. The cells were left to adhere to the confluent cell monolayers at 37°C during 30 min in the case of PMA stimulation or 5 min in the case of SDF-1α stimulation.

The fluorescence of the initial input cells was determined using a fluorescence plate reader with excitation and emission wavelengths of 485 nm and 535 nm, respectively. Non-adherent cells were then progressively removed by flick washes of the microtiter plate. The wells were replenished with 200 µl HHMC and the fluorescence of the remaining adherent cells was measured. The flick washes were continued until the fluorescence values attained approx. 10 % of the input value. All experiments were done in triplicate. Adhesion was expressed as the percentage of input cells. Where appropriate, background binding of unstimulated cells was subtracted from the overall adhesion values.

For static adhesion assays of CHO cell suspension cultures to LFA-1 as an adhesion target, the protein was immobilized in a flat-bottom 96-well microtiter plate at a concentration of 3 µg/ml in 10 mM Tris pH 9.0 using 40 µl/well O/N at 4°C. Likewise soluble ICAM-1–Fc was adsorbed at 10 µg/ml for adhesion assays with PMA-stimulated (100 ng/ml) J-β_2.7/α_M cells. The purified LFA-1 was derived from lysates of human tonsil and spleen and isolated by immunoaffinity chromatography (Klickstein *et al.*, 1996; Dustin *et al.*, 1989), soluble ICAM-1–Fc was purified from CHO Lec 3.2.8.1 cells (Weber *et al.*, 1999a). Non-specific adhesion was blocked for 2 h with 200 µl HHMC/0.5 % BSA. Where indicated, immobilized LFA-1 was preincubated with TS1/18 mAb or an IgG_1 isotype control. Cells in suspension were labeled with BCECF/AM.

CHO cells were pretreated with anti–JAM-1 or preimmunization serum, J-β_2.7/α_M cells with the α_L mAb TS1/22 or the α_M mAb CBRM1/29, as indicated. They were aliquoted into the microtiter plate with 10^5 cells/50 µl/well and left to adhere to immobilized LFA-1 respective ICAM-1 for 30 min at 37°C. The assay was continued as described above. All experiments were done in triplicate. Adhesion was expressed as the percentage of input cells.

3.7.2. Transmigration assay (chemotaxis)

In vitro transmigration under static conditions was investigated using transwell-filter inserts (**fig. 3**). Cells in suspension were allowed to transmigrate towards a chemokine gradient (chemotaxis) through HUVEC monolayers grown on the 5.0-µm filters.

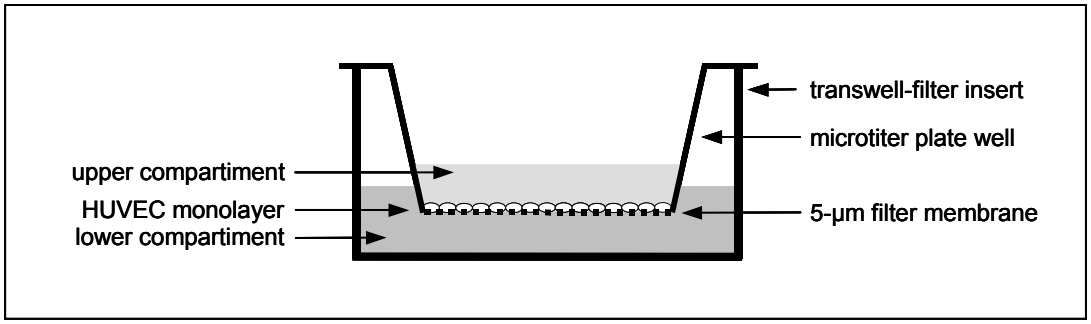

fig. 3: Schematic representation of a chemotactic transmigration assay with a transwell-filter insert (6.5 mm in diameter) placed in the slot of a 24-well microtiter plate. The polycarbonate membrane of the transwell-filter consists of pores with 5.0 µm in size. It provides a substrate for seeding HUVEC monolayers that in combination with the filter membrane divides the transwell assay into an upper compartment (filter insert) and a lower compartment (well). This allows chemotaxis of cells in suspension from the upper to the chemokine-containing lower compartment by their interaction with the confluent endothelial monolayer.

HUVECs were grown to confluence on the collagenized membrane of the transwell-filter insert within 1-2 days at 37°C. Some HUVEC monolayers were preincubated for 30 min with anti–JAM-1 or preimmunization serum, ICAM-1 mAb, ICAM-1 Fab or IgG_1 isotype control, as indicated. $CD4^+CD45RO^+$ T cells and neutrophils, respectively, were resuspended in RPMI 1640 medium supplemented with 0.5 % BSA and were incubated for 30 min with TS1/22 or IgG_1 isotype control as indicated. Neutrophils were additionally pretreated for 30 min with 5 % human serum to block Fc receptors. The chemokine gradient was established by filling the lower compartment with chemokine-supplemented RPMI 1640 medium. The HUVEC-coated transwell-filter insert was placed in the well and the cell suspension was added over the unstimulated endothelial monolayer. Cells were allowed to transmigrate at 37°C for 90 min towards a SDF-1α (1 µg/ml) gradient (for $CD4^+CD45RO^+$ T cells) or for 60 min towards an IL-8 (100 ng/ml) gradient (for neutrophils), respectively. Cell input and transmigrated cells were counted by flow cytometry.

3.7.3. Cell-cell interaction under conditions of laminar flow

A flow chamber with parallel plate geometry (**fig. 4**) was used to investigate cell-cell interactions (*i.e.* intercellular adhesion and cell spreading/transmigration) under laminar flow conditions (see **fig. 28**), simulating *in vitro* the physiological fluid shear stress present in the human microvasculature (Lawrence *et al.*, 1991).

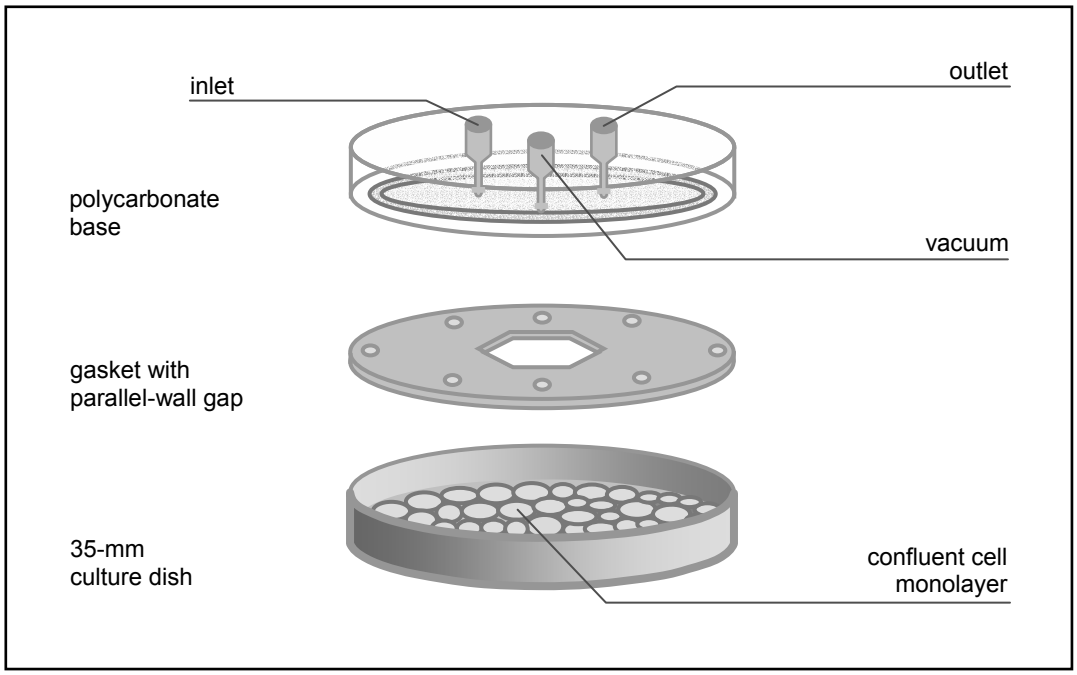

fig. 4: Parallel plate flow chamber with transparent polycarbonate base, rubber gasket and interchangeable 35-mm tissue culture dish. The chamber was mounted on the stage of a phase-contrast microscope equipped with a video camera system. Polycarbonate base and rubber gasket were held in place by vacuum application. The cell suspension was passed through the inlet manifold by an automatic syringe pump connected to the outlet manifold. The shear stresses acting at the chamber walls were regulated by the applied flow rate.

HUVECs were seeded on a 35-mm tissue culture dish and grown to confluence within 1-2 days. The monolayer was stimulated with TNF-α (100 U/ml) or costimulated with TNF-α (100 U/ml) + IFN-γ (200 U/ml) O/N at 37°C. SDF-1α was immobilized on the HUVECs at a concentration of 1 µg/ml 30 min prior to the flow experiment, except for assays with neutrophils. HUVECs were preincubated with anti–JAM-1 or preimmunization serum, ICAM-1 mAb, ICAM-1 Fab or IgG_1 isotype control, as indicated, for 30 min at 37°C. Subsequently the culture dish was inserted into the flow chamber.

Cells in suspension subjected to adhesion under flow conditions were preincubated with TS1/22, TS1/18 or IgG_1 isotype control, as indicated, for 30 min at 37°C. In the case of cytokine-stimulation of the HUVEC monolayer, T lymphocytes were likewise pretreated with VLA-4 mAb. Neutrophils were pretreated with 5 % human serum to block Fc receptors. The cell suspension was adjusted to $5 \cdot 10^5$ cells/ml in RPMI 1640 medium and tempered to 37°C.

The HUVEC monolayer and the polycarbonate base were assembled together with a rubber gasket that held their flat surfaces approx. 250 µm apart in the area of the gasket gap. Here, a well-defined laminar flow of suspension cells was induced over the cell monolayer, generated by an automatic syringe pump. The cells were perfused through the flow chamber at a controlled flow rate of 0.1 ml/s effecting a wall shear stress[5] of 1.5 dyn/cm^2. Cell-cell interactions were directly visualized and documented by video microscopy.

Experiments were video-analyzed by quantification of interaction events in between multiple 0.25-mm^2 fields of view, starting after a flow equilibration period of 5 min. Adhesion was defined as occurring when cells formed a firm contact with the HUVEC monolayer for at least 10 s under flow conditions. Transmigrating cells were defined as firmly adhesive cells that underwent shape change indicative of spreading and migration beneath the cells of the endothelial monolayer. Results were expressed as cells/mm^2.

3.7.4. Materials

Biomaterials

ICAM-1, soluble	ICAM-1–Fc purified from CHO Lec 3.2.8.1 cells from L.B. Klickstein, Harvard Medical School, Boston, MA
IFN-γ	human recombinant; PeproTech (Rocky Hill, NJ)
IL-8	human recombinant; PeproTech (Rocky Hill, NJ)
LFA-1, purified	from L.B. Klickstein, Harvard Medical School, Boston, MA
SDF-1α	human recombinant; PeproTech (Rocky Hill, NJ)
TNF-α	human recombinant; PeproTech (Rocky Hill, NJ)

Reagents

BCECF/AM	2',7'-bis-(2-carboxyethyl)-5-(and-6)-carboxy-fluorescein/ acetoxymethylester; Molecular Probes (Leiden, Netherlands) stock: 1 µg/µl (~1.6 mM) in dry DMSO (Merk) at –20°C
PMA	Promega (Mannheim, Germany)

[5] The existing wall shear stresses were calculated from the chamber geometry and the volumetric flow rate as described (Lawrence *et al.*, 1987).

Equipment and materials

96-well tissue culture plates	ICN (Costa Mesa, CA)
flow chamber polycarbonate base	from L.V. McIntire (Rice University, Houston, TX)
flow chamber rubber gasket	PharmElast SF1332; SF Medical Ltd. (Watford, UK)
fluorescence plate reader	SpectraFluor Plus; software: easyWin fitting; TECAN (Crailsheim, Germany)
syringe pump	model 210; Fabrique Auxetatis-Unis (USA)
transwell-filter inserts	Costar, Corning Inc. (Acton, MA)
video system	videotimer VTG-10; FoR.A time-lapse videocasette recorder SR-L900E; JVC (Japan) Trinitron color video monitor SSM-1; Sony (Park Ridge, NJ) video camera 3-CCD; JVC (Japan)

3.7.5. Statistical analysis

Statistical analysis was performed with InStat software (GraphPad Software, San Diego, CA), using analysis of variance (ANOVA) and signed-rank tests according to Kruskal-Wallis as multiple comparison procedures, and Tukey tests, Student's t-tests and Bonferroni tests to determine the statistical significance between two interventions, where appropriate. A statistically significant difference for a particular comparison was only claimed when the criterion $P < 0.05$ or better was fulfilled. Similarly, the effect of a JAM-1 and ICAM-1 antibody combination was only considered as additive when the level of significance, as indicate by the P-value, was lower for the combination than for either antibody alone, and the combination was statistically different with $P < 0.05$, as compared to either intervention alone.

3.8. Yeast two-hybrid system screening procedures

3.8.1. Introduction: the yeast two-hybrid system

The yeast two-hybrid (YTH) system, initially developed by Fields *et al.*, 1989, is a yeast-based genetic assay to detect protein-protein interactions *in vivo*. The consequent transcriptional induction of one or more reporter genes is used to detect such positive interactions (Fields *et al.*, 1994).

3.8.1.1. Modular nature of transcriptional activators: DNA-binding and activation domains

Detection of protein-protein interactions using the YTH system relies on the modular nature of many site-specific eukaryotic transcriptional activators. These factors include a DNA-binding domain (DBD) and a transcriptional activation domain (AD). The DBD mediates binding of the transcriptional activator to a specific DNA sequence located upstream of a reporter gene. The AD of the transcription factor interacts with proteins of the basal transcriptional machinery, recruiting them to the promoter and thus inducing transcription initiation. The DBD and AD do not necessarily need to be covalently linked to mediate transcriptional activation (Brent *et al.*, 1985; Keegan *et al.*, 1986). Hence, if these domains are fused separately to any two interacting proteins X and Y, the principle of the YTH system, they can subsequently be brought into proximity as a result of this protein-protein interaction, and thereby reconstitute a functional transcription factor. In this way, the interaction between two such hybrid proteins (*i.e.* DBD-X and AD-Y), directed to the yeast nucleus, enables transcription activation of the appropriate reporter gene, and thus constitutes a positive signal in the YTH assay.

3.8.1.2. Bait and prey: the library screening application of the YTH system

A protein of interest fused to a DBD can be used as a so-called ”bait” to screen a library for a unknown interacting protein partner, termed ”prey”. The cDNA library consists of a collection of plasmids that encode AD-fusion proteins. The generation of the two protein hybrids, bait and prey, is performed at the DNA level by subcloning the appropriate coding sequences into YTH vectors, *i.e.* the DBD-fusion vector pAS2-1 for the bait and the AD-fusion vector pGAD10 for library cDNAs. Both plasmids are sequentially transformed into the host strain *S. cerevisiae* CG-1945, yielding a yeast population where the cDNA library is expressed at the protein level. Consequently, each yeast cell expresses both the bait and one library protein, ensured by nutritional selection for co-transformed cells. The yeast strain phenotype maintains auxotrophy for these nutritional markers (*i.e.* tryptophan and leucine). In addition, CG-1945 contains two chromosomally integrated reporter gene constructs, the yeast *HIS3* gene and the bacterial *lacZ* gene, upstream of which are positioned binding sites for the transcriptional DBD. A positive bait-prey interaction causes the physical reconstitution of a functional DBD-AD transcription factor due to steric proximity of these domains on the coat-tails of the bait and prey hybrids and leads to activation of the reporter genes. Transcriptional activation of *HIS3* confers histidine prototrophy and allows in a first screening step the nutritional selection for yeast cells bearing an interacting hybrid pair. These pre-selected cells are additionally tested by an enzymatic colour assay for the action of *lacZ*-encoded β-galactosidase. From a candidate yeast colony positive for expression of both reporter genes, the unique bait-encoding plasmid is segregated. The prey

plasmid encoding the potential interaction partner of the bait is isolated, amplified and subsequently characterized by sequencing its library cDNA insert.

3.8.2. Yeast strain *S. cerevisiae* CG-1945

genotype:	*MATa, ura3-52, his3-200, ade2-101, lys2-801, trp1-901, leu2-3, 112, gal4-542, gal80-538, cyh^{r}2, LYS2::GAL1$_{UAS}$-GAL1$_{TATA}$-HIS3, URA3::GAL4$_{17\text{-mers(x3)}}$-CyC1$_{TATA}$-lacZ*
transformation markers:	*trp1, leu2, cyh^{r}2*
reporter genes:	*HIS3, lacZ*

3.8.3. Culturing *S. cerevisiae*

Yeast strains were grown by shaking at 30°C in liquid culture medium or were spread on dry agar plates as described for bacteria and grown for 2-3 days at 30°C in the inverted position. Liquid cultures were obtained by inoculation with a single yeast colony picked from an agar plate. The growth phase was determined by measurement of the optical density (OD_{600}) as described for bacteria. Transformed cells were selectively grown on synthetic dropout (SD) medium depleted from the corresponding nutritional marker(s) in turn provided by the transformed plasmid(s) (see below). For long-term storage of yeast strains, single colonies were resuspended in 1 ml of the appropriate medium supplemented with sterile glycerol to a final concentration of 25 % and frozen at –70°C.

3.8.4. Media for culturing *S. cerevisiae*

Media were autoclaved for 20 min at 121°C and cooled to approximately 55°C before adding glucose or dropout solutions. Glucose stock solutions were autoclaved separately and dropout solutions were filter-sterilized.

YPD: (yeast extract/peptone/dextrose)

complete medium for non-selective routine growth of yeast

yeast extract	10 g/l
peptone	20 g/l
glucose, 40% (w/v)	50 ml/l (= 20 g/l)
agar	20 g/l (where appropriate)

SD medium: (synthetic dropout medium; ”THLA medium”)

SD is a synthetic minimal medium used in yeast transformations to select for specific phenotypes. It consists of yeast nitrogen base (YNB) without amino acids and glucose as carbon sources. The medium is supplemented with various dropout solutions that contains essential amino acids or nucleotides for which the strain to be selected is auxotrophic.

YNB without amino acids	6.7 g/l
-Leu/-Trp/-His DO supplement	0.6 g/l
dropout solutions T, H, L, A	added as appropriate, concentrations see below
glucose, 40% (w/v)	50 ml/l (= 20 g/l)
agar	20 g/l (where appropriate)

SD/Trp$^-$ (HLA) medium:

selecting for strains containing pAS2-1(*TRP1*)

SD/Trp$^-$/Leu$^-$ (HA) medium:

selecting for strains containing pAS2-1(*TRP1*) and pGAD10(*LEU2*)

SD/Trp$^-$/Leu$^-$/His$^-$ (A) medium:

selecting for yeast colonies bearing a positive YTH protein-protein interaction (*HIS3* expression) under continuous selection for the bait expression vector pAS2-1(*TRP1*) and the library protein expression vector pGAD10(*LEU2*)

SD/Trp$^-$/His$^-$ (LA) medium:

medium to test for bait-mediated non-specific self-activation of the *HIS3* reporter gene in yeast strains transformed with the bait-encoding expression vector pAS2-1(*TRP1*)

SD/Leu$^-$ (THA) medium:

selecting for yeast strains containing the library vector pGAD10 (*LEU2*);
supplemented with 1 µg/ml cycloheximide where appropriate; THA/cycloheximide medium selects for the segregation of bait-expressing pAS2-1(*TRP1*) vectors in co-transformed yeast cells (see 3.8.9.)

Dropout solutions for SD media:

abbr.	*dropout sol.*	*final conc.*	*stock sol.*
T	L-tryptophan	20 µg/ml	500x
H	L-histidine·HCl·H_2O	20 µg/ml	500x
L	L-leucine	100 µg/ml	100x
A	adenine hemisulfate	20 µg/ml	100x

3.8.5. YTH cloning and control vectors

3.8.5.1. Bait-fusion vector pAS2-1

pAS2-1 enables the fusion of a bait-encoding cDNA to the Gal4 DBD-encoding sequence by subcloning into the MCS. The bait hybrid is expressed under the control of the *S. cerevisiae alcohol dehydrogenase 1* (*ADH1*) promoter and targeted to the yeast nucleus by a nuclear localization signal in the N-terminus of Gal4. pAS2-1(*TRP1*) contains the *TRP1* nutritional gene that allows yeast auxotrophs to grow on tryptophan-deficient synthetic medium (SD/Trp^-) and confers cycloheximide sensitivity to CG-1945 by encoding the CYH2 protein (see 3.8.9.).

cDNA encoding the cytoplasmic domain of CD11a was subcloned into the DBD-fusion vector pAS2-1 as described (see 3.11.2.). The subsequently transformed yeast strain CG-1945 expressing the bait hybrid failed to grow on selective histidine-depleted LA medium, indicating that the DBD-fused bait itself did not activate the reporter gene *HIS3* in a non-specific way[6].

3.8.5.2. Prey-fusion library vector pGAD10

The cDNA library screened against the bait hybrid consisted of prey-encoding cDNAs subcloned into the *Eco*RI site of pGAD10(*LEU2*), a Gal4 AD-fusion vector. The prey hybrids are expressed under the control of the *ADH1* promotor and targeted to the yeast nucleus by a heterologous nuclear localization signal included in the AD. The nutritional gene *LEU2* allows yeast auxotrophs to grow on leucine-deficient synthetic medium (SD/Leu^-).

[6] In the case of non-specific activation, the false-positive background can be suppressed to a level that is only overcome by a specific *HIS3* activation when using medium supplemented with 3-amino-1,2,3-triazole (3-AT), a competitive inhibitor of the *HIS3* gene product (Kishore *et al.*, 1988).

3.8.5.3. Control vectors

The control plasmids pVA3-1(*TRP1*) and pTD1-1(*LEU2*) were sequentially introduced into wild-type CG-1945 strain by small-scale transformations. This co-transformed yeast strain provides a positive control for the YTH assay as it expresses two interacting hybrids, the murine p53 fused to a DBD (encoded by pVA3-1) and the Simian virus 40 (SV40) large T-antigen fused to an AD (encoded by pTD1-1), thereby leading to histidine prototrophy and a positive signal in the β-Gal assay (Bartel *et al.*, 1993).

3.8.6. Amplification of the human leukocyte cDNA library

The AD-fused cDNA library was prepared from a commercially purchased library culture of *E. coli* DH5α. The library based on mRNA of peripheral blood leukocytes pooled from 350 humans 18-40 in age. cDNA inserts (0.8-5.0 kb, 1.7 kb in average) were generated by oligo(dT) and random priming and subcloned into the *Eco*RI site of the YTH library vector pGAD10 (Clontech). The number of independent clones was $1.6 \cdot 10^6$. The library had to be amplified to yield enough plasmid DNA for a representative screening and for long-term storage.

The *E. coli* library culture was spread on large LB/amp agar plates with a number of colony forming units (cfu) that was six times the number of independent clones (40,000 cfu/plate) and incubated overnight at 37°C. The colonies were scraped off the agar using 5-8 ml LB/amp medium per plate, pooled on ice and cultured for 4 h at 37°C. The plasmids were isolated in large-scale plasmid preparations (gigapreps; see 3.10.7.) and the obtained plasmid cDNA library was aliquoted at a concentration of 1 µg/µl. The titre was determined to be $5.8 \cdot 10^9$ cfu/ml of library suspension, ensuring that the amplified plasmid cDNA library was representative.

3.8.7. Lithium acetate-mediated yeast transformation

For both small-scale and large-scale transformations of yeast with plasmid cDNA the lithium acetate (LiOAc) method (Ito *et al.*, 1983; Schiestl *et al.*, 1989) was used in a modified protocol. Competence in yeast cells is induced by the monovalent alkali cation Li^+ in combination with polyethylene glycol (PEG), and DMSO-enhanced DNA-uptake is effected by a heat pulse.

3.8.7.1. Simple plasmid transformation – small-scale

The small-scale preparation produces 2 ml of competent cells sufficient for 20 simple plasmid transformations. After transformation the yeast cells were grown under nutritional selection for

the corresponding plasmid. For YTH screening, the small-scale transformation is the first of two sequential transformations, shuttling the bait plasmid into wild-type CG-1945 cells. The resulting bait-expressing strain is tryptophan prototrophic and can be selectively grown on SD/Trp$^-$ (HLA) medium.

A stationary phase culture of wild-type CG-1945[7], grown overnight in 10 ml YPD at 30°C, was used to inoculate 50 ml of fresh medium to an OD_{600} of 0.5. The culture was shaken for 3 h at 30°C to mid-log phase and centrifuged at 2,500 rpm for 5 min. The pellet was resuspended in 40 ml TE, centrifuged, resuspended in 2 ml of LiOAc/TE and left at room temperature for 10 min. 100 µl of these competent yeast cells (sufficient for a single transformation) were transferred to a DNA mix composed of 100 µg denatured carrier DNA and 1-2 µg (1 µg/µl) of the bait-encoding fusion vector pAS2-1(*TRP1*). After addition of 700 µl LiOAc/PEG/TE the transformation mix was vortexed vigorously and incubated for 30 min at 30°C. 88 µl DMSO was added and the suspension was mixed by pipetting. The cells were then treated for 7 min with a heat shock of 42°C and centrifuged twice at 10,000 rpm for 10 s with subsequent resuspension in 1 ml TE. The transformed cells were spread on SD/Trp$^-$ plates (100 µl of non-diluted, 1:10 or 1:50 diluted cell suspension to ensure growth of well-separated single colonies) and incubated for approx. 3 days at 30°C.

3.8.7.2. cDNA library transformation – large-scale

A large-scale protocol was used to transform in a second step the pGAD10(*LEU2*) cDNA library plasmids into the bait-transformed yeast strain. This procedure yields 1 ml of competent cells sufficient for a single library transformation. The resulting yeast population expressing bait and individual prey hybrids is tryptophan and leucine prototrophic and can be selectively grown on SD/Trp$^-$/Leu$^-$ (HA) medium.

Five, 4-ml aliquots of SD/Trp$^-$ (HLA) medium were inoculated with the bait-expressing yeast strain and incubated for 20 h at 30°C. The cultures were transferred into 100 ml YPD medium to a final OD_{600} of 0.3. The cells were shaken for 3-4 h at 30°C to reach mid-log phase (OD_{600} of 0.6-0.8) and centrifuged at 2,500 rpm for 5 min. The pellet was resuspended in 50 ml TE, recentrifuged, resuspended in 2 ml of LiOAc/TE and left at room temperature for 10 min. A DNA mix composed of 2 mg denatured carrier DNA and 200 µg of cDNA library plasmids was then added. After addition of 14 ml LiOAc/PEG/TE, the transformation mix was vortexed vigorously and incubated for 30 min at 30°C. 1.8 ml DMSO was added and the suspension was

[7] Note: The yeast strain and culture media described here correspond to a bait transformation of wild-type cells within a YTH screening procedure. For transformation of an ulterior plasmid type, the SD medium after transformation has to be adapted to the nutritional marker of this plasmid. In the case of shuttling a plasmid into a pretransformed yeast strain, these cells have to be

mixed by pipetting. The yeast cells were treated for 7 min by a heat shock of 42°C with occasional swirling and cooled down to room temperature in a water bath. They were centrifuged, washed with 50 ml TE, recentrifuged and resuspended in 100 ml YPD. The culture was shaken for 1 h at 30°C and then centrifuged twice. The pellet was resuspended first in 50 ml TE and then in 100 ml selective SD/Trp^-/Leu^- (HA) medium. In between, in order to measure the efficiency of the library transformation, a 10-µl and 100-µl aliquot of the HA culture was spread on small HA agar plates and incubated for 2-3 days at 30°C. The library transformation efficiency was then determined as the number of transformants/µg plasmid DNA grown on these agar plates. The 100-ml HA culture itself was further grown for 16 h at 30°C. The suspension was centrifuged three times and the pellet resuspended twice in 50 ml TE and once in 6 ml TE. Subsequently the cells were subjected to nutritional selection for *HIS3* reporter gene activation without delay.

3.8.8. Detection of reporter gene activation

3.8.8.1. Nutritional selection for *HIS3* reporter gene-activated yeast cells

Histidine prototrophy is the first selectable marker for a bait-prey protein interaction in the YTH system. Hence, in a first step, yeast cells were screened by nutritional selection on histidine-depleted SD/Trp^-/Leu^-/His^- (A) medium.

The complete culture of previously library-transformed yeast cells (see 3.8.7.2.) was directly spread on large selective A agar plates using 100 µl cell suspension/plate to allow growth of isolated cell colonies. The plates were incubated for several days at 30°C. Candidate clones that have grown by day 8 were transferred to and collected on fresh A agar plates (master plates) and subsequently subjected to a β-Gal filter assay.

3.8.8.2. β-Gal filter assay

Activation of the *lacZ* reporter gene and subsequent expression of β-galactosidase (β-Gal) is the second marker in the YTH system and provides a screenable color phenotype for yeast cells that contain an interaction between the bait and prey hybrid proteins.

Candidate His^+ yeast colonies from master plates and a positive control yeast strain (pVA3-1/pTD1-1–transformed) were spread on a selective A plate and grown for 3 days at 30°C. An aluminium boat with a flat bottom was constructed and floated on liquid nitrogen. A

---

grown in SD medium lacking the nutritional marker of the pretransformed plasmid and afterwards in SD medium additionally depleted for the nutritional marker of the second plasmid.

Whatman filter paper of appropriate size was laid over the yeast colonies on the A plate and both filter paper and agar medium were marked with asymmetric stitches. The filter paper was removed and placed colony-side-up on the pre-cooled aluminium boat. After 30 s, boat and filter paper were immersed in the liquid nitrogen for 5 s. The filter paper was removed and placed colony-side-up in a petri dish until thawed. 3.2 ml of Z buffer and 63 µl of 2 % X-Gal were placed in the lid of a petri dish (volumes calculated for small petri dishes, 90 mm diameter). A fresh piece of Whatman filter paper and then the yeast-bearing filter paper (colony-side-up) were placed in the liquid. The dish was covered with its bottom, sealed with parafilm and incubated at 37°C in the darkness. The colour of the yeast colonies was checked from time to time. Development of the blue color took from 30 min to 1 h.

3.8.9. Cycloheximide counterselection of yeast segregants

Further analysis of a $His^+/\beta\text{-}Gal^+$ candidate yeast strain found positive in a YTH screen requires the generation of a segregant strain that has lost the known bait-expressing vector pAS2-1(*TRP1*) and retains only the library vector pGAD10(*LEU2*) encoding the as yet unknown bait-interacting prey protein. Candidate clones are grown on SD/Trp^+/Leu^- (THA) medium supplemented with cycloheximide (naramycin A). The THA medium allows spontaneous segregation of pAS2-1(*TRP1*) while maintaining the selective pressure for pGAD10(*LEU2*). Only yeast cells that undergo this spontaneous pAS2-1–segregation can survive on THA/cycloheximide medium due to cycloheximide sensitivity conferred by the pAS2-1 plasmid[8].

A single colony of a candidate $His3^+/lacZ^+$-clone was resuspended in 100 µl TE and spread on a THA/cycloheximide agar plate. The plate was incubated for 3-5 days at 30°C until cycloheximide-resistant colonies appeared. Individual colonies were checked for the loss of pAS2-1(*TRP1*) by negative selection on tryptophan-depleted HA medium. A verified colony, bearing only the library plasmid, was subjected to a yeast miniprep to isolate this vector for further analysis of the candidate prey cDNA.

3.8.10. Yeast miniprep and isolation of the prey-encoding library vector

The prey-encoding library vector is isolated from the candidate colony by a yeast miniprep and used to transform *E. coli* DH5α for further amplification and purification purposes. Vector

[8] pAS2-1 confers cycloheximide sensitivity by the *CYH2* gene. Cycloheximide acts on the CYH2 protein and thereby inhibits protein translation in yeast. The strain CG-1945 is normally cycloheximide resistant due to its *cyh2* mutant allele that encodes a mutated CYH2 protein and is so not affected by this drug. Nevertheless pAS2-1–transformed CG-1945 fails to grow on cycloheximide since the wild-type *CYH2* gene of the vector is dominant to the *cyh2* mutant allele in the strain genome (Guthrie *et al.*, 1991).

shuttling form yeast to bacteria is necessary due to genomic DNA contamination in yeast plasmid preparations.

5 ml of THA medium were inoculated with a bait-plasmid–segregated candidate yeast colony. The culture was incubated for 1-2 days at 30°C until saturation and centrifuged at 2,500 rpm for 5 min. The pellet was resuspended in 300 µl yeast cell breaking buffer and transfered to an Eppendorf tube filled to a volume of 150 µl with acid-washed glass beads that were used as a physical agent for yeast cell wall disruption. 400 µl phenol/chloroform/isoamyl alcohol was added. The tube was vortexed vigorously for 2 min and centrifuged at 14,000 rpm for 5 min. The aqueous phase was extracted with chloroform and centrifuged at 14,000 rpm for 1 min. The yeast plasmid DNA was ethanol precipitated, resuspended in 25 µl TE and used for *E. coli* transformation by electroporation. The prey-encoding library vector was subsequently amplified in DH5α, isolated in a plasmid maxiprep and identified by sequence analysis.

3.8.11. Materials, solutions and reagents

Biomaterials and materials

carrier DNA	sheared, denatured Herring testis DNA, 10 µg/µl in TE; Clontech (Palo Alto, CA); denatured at 95°C for 20 min and cooled immediately on ice just prior to use
cDNA library	human leukocyte cDNA MATCHMAKER library, subcloned into pGAD10 (GenBank accession number U13188), provided in *E. coli* DH5α; Clontech
glass beads	acid-washed glass-beads, 0.4-0.6 mm; Sigma
parafilm	American National Can (Menasha, WI)
pAS2-1	YTH cloning vector, GenBank accession number U30497; Clontech
pTD1-1	YTH control vector; Clontech
pVA3-1	YTH control vector; Clontech
S. cerevisiae CG-1945	Clontech
Whatman filter paper	Qualitative #1; Whatman (Maidstone, UK)

Solutions and buffers

LiOAc/PEG/TE	100 mM LiOAc/40 % (w/v) PEG-4000/1x TE, prepared immediately prior to use from sterile stock solutions, *i.e.* 1 M LiOAc, 10x TE and 50 % (w/v) PEG-4000
LiOAc/TE	100 mM LiOAc/0.5x TE, prepared immediately prior to use from sterile stock solutions, *i.e.* 1 M LiOAc and 1x TE

PEG-4000	polyethylene glycol, 4000 g/mol average molecular weight, prepared as 50 % (w/v) stock solution and autoclaved	
TE (10x)	Tris-base	200 mM
	EDTA	10 mM
X-Gal, 2 %	5-bromo-4-chloro-3-indolyl-β-D-galactopyranoside, 20 mg/ml in *N,N*-dimethylformamide (DMF), stored at –20°C	
yeast cell breaking buffer	LiCl	2.5 mM
	Tris, pH	850 mM
	Triton X-100	4 %
	EDTA	62.5 mM
Z buffer	Na_2HPO_4	60 mM
	NaH_2PO_4	40 mM
	KCl	10 mM
	$MgSO_4$	1 mM
	pH 7	

Reagents

Reagents used in the YTH assay were mainly from Difco Laboratories (Detroit, MI) and are listed if not from Sigma (St. Louis, MO) or mentioned elsewhere.

agar (Bacto-agar)	Difco Laboratories
chloroform	Merck (Darmstadt, Germany)
D-(+)-glucose (dextrose)	Fluka (Buchs, Switzerland)
-Leu/-Trp/-His DO supplement	Clontech
PEG-4000	Fluka (Buchs, Switzerland)
peptone (Bacto-peptone)	Difco Laboratories
phenol/chloroform/isoamyl alcohol	25:24:1; Roth (Karlsruhe, Germany)
X-Gal	Amersham
yeast extract (Bacto-Yeast extract)	Difco Laboratories
yeast nitrogen base (YNB)	(without amino acids); Difco Laboratories

3.9. Work with *E. coli*

3.9.1. General

E. coli were cultured at 37°C with LB medium autoclaved for 20 min at 121°C. Bacteria transformed with an ampicillin resistance-conferring plasmid were selectively propagated by supplementing the LB medium with 100 µg/ml ampicillin (LB/amp medium). All solutions and

supplements used for work with *E. coli* were autoclaved or filter-sterilized. Bacterial strains were long-term stored at –70°C in LB medium supplemented with glycerol to a final concentration of 15 %.

3.9.2. Culturing bacteria

3.9.2.1. Growth on solid media

Dry LB agar plates were inoculated with a single bacterial colony or with a bacterial suspension by spreading with a sterile inoculation loop or a glass spreader, respectively, to achieve single colony growth. The plates were incubated inverted overnight at 37°C.

3.9.2.2. Growth of liquid cultures

For small liquid cultures 5-10 ml LB or LB/amp medium were inoculated with a single bacterial colony and incubated overnight. Bacteria were harvested by centrifugation. Starter cultures were incubated for 8 h and used to inoculate fresh liquid medium.

For large liquid cultures 100-250 ml LB or LB/amp medium were inoculated with a starter culture to a dilution of 1:500 - 1:1000 and incubated overnight at 37°C with shaking. Bacteria were harvested by centrifugation.

3.9.3. Optical density of bacterial cultures

The optical density of liquid bacterial cultures at a wavelength of 600 nm (OD_{600}) was measured in plastic cuvettes against pure medium as a blank in a spectrophotometer. Each 0.1 OD_{600} unit corresponds to approx. 10^8 cells/ml (~$3 \cdot 10^6$ cells/ml in the case of yeast cells) for $OD_{600} < 1$.

3.9.4. Transformation of *E. coli* with plasmids

3.9.4.1. Preparation of competent cells by $CaCl_2$ treatment

100 ml LB medium were inoculated with an overnight culture of *E. coli* DH5α and grown at 37°C with shaking to an OD_{600} of 0.4. The culture was centrifuged at 4,000 rpm for 15 min at 4°C. The pellet was resuspended in 50 ml ice-cold 100 mM $MgCl_2$, incubated for 30 min on ice, centrifuged at 4°C and resuspended in 50 ml ice-cold 100 mM $CaCl_2$. The suspension was

incubated for 30 min on ice and centrifuged at 4°C. The cells were resuspended in 2 ml ice-cold 100 mM $CaCl_2$, incubated for 24 h at 4°C, supplemented with ice-cold 0.5 ml glycerin and 2.5 ml 100 mM $CaCl_2$ and stored in 100-µl aliquots at –70°C.

3.9.4.2. Heat-shock transformation of *E. coli*

Treatment of competent bacteria with a brief heat shock enables transformation by DNA. Plasmid DNA or a plasmid ligation reaction, were mixed at an appropriate concentration with 50 µl thawed competent bacteria and incubated for 30 min on ice. The bacteria were treated for 90 s by a heat shock of 42°C, placed on ice, diluted with 300 µl LB medium and incubated for 1 h at 37°C with shaking. An aliquot of 50-200 µl was spread on a LB/amp agar plate and incubated overnight at 37°C to select for transformed bacteria.

3.9.4.3. Preparation of electrocompetent cells

100 ml of LB medium were inoculated with an overnight culture of *E. coli* DH5α. Cells were grown at 37°C with shaking to an OD_{600} of 0.4, chilled for 20 min on ice and centrifuged at 4,000 rpm for 20 min at 4°C. The pellet was resuspended in 100 ml ice-cold water. Bacteria were then successively recentrifuged and resuspended in each of the following ice-cold solutions: 100 ml water, 16 ml 10 % glycerol and finally 2 ml 10 % glycerol. The cells were then aliquoted and stored at –70°C.

3.9.4.4. Electroporation of *E. coli*

Electroporation with high voltage is the most efficient method for transforming *E. coli*. An efficiency of about 10^9 transformants/µg input plasmid DNA can be achieved. This method was used to transform yeast plasmid DNA into *E. coli* DH5α.

50 µl of thawed electrocompetent cells were mixed with up to 1 µg yeast plasmid DNA and transferred into an ice-cold electroporation cuvette with a 0.2 cm electrode gap. The cuvette was placed into an electroporator and pulsed with 2.5 kV, 25 µF and a pulse control of 200 Ω. Immediately 1 ml LB medium was added and the culture was grown for 1 h at 37°C with shaking. An aliquot of 50-200 µl was spread on a selective LB/amp agar plate and grown overnight at 37°C.

3.9.5. Materials

ampicillin	stock: 100 µg/µl, stored at –20°C
E. coli DH5α	MaxEfficiency DH5α competent cells; GibcoBRL genotype: F⁻ Φ80d*lac*ZΔM15 Δ(*lac*ZYA-*arg*F)U169 *deo*R *rec*A1 *end*A1 *hsd*R17(r_k^-, m_k^+) *pho*A *sup*E44 λ⁻ *thi*-1 *gyr*A96 *rel*A1
electroporation cuvette	0.2 cm; Eurogentec (Seraing, Belgium)
electroporator	Gene Pulser II; Bio-Rad

3.10. DNA processing and manipulation

3.10.1. Restriction endonuclease digestion of DNA

Type II restriction endonucleases were used to digest double-stranded DNA for analytical or preparative purposes. These restriction enzymes bind to short, specific nucleotide sequences and cleave the DNA within this region by hydrolyzing a phosphodiester bond in each strand. The recognition sequences (palindromes) possess twofold rotational symmetry. Staggered cleavage generates complementary, cohesive 5' and 3' ends (sticky ends). Cleavage in the axis of symmetry yields blunt ends.

For preparative purposes, 1-10 µg DNA were digested with 1-20 U of restriction enzyme in a volume of 50-100 µl. Complete digestion was confirmed by agarose gel electrophoresis. For analytical purposes, 0.2-2 µg DNA were digested with 1-5 U enzyme in a volume of 20-50 µl. In both cases digests were incubated for 2 h at 37°C. Reaction buffers were supplied by the manufacturer. Enzymes were heat-inactivated as recommended by the supplier or removed by phenol:chloroform extraction.

3.10.2. Phenol:chloroform extraction

To inactivate and remove proteins, e.g. restriction enzymes, nucleic acid solutions were extracted with phenol:chloroform. Thereby denatured proteins form a layer at the interface between aqueous and organic phases during centrifugation. The aqueous phase contains the purified DNA that can subsequently be concentrated by ethanol precipitation or directly used for further manipulations.

An equal volume of phenol:chloroform:isoamyl alcohol (25:24:1) was added to the DNA sample. After vortexing vigorously the emulsion was centrifuged at 13,000 rpm for 1 min and the upper aqueous phase was carefully separated from the interface and organic phase. An additional chloroform extraction was performed in order to remove residual phenol.

3.10.3. Ethanol precipitation of DNA

In the presence of relatively high concentrations of monovalent cations, ethanol induces a structural transition in nucleic acid molecules which causes them to aggregate and precipitate from solution. Ethanol precipitation was used to concentrate and/or desalt DNA solutions and to remove any residual organic phase following a phenol:chloroform extraction.

5 M NaCl solution was added to the DNA sample to a final concentration of 250 mM. Three volumes of ethanol (-20°C) were added, the solution was stored on ice for 10 min and then centrifuged at 13,000 rpm for 15 min at 4°C. The pellet was washed with one volume of ice-cold 70 % ethanol, recentrifuged for 5 min and dried in a speedvac evaporator. The DNA was dissolved in water or TE (pH 8) for 20 min at 37°C at an appropriate concentration.

3.10.4. Dephosphorylation of linearized plasmid DNA by CIP

In order to prevent self-ligation of vector ends in cloning strategies, linearized plasmid DNA was treated with calf intestine alkaline phosphatase (CIP). CIP catalyzes the hydrolysis of 5'-phosphate residues to 5'-hydroxyl ends. Since T4 DNA ligase requires 5'-phosphate residues to catalyze new phosphodiester bonds, ligation is only possible between vector ends and inserts, but not between vector ends themselves.

Dephosphorylation was carried out directly following plasmid linearization. CIP was added to the digestion mixture at a concentration of 1 U per pmol linearized vector DNA. After 45 min incubation at 37°C, CIP and the restriction enzymes were removed by phenol:chloroform extraction. The plasmid was recovered by ethanol precipitation.

3.10.5. Ligation of DNA fragments

DNA fragments bearing either sticky or blunt ends can be ligated *in vitro* with bacteriophage T4 DNA ligase. This enzyme catalyzes the formation of new phosphodiester bonds between a 5'-phosphate residue of one and a 3'-hydroxyl residue of another double-stranded DNA fragment generated by restriction endonucleases.

Ligation occured overnight at 16°C in a volume of 10-20 µl containing 1x ligation buffer supplied by the manufacturer and 1-2 U ligase. The insert DNA was employed at a 2-5 molar excess relative to the linearized and dephosphorylated vector DNA.

3.10.6. Miniprep: small-scale preparation of plasmid DNA

Plasmid DNA was purified from bacteria cultures by alkaline lysis of the bacterial cells and subsequent silica-based anion exchange column chromatography. A small culture of bacteria is grown in order to amplify *in vivo* the plasmid of interest. The bacteria are harvested and resuspended in buffer P1 (50 mM Tis·Cl pH 8.0, 10 mM EDTA, 100 µg/ml RNase A). Treatment with lysis buffer P2 (0.2 N NaOH, 1 % SDS) causes denaturation of the DNA by NaOH and of the bacterial proteins by SDS. The mixture is neutralized by buffer P3 (3 M potassium acetate, pH 5.5) causing reannealing of plasmid DNA and precipitation of SDS. Proteins, chromosomal DNA, SDS and cell debris are removed by centrifugation while the plasmid DNA stays in solution.

3 ml of a small overnight culture was centrifuged at 13,000 rpm for 1 min at room temperature. The bacterial pellet was resuspended in 250 µl P1. 250 µl P2 and 350 µl P3 were added, followed by gently mixing. The suspension was centrifuged at 13,000 rpm for 10 min and an equilibrated spin column was loaded with the supernatant. After washing of the column, the DNA was eluted by adding 50 µl water or TE and centrifugation of the column at 13,000 rpm for 1 min.

3.10.7. Midiprep, maxiprep and gigaprep: large-scale preparations of plasmid DNA

The alkaline lysis method, as described for minipreps, was used to produce high yields of plasmid DNA from large-scale bacterial cultures.

For midipreps, a bacteria culture of 100 ml was centrifuged at 4,000 rpm for 15 min at 4°C. The pellet was resuspended in 4 ml P1, supplemented with 4 ml P2 and incubated at room temperature for 5 min. After addition of 4 ml ice-cold P3 the mixture was incubated on ice for 15 min and centrifuged at 4,000 rpm for 30 min at 4°C. The supernatant was filtered over a pre-wetted folded filter and placed on an equilibrated anion exchange column that was subsequently washed twice. The absorbed DNA was eluted with elution buffer by gravity according to the manufacture's instruction. The eluate was precipitated by adding 0.7 volumes room-temperature isopropanol and subsequent centrifugation at 9,000 rpm for 30 min at 4°C. The pellet was washed with 2 ml 70 % ethanol, recentrifuged for 10 min, dried under vacuum and redissolved in 100 µl water or TE to an appropriate concentration. Maxipreps (for 250-ml cultures) and

gigapreps (for library cDNA isolation, see 3.8.6.) were performed likewise using appropriate columns and scaled-up protocols.

3.10.8. Quantification of DNA and RNA solutions

The concentration of nucleic acid solutions was determined by spectrophotometry. The ultraviolet (UV) absorption was measured at a wavelength of 260 nm (OD_{260}) using a quartz cuvette of 1 cm width. For double-stranded DNA an $OD_{260} = 1.0$ corresponds to approximately 50 µg DNA/ml. For RNA an $OD_{260} = 1.0$ corresponds to approximately 40 µg RNA/ml. In addition the OD_{280} was measured to estimate the purity of the nucleic acid sample. A ratio OD_{260}/OD_{280} of significantly less than 1.8-2.0 indicates phenol or protein contamination.

DNA samples were diluted 1:200, RNA samples 1:250, and measured in a spectrophotometer against a blank of pure water. An OD_{260} of 1.0 corresponds to a concentration of 10 µg DNA/µl respectively 10 µg RNA/µl of the original, non-diluted solution.

3.10.9. Agarose gel electrophoresis

Agarose gel electrophoresis was used for analytical and preparative purposes. The method is based on the migration of the negatively charged DNA towards the anode in an electric field. The fragments migrate through the gel matrix at rates inversely proportional to the logarithm (log_{10}) of the number of base pairs. Visualizing of DNA bands within an agarose gel is performed by DNA staining with the intercalating fluorescent dye ethidium bromide and subsequent illumination under UV light. The length of a DNA fragment is determined by comparison of its mobility to that of DNA standards.

The agarose gel, 1-2 % (w/v) agarose melted in 1x TBE electrophoresis buffer and supplemented with 0.5 µg/ml ethidium bromide, was placed in a electrophoresis tank and submerged in 1x TBE buffer. The DNA samples were mixed with DNA loading buffer and loaded into the gel wells. In addition 10 µl of a DNA standard was loaded in parallel with the samples. Horizontal electrophoresis was carried out at approximately 110 V. The stained gel was photographed under UV light.

3.10.10. Recovery of DNA from agarose gels

For preparative purposes DNA fragments of interest were cut out from stained agarose gels with a razor blade under UV illumination. The gel slides were solubilized and DNA was recovered by column chromatography.

Agarose gel slide were weighed (= 1 volume) and dissolved in 3 volumes of solubilization buffer by incubation for 10 min at 50°C. 1 volume isopropanol was added and the solution was applied to a silica-gel spin column. The column was centrifuged at 13,000 rpm for 1 min, washed with buffer and centrifuged again. DNA was eluted by adding 50 µl water or TE and centrifugation of the column at 13,000 rpm for 1 min. All buffers were provided by the manufacturer.

3.10.11. Sequencing of DNA

The sequence of specific target regions in between plasmid DNA was determined by a commercial sequencing service (MWG Biotech, Ebersberg, Germany). The sequence data were verified on the basis of the corresponding fluorescence electropherogram and subjected to computer analysis.

3.10.12. Computer-assisted sequence analysis

The GCG program (Wisconsin Sequence Analysis Package, Version 8.1-UNIX, 1995; Genetics Computer Group, Madison, WI, USA) was used together with public scientific internet applications for computer-assisted DNA and protein sequence analysis and database alignments.

3.10.13. Materials

Biomaterials and enzymes

agarose	agarose NA; Amersham Pharmacia Biotech (Uppsala, Sweden)
calf intestine alkaline phosphatase (CIP)	Boehringer Mannheim (Mannheim, Germany)
restriction enzymes	New England Biolabs (Fankfurt, Germany) and Boehringer Mannheim (Mannheim, Germany)
T4 DNA ligase	Boehringer Mannheim (Mannheim, Germany)

Reagents and solutions

chloroform	Merck
DNA loading buffer (6x)	0,25% (w/v) bromophenol blue 0,25% (w/v) xylene cyanol 30% (v/v) glycerol 50 mM EDTA
DNA standard	Gene Ruler DNA ladder mix; MBI Fermentas (Souffelweyersheim, France)
ethidium bromide	1 % (w/v); Serva, Boehringer Ingelheim (Heidelberg, Germany)
phenol/chloroform/isoamyl alcohol (25:24:1)	Roth (Karlsruhe, Germany)
TBE buffer (5x)	Tris-base 108 g boric acid 55 g EDTA 40 ml of 0.5 M, pH 8.0 ad 2 l
TE	10 mM Tris (pH 7.6), 1 mM EDTA (pH 8.0)

Equipment and materials

electrophoresis system	Sub-Cell GT agarose gel electrophoresis system; Bio-Rad
gel extraction kit	QIAquick Gel Extraction Kit; Qiagen (Hilden, Germany)
midiprep, maxiprep and gigaprep kits	QIAGEN Plasmid Midi, Maxi and Giga Kits; Qiagen (Hilden, Germany)
miniprep kit	QIAprep Spin Miniprep Kit; Qiagen (Hilden, Germany)
photographic film	Polapan; Polaroid (Offenbach, Germany)
photo camera	MP-4 Land Camera, model 44-31; Polaroid (Cambridge, MA)
speedvac	Vacuum cncentrator centrifuge Univapo 150 H; UniEquip (Martinsried, Germany)
UV illuminator	model N90M; UniEquip (Martinsried, Germany)

3.11. PCR applications

3.11.1. DNA amplification by PCR

The polymerase chain reaction (PCR) constitutes an enzymatic *in vitro* amplification of specific DNA segments. Amplification occurs in automated, temperature-controlled cycles of denaturation, annealing and elongation in a thermal cycler. Initially, double-stranded template

DNA is separated into its complementary single strands by heating (denaturation). At a lower temperature two oligonucleotide primers, flanking the DNA region to be amplified, hybridize to their respective complementary sequences on opposite strands (annealing) and serve as primers for DNA synthesis in a 5'→3' direction (elongation). Primer extension is catalyzed at a slightly increased temperature by a thermostable DNA polymerase that adds deoxyribonucleotide triphosphates (dNTPs) to the recessed 3'-hydroxyl end of extending strands, thereby generating new double-stranded DNA across the primer-flanked region. The products of each reaction cycle are then denatured to permit a new amplification cycle. Theoretically, for n cycles a 2^n-fold amplification of a specific DNA sequence is obtained.

Primers were commercially synthesized (MWG Biotech, Ebersberg, Germany). They were designed corresponding to the DNA segment to be amplified, provided with restriction sites for endonuclease digestion or epitope-encoding sequences for immunological purposes where appropriate. Pairs of primers were designed to have equivalent melting temperatures (T_m), calculated according to the formula[9] T_m [°C] = (A+T)·2 + (G+C)·4. The annealing temperature for each PCR was typically estimated by T_m minus 5°C and optimized experimentally. For preparative DNA amplification as part of cloning strategies, Deep $Vent_R$ DNA polymerase was used in preference to *Taq* DNA polymerase, due to its 3'→5' proofreading exonuclease activity which minimizes the risk of nucleotide misincorporation during elongation.

Reaction parameters for DNA amplification were as follows:

template DNA	~200 ng (except in negative control PCR)
sense-primer (forward)	1 µM
antisense-primer (reverse)	1 µM
DNA polymerase	1-2 U
PCR reaction buffer	1x
dNTPs	each 200 µM
final reaction volume	100 µl (preparative PCR), 30-50 µl (analytical PCR)

Thermal cycle parameters for PCRs were as follows:

initial denaturation	94°C, 5 min
denaturation	94°C, 30-60 s
annealing	60-65°C (primer pair and template specific), 30-60 s
elongation	72°C for *Taq* DNA polymerase, approx. 60 s/kb 74°C for Deep VentR DNA polymerase, approx. 60 s/kb
cycles	30
final elongation	72°C/74°C, 10 min

[9] A, T, G, C: number of the 2'-deoxynucleosides adenosine (A), thymidine (T), guanosine (G) and cytidine (C) within a primer sequence.

A negative control was included in each PCR experiment using H_2O instead of template DNA to allow the detection of amplified DNA molecules due to contamination. PCR products were analyzed by agarose gel electrophoresis. In preparative experiments, the DNA fragments were subcloned into appropriate vectors and sequenced to exclude errors.

3.11.2. Synthesis of a cDNA insert encoding the cytoplasmic region of CD11a

The DNA sequence encoding the cytoplasmic tail of CD11a (nt 3425-3649)[10] was subcloned within the *Nde*I (5971)/*Eco*RI (5988) restriction site of the YTH vector pAS2-1 (Dr. G. Heiss).

Primers[11] used for the amplification of this cDNA insert were

5'-*CGT***CATATG**AAGGTTGGTTTCTTCAAACGGAAC-3' (forward) and

5'-*CCG***GAATTC**GGCATCCTGAGTCCAGTTCTG-3' (reverse).

The plasmid paαL, full-length *CD11a* cDNA subcloned into the *Hind*III/*Xba*I restriction site of pAPRM8 (Klickstein *et al.*, 1996), served as template DNA for the PCR.

3.11.3. Synthesis of *JM1121* and *JAM$^{(HA)}$* cDNA inserts

cDNA sequences encoding full-length human JAM-1 without (*JM1121*) and with (*JAM$^{(HA)}$*) the hemagglutinin (HA) epitope YPYDVPDYA were subcloned into the *Kpn*I (895)/ *Bam*HI (907) site of the mammalian expression vector pcDNA3.

Primers used for the amplification of *JM1121* cDNA were

JM101 5'-*GCGG***GGTACC**ATGGGGACAAAGGCGCAAGTCGA-3' (forward) and

JM102 5'-*GCGG***GGATCC**TCACACCAGGAATGACGAGGTCT-3' (reverse).

Primers used for the amplification of *JAM$^{(HA)}$* cDNA were JM101 (forward) and

JM302 5'-*GCGG***GGATCC**TCAAGCGTAATCTGGAACATCGTATGGGTA-

*TCCAGC*CACCAGGAATGACGAGGTCT-3' (reverse).

The prey-encoding library vector isolated from the *bona fide* yeast colony αLMC3 during the YTH screening (see 4.1.) served as *JAM-1* DNA template for the synthesis of both fragments.

---

[10] Nucleotide numbers of *CD11a* refer to GenBank accession number Y00796 (Larson *et al.*, 1989).

[11] normal: gene-specific DNA sequence, bold: restriction site; underlined: start/stop codon; underlined dotted: tag-encoding sequence; italic: clamp or bridge.

3.11.4. Synthesis of Ig-like domain–deleted *JAM-1* cDNA constructs by PCR overlap extension (deletion mutagenesis)

The overlap extension method (Horton *et al.*, 1989) enables the fusion of two independent but overlapping DNA fragments without the use of restriction enzymes or ligase. After initial denaturation of both molecules, the single strands of each fragment that include the overlapping sequence at their 3' ends can anneal to each other and serve as primers for one another (strand self-priming). By the action of DNA polymerase the single strands are extended in 5'-3' direction starting at the particular 3' end of the overlapping region (overlap extension). Thereby the different strands serve as template DNA for one another to ultimately generate a single, fused double-stranded DNA molecule that itself is further amplified during subsequent PCR steps in the presence of two primers flanking the DNA region on the ”ligated” fragment to be amplified.

Two PCR fragments, N_{JAM} and C_{JAM}, were synthesized using JAM-1–encoding pJM1121 as template DNA (**table 2**). N_{JAM} contained the 5' part of *JAM-1* ending just before the Ig-like domain to be deleted. Its 3' end consisted of the last 25 nt before and the first 25 nt after this domain, accomplished by the appropriate design of the antisense primer (Ig1D-N02 respective Ig2D-N02). Conversely, C_{JAM} based on the 3' part of *JAM-1*, beginning just after the Ig-like domain to be deleted. The 5' end of C_{JAM} constituted the same DNA sequence as the 3' end of N_{JAM}, accomplished by the sense primer used (Ig1D-C01 respective Ig2D-C01). Thus, both fragments provided a mutual overlapping sequence of approximately 50 bp, containing sequence areas before and after the Ig-like domain to be deleted but specifically excluding the domain sequence itself. This sequence overlap was used to fuse both molecules by PCR overlap extension (**table 3**). N_{JAM} and C_{JAM} were purified by preparative agarose gel electrophoresis, mixed together, supplemented with primers flanking the terminal ends of *JAM-1* and subjected to PCR. Strand self-priming, overlap extension and PCR amplification yielded the synthesis of hybrid *JAM-1* molecules deleted for the corresponding Ig-like domain. The fragment was electrophoretically purified and subcloned into the expression vector pcDNA3. The identity and integrity of the hybrid molecule was confirmed by complete DNA sequencing.

fragment	nt numbers	sense primer	antisense primer
$N_{JAM}^{\Delta D1}$	1-123, 394-418	JM101	Ig1D-N02
$C_{JAM}^{\Delta D1}$	99-123, 394-900	Ig1D-C01	JM102
$C_{JAM}^{\Delta D1(HA)}$	99-123, 394-897, HA	Ig1D-C01	JM302
$N_{JAM}^{\Delta D2}$	1-393, 652-676	JM101	Ig2D-N02
$C_{JAM}^{\Delta D2}$	369-393, 652-900	Ig2D-C01	JM102
$C_{JAM}^{\Delta D2(HA)}$	369-393, 652-897, HA	Ig2D-C01	JM302

table 2: Sense and antisense primers used for generation of N_{JAM} and C_{JAM} fragments for use in PCR overlap extension synthesis. Nucleotide numbers refer to the coding sequence of human JAM-1 (nt 1-900); ”HA” indicates implementation of a HA-encoding tag sequence at the 3’ end of the fragment.

fused DNA	nt numbers	self-priming molecules	flanking primers
$JAM^{\Delta D1}$	1-123, 394-900	$N_{JAM}{}^{\Delta D1}$, $C_{JAM}{}^{\Delta D1}$	JM101, JM102
$JAM^{\Delta D1(HA)}$	1-123, 394-897, HA	$N_{JAM}{}^{\Delta D1}$, $C_{JAM}{}^{\Delta D1(HA)}$	JM101, JM302
$JAM^{\Delta D2}$	1-393, 652-900	$N_{JAM}{}^{\Delta D2}$, $C_{JAM}{}^{\Delta D2}$	JM101, JM102
$JAM^{\Delta D2(HA)}$	1-393, 652-897, HA	$N_{JAM}{}^{\Delta D2}$, $C_{JAM}{}^{\Delta D2(HA)}$	JM101, JM302

table *3: Flanking sense and antisense primers used for the fusion of self-priming N_{JAM} and C_{JAM} fragments by PCR overlap extension to synthesize mutagenized *JAM-1* DNA molecules deficient for the sequence region encoding the N-terminal Ig-like domain 1 ($JAM^{\Delta D1}$) or the membrane-proximal Ig-like domain 2 ($JAM^{\Delta D2}$) of human JAM-1. Nucleotide numbers refer to the coding sequence of human *JAM-1* (nt 1-900); "HA" indicates implementation of a HA-encoding tag sequence at the 3' end of the fragment.

Primers[12] used to generate self-priming molecules were

Ig1D-C01 (forward)
5'-T^{099}TCTGAACCTGAAGTCAGAATTCCT^{123}‖**C^{394}CATCCAAGCCTACAGTTAACAT^{416}**-3'
Ig1D-N02 (reverse)
5'-**G^{418}GATGTTAACTGTAGGCTTGGATGG^{394}**‖A^{123}GGAATTCTGACTTCAGGTTCAG^{101}-3'
Ig2D-C01 (forward)
5'-G^{369}GTCAAGCTCATCGTGCTTGTGCCT^{393}‖**T^{652}ATGGGACACCCATGACTTCAAA^{674}**-3'
Ig2D-N02 (reverse)
5'-**C^{676}ATTTGAAGTCATGGGTGTCCCATA^{652}**‖A^{393}GGCACAAGCACGATGAGCTTG^{372}-3'.

3.11.5. Analytical PCR

Gene expression analysis of *JAM-1* and *β-actin* at the RNA level using RT-PCR included analytical PCR and is described below (see 3.12.).

Prior to sequencing of prey-encoding cDNA inserts from pGAD10-based library vectors of candidate $HIS3^{+}/lacZ^{+}$ yeast colonies the insert sizes were determined by analytical PCR.

Primers[13] used for the amplification of these inserts flanked the *Eco*RI restriction site within the MCS of pGAD10 and were

GAD101 5'-G^{797}ATGAAGATACCCCACCAAACCCA^{821}-3' (forward) and
GAD102 5'-C^{888}TTGCGGGGTTTTTCAGTATCTAC^{864}-3' (reverse).

[12] normal: sequence region before the Ig-like domain to be deleted; bold: sequence region after the Ig-like domain to be deleted; "‖" indicates the position of the omitted Ig-like domain sequence (fusion locus). The nucleotide numbers indicated with superscripts correspond to the coding sequence of human *JAM-1*.
[13] Nucleotide numbers indicated with superscripts correspond to the sequence of pGAD10.

3.11.6. Materials

Deep Vent$_R$ DNA polymerase	New England Biolabs
dNTPs	PCR nucleotide mix, contains the deoxynucleotides dATP, dGTP, dCTP, dTTP each at 10 mM; Roche Diagnostics (Mannheim, Germany)
oligonucleotide primers	synthesized to order by MWG Biotech (Ebersberg, Germany); dissolved in water to final 100 pmol/µl
PCR reaction buffer	10x buffer as provided by the supplier of the appropriate DNA polymerase
Taq DNA polymerase	Qiagen (Hilden, Germany)
thermal cycler	Mastercycler gradient; Eppendorf (Hamburg, Germany)

3.12. Gene expression analysis at the RNA level using RT-PCR

Gene expression analysis at the RNA level, *i.e.* determination of target-specific mRNA transcripts in the cell, includes isolation of total RNA, reverse transcription of mRNA to cDNA and amplification of the target cDNA by PCR. Cells were dissolved by a mono-phasic solution of phenol and guanidine isothiocyanate (Trizol Reagent). Addition of chloroform and subsequent centrifugation lead to phase separation under conditions at which RNA remained water-soluble and proteins or DNA were found in the organic phase or the interphase. The total RNA was subsequently isolation from the aqueous phase and served as template for the synthesis of cDNA via reverse transcriptase polymerase chain reaction (RT-PCR) using viral reverse transcriptase and random hexamer primers. The cDNA pool was subsequently subjected to analytical PCR using gene-specific oligonucleotide primers.

$5 \cdot 10^6$ CHO cells were harvested, washed in PBS, homogenized in 1 ml Trizol reagent and incubated for 5 min at room temperature. Phase separation was generated by addition of 200 µl chloroform and centrifugation at 13,000 rpm for 15 min at 4°C. The RNA was precipitated from the aqueous phase by addition of 500 µl isopropanol, incubation for 10 min at room temperature and centrifugation at 13,000 rpm for 10 min at 4°C. The pellet was washed with 1 ml 75 % ethanol, recentrifuged at 7,500 rpm for 5 min at 4°C, and dried for 5-10 min at 55°C. The RNA was redissolved in 100 µl water with incubation for 10 min at 55°C and its concentration was determined by spectrophotometry (see 3.10.8.). Samples were stored at –70°C. To prevent degradation of RNA due to RNase contamination, only diethylpyrocarbonate (DEPC)-treated water was used. For this the water was supplemented with DEPC to final 0.1 % (v/v), incubated

overnight at room temperature and autoclaved. The utilized glassware was baked overnight at 140°C prior to use. Work with RNA was performed wearing gloves.

Reaction parameters for the first strand cDNA synthesis by RT-PCR were as follows:

template RNA	5 µg (volume respective to the RNA concentration)
random hexamer primers	5 µM
first strand buffer	1x
DTT (dithiothreitol)	10 mM
dNTPs	each 0.5 mM
reverse transcriptase	200 U
final reaction volume	20 µl

Template RNA and random hexamer primers were mixed with water to a final volume of 12 µl and incubated for 10 min at 70°C. The remaining components excluding the enzyme were added and the solution was incubated for 10 min at 25°C and additionally for 2 min at 42°C. The reverse transcriptase was supplemented and the RT-PCR was performed for 50 min at 42°C. The enzyme was heat-inactivated for 15 min at 70°C and the first strand cDNA samples were stored at –20°C.

Subsequently, for gene expression analysis, 10 % of a cDNA-containing first strand reaction mix was subjected to analytical PCR (see 3.11.) in order to amplify cDNA fragments derived from expressed target gene-specific mRNA transcripts, i.e. *JAM-1*–related cDNA and as a control *β-actin* cDNA.

Primers used for amplification of *JAM-1*–related cDNA were JM101 (forward) and JM102 (reverse). JM101 (forward) and JM302 (reverse) were used to amplify HA-tagged sequences (see 3.11.3.).

Primers used for the amplification of *β-actin* cDNA were

5-bAct `5'-AGAGATGGCCACGGCTGCTT-3'` (forward) and

3-bAct `5'-ATTTGCGGTGGACGATGGAG-3'` (reverse)

and allowed amplified *β-actin* fragments derived from genomic DNA contamination or spliced mRNA transcripts to be distinguished (see 4.7.). A human foreskin fibroblast preparation served as positive control for *β-actin* cDNA amplification.

Materials

dNTPs	(see 3.11.6.)
DTT (0.1 M)	GibcoBRL
ethanol (75 %)	prepared with DEPC-treated water

first strand buffer	GibcoBRL
human foreskin fibroblast preparation	kind gift of K. Bauer (IPEK, University Hospital, Munich)
random hexamer primers	Primer ”random”; Boehringer Mannheim
reverse transcriptase	Superscript II, Rnase H^- reverse transcriptase, derived from moloney murine leukemia virus (MMLV); GibcoBRL
Trizol reagent	total RNA isolation reagent; GibcoBRL

3.13. Protein analysis

3.13.1. Measurement of protein concentrations (BCA method)

Bicinchoninic acid (BCA) is a selective detection reagent for the cuprous cation Cu^{1+} that is generated by protein-mediated reduction of Cu^{2+} in an alkaline environment. The complex of two BCA molecules with a Cu^{1+} ion exhibits an absorption maximum at a wavelength of 562 nm, allowing spectrophotometric quantification of proteins in aqueous solution.

Proteins were quantitative precipitated by addition of 1 ml ice-cold 12 % trichloroacetic acid (TCA), incubation for 30 min on ice and centrifugation at 13,000 rpm for 30 min at 4°C. The supernatant was removed and the pellet was resuspended in 100 µl water. Using a BSA stock solution, a set of protein standards with 0-25 µg BSA/100 µl was prepared. To each set of protein standards and protein samples, 2 ml of freshly prepared BCA working solution was added. The protein solutions were incubated for 30 min at 60°C, cooled to room temperature and their absorption was measured at the wavelength of 562 nm in a spectrophotometer. Based on the absorption values of the protein standards a calibration curve was calculated and used for determination of the protein concentrations in the samples. All protein standards and samples were prepared in duplicate.

Materials

BSA stock solution	2.0 µg/µl BSA standard; Pierce Chemicals (Rockford, IL)
BCA Protein Assay Kit	Pierce Chemicals (Rockford, IL)

3.13.2. Whole cell lysates

Mammalian cells were harvested, washed with PBS and counted in a Neubauer hemacytometer. Approximately $2 \cdot 10^6$ cells were centrifuged at 1,200 rpm for 5 min at 25°C. The pellet was resuspended on ice in 200 µl ice-cold 1x SDS sample buffer supplemented with protease inhibitors and where appropriate with DTT by drawing through a 20G needle with a 1-ml insulin syringe. The cell lysates were heated for 5 min at 96°C and subjected to SDS-PAGE or long-term storage at –70°C.

Materials

DTT supplementation	25 mM (where appropriate); GibcoBRL	
protease inhibitor supplementation	aprotein	2 µg/ml (stock solution at –20°C: 10 µg/µl)
	leupeptin	5 µg/ml (stock solution –20°C: 5 µg/µl)
SDS sample buffer (2x)	(see 3.13.4.)	

3.13.3. Fractionated cell lysates

Intact cells were lysed and separated into membrane and cytosolic cell fractions for protein analysis. Approximately $3 \cdot 10^7$ CHO cells were washed twice in PBS and then resuspended in 500 µl ice-cold hypotonic lysis buffer and disrupted by 60-80 strokes in a glass Dounce homogenizer on ice. The homogenate was incubated on ice for 10 min and centrifuged at 110 g for 5 min at 4°C to remove nuclei, unbroken cells and large debris. The postnuclear supernatant was ultracentrifuged at 100,000 g for 30 min at 4°C, resulting in a supernatant containing the cytosolic cell fraction. The pellet was washed with 1 ml lysis buffer by passage 5 times through a 26G syringe canula and then ultracentrifuged again. The supernatant was discarded and the pellet, containing membranes and cytoskeletons, was resuspended in 400 µl hypotonic lysis buffer supplemented with 1 % (v/v) Igepal CA-630 detergent. This membrane fraction was incubated on ice for 10 min. The fractionated protein samples were stored at -70°C.

Materials

hypotonic lysis buffer	HEPES	10 mM
	KCl	10 mM
	$MgCl_2$	10 mM
	EDTA	0.5 mM
	Complete, mini	1 tablet/8.4 ml buffer
	pH	7.9
Igepal CA-630	(Octylphenoxy)polyethoxyethanol; formerly Nonidet P-40	

Complete, mini	EDTA-free protease inhibitor cocktail tablets; Roche Diagnostics (Mannheim, Germany)
ultracentrifugation tubes	Microfuge tube polyallomer; Beckman Instruments (Palo Alto, CA)
ultracentrifuge	Optima TLX Ultracentrifuge; Beckman Instruments (Palo Alto, CA)

3.13.4. SDS-PAGE

Whole cell lysates and protein samples were resolved for analytical purposes by polyacrylamide gel electrophoresis (PAGE). The use of the anionic detergent sodium dodecyl sulfate (SDS) enables separation according to the molecular weight of the proteins. It binds to the polypeptides and confers a negative charge which is in direct proportion to their size. The gel matrix is prepared by polymerization of acrylamide and *N,N′*-methylenebisacrylamide via free radicals. Initial radicals arise from chemical decay of ammonium persulfate (APS) catalyzed by *N,N,N′,N′*-tetramethylethylenediamine (TEMED). The electrophoresis towards the anode is carried out in a discontinuous buffer system that first concentrates SDS-protein complexes within a stacking gel before they migrate into the resolving gel. The size of proteins is determined by comparing their mobility with that of a protein standard.

The resolving gel solution was prepared, poured between two glass plates and overlaid with butanol. After polymerization, the top of the gel was washed with water. Freshly prepared stacking gel solution was filled and allowed to polymerize. Subsequently the gel was placed in a vertical electrophoresis apparatus filled with 1x running buffer. Protein samples were diluted 1:1 with 2x SDS sample buffer if not already prepared with 1x SDS sample buffer. The SDS sample buffer was supplemented with (reducing conditions) or without (non-reducing conditions) dithiothreitol (DTT). The protein samples and a protein standard were denatured by boiling for 5 min and loaded onto the gel. Electrophoresis was carried out at 200 V. The resolving gel was subsequently subjected to western blot analysis or silver staining.

Materials

acrylamide/bis-acrylamide	30 % (w/v) solution, mix ratio 29:1; Bio-Rad
APS	Bio-Rad
DTT	stock solution: 1 M in 10 mM NaOAc, stored at –20°C
electrophoresis apparatus and supplies	Mini-PROTEAN II Cell; Bio-Rad
protein standards	prestained SDS-PAGE standards: low range (20-112 kDa), broad range (7-207 kDa); Bio-Rad

resolving gel (10 %)	5 ml 1.5 M Tris, pH 8.8 8.2 ml water 6.7 ml acrylamide/bis-acrylamide solution 125 µl 10 % (w/v) APS 7.5 µl TEMED
running buffer (10x)	30 g Tris-base 142 g glycine 50 ml 20 % SDS ad 1 l
SDS sample buffer (2x)	100 mM Tris·HCl (pH 6.8) 20 % (v/v) glycerol 4 % (w/v) SDS 0.01 % (w/v) bromphenol blue 50 mM DTT (where appropriate)
stacking gel	1.25 ml 0.5 M Tris, pH 6.8 3.25 ml water 0.5 ml acrylamide/bis-acrylamide 30 µl 10 % APS 5 µl TEMED

3.13.5. Western blot analysis

Western blotting consists of the transfer of electrophoretically separated proteins from a SDS-PAGE gel to a nitrocellulose membrane by electrophoresis. The membrane-immobilized target protein is immunologically identified by an appropriate primary antibody and a horseradish peroxidase (HRP)-conjugated secondary antibody directed against the primary antibody. Detection of the antigen-antibody-antibody complex occurs by HRP-mediated oxidation of the chemiluminescent substrate luminol, a cyclic diacylhydrazide. The reaction product exhibits an excited state which decays to ground state via a light emitting pathway, and is detectable by exposure of the membrane to an autoradiography film.

A nitrocellulose membrane was placed onto the polyacrylamide gel and both were sandwiched between electrode papers, pads and a plastic support. The proteins were transferred to the membrane by electrophoresis towards the anode at 200 mA for 1 h at 4°C in ice-cold transfer buffer. Non-specific binding sites on the blotted membrane were blocked by shaking in TBS/milk for 1 h at room temperature. The membrane was successively incubated with the primary and secondary antibodies for 1 h at room temperature, with washing by rinsing in TBST three times for 10 min. Antibodies used were diluted in TBST/milk to appropriate concentrations. The freshly prepared chemiluminescent substrate working solution was added to the surface of the membrane (approx. 0.2 ml/cm^2) and incubated for 4 min at room temperature.

The membrane was wrapped in plastic foil and exposed in the darkroom for 10 s - 30 min to an autoradiographic film that was subsequently developed in dark room conditions.

Materials

antibodies, primary	for source and concentrations see 3.14.1.
antibodies, secondary	HRP-conjugated; for source and concentrations see 3.14.2.
autoradiography film	Hyperfilm ECL high performance chemiluminescence film; Amersham Pharmacia (Buckinghamshire, UK)
blocking milk	non-fat dry milk, blotting grade blocker; Bio-Rad
blotting apparatus and supplies	Mini Trans-Blot Cell; Bio-Rad
chemiluminescent substrate	SuperSignal West Pico Chemiluminescent Substrate (for normal applications) and SuperSignal West Dura Extended Duration Substrate (for applications requiring higher sensitivity); comprises luminol/enhancer solution and stable peroxide solution mixed 1:1 to prepare the working solution; light emission wavelength: 425 nm; Pierce (Rockford, IL)
electrode paper Novablot	Filter Paper, Grade 1F, Amersham
film developer	G150 developer; Agfa-Gevaert (Mortsel, Belgium)
film fixing bath	G354 fixing bath; Agfa-Gevaert (Mortsel, Belgium)
nitrocellulose membrane	Hybond-C super; Amersham Life Science (Buckinghamshire, UK)
TBS	10 ml 1M Tris 33 ml 5 M NaCl ad 1 l
TBS/milk	TBS supplemented with 5 % (w/v) blocking milk
TBST	TBS supplemented with 0.05 % (v/v) tween 20
TBST/milk	TBST supplemented with 5 % (w/v) blocking milk
transfer buffer	3.03 g Tris 14.4 g glycin 200 ml methanol ad 1 l
tween 20	polyoxyethylenesorbitan monolaurate; Bio-Rad

3.13.6. Silver staining of polyacrylamide gels

Silver staining of polyacrylamide gels allows the detection of proteins separated by SDS-PAGE to a limit of 2-5 ng protein/band. The staining relies on differential reduction of silver ions close-to protein bands.

Fixation	2 x 30 min	CH_3OH/H_2O/glacial acetic acid (4:3:1)
	2 x 10 min	H_2O wash
	1 x 15 min	2.4 g sodium tetraborate ($Na_2B_4O_7$) decahydrate
		ad 148 ml H_2O
		2 ml 25 % glutaraldehyde
	3 x 30 min	H_2O wash
Incubation	1 x 15 min	merge in order as indicated:
		24 ml H_2O
		2.3 ml 1 M NaOH
		2,5 ml 25 % NH_3 solution
		5 ml 20 % (w/v) $AgNO_3$
		ad 125 ml H_2O
	2 x 5 min	H_2O wash
Development		until desired staining level with:
		13 ml ethanol
		750 µl 1 % (w/v) citric acid
		90 µl 37 % formaldehyde
		ad 150 ml H_2O
Reduction termination		
	1 x 10 min	3.7 g Tris·HCl
		2.5 g $Na_2S_2O_3$
		ad 100 ml H_2O
Backround destaining		exposure until desired background attenuation with
		Farmer's Reducer:
		2.5 ml 20 % (w/v) $Na_2S_2O_3$
		2.5 ml 1 % (w/v) $K_3[Fe(CN)_6]$
		ad 220 ml H_2O
	3 x 10 min	H_2O wash

For storage purpose the stained polyacrylamide gel was incubated in 20 % glycerin for 2 h. The gel was then placed between a wet Whatman 3MM paper and a cellophane sheet on the top and dried under vacuum for 2 h at 85°C.

Materials

cellophane sheets	Amersham
gel dryer	model 583; Bio-Rad
Whatman 3MM paper	3MM-Chr chromatography paper, Whatman (Maidstone, UK)

3.13.7. Flow cytometry

Flow cytometry analysis enables the determination of optical and immunofluorescence characteristics of a single cell. Inside a flow cytometer the cell suspension passes the measurement cell as a laminar flow of single cells in isotonic shear fluid, where they are intersected by monochromatic light (488-nm argon ion laser). Measurement of light diffraction allows determination of the physical properties of the cell, such as the size (represented by forward scatter, FSC) and internal complexity (represented by side scatter, SSC) that was used to determine the cell number within cell suspensions in chemotaxis assays. Measurement of fluorescence activation further allows the quantification of the fluorescent dye uptake of immunofluorescence-labeled cells that enables the analysis of cellular protein expression. The flow cytometry results were digitized, computer analyzed and subsequently displayed as histograms describing the logarithmic distribution of the measured fluorescence intensity over the cell population.

Cells were harvested, resuspended in HHMC, placed into round-bottom 96-well microtiter plates with $0.5 \cdot 10^6$ cells/200 µl/well and centrifuged. Each centrifugation step comprised capping of the plate with a self-adhesive plate sealer, centrifugation at 1,200 rpm for 3 min at 25°C and supernatant removal by a precipitous flick. In the case of intracellular immunofluorescence staining, cells were permeabilized with 50 µl 0.2 % (v/v) Triton X-100 for 2 min on ice, the cell suspension was diluted with 150 µl HHMC, centrifuged, washed with 200 µl HHMC and recentrifuged. For staining, the cells were resuspended in 50 µl HHMC supplemented with either a primary antibody directed against the target gene, an IgG isotype control or preimmunization serum. The cell suspension was incubated for 30 min at room temperature, diluted with 150 µl HHMC, centrifuged, washed with 200 µl HHMC and then recentrifuged. The cells were immunofluorescence labeled by resuspension in 50 µl HHMC supplemented with a corresponding secondary antibody conjugated with the fluorochrome fluorescein-5(6)-isothiocyanate (FITC). Subsequent incubation and washing was performed as before but in darkness. The stained cells were finally resuspended in 500 µl HHMC, transferred into FACS-tubes and subjected to flow cytometry measurement. In general a constant number of 10,000 cells was analyzed. Protein expression was indicated by a positive shift in the fluorescence intensity of the two histograms obtained for i) cell populations incubated with an IgG isotype control or preimmunization serum and ii) antigen-labeled cell populations.

Materials

antibodies, primary	for source and concentrations used see 3.14.1.
antibodies, secondary	FITC-conjugated; for source and concentrations used see 3.14.2.
FACS-tubes	5-ml Falcon polystyrene tubes; Becton Dickinson (Meylan, France)

flow cytometer	FACScan, fluorescence-activated cell analyzer; software: CellQuest; Becton Dickinson Immunochemistry Systems (San Jose, CA)
IgG isotype controls	for source and concentrations used see 3.14.3.
isotonic shear fluid	FACSFlow shear fluid; Becton Dickinson
plate sealer	Linbro plate sealer with adhesive back; ICN Biomedicals (Aurora, OH)
Triton X-100, 0.2 %	t-octylphenoxypolyethoxyethanol; used at a concentration of 0.2 % (v/v) in PBS

3.14. Antibodies and sera

3.14.1. Primary antibodies

α_L (CD11a) pAb C-17	goat IgG, directed against the cytosolic domain of CD11a, 200 µg/ml; Santa Cruz Biotechnology western blotting: 1:300 dilution, non-reducing conditions
α_L (CD11a) mAb MCA502	rat IgG_{2a}, 2 mg/ml; Serotec (Oxford, UK) western blotting: 1:1000 dilution, non-reducing conditions
α_M (CD11b) mAb CBRM 1/29	mouse IgG_1,1 mg/ml; from T.A. Springer (Center of Blood Research, Boston, MA) used: 10 µg/ml
β_2 (CD18) mAb MEM48	mouse IgG_1, 100 µg/ml; R&D Systems (Wiesbaden, Germany) Western blotting: 1:200 dilution, non-reducing conditions
HA pAb Y-11	rabbit IgG, 200 µg/ml; Santa Cruz Biotechnology flow cytometry: 10 µg/ml western blotting: 1:300 dilution
ICAM-1 Fab	Fab fragment of the ICAM-1 mAb RR1/1; from R. Rothlein (Boehringer Ingelheim Pharmaceuticals, Ridgefield, CT) used: 10 µg/ml
ICAM-1 mAb RR1/1	mouse IgG_1, 1.7 µg/µl; from R. Rothlein (Boehringer Ingelheim Pharmaceuticals, Ridgefield, CT) used: 10 µg/ml
JAM-1 pAb	(see 3.14.4. and 3.15.2.)
TS1/18	hybridoma cell line secreting mouse IgG_1 mAb directed against the LFA-1 β_2 subunit (CD18); ATTC (Sánchez-Madrid *et al.*, 1982) used: 1:2 dilution of hybridoma supernatant or 10 µg/ml

TS1/22 hybridoma cell line secreting mouse IgG_1 mAb directed against the LFA-1 α_L subunit (CD11a); ATTC (Sánchez-Madrid *et al.*, 1982)
used: 1:2 dilution of hybridoma supernatant or 10 µg/ml

VLA-4 mAb HP1/2 α_4 (CD49d) mAb, mouse IgG_1, 4.9 µg/µl; from M.E. Hemler (Harvard Medical School, Boston, MA)
used: 10 µg/ml

3.14.2. Secondary antibodies

horseradish peroxidase (HRP)-conjugated (for western blotting) or
fluorescein-5(6)-isothiocyanate (FITC)-conjugated (for flow cytometry) mAbs

anti-goat IgG HRP-conjugated
from rabbit, 400 µg/ml; Santa Cruz Biotechnology
used: 1:3000 dilution

anti-mouse IgG (Fc specific) FITC-conjugated,
$F(ab')_2$ fragment, from goat, 2.2 µg/µl; Sigma
used: 1:200 dilution

anti-mouse IgG HRP-conjugated
from sheep, 500 µg/ml; Amersham Life Science
used: 1:3000 dilution

anti-rabbit IgG FITC-conjugated
from goat, 400 µg/ml; Santa Cruz Biotechnology
used: 1:50 dilution

anti-rabbit IgG HRP-conjugated
from goat, 400 µg/ml; Santa Cruz Biotechnology
used: 1:2500 dilution

3.14.3. IgG isotype controls

mouse IgG_1, κ (MOPC 21) 200 µg/ml; Sigma
used: 10 µg/ml
flow cytometry: 1:100 dilution

rabbit IgG 500 µg/ml; Santa Cruz Biotechnology
used: 1:250 dilution

3.14.4. Sera

human serum	Bio-Whittaker (Walkersville, MD); used in concentrations as indicated
JAM-1 pAb	polyclonal mouse serum; generated to order by Eurogentec (Herstal, Belgium) as described (see 3.15.2.) Antibody inhibition studies were performed with polyclonal serum of mouse TS, western blot analysis with polyclonal serum of mouse DS. used: 1:50 dilution flow cytometry: 1:100 dilution western blotting: 1:1500 dilution
preimmunization serum	murine control serum for JAM-1 polyclonal Ab gathered from mouse TS and mouse DS, respectively, prior to DNA-mediated immunziation (Eurogentec); used in concentrations equivalent to anti–JAM-1

3.15. Antibody preparation

3.15.1. Hybridoma cell lines: maintainance and antibody isolation

3.15.1.1. Propagation

B cell hybridomas are immortalized cell lines derived by cell fusion between a normal B lymphocyte from an immunized animal and a myeloma cell of an immortalized tumor line. B cell hybridomas secrete individual monoclonal antibodies of a single antigen-specificity derived from the normal B lymphocyte cell.

The hybridoma cell lines TS1/22 and TS1/18 (Sánchez-Madrid *et al.*, 1982) were cultured in a 5 % CO_2 atmosphere at 37°C in DMEM medium containing 4.5 g/l glucose, 1 mM sodium pyruvate and 4 mM L-glutamine and supplemented with 10 % heat-inactivated FCS and 50 mg/l gentamicin. The cultures were maintained between 10^5-10^6 cells/ml and then subcultured by centrifugation and subsequent seeding in fresh medium. The remaining medium supernatant was stored at 4°C for further experimental applications or antibody extraction.

3.15.1.2. Isolation of hybridoma-secreted monoclonal antibodies

Protein G, a cell surface protein of group G streptococci, is a type III Fc receptor that binds to the Fc region of IgG. It was used for isolation of the secreted IgG_1 mAbs TS1/22 (anti-CD11a) and TS1/18 (anti-CD18) from hybridoma medium supernatant by affinity chromatography.

An agarose bead-coupled protein G-affinity column was equilibrated with 10 volumes of binding buffer. The hybridoma medium supernatant was applied to the column until saturation (determined by flow cytometry analysis of Jurkat cells stained with different fractions of the effluents). The column was washed with 10 volumes binding buffer and the antibodies were eluted with 4 volumes acidic elution buffer. Thereby the eluate was partitioned into collection tubes filled with 30 µl neutralization buffer to a final volume of 500 µl. Fractions with high antibody concentrations, estimated by measurement of OD_{280}, were pooled and subjected to protein concentration determination by the BCA method. All solutions used were filter-sterilized.

3.15.1.3. Materials

affinity column	HiTrap Protein G Sepharose column, 1 ml volume; Amersham
binding buffer	20 mM sodium phosphate, pH 7.0, prepared from 1 M Na_2HPO_4 and 1 M NaH_2PO_4 according to the Henderson-Hasselbalch equation
DMEM	Dulbecco's modified Eagle's medium; GibcoBRL
elution buffer	0.1 M glycine, pH 2.7, titrated with HCl
hybridoma cell lines	(see 3.14.1.)
neutralization buffer	1 M Tris, pH 9.0, titrated with HCl

3.15.2. DNA-mediated immunization of mice

Mouse anti-JAM-1 polyclonal antisera were commercially produced to order by DNA-mediated immunization (Eurogentec, Herstal, Belgium). The immune response against a foreign protein is induced in mice by direct gene transfer of plasmid DNA and subsequent *in vivo* expression of the vector-encoded antigen (Davis *et al.*, 1995). The DNA is injected into young myofibres of regenerating skeletal muscles that have been degenerated by injection of necrotizing snake-venom cardiotoxin.

For mice immunization, the JAM-1 antigen-encoding mammalian expression vector pJM1121 was amplified and isolated by a endotoxin-free maxiprep. 100 µg pJM1121 in endotoxin-free

PBS was injected at a concentration of 1 µg/µl into regenerating mouse *tibialis anterior* (TA) muscle 5 days postdegeneration (Eurogentec). Final bleedings were taken after 102 days and antisera were tested under experimental conditions versus preimmunization sera withdrawn from each mouse prior to their immunization. The polyclonal serum of mouse DS was sufficient for western blot analysis, whereas flow cytometry, transmigration and adhesion assays were carried out using the anti-JAM-1 serum of mouse TS.

Materials

endotoxin-free maxiprep	EndoFree Plasmid Maxi Kit; Qiagen (Hilden, Germany)
PBS (1x)	sterile and endotoxin-free; Sigma
TE (100x)	sterile and endotoxin-free; Sigma

4. Results

4.1. Determination of JAM-1 as CD11a-interacting protein

A yeast two-hybrid screen (as described in detail in 3.8.) was used to investigate new specific interaction partners of the β_2 integrin lymphocyte function-associated antigen-1 (LFA-1) α_L subunit, CD11a. The cDNA sequence of the cytoplasmic domain of CD11a was subcloned into the yeast two-hybrid (YTH) vector pAS2-1 and used to transform *S. cerevisiae* CG-1945. After a second transformation of this bait-expressing yeast strain with a human leukocyte cDNA library, CD11a was screened *in vivo* with cDNA library-encoded leukocyte proteins (**table 4**).

transformation efficiency (cfu/µg library DNA)	$1.7 \cdot 10^3$
screened clones	$3.4 \cdot 10^5$
His^+ clones	615
β-Gal^+ clones	3

table 4: Results of the YTH screening experiment for CD11a against a human leukocyte cDNA library.

Out of $3.4 \cdot 10^5$ clones screened, three candidate colonies (αLMC1 – αLMC3) appeared positive for β-galactosidase (β-Gal) expression indicating *lacZ* reporter gene activation (**fig. 5^A**). Isolation of library plasmid DNA from these clones allowed the sequence analysis of the respective prey-encoding cDNA inserts (**fig. 5^B**). Subsequent database alignment revealed one relevant candidate (αLMC3) plus two false-positives that contained library plasmids with cDNA inserts generating an *Alu*I repetitive sequence warning. The library plasmid of the *bona fide* candidate contained a cDNA insert of approximately 1.8 kb with an open reading frame (ORF) of 900 bp. The coding sequence encoded a prey protein that exhibited 75 % homology with the recently published junctional adhesion molecule (JAM)-1 of mice (Martìn-Padura *et al.*, 1998) and was previously identified as the human homologue (Ozaki *et al.*, 1999; Williams *et al.*, 1999). Hereafter a cDNA sequence of ~800 bp 3' to the ORF was shown to be identical to the published 3'-UTR[1] of human JAM-1 (Naik *et al.*, 2001). Thus, human JAM-1 was identified by the YTH system as a candidate CD11a-interacting protein.

[1] GenBank accession number AF172398

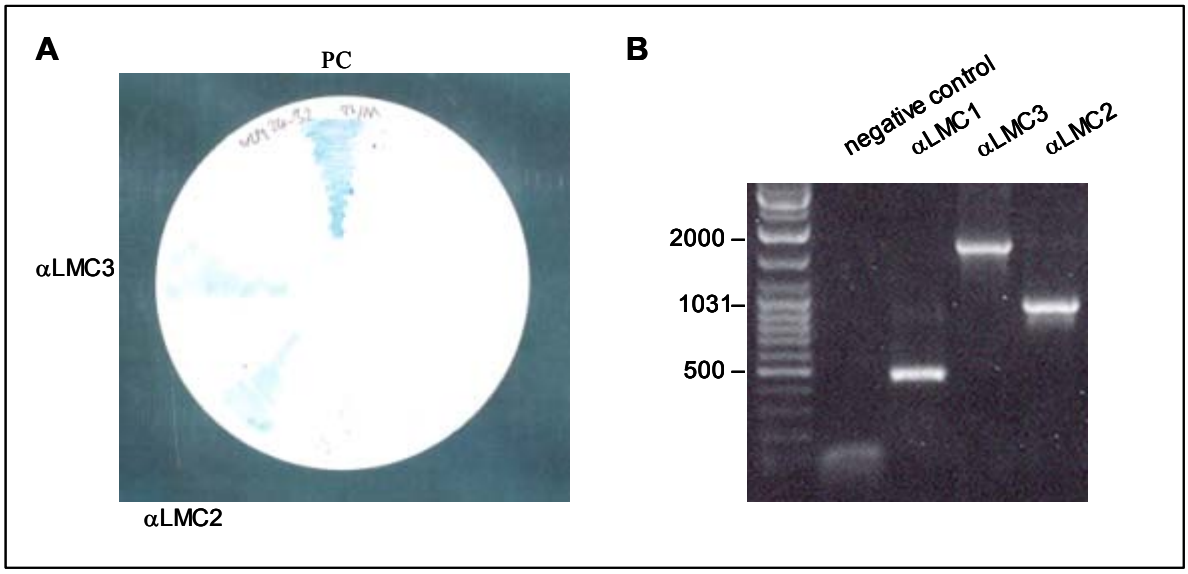

figure 5: **(A)** β-Gal filter assay for detection of *lacZ* reporter gene activated yeast cells. *HIS3*$^+$ colonies that survived primary nutritional selection together with a yeast positive control were replicated on filter paper and subjected to an enzymatic β-Gal assay that results in blue coloration of candidate positive clones bearing interacting bait and prey proteins due to the activity of *lacZ*-encoded β-galactosidase. *lacZ*-negative yeast colonies (not marked) showed no coloration. PC: positive control yeast strain (see 3.8.5.3.); αLMC2: second candidate yeast colony; αLMC3: third candidate yeast colony (*bona fide*). The β-Gal filter with the candidate yeast colony αLMC1 is not shown. **(B)** Analysis of the cDNA inserts of library plasmids isolated from the candidate yeast colonies αLMC1 (500 bp; lane 3), αLMC2 (1 kb; lane 5) and the *bona fide* candidate αLMC3 (1.8 kb; lane 4) by analytical PCR. Primers flanking the MCS of the YTH library vector pGAD10 allowed amplification of the prey-encoding cDNA inserts (see 3.11.5.). A complete reaction mix without template DNA served as a negative control for the PCR (lane 2). The PCR samples were subjected to analytical agarose gel electrophoresis. A representative 1 % agarose gel is shown stained with ethidium bromide and visualized under UV light. Molecular size markers are indicated in bp (lane 1).

4.2. Expression of JAM-1 in CHO transfectants and various cell types

To further elucidate the *in vivo* findings in yeast and to explore functional consequences of the supposed interaction between LFA-1 and JAM-1, both an eukaryotic cell model for JAM-1 surface expression and a polyclonal antibody directed against human JAM-1 were established. Isolation of the YTH library plasmid from the *bona fide* candidate yeast colony αLMC3, encoding the full-length prey protein, enabled the direct subcloning of human *JAM-1* cDNA into the mammalian expression vector pcDNA3 (pJM1121). Chinese hamster ovary (CHO) cells, adherent cells which grow to confluent monolayers but do not express endogenous JAM-1, were transfected with pJM1121 (CHO-JAM cells) or the pcDNA3 alone (CHO-vector cells). Polyclonal sera raised against human JAM-1 (anti–JAM-1) were generated by DNA-mediated immunization of mice with pJM1121 and enabled expression analysis of JAM-1 in CHO transfectants and various other cell types.

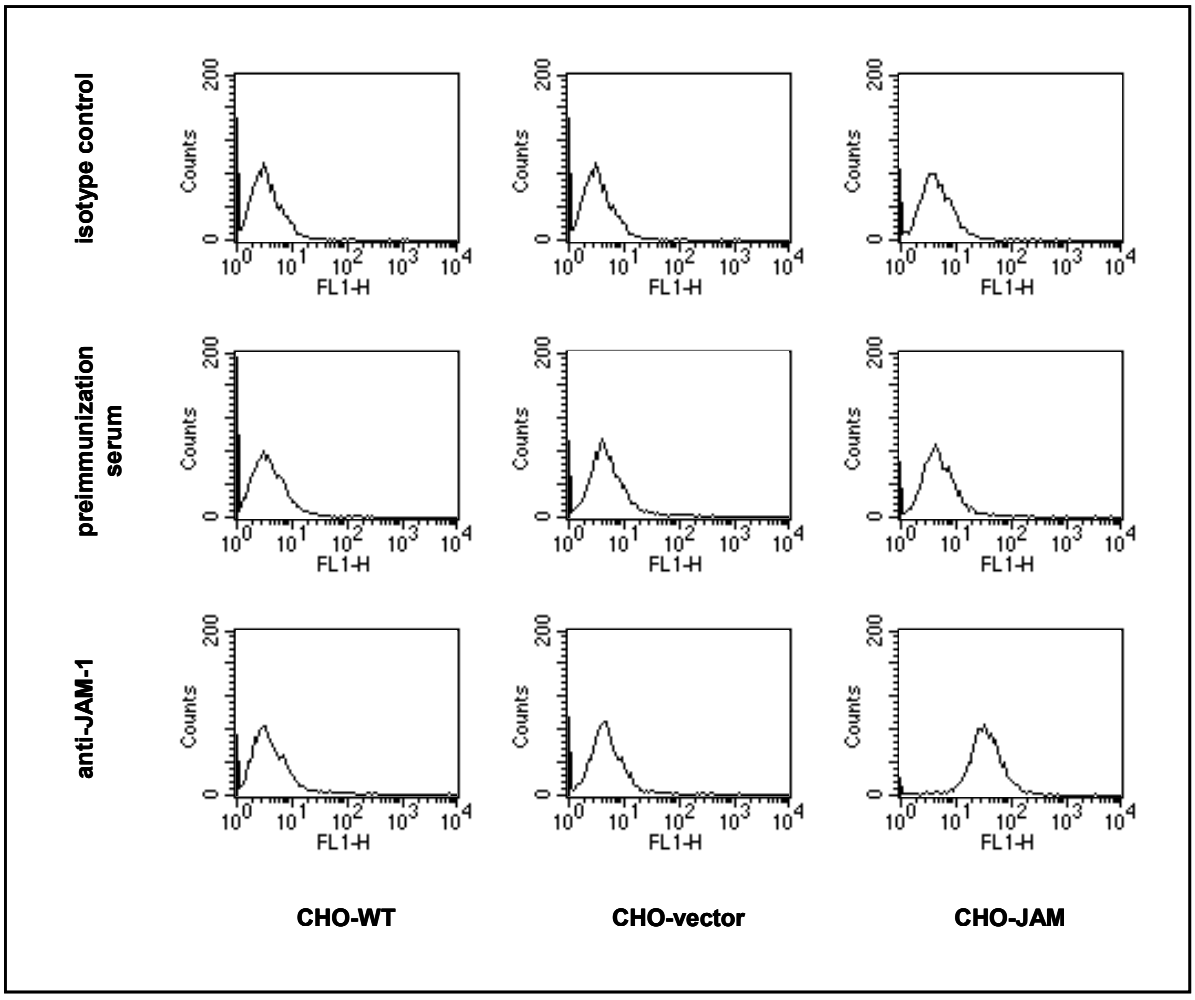

figure 6: Wild-type CHO cells (CHO-WT), CHO-vector and CHO-JAM transfectants were stained with an IgG_1 isotype control (upper plots), murine preimmunization serum (mid plots) or anti–JAM-1 (lower plots) for JAM-1 surface expression analysis by flow cytometry. "FL1-H" represents the logarithmic fluorescence intensity. Representative histograms are shown.

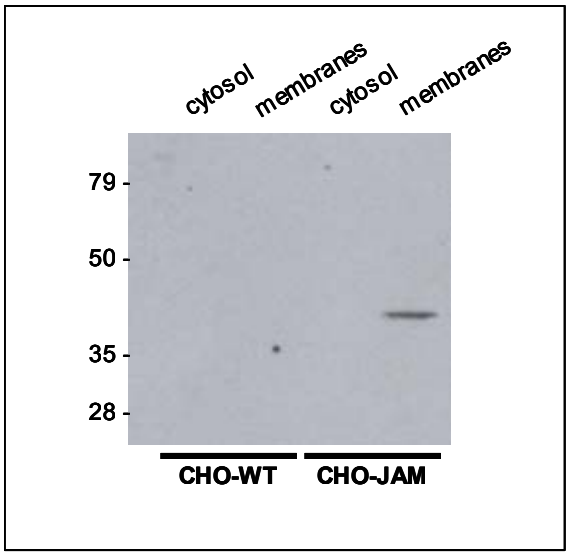

figure 7: Cytosolic (lane 1, 3) and membrane fractions (lane 2, 4) of whole cell lysates from wild-type CHO cells (CHO-WT; lane 1, 2) and CHO-JAM transfectants (lane 3, 4) were separated by SDS-PAGE and subjected to western blot analysis using anti–JAM-1. The antigen was detected as a single band at ~40 kDa, as indicated. The size of protein molecular weight markers is expressed in kDa. A representative blot is shown.

Flow cytometry analysis with anti–JAM-1 revealed surface expression of heterogeneous JAM-1 in CHO-JAM but not in CHO-vector transfectants (**fig. 6**). Specificity of the polyclonal antibody was demonstrated by the use of an isotype control and in particular murine preimmunization serum, both of which did not induce any shift in the distribution of fluorescence intensities for CHO transfectants or wild-type (CHO-WT) cells (**fig. 6**). Expression and localization of JAM-1 was further confirmed by immunoblotting, where the protein was detected by anti–JAM-1 exclusively in membrane but not in cytosolic fractions of whole cell lysates from CHO-JAM cells (**fig. 7**). Consistent with the lack of endogenous JAM-1 expression, wild-type CHO cells were not detected by anti–JAM-1 by either flow cytometry or immunoblotting analysis (**fig. 6, 7**).

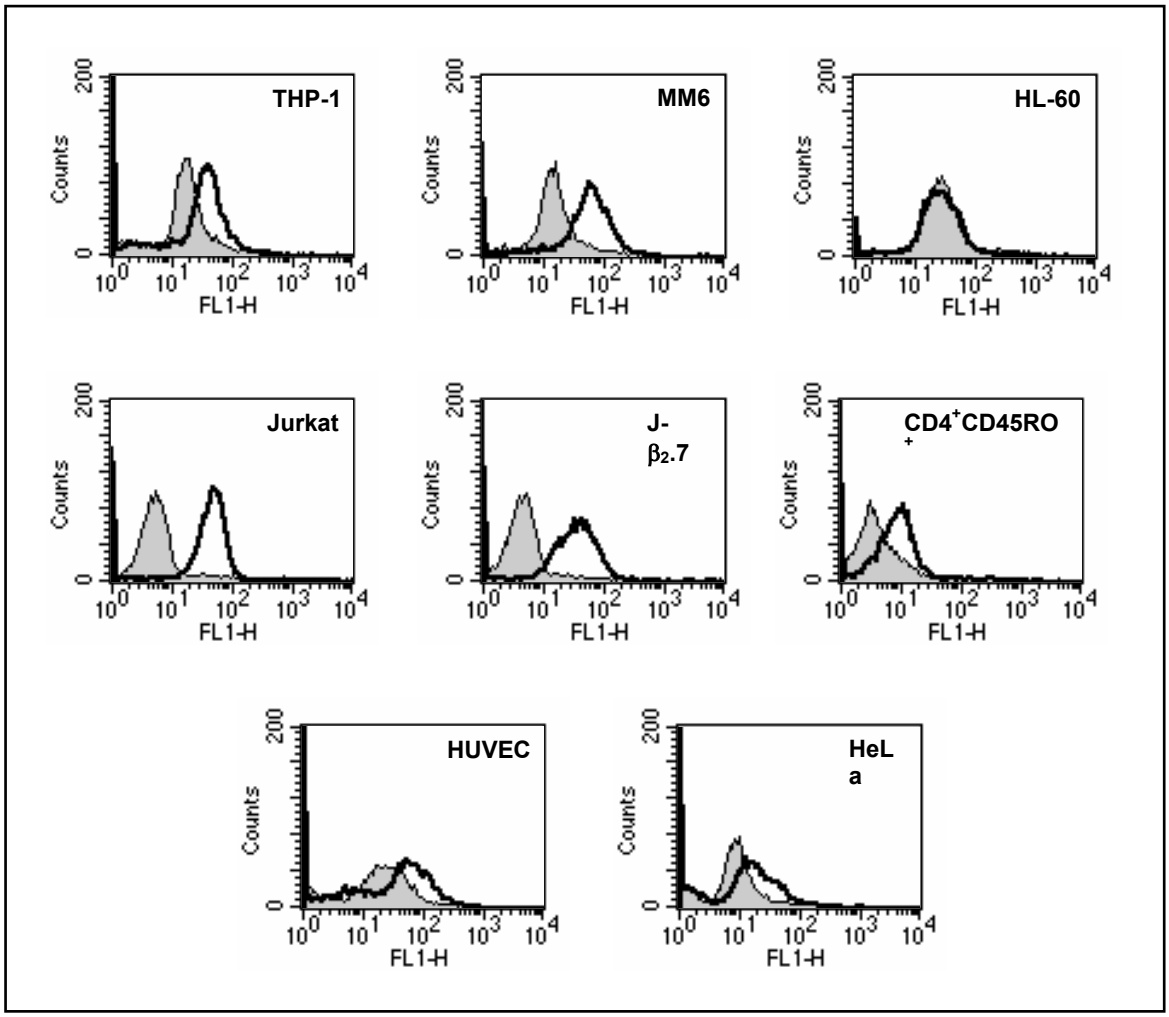

figure 8: Flow cytometry analysis of endogenous JAM-1 expressed on the surface of endothelial, epithelial and leukocytic cells in culture or isolated from the human vasculature, as indicated. The charts shown display overlaid histograms of cells stained with murine preimmunization serum (grey plots with thin line) and mouse anti–JAM-1 (white plots with thick line), respectively. JAM-1 was not detectable on the surface of myeloid HL-60 cells preincubated with 5 % human serum to block Fc receptors. "FL1-H" represents the logarithmic fluorescence intensity. Histograms shown are representative.

Native JAM-1 surface expression could be detected by anti–JAM-1 to a variable extent in different immortalized lines, *i.e.* epithelial-like HeLa cells, monocytic Mono Mac 6 and THP-1 cells, Jurkat and J-β_2.7 T lymphoid cells, and in several cells isolated from the human vascular system, *i.e.* $CD4^+CD45RO^+$ memory T cells and endothelial HUVECs, but was barely detectable on myeloid HL-60 cells (**fig. 8**). These results are consistent with published data (Ozaki *et al.*, 1999; Williams *et al.*, 1999).

4.3. Specific ability of CHO-JAM transfectants to support LFA-1–mediated leukocyte adhesion

Notably, the sequence of JAM-1 revealed structural homology with the LFA-1 ligands, IgSF proteins which are all members of the ICAM family. Given the importance of ICAMs in the formation of firm adhesive cell-cell interactions by integrins, a functional role for JAM-1 in leukocyte adhesion was assumed. To test this hypothesis and to verify the finding of a potential interaction between LFA-1 and JAM-1 identified in the YTH system, CHO transfectants were subjected to static leukocyte adhesion assays.

Incubation of fluorescence-labeled Jurkat T cells in suspension with adherent CHO cell monolayers grown in 96-well microtiter plates allowed the measurement of their mutual adhesion under static conditions by fluorescence spectrometry. Jurkat T cells, which express LFA-1 on their cell surface (see **fig. 12^B**), were transformed in an integrin-activated state by pretreatment with phorbol-12-myristate-13-acetate (PMA). Thus, stimulated Jurkat T cells showed significant binding to CHO-JAM but not to CHO-vector (**fig. 9^A**, black column) or wild-type CHO cells (data not shown), confirming JAM-1 may function as a heterophilic cell adhesion molecule (CAM). Shielding of JAM-1 surface ligands with anti–JAM-1 led to a significant decrease of the four-fold enhanced values for leukocyte adhesion on CHO-JAM cell monolayers to the background levels observed on cell monolayers lacking JAM-1 expression (**fig. 9^A**, grey column). To validate the involvement of leukocyte LFA-1 in the observed attachment, static adhesion assays were performed using Jurkat T cells preincubated with the CD18-blocking mAb TS1/18. In this case, adhesion of Jurkat T cells to JAM-1–expressing CHO cells was reduced to background levels, indicating that the binding was specifically mediated by leukocytic β_2 integrins (**fig. 9^A**, white column). An isotype control for TS1/18 and preimmunization serum directed against Jurkat and CHO-JAM cells, respectively, had no effect on adhesion (data not shown).

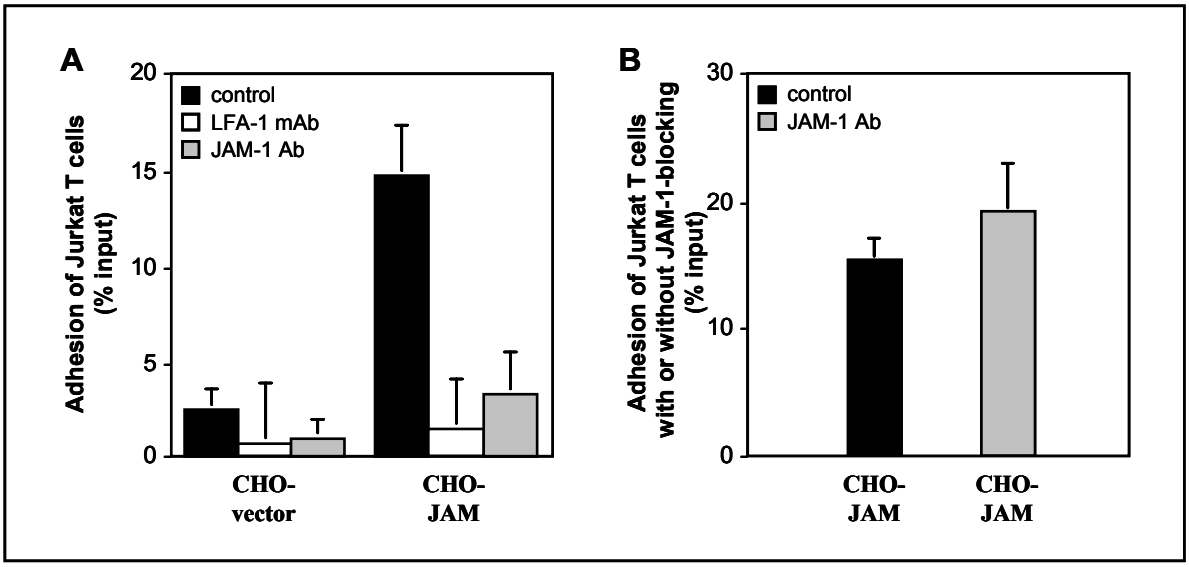

figure 9: **(A)** Adhesion of PMA-stimulated Jurkat T cells to adherent monolayers of CHO-vector and CHO-JAM cells, as indicated, under static conditions. Experiments were performed without application of antibodies (control; black column) or involving pretreatment of Jurkat T cells with the CD18-blocking mAb TS1/18 (white column) and preincubation of CHO cell monolayers with anti–JAM-1 (grey column). **(B)** Adhesion of PMA-stimulated Jurkat T cells without (control) or with anti–JAM-1 pretreatment, as indicated, to adherent CHO-JAM cell monolayers under static conditions. **(A-B)** Background binding of unstimulated Jurkat cells was negligible and was subtracted from stimulated binding. Adhesion was measured as the percentage of input Jurkat cells. Data are expressed as the mean ± s.d. of four separate experiments performed in triplicate.

Extracellular, homophilic interactions between JAM-1 proteins on opposite cells had previously been reported to occur (Martìn-Padura *et al.*, 1998; Liu *et al.*, 2000b). Since Jurkat T cells themselves express JAM-1 (see **fig. 8**) a homophilic interaction *in trans* between leukocytic JAM-1 and CHO cell-expressed JAM-1 in the observed cellular arrest was possible. Therefore, Jurkat T cells were pretreated with anti–JAM-1 and then subjected in a control experiment to adhesion on CHO-JAM cell monolayers (**fig. 9^{B}**). The pretreatment had no significant effect on cellular adhesion, thus excluding a significant participation of homophilic JAM-1 interactions in the firm arrest of Jurkat cells.

Static adhesion experiments therefore revealed that leukocyte arrest to CHO-JAM transfectants was specifically mediated by a heterophilic interaction between LFA-1 and JAM-1 and thus confirmed both the YTH findings and the presumed functional role of JAM-1 as a CAM.

4.4. Recognition of surface-expressed JAM-1 by purified LFA-1 receptor molecules

To further confirm a specific receptor-ligand interaction between LFA-1 and JAM-1 in cell adhesion, JAM-1–expressing CHO cells in suspension were exposed to purified and immobilized LFA-1 molecules instead to LFA-1 expressing Jurkat cells. Consistent with the previous findings, only JAM-1–transfected CHO cells but not CHO-vector transfectants developed adhesive binding to immobilized LFA-1 (**fig. 10**, black column). In turn, treatment of CHO cells with anti–JAM-1 (**fig. 10**, grey column) or neutralization of immobilized LFA-1 with TS1/18 (**fig. 10**, white column) completely inhibited the specific adhesion of CHO-JAM cells to the integrin receptor.

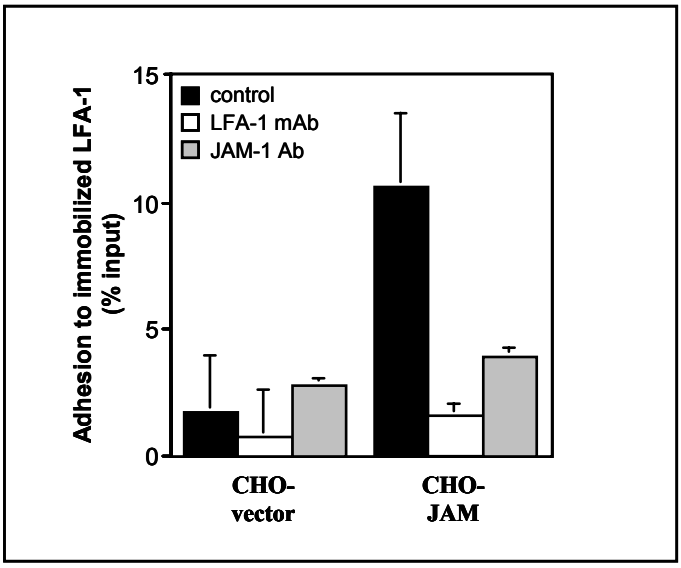

figure 10: Adhesion of CHO-vector and CHO-JAM cells, as indicated, to purified and immobilized LFA-1 receptor molecules under static conditions. Experiments were performed without application of antibodies (control; black column) or by blocking LFA-1 molecules with anti–CD18 mAb TS1/18 (white column) and preincubation of CHO cells in suspension with anti–JAM-1 (grey column). Isotype control and preimmunization serum had no effect on adhesion (data not shown). Adhesion was measured as the percentage of input CHO cells. Data are the mean ± s.d. of four separate experiments performed in triplicate.

Both the α_L (CD11a; 180 kDa) and the β_2 (CD18; 95 kDa) integrin chain could be detected in the LFA-1 preparation after SDS-PAGE by immunoblotting using appropriate antibodies (**fig. 11**). However, the polyclonal serum anti–JAM-1 failed to detect any JAM-1 impurity at the concentrations of LFA-1 used for the coating in static adhesion assays (**fig. 11**). Similarly, silver staining of the LFA-1 preparation after gel electrophoresis revealed distinct bands for the LFA-1 subunits (**fig. 11**) but did not indicate any JAM-1 impurity. An appreciable co-purification of JAM-1 in the course of LFA-1 isolation from human organs could therefore be excluded, which

was in principle possible, given the evidence for a receptor-ligand interaction between LFA-1 and JAM-1.

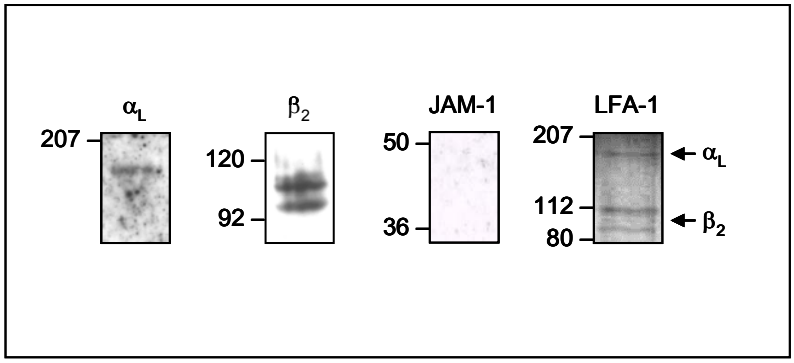

figure 11: Protein analysis of the molecular LFA-1 preparation. Purified LFA-1 was subjected to SDS-PAGE at the same concentrations used in static adhesion assays. Immunoblot analysis with anti-α_L C-17 (also verified with the mAb MCA 502; data not shown) and β_2 mAb MEM48, respectively, under non-reducing conditions **(left panels)** revealed a distinct band for α_L at ~180 kDa and a double band for β_2 between 100-120 kDa, presumably due to differential glycosylation. JAM-1 impurity that would be expected at ~40 kDa was not detectable by western blotting with anti–JAM-1 **(third panel)**. Protein detection by silver staining **(right panel)** did not indicate any protein impurities and revealed distinct bands corresponding to the α and β chains of LFA-1 as observed in the corresponding immunoblots. Protein molecular weight markers are indicated in kDa. Representative blots and gels are shown.

The results obtained using purified LFA-1 (in this way excluding the cellular background provided by the LFA-1–expressing Jurkat T cells used in the previous static adhesion experiments), strongly support a functional role for the cell-surface expressed JAM-1 as a specific ligand for the integrin receptor LFA-1 in cell-cell adhesion. The lack of leukocytic JAM-1 as a potential adhesion target for CHO-JAM transfectants in these experiments on immobilized LFA-1, confirmed the heterophilic nature of the cell adhesion-mediating molecular interaction and revealed that Jurkat T cell arrest on CHO-JAM cells (see **fig. 9**) was not supported by homophilic interactions with leukocytic JAM-1. These results are consistent with findings that recombinant solid-phase JAM-1 does not mediate adhesion of JAM-1–transfected COS cells (Williams *et al.*, 1999).

4.5. Receptor specificity of JAM-1 for the β_2 integrin LFA-1

The cell line J-β_2.7 is a mutant Jurkat T cell line deficient in α_L (CD11a) expression due to chemical mutagenesis (Weber *et al.*, 1997b). Since subunit heterodimerization is required for integrin translocation to the plasma membrane, integrin α and β chains are interdependent for their cell surface expression (Anderson *et al.*, 1987; Arnaout, 1990). The α_L-deficient J-β_2.7 cells

are therefore characterized as a lymphoid cell line lacking LFA-1 cell surface receptors despite normal expression of endogenous β_2 (CD18) chains. They provided an ideal system to investigate the specific involvement of LFA-1 in cellular arrest of the primordial Jurkat T cells to JAM-1–expressing CHO cells.

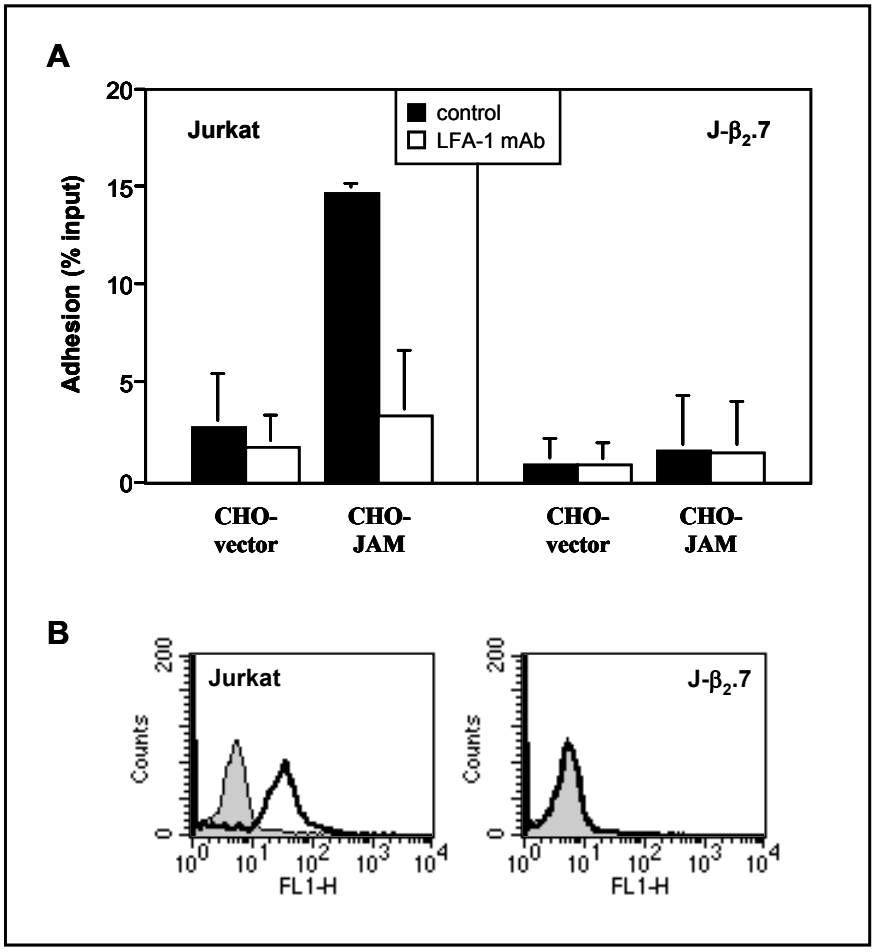

figure 12: **(A)** Adhesion of **(left panel)** PMA-stimulated wild-type Jurkat cells and **(right panel)** PMA-stimulated α_L-deficient Jurkat J-β_2.7 cells to adherent monolayers of CHO-vector and CHO-JAM cells, as indicated, performed in parallel under static conditions. Experiments were performed without (control; black column) or with (white column) preincubation of Jurkat cells with the β_2-blocking mAb TS1/18. Background binding of unstimulated wild-type and mutant Jurkat cells was negligible and was subtracted from stimulated binding. Adhesion was measured as percentage of input Jurkat cells. Data are mean ± s.d. of four separate experiments performed in triplicate. **(B)** Flow cytometry control analysis of LFA-1 surface expression in wild-type Jurkat cells **(left plot)** and mutant Jurkat J-β_2.7 cells **(right plot)**. The charts shown display overlaid histograms of cells stained with a mouse IgG_1 isotype control (grey plots with thin line) and TS1/18 mAb (white plots with thick line). "FL1-H" represents the logarithmic fluorescence intensity. Representative histograms are shown.

Static leukocyte adhesion assays on CHO cell monolayers were performed in parallel with PMA-stimulated wild-type Jurkat cells (**fig. 12**$^{\mathbf{A}}$, left panel) and mutant Jurkat J-β_2.7 cells (**fig. 12**$^{\mathbf{A}}$, right panel). Wild-type Jurkat cells adhered exclusively to CHO-JAM cell monolayers. This specific cell-cell interaction was suppressed by neutralization of leukocytic LFA-1 receptors with the blocking β_2 mAb TS1/18 (**fig. 12**$^{\mathbf{A}}$, left panel) as has been shown in previous experiments

(see **fig. 9^{A}**). In contrast to the wild-type cells, PMA-stimulated J-β_2.7 mutants completely failed to adhere onto CHO-JAM transfectants (**fig. 12^{A}**, right panel). This clearly confirms the reliance on LFA-1 for leukocyte binding to JAM-1–presenting cells. As expected for α_L-deficient cells, incubation of J-β_2.7 cells with TS1/18 had no effect on adhesion values (**fig. 12^{A}**, right panel). As a control, LFA-1 expression profiles of Jurkat and J-β_2.7 cells were verified by flow cytometry (**fig. 12^{B}**).

Transfection of J-β_2.7 cells with α_L-encoding cDNA (referred to hereafter as J-β_2.7/α_L cells) reconstituted LFA-1 surface expression formerly knocked out in J-β_2.7 cells, as confirmed by flow cytometry analysis (**fig. 14^{A}**). Compared to its parental cell line, transfected J-β_2.7/α_L cells showed restored adhesion to CHO-JAM cells under static conditions that was not observable on CHO-vector cell monolayers (**fig. 13**, left panel). This reconfirmed the requirement of intact LFA-1 surface expression for adhesion of Jurkat T cells to JAM-1–presenting cells.

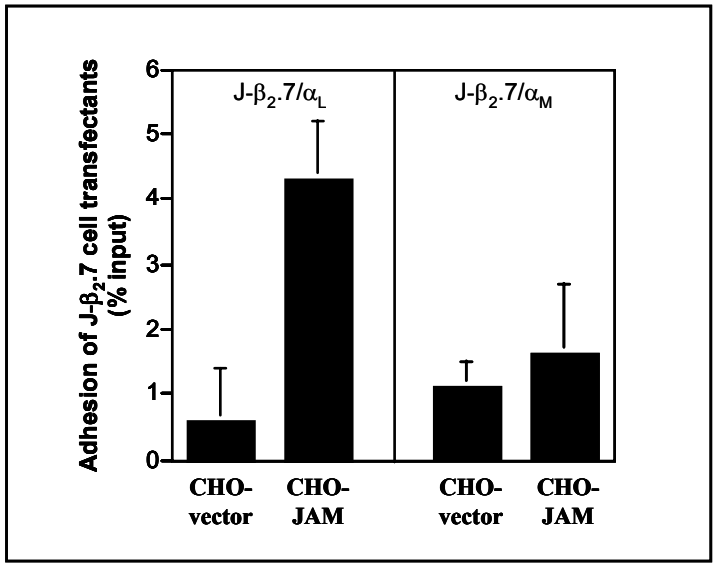

figure 13: Adhesion of **(left panel)** PMA-stimulated J-β_2.7/α_L cells expressing reconstituted LFA-1 and **(right panel)** PMA-stimulated J-β_2.7/α_M cells expressing heterotopic Mac-1 to adherent monolayers of CHO-vector and CHO-JAM cells, as indicated, under static conditions. α chain-transfected J-β_2.7 cells without PMA-stimulation showed negligible background binding that was subtracted from stimulated binding. Adhesion was measured as the percentage of input cells. Data are the mean ± s.d. of four separate experiments performed in triplicate.

Although the YTH data implied an interaction between JAM-1 and CD11a and thus a specific interaction with the β_2 integrin LFA-1 ($\alpha_L\beta_2$; CD11a/CD18), affinity of JAM-1 for other members of the β_2 integrin family could not be excluded. This possibility was tested by static adhesion assays of J-β_2.7/α_M cells to CHO-JAM cell monolayers. Due to transfection of J-β_2.7 cells with α_M–encoding cDNA, J-β_2.7/α_M cells expressed heterotopic α_M. Heterodimerization of this α subunit with the endogenously translated β_2 subunit led to the formation and subsequent

surface expression of the β_2 integrin Mac-1 ($\alpha_M\beta_2$; CD11b/CD18) normally not expressed by lymphoid cells (Weber *et al.*, 1999a). The J-β_2.7/α_M cells, still deficient in α_L, thus carried Mac-1 ($\alpha_M\beta_2$) but not the homologous LFA-1 ($\alpha_L\beta_2$) receptors on their cell membrane.

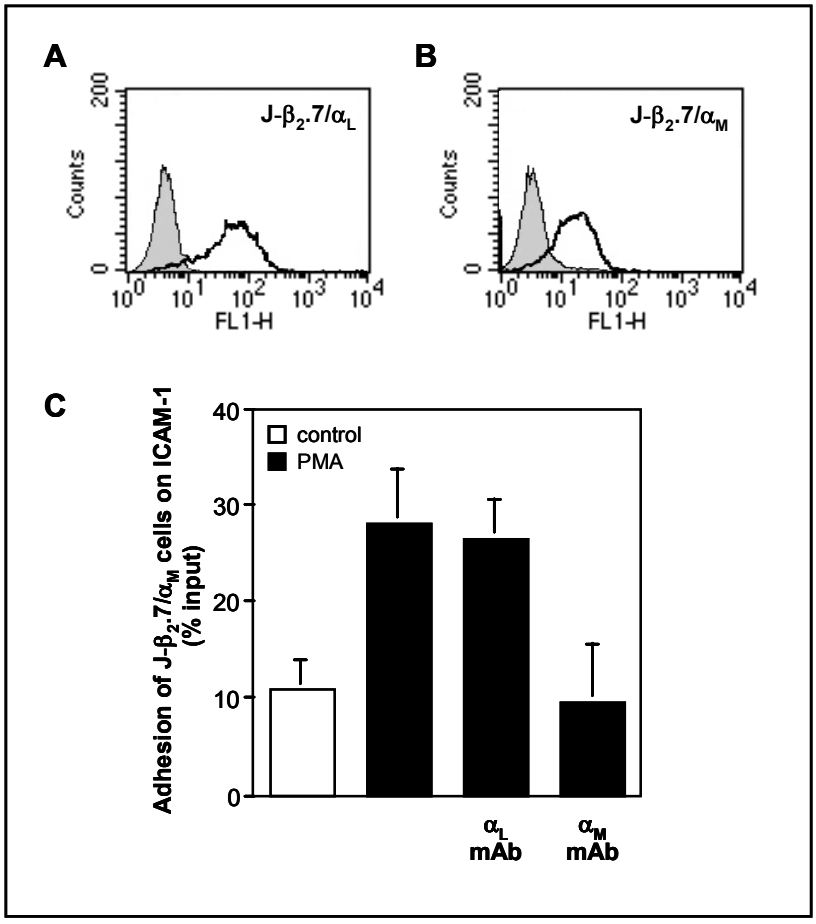

figure 14: Control experiments. **(A-B)** Flow cytometry analysis for surface expression of **(A)** reconstituted LFA-1 on J-β_2.7/α_L cells and **(B)** heterotopic Mac-1 on J-β_2.7/α_M cells. Charts shown display overlaid histograms of cells stained with an IgG_1 isotype control (grey plots) and α_L mAb TS1/22 respective α_M mAb CBRM1/29 (white plots). "FL1-H" represents the logarithmic fluorescence intensity. Histograms shown are representative. **(C)** Adhesion of J-β_2.7/α_M cells expressing heterotopic Mac-1 onto purified and immobilized ICAM-1 molecules under static conditions. Experiments were performed without (control; white column) or with PMA-stimulation (black column) of J-β_2.7/α_M cells and application of blocking α_L mAb TS1/22 respective blocking α_M mAb CBRM1/29, as indicated. An IgG_1 isotype control had no effect on adhesion (data not shown). Adhesion was measured as the percentage of input J-β_2.7/α_M cells. Data are the mean ± s.d. of three separate experiments performed in triplicate.

In contrast to J-β_2.7/α_L cells (**fig. 13**, left panel), J-β_2.7/α_M cells failed to develop adhesive cell-cell interactions with monolayers of CHO-JAM transfectants (**fig. 13**, right panel) despite surface expression of Mac-1, as revealed by flow cytometry analysis (**fig. 14^B**). Nevertheless, Mac-1 expression on the plasma membrane was functional as determined by Mac-1–dependent adhesion of PMA-stimulated J-β_2.7/α_M cells onto purified ICAM-1 (**fig. 14^C**) consistent with

previous data (Weber *et al.*, 1999a). Thus, JAM-1 specifically interacts with LFA-1 and not with the homologous β_2 integrin Mac-1.

4.6. Inability of homophilic JAM-1 interactions to support leukocyte adhesion

Murine as well as human JAM-1 functions as CAMs between endothelial and epithelial cells in a homophilic manner. However, as both LFA-1–bearing wild-type Jurkat cells and α_L-deficient Jurkat J-β_2.7 cells showed equivalent JAM-1 expression on their cell membranes (see **fig. 8**), the marked difference in their adhesion to JAM-1–presenting CHO cell monolayers (see **fig. 12^A**) indicated that homophilic interactions of JAM-1 do not contribute to such a cell-cell interaction. The complete suppression of Jurkat cell adhesion to CHO-JAM cell monolayers to background levels by the use of a LFA-1 blocking mAb (see **fig. 9^A**) led to the prediction that leukocytic JAM-1 does not bind to CHO cell–expressed JAM-1 in a homophilic manner that would be sufficient to mediate firm cell-cell adhesion.

To further test for a possible involvement of homophilic JAM-1 interactions in cellular adhesion, CHO-JAM cells in suspension, that showed significant arrest on immobilized LFA-1 (see **fig. 10**), were subjected to static adhesion on CHO-JAM cell monolayers. The adhesion values did not differ from those of wild-type CHO cells in suspension (**fig. 15**). This indicated that CHO-JAM transfectants were not capable to perform mutual cellular arrest via homophilic JAM-1 binding *in trans*.

Leukocyte adhesion due to homophilic JAM-1 interactions was also ruled out by experiments with HL-60 cells. Consistent with published data (Williams *et al.*, 1999), this myeloid cell line lacked detectable JAM-1 surface expression as verified by flow cytometry (see **fig. 8**). However, HL-60 cells were able to form adhesive cell contact with CHO-JAM cells mediated by their LFA-1 receptor as shown in adhesion studies using the LFA-1 α_L mAb TS1/22 (**fig. 16**).

Together, these data showed that homophilic interactions of surface JAM-1 appear to be insufficient to mediate firm cellular arrest of leukocytes.

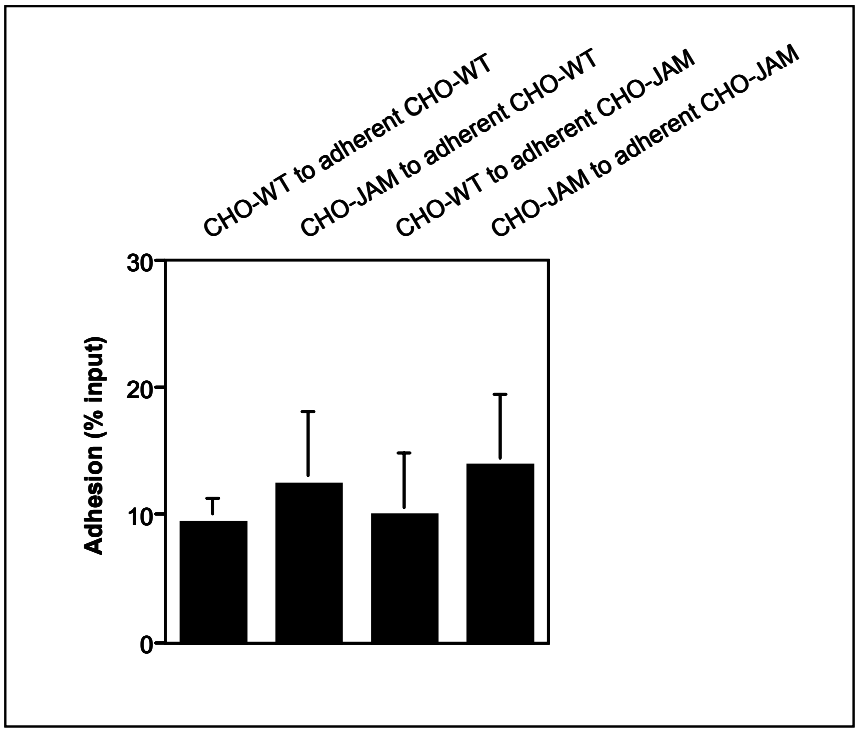

figure 15: Adhesion of wild-type CHO cells and CHO-JAM transfectants in suspension to adherent monolayers of wild-type CHO and CHO-JAM cells, as indicated, under static conditions. Adhesion was measured as the percentage of input of CHO suspension cells. Data are the mean ± s.d. of four separate experiments performed in triplicate.

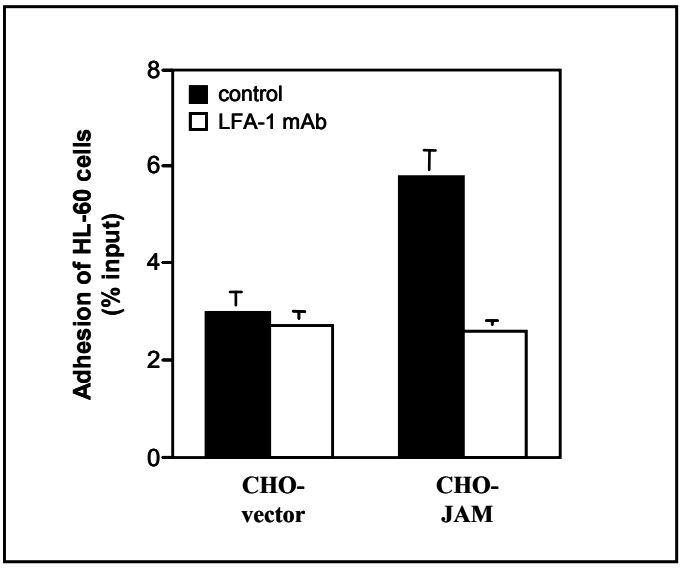

figure 16: Adhesion of PMA-stimulated myeloid HL-60 cells on adherent CHO-vector or CHO-JAM cell monolayers, as indicated, under static conditions. HL-60 cells were preincubated with 5 % human serum to block Fc receptors. Experiments were performed without (control; black column) or with (white column) preincubation of HL-60 cells with the α_L-blocking mAb TS1/22. Background binding of unstimulated HL-60 cells was negligible and was subtracted from stimulated binding. Adhesion was measured as the percentage of input HL-60 cells. Data are the mean ± s.d. of four separate experiments performed in triplicate.

4.7. Dependence on Ig-like domain 2 for LFA-1 receptor binding of JAM-1

Given that the IgSF member JAM-1 might function as a counter-receptor for the integrin LFA-1, it was of special interest to investigate which regions within the extracellular part of JAM-1 could be essential for mediating this protein interaction. Considering the molecular structure of JAM-1 (**fig. 17**), a requirement of either the N-terminal Ig-like domain 1 or the membrane-proximal Ig-like domain 2 for heterophilic interaction was conceivable. Therefore mutant *JAM-1* cDNA constructs were generated by PCR overlap extension that were each deficient in one of the extracellular domains (referred to hereafter as $JAM^{?D1}$ and $JAM^{?D2}$, respectively; **fig. 17**).

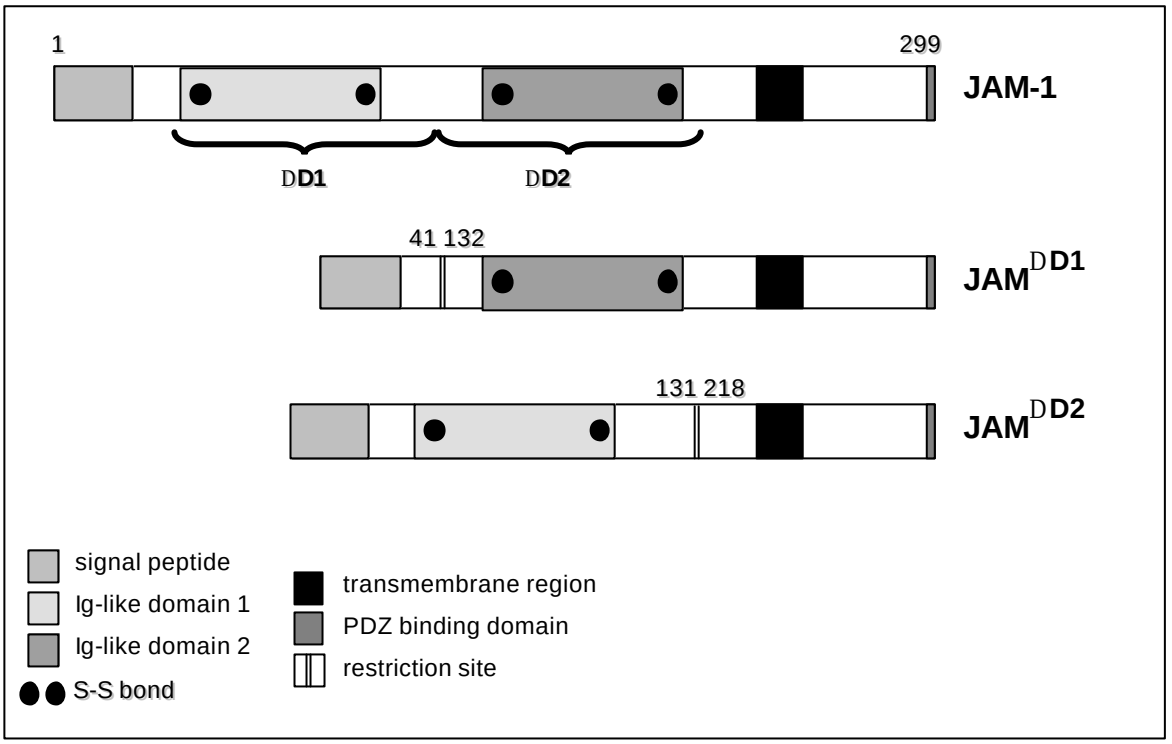

figure 17: Schematic representation of the full-length human JAM-1 protein (aa 1-299) and the mutant JAM-1 protein constructs $JAM^{?D1}$ and $JAM^{?D2}$ as expressed in CHO transfectants. The N-terminal signal peptide (aa 1-27) is shown in light grey, the predicted transmembrane region (aa 236-260) in black. The C-terminal PDZ domain-binding motif FLV (aa 297-299) is shown in grey. The N-terminal Ig-like domain 1 and the membrane-proximal Ig-like domain 2 are shown striated, as indicated. Their Ig-like loop-confining disulfide bonds are each marked with two black points. cDNAs encoding the mutant JAM-1 proteins were generated by PCR overlap extension as described. Deleted regions are marked by curly brackets: region D1 (aa 42-131) in $JAM^{?D1}$ and region D2 (aa 132-217) in $JAM^{?D2}$. Resulting restriction sites are marked by a double-slash (||). $JAM^{(HA)}$, $JAM^{?D1(HA)}$ and $JAM^{?D2(HA)}$ protein constructs (not shown) correspond to the illustrated proteins with an additional hemagglutinin (HA) epitope fused to the respective C-terminus.

The mutant *JAM-1* cDNA constructs were subcloned into the mammalian expression vector pcDNA3 and subsequently transfected into wild-type CHO cells (CHO-$JAM^{?D1}$ and CHO-$JAM^{?D2}$ cells, respectively). However, anti–JAM-1 failed to detect mutant JAM-1 proteins in transfected cells (data not shown). Expression of $JAM^{?D1}$ and $JAM^{?D2}$ was therefore analyzed at the transcriptional level by reverse transcriptase polymerase chain reaction (RT-PCR) using

total RNA isolated from wild-type and transfected CHO cells (**fig. 18^{A}**). Agarose gel electrophoresis of the PCR products obtained by amplification with specific primers for human *JAM-1* cDNA revealed transcription of full-length *JAM-1* mRNA (900 bp) in CHO-JAM transfectants but not in CHO-vector transfectants nor in wild-type CHO cells (**fig. 18^{A}**). Likewise, expression of domain 1-deficient *JAM-1* mRNA (660 bp) in CHO-JAM$^{\Delta D1}$ cells and domain 2-deficient *JAM-1* mRNA (672 bp) in CHO-JAM$^{\Delta D2}$ cells was confirmed at the transcriptional level (**fig. 18^{A}**).

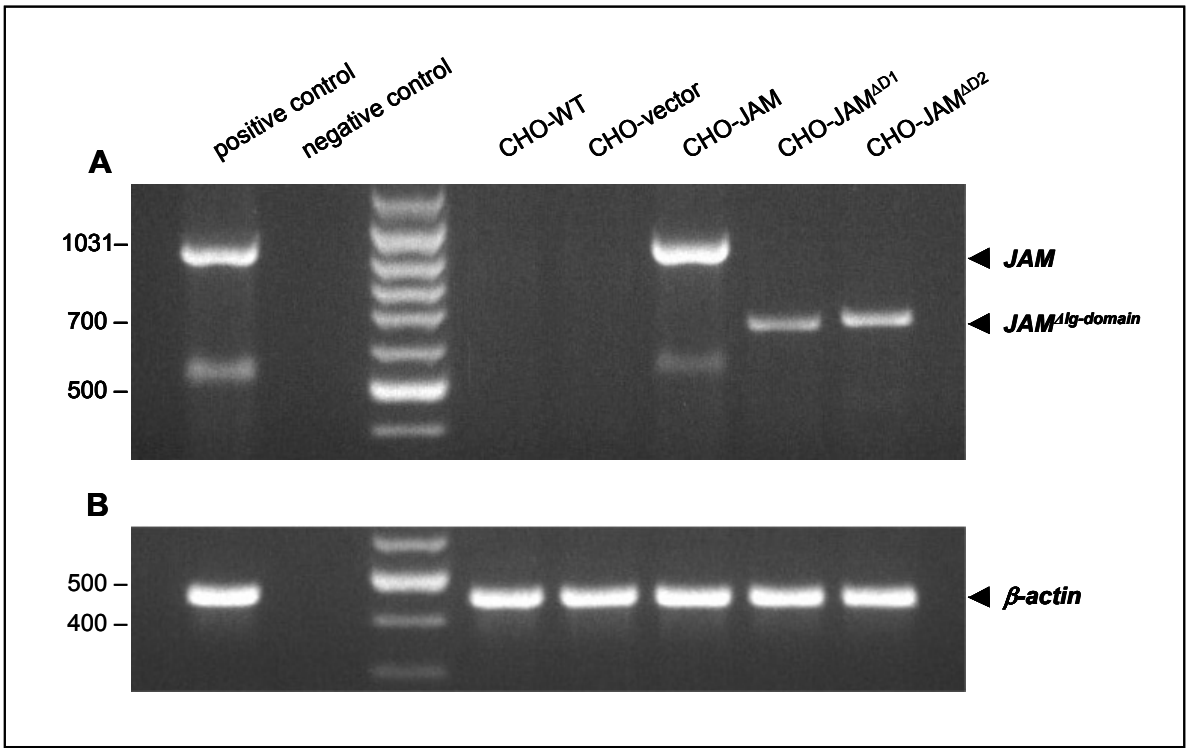

figure 18: **(A)** Expression analysis of transcribed full-length human *JAM-1* mRNA (900 bp) in wild-type CHO (lane 4), CHO-vector (lane 5) and CHO-JAM cells (lane 6), and of mutant *JAM-1* mRNA deficient in either the N-terminal Ig-like domain 1 (*JAM$^{\Delta D1}$*; 660 bp; lane 7) or the membrane-proximal Ig-like domain 2 (*JAM$^{\Delta D2}$*; 672 bp; lane 8) expressed in CHO-JAM$^{\Delta D1}$ and CHO-JAM$^{\Delta D2}$ transfectants, respectively. PCR on pJM1121 plasmid DNA served as a positive control (900 bp; lane 1) for amplification of *JAM-1*–related cDNA. An unspecific band of ~580 bp appeared by amplification of the full-length *JAM-1* cDNA due to the primer design (lanes 1 and 6). A complete reaction mix without template DNA served as negative control (lane 2) for the PCR. **(B)** Control expression analysis of *β-actin* mRNA transcripts (446 bp) in identical preparations of total RNA from CHO cells as used in (A). DNA contamination in the RNA samples was excluded by failure of a longer 652-bp fragment amplified from intron-containing genomic *β-actin* DNA. Thus, amplified cDNA fragments in (A) resulted exclusively from transcribed *JAM-1* mRNA. A human foreskin fibroblast preparation served as positive control (446 bp; lane 1) for *β-actin* cDNA amplification. A complete reaction mix without template DNA served as negative control (lane 2). **(A-B)** Total RNA was isolated from CHO cells and mRNA was reverse transcribed by RT-PCR using random hexamer primers. For each investigated CHO cell line, target cDNAs were amplified in separate PCRs but from identical RNA preparations using primers specific for *JAM-1*–related and *β-actin* DNA, respectively. PCR samples were subjected to analytical agarose gel electrophoresis. Shown are representative 1 % agarose gels stained with ethidium bromide and visualized under UV light. Molecular size markers (lane 3) are indicated in bp.

Possible DNA contamination of RNA extracts, leading to false-positive detection of genomic *JAM-1* sequences instead of *in vivo* transcribed *JAM-1* mRNA, was excluded by a control PCR using the respective RT-PCR samples and primers specific for the housekeeping gene *β-actin*

(**fig. 18^{B}**). In the case of a DNA contamination this PCR would lead to additional amplification of a genomic *β-actin* fragment including intron sequences (652 bp; data not shown) in addition to the fragments derived from spliced *β-actin* mRNA transcripts (446 bp; **fig. 18^{B}**).

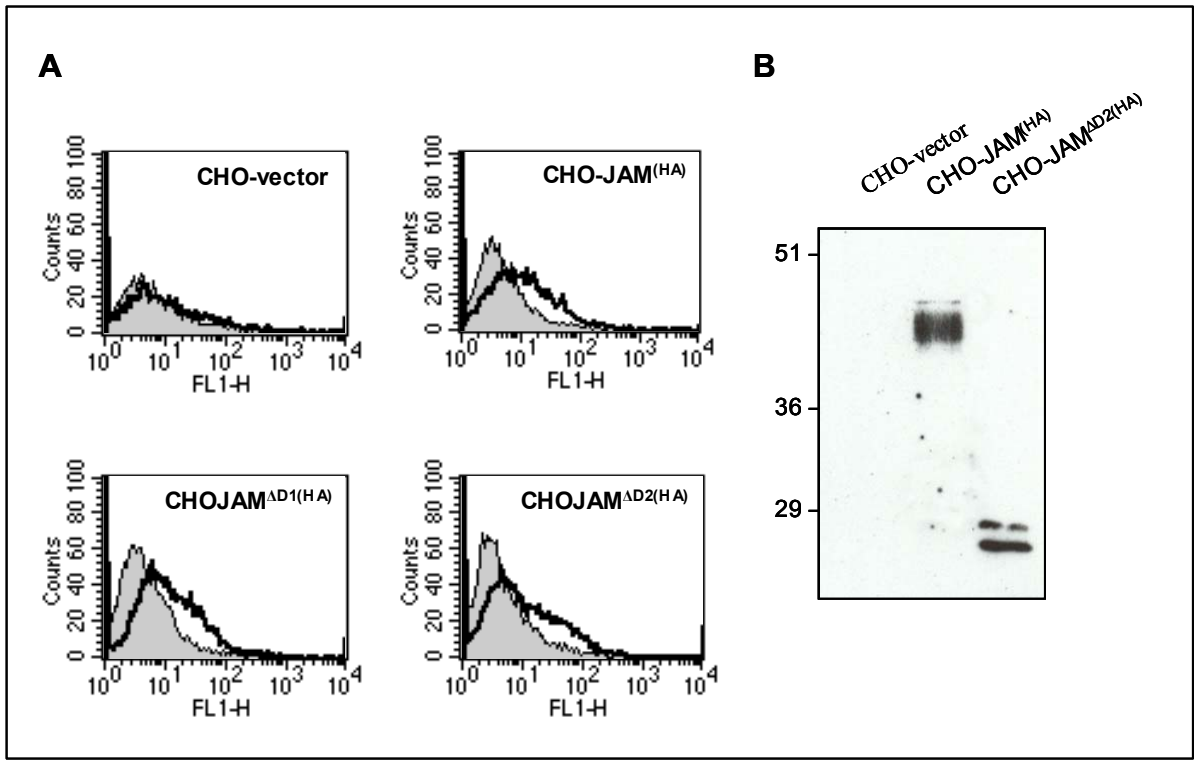

figure 19: **(A)** Expression analysis of HA-tagged full-length and mutant JAM-1 proteins in permeabilized CHO-vector, CHO-JAM$^{(HA)}$, CHO-JAM$^{\Delta D1(HA)}$ and CHO-JAM$^{\Delta D2(HA)}$ transfectants, as indicated, by flow cytometry. Charts shown display overlaid histograms of cells stained with a rabbit IgG isotype control (grey plot with thin line) and anti-HA Y-11 (white plot with thick line), respectively. "FL1-H" represents the logarithmic fluorescence intensity. Histograms shown are representative. **(B)** Western blot analysis of whole cell lysates from CHO-vector, CHO-JAM$^{(HA)}$ and CHO-JAM$^{\Delta D2(HA)}$ transfectants, as indicated. Protein samples were separated by SDS-PAGE and subjected to western blot analysis using anti-HA Y-11. Mutant JAM$^{\Delta D2(HA)}$ appeared in multiple bands at ~26 kDa. Molecular weight markers are expressed in kDa. A representative blot is shown.

Despite confirmation of *JAM$^{\Delta D1}$* and *JAM$^{\Delta D2}$* mRNA transcription in the corresponding CHO transfectants, the presence of normal mRNA translation, absence of protein degradation and sufficient surface expression of the mutant JAM-1 molecules remained untested. For this reason, cDNA constructs were generated and transfected into wild-type CHO cells that allowed expression of full-length and mutant JAM-1 proteins fused to a C-terminal hemagglutinin (HA) epitope (CHO-JAM$^{(HA)}$, CHO-JAM$^{\Delta D1(HA)}$ and CHO-JAM$^{\Delta D2(HA)}$ cells, respectively). Expression of the HA-tagged constructs at the mRNA level was again verified by RT-PCR (data not shown). In addition, flow cytometry analysis of permeabilized CHO transfectants with anti-HA confirmed equivalent protein expression for all HA-tagged JAM-1 constructs (**fig. 19^{A}**). Western blot analysis revealed the molecular size for mutant JAM$^{\Delta D2(HA)}$ to be approximately 26 kDa (**fig. 19^{B}**).

Both types of CHO transfectants, expressing JAM-1 constructs with or without HA epitope, were grown to confluence and used as substrates for static adhesion assays with PMA-stimulated Jurkat T cells (**fig. 20^{A+B}**). CHO-JAM$^{\Delta D1}$ cells supported considerable adhesion of Jurkat T cells equivalent to that seen on CHO-JAM transfectants presenting full-length JAM-1 on their surface (**fig. 20^{A}**). In contrast, adhesion of Jurkat T cells on CHO-JAM$^{\Delta D2}$ cell monolayers did not show substantial differences from background binding on CHO-vector cell monolayers (**fig. 20^{A}**). Equivalent results were obtained for leukocyte binding to CHO-JAM$^{(HA)}$, CHO-JAM$^{\Delta D1(HA)}$ and CHO-JAM$^{\Delta D2(HA)}$ cells, indicating that the cytoplasmic HA epitope did not altered the binding characteristics of the transfected cells (**fig. 20^{B}**).

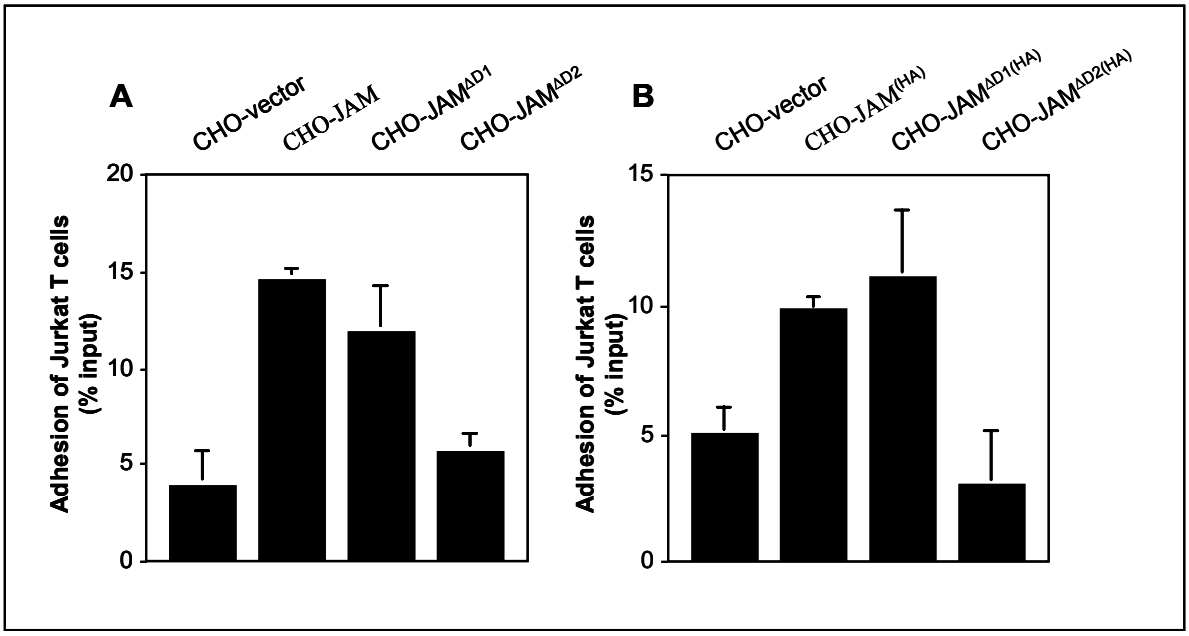

figure 20: **(A)** Adhesion of PMA-stimulated Jurkat T cells to CHO-vector cell monolayers and to CHO cell monolayers expressing wild-type JAM-1 (CHO-JAM) or mutant JAM-1 lacking the N-terminal Ig-like domain 1 (CHO-JAM$^{\Delta D1}$) or the membrane-proximal Ig-like domain 2 (CHO-JAM$^{\Delta D2}$), as indicated, under static conditions. JAM-1 and related proteins were expressed without HA epitope tag. **(B)** Adhesion of PMA-stimulated Jurkat cells as described for (A) but subjected to monolayers of CHO transfectants that expressed full-length and mutant JAM-1 with a C-terminal HA epitope tag, *i.e.* CHO-JAM$^{(HA)}$, CHO-JAM$^{\Delta D1(HA)}$ and CHO-JAM$^{\Delta D2(HA)}$ cells. **(A-B)** Background binding of unstimulated Jurkat cells was negligible and was subtracted from stimulated binding. Adhesion was measured as the percentage of input Jurkat cells. Data are the mean ± s.d. of four separate experiments performed in triplicate.

Static adhesion assays with purified LFA-1 as adhesion target for CHO transfectants in suspension confirmed the importance of the membrane-proximal domain 2 of JAM-1 for receptor recognition. CHO-JAM$^{\Delta D2}$ cells lacking this specific region failed to bind to immobilized LFA-1 and showed only nonspecific background binding similar to that of CHO-vector transfectants (**fig. 21^{A}**). However, the absence of the N-terminal domain 1 in JAM-1 did not interfere with normal receptor recognition and binding, leading to similar adhesion values for CHO-JAM$^{\Delta D1}$ cells to those obtained with CHO-JAM cells on molecular LFA-1 (**fig. 21^{A}**). Again, performance of the binding assay with CHO transfectants expressing HA-tagged JAM-1 proteins resulted in equivalent adhesion characteristics (**fig. 21^{B}**).

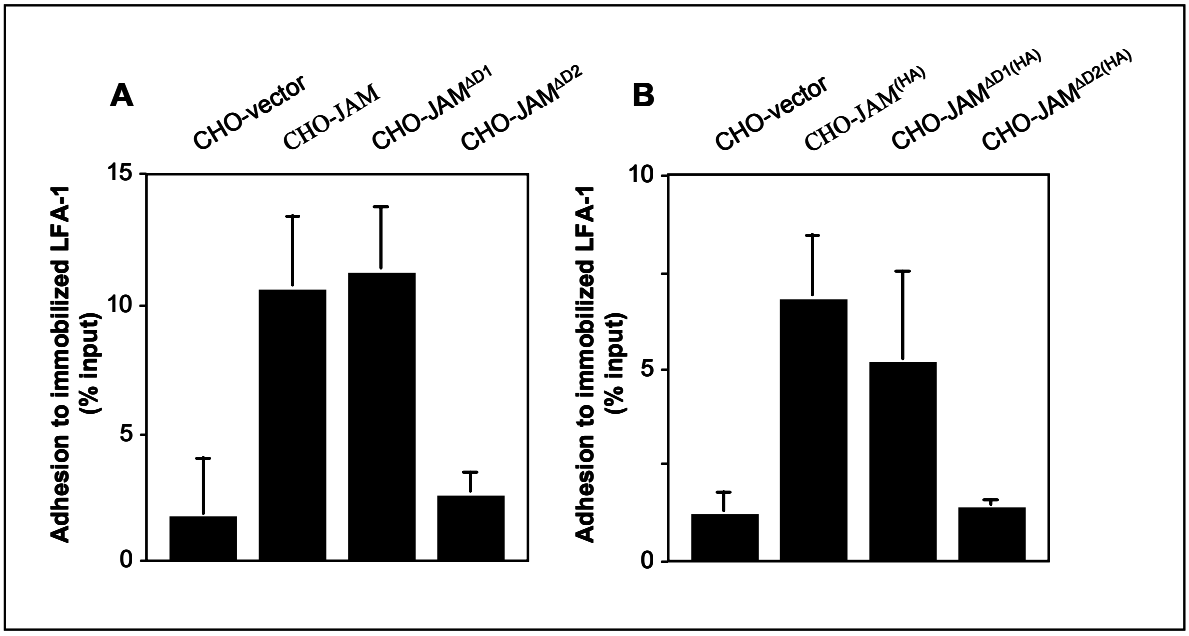

figure 21: Adhesion of CHO transfectants in suspension to purified and immobilized LFA-1 under static conditions. Wild-type and mutant JAM-1 proteins were expressed **(A)** without or **(B)** with C-terminal fused HA epitope tag (compare to fig. 20). Adhesion was measured as the percentage of input CHO cells. Data are the mean ± s.d. of four separate experiments performed in triplicate.

Deletion analysis indicated that the membrane-proximal Ig-like domain 2 of JAM-1 is both crucial and sufficient to support direct interaction of JAM-1 with its receptor LFA-1.

4.8. Contribution of JAM-1 in LFA-1–dependent adhesion of memory T cells to inflammatory stimulated endothelium

The initial experiments designed to confirm a functional role for JAM-1 in LFA-1–mediated adhesion were performed using Jurkat T cells and CHO transfectants. Inevitably, the results of these experiments are based to some extent on the cellular background of these immortalized cell lines. To investigate the cooperation of LFA-1 and JAM-1 in a more physiological context, cells of the human vascular system were subjected to cell-cell adhesion assays under static conditions. Human umbilical vein endothelial cells (HUVECs) were isolated from the veins of umbilical cords freshly obtained after birth. $CD4^+CD45RO^+$ memory T lymphocytes were isolated from the blood of normal volunteers by magnetic cell separation and immediately subjected to HUVEC monolayer adhesion. HUVECs were left untreated or stimulated simultaneously with the inflammatory cytokines tumor necrosis factor (TNF)-α and interferon (IFN)-γ, the latter inducing a redistribution of junctional located JAM-1 to the endothelial cell surface (Ozaki *et al.*, 1999; Shaw *et al.*, 2001c). TNF-α–activation of HUVECs induces expression of VCAM-1 that leads to stable arrest of $CD4^+$ T cells under static and flow conditions (Luscinskas *et al.*, 1995).

To exclude such an influence on $CD4^+CD45RO^+$ T cell adhesion exercised by VLA-4/VCAM-1 interactions, all experiments on cytokine-stimulated HUVEC monolayers were performed with VLA-4–blocked memory T cells and in the presence of VLA-4 mAb.

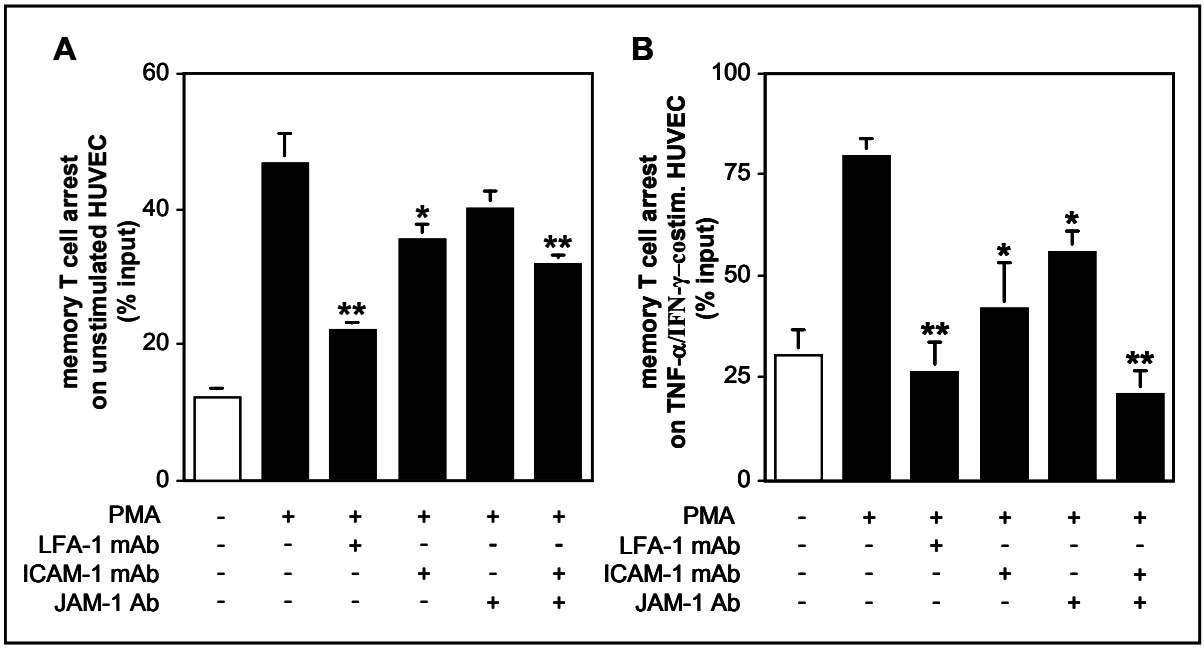

figure 22: **(A)** Adhesion of PMA-stimulated $CD4^+CD45RO^+$ T cells to unstimulated HUVECs under static conditions. **(B)** Adhesion of PMA-stimulated $CD4^+CD45RO^+$ T cells to HUVECs costimulated with the inflammatory cytokines TNF-α and IFN-γ under static conditions. Experiments on cytokine-stimulated HUVECs were performed with VLA-4–blocked $CD4^+CD45RO^+$ T cells and in the presence of VLA-4 mAb to exclude VLA-4/VCAM-1–mediated cell adhesion. **(A-B)** Cell binding experiments with the exclusion of PMA stimulation were performed as controls (white columns). Antibody studies included the treatment of $CD4^+CD45RO^+$ T cells with LFA-1 mAb TS1/22 and preincubation of HUVEC monolayers with ICAM-1 mAb, anti–JAM-1 or ICAM-1 mAb/anti–JAM-1 in combination, as indicated. An IgG_1 isotype control or preimmunization serum had no significant effects, whereas ICAM-1 Fab was as effective as ICAM-1 mAb (data not shown). Adhesion was measured as the percentage of input $CD4^+CD45RO^+$ T cells. Data are the mean ± s.d. of four separate experiments performed in triplicate. $^*P < 0.05$, $^{**}P < 0.01$.

PMA-induced adhesion of $CD4^+CD45RO^+$ T cells on untreated HUVECs was largely decreased when the lymphocytes were preincubated with LFA-1 mAb TS1/22 (**fig. 22^A**). This inhibition was more significant in experiments with inflammatory stimulated HUVECs, where adhesion was reduced to the background values observed with unstimulated memory T cells (**fig. 22^B**). Stimulated $CD4^+CD45RO^+$ T cell arrest therefore appeared to be largely dependent on the presence of leukocytic LFA-1 receptors. In contrast, neutralization of the LFA-1 ligand ICAM-1 on untreated or TNF-α/IFN-γ–costimulated HUVEC monolayers led to a far less pronounced inhibition of T cell arrest than achieved by receptor blockage (**fig. 22^{A+B}**). Thus, LFA-1 ligand(s) in addition to ICAM-1 appeared to be involved in PMA-induced T cell arrest. This finding was also consistent with published results (Rothlein *et al.*, 1986; Nortamo *et al.*, 1991; de Fougerolles *et al.*, 1992; Springer, 1994; Bleijs *et al.*, 2000) and, together with the own previous results, allowed to postulate an interplay between ICAM-1 and JAM-1 as concerted LFA-1 ligands in cell-cell adhesion. Shielding JAM-1 on costimulated HUVECs by the use of anti–JAM-1 indeed significantly reduced LFA-1–mediated adhesion of activated $CD4^+CD45RO^+$ T cells (**fig. 22^B**).

Moreover, combined treatment with ICAM-1 mAb and anti–JAM-1 completely impeded this adhesive cell interaction, resulting in the binding levels observed with unstimulated or LFA-1–blocked stimulated $CD4^+CD45RO^+$ T cells (**fig. 22^B**). In contrast, resting HUVECs underwent no significant changes in activated T lymphocyte binding when treated with anti–JAM-1 alone or together with ICAM-1 mAb and anti–JAM-1 (**fig. 22^A**). Equivalent findings were obtained when T lymphocyte binding was induced by the more physiological stimulus of stromal cell-derived factor (SDF)-1α (CXCL12) instead of PMA (data not shown).

The usage of $CD4^+CD45RO^+$ T lymphocytes and HUVECs isolated from the human vascular system confirmed the interaction between LFA-1 and JAM-1 in cell-cell adhesion in a more physiological context, but only under the specific conditions of inflammatory stimulation of endothelial monolayers with TNF-α and IFN-γ. The results additionally suggested that under these inflammatory conditions ICAM-1 works in tandem with JAM-1 to mediate LFA-1–dependent adhesion of memory T cells. Thus JAM-1 could play an important role in the process of leukocyte recruitment in inflammation.

4.9. Insistency of LFA-1/JAM-1–based cell adhesion under physiological conditions of flow

Circulating leukocytes *in vivo* must resist the physical shear forces that act on them at the vessel wall and that oppose their adhesion to the endothelium or recruitment to sites of inflammation and during lymphocyte homing (see **fig. 28**).

To further investigate the physiological relevance of the LFA-1/JAM-1 interplay, leukocyte adhesion assays were performed under laminar flow conditions to simulate *in vitro* the physiological fluid shear stress present in the human microvasculature. Memory T cells were perfused through a parallel plate flow chamber (see **fig. 4**) causing a laminar flow of cell suspension over embedded HUVEC monolayers that induced a regulated wall shear stress of 1.5 dyn/cm^2. Cell-cell interactions, *i.e.* leukocyte rolling, adhesion and transendothelial migration, was directly visualized by video microscopy. Inflamed HUVEC monolayers were immobilized with the chemokine SDF-1α to trigger integrin-mediated firm arrest of memory T cells under conditions of shear forces, as has been described for $CD34^+$ progenitors (Peled *et al.*, 1999). Despite a redundancy of cell adhesion-mediating receptor-ligand pairs, flow experiments were performed under conditions blocking leukocytic VLA-4 integrins. This excluded intercellular VLA-4/VCAM-1 interactions enhanced by induction of endothelial VCAM-1 expression through cytokine stimulation of HUVECs.

SDF-1α–triggered T lymphocyte adhesion to cytokine-stimulated HUVECs under flow appeared to be in large part mediated by LFA-1 as demonstrated with the mAb TS1/22 (**fig. 23^{A+B}**). On TNF-α–stimulated HUVECs, ICAM-1 served exclusively as the LFA-1 ligand, whereas anti–JAM-1 did not effect cellular interaction and thus had no additive effect when applied together with an ICAM-1 mAb (**fig. 23^{A}**). In contrast, under conditions of costimulation with TNF-α and IFN-γ where JAM-1 is redistributed from cell-cell junctions to the cell surface, anti–JAM-1 efficiently reduced adhesion of $CD4^+CD45RO^+$ T cells (**fig. 23^{B}**). The cell binding inhibition was additively increased by simultaneous blocking of ICAM-1 and JAM-1 on the endothelial surface, attaining the levels observed for neutralization of the LFA-1 receptor (**fig. 23^{B}**). The results from flow chamber experiments correlated with those obtained in the corresponding assays under static conditions (see **fig. 22**).

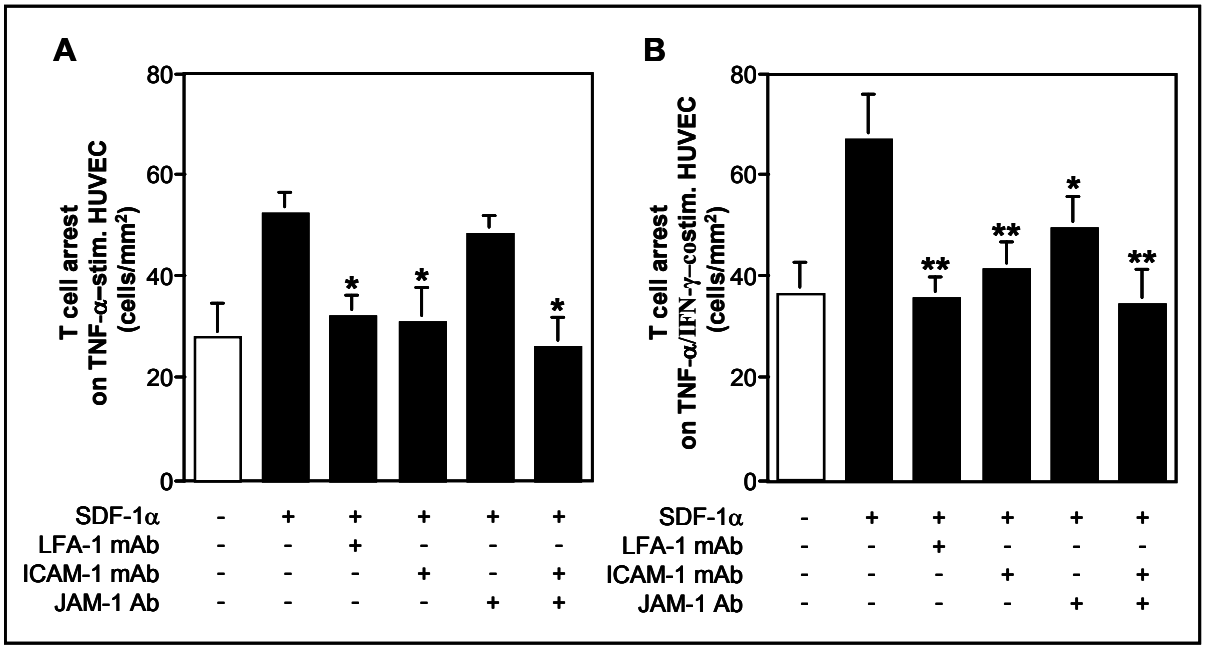

figure 23: Flow chamber experiments to study memory T cell adhesion to **(A)** TNF-α–stimulated HUVEC monolayers and to **(B)** TNF-α/IFN-γ–costimulated HUVEC monolayers under flow conditions. $CD4^+CD45RO^+$ T cells tempered to 37°C were perfused through the flow chamber at controlled flow rates of 0.1 ml/s effecting a wall shear stress of 1.5 dyn/cm^2. T cell arrest was triggered by SDF-1α immobilized on HUVEC monolayers (black columns). Control experiments were performed without SDF-1α stimulation (white columns). Experiments were each performed with VLA-4–blocked $CD4^+CD45RO^+$ T cells and in the presence of VLA-4 mAb. Antibody studies included the treatment of $CD4^+CD45RO^+$ T cells with LFA-1 mAb TS1/22 and preincubation of HUVEC monolayers with ICAM-1 mAb, anti–JAM-1 or ICAM-1 mAb/anti–JAM-1 in combination, as indicated. An IgG_1 isotype control and preimmunization serum had no significant effects, whereas ICAM-1 Fab was as effective as ICAM-1 mAb (data not shown). Firmly adherent T cells were counted after a 5-min equilibration of flow conditions and expressed as cells/mm^2. Data are the mean ± s.d. and are representative of at least three experiments performed in duplicate. *$P < 0.05$, **$P < 0.01$.

Even under the effect of physical shear stress forces, JAM-1 appeared able to engage in adhesive molecular interactions with the integrin receptor LFA-1 and thus to participate in the firm arrest of memory T cells on inflamed endothelium. The additive effect of ICAM-1 mAb and anti–JAM-1 on LFA-1–mediated cell adhesion suggested that both IgSF proteins might function as alternative ligands for LFA-1 under certain inflammatory conditions. Experiments on HUVECs

solely stimulated with TNF-α revealed the requirement of JAM-1 redistribution from junctional structures to the apical surface to enable its participation in T cell binding. These findings strengthened the hypothesis of a crucial role for JAM-1 in leukocyte binding during inflammation in a more physiological context.

4.10. Involvement of JAM-1 in memory T cell transmigration

Dissociation of endothelial JAM-1 from TJs caused by combined cytokine treatment with TNF-α and IFN-γ interfere with the intercellular junctional integrity and the endothelial permeability (Ozaki *et al.*, 1999; Shaw *et al.*, 2001c). Such a process could enable leukocyte transmigration during inflammation. Given the ability of JAM-1 to participate under inflammatory conditions in firm leukocyte adhesion, an additional functional role for JAM-1 in leukocyte recruitment, *i.e.* diapedesis across the endothelial barrier, could be envisioned. To address this hypothesis, transendothelial migration of memory T cells was investigated under static and flow conditions.

In static chemotaxis experiments, $CD4^+CD45RO^+$ T cells were allowed to transmigrate across resting HUVEC monolayers grown to confluence on 5.0-μm filter membranes towards a SDF-1α chemokine gradient (see **fig. 3**). Lymphocyte transmigration appeared dependent on SDF-1α stimulation and was mainly mediated by LFA-1 and its ligand ICAM-1 (**fig. 24**). In static adhesion assays, anti–JAM-1 did not effect PMA or SDF-1α–triggered lymphocyte adhesion on unstimulated HUVECs, either alone or in combination with an ICAM-1 mAb (see **fig. 22^A**). In contrast, transendothelial chemotaxis under the same conditions was significantly impaired by anti–JAM-1 and completely inhibited to a level observed for LFA-1–independent background transmigration by the combined action with the ICAM-1 mAb (**fig. 24**).

Similar results were obtained for transendothelial migration induced by SDF-1α under shear forces in flow chamber experiments, a phenomenon that has also been termed chemorheotaxis (Cinamon *et al.*, 2001b; Luscinskas *et al.*, 2001). In these assays, migration of firmly adherent memory T cells through the endothelial monolayer (indicated by leukocyte shape change and subsequent spreading), was directly visualized by video microscopy. The number of cells undergoing shape changes on inflamed endothelium was significantly reduced by each anti–JAM-1 and ICAM-1 mAb alone (**fig. 25)**. Notably, blocking JAM-1 attenuated also lymphocyte spreading on resting endothelium (data not shown). A combined treatment of inflamed ECs with both antibodies showed an additive effect and impaired lymphocyte shape change to a similar extent to that observed for LFA-1–blocked lymphocytes (**fig. 25**).

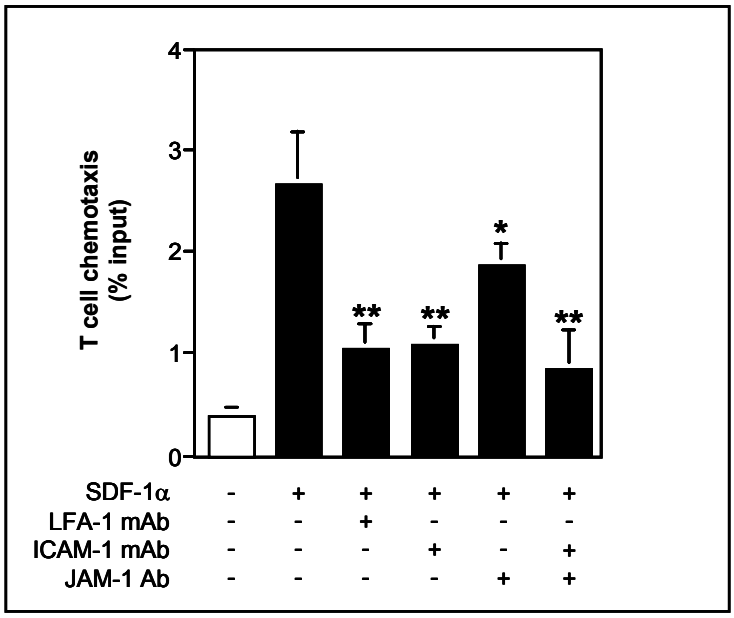

figure 24: Transendothelial chemotaxis of $CD4^+CD45RO^+$ T cells across unstimulated HUVEC monolayers triggered by SDF-1α. Experiments were performed in 5.0-µm transwell-filters with (black columns) or without (white column) chemokine stimulation. Antibody applications included the treatment of $CD4^+CD45RO^+$ T cells with LFA-1 mAb TS1/22 and preincubation of resting HUVEC monolayers with ICAM-1 mAb, anti–JAM-1 or ICAM-1 mAb/anti–JAM-1 in combination, as indicated. An IgG_1 isotype control and preimmunization serum had no significant effects, whereas ICAM-1 Fab was as effective as ICAM-1 mAb (data not shown). Transmigrated cells were counted by flow cytometry and expressed as the percentage of input lymphocytes. Data are the mean ± s.d. of four separate experiments performed in duplicate. $*P < 0.05$, $**P < 0.01$.

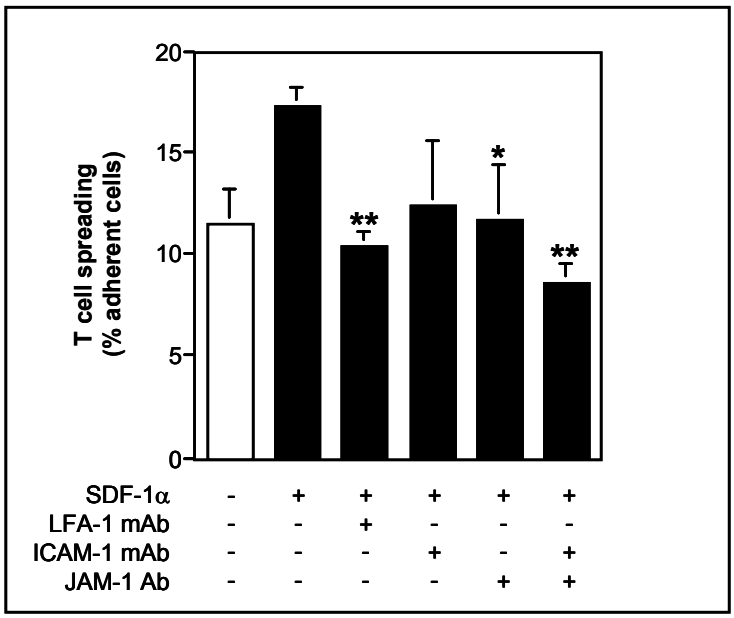

figure 25: Spreading and transmigration of $CD4^+CD45RO^+$ T cells induced by SDF-1α immobilized on HUVEC monolayers costimulated with TNF-α and IFN-γ under flow conditions. $CD4^+CD45RO^+$ T cells tempered to 37°C were perfused through the flow chamber at controlled flow rates of 0.1 ml/s effecting a wall shear stress of 1.5 dyn/cm^2. Control experiments were performed without SDF-1α immobilization (white column). Experiments were each performed with VLA-4–blocked $CD4^+CD45RO^+$ T cells and in the presence of VLA-4 mAb. Antibody applications included the treatment of $CD4^+CD45RO^+$ T cells with LFA-1 mAb TS1/22 and preincubation of HUVEC monolayers with ICAM-1 mAb, anti–JAM-1 or ICAM-1 mAb/anti–JAM-1 in combination, as indicated. An IgG_1 isotype control and preimmunization serum had no significant effects, whereas ICAM-1 Fab was as effective as ICAM-1 mAb (data not shown). Firm adherent cells undergoing shape change indicative of spreading and subsequent transmigration were analyzed by video microscopy and expressed as the percentage of adherent cells. Data are the mean ± s.d. and are representative of at least three experiments performed in duplicate. $*P < 0.05$, $**P < 0.01$.

Chemotaxis and flow experiments suggested that JAM-1 participates not only in leukocyte adhesion but also in transendothelial leukocyte migration. Inhibition of cell spreading appeared thereby to be largely independent from inflammatory stimulation of the endothelium. The influence of specific antibodies on T cell transmigration gave further confirmation for JAM-1 acting as an interaction partner and alternative ligand of LFA-1.

4.11. Involvement of JAM-1 in transmigration but not adhesion of neutrophils

The studies concerning an involvement of JAM-1 in leukocyte-EC interactions were further extended to myeloid cells. At first, neutrophil adhesion on HUVEC monolayers inflamed by combined treatment with TNF-α plus IFN-γ was investigated under laminar flow conditions exerting shear stress forces of 1.5 dyn/cm^2. This CXCR2-triggered adhesion was not affected by the α_L mAb TS1/22 but markedly decreased after neutrophil treatment with the β_2 mAb TS1/18 directed against both β_2 integrins LFA-1 and Mac-1 (**fig. 26^A**). Given the negligible effect of TS1/22, the failure of anti–JAM-1 to block neutrophil adhesion under the experimental conditions was expected (**fig. 26^A**). Even the combined application of ICAM-1 mAb and anti–JAM-1 did not reduce neutrophil adhesion more than ICAM-1 mAb alone. The latter itself showed a much more significant effect to that observed with LFA-1 mAb. This was most likely due to the capability of ICAM-1 to function not only as ligand for LFA-1 but also for Mac-1 expressed on neutrophils (**fig. 26^A**). In contrast to ICAM-1 mAb, the negligible effect of anti–JAM-1 on neutrophil adhesion suggested that it did not interfere with the β_2 integrin Mac-1. This further strengthened the notion of receptor-specificity of JAM-1.

Transendothelial chemotaxis of neutrophils across resting HUVECs towards an interleukin (IL)-8 (CXCL8) gradient (**fig. 26^B**) led to results similar to those obtained for SDF-1α–triggered chemotaxis of memory T cells (see **fig. 24**). LFA-1–dependent neutrophil transmigration under static conditions was reduced by ICAM-1 mAb or anti–JAM-1 alone, and simultaneous treatment of neutrophils with both antibodies appeared to have an additional inhibitory effect (**fig. 26^B**).

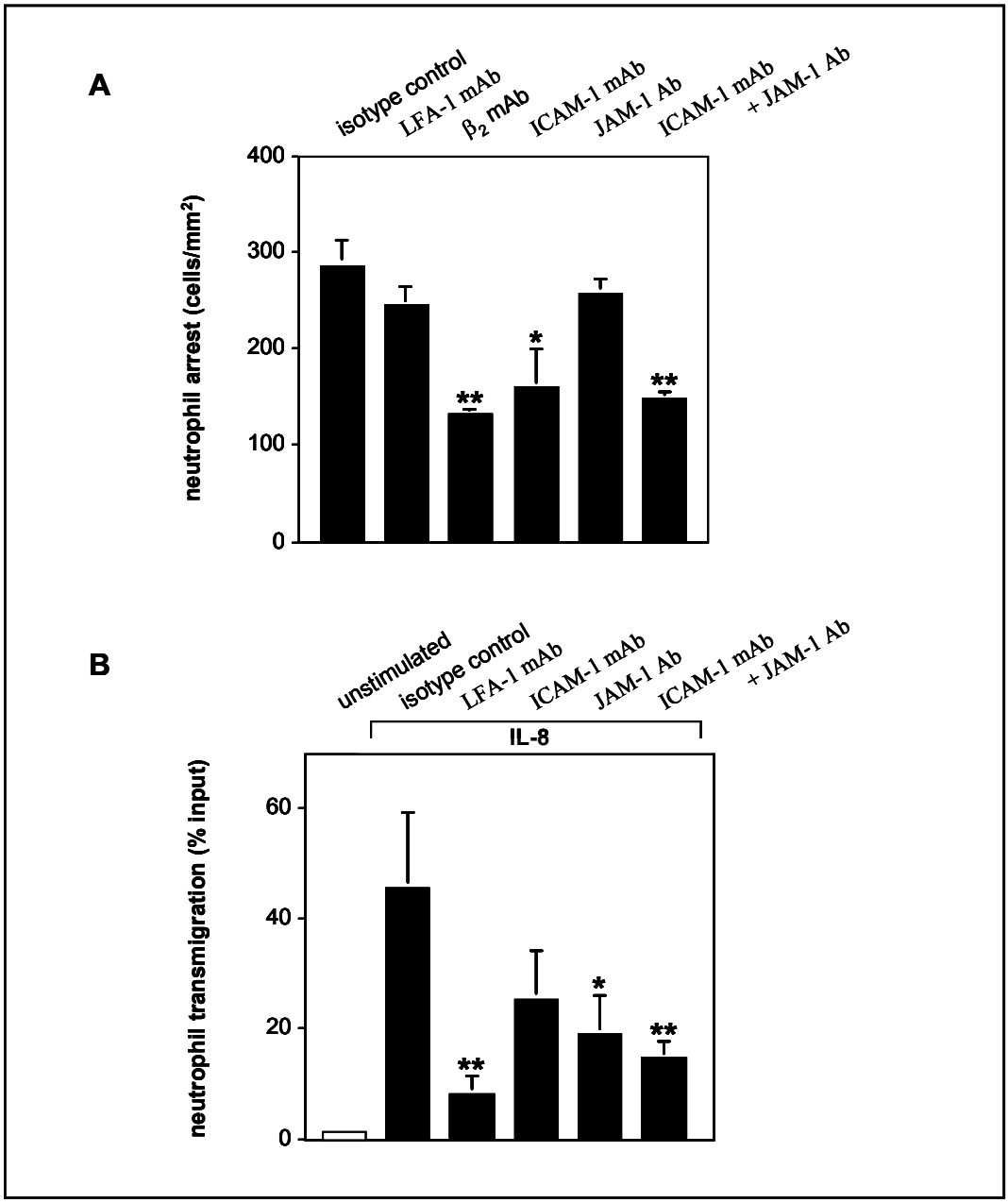

figure 26: **(A)** Flow chamber experiments to study neutrophil adhesion on HUVEC monolayers costimulated with TNF-α and IFN-γ under flow conditions. Neutrophils were pretreated with 5 % human serum to block Fc receptors, tempered to 37°C and perfused through the flow chamber at controlled flow rates of 0.1 ml/s effecting a wall shear stress of 1.5 dyn/cm^2. Antibody studies included neutrophils treatment with an IgG_1 isotype control, LFA-1 α_L mAb TS1/22 or β_2 integrin mAb TS1/18 and preincubation of inflammatory stimulated HUVEC monolayers with ICAM-1 mAb, anti–JAM-1 or ICAM-1 mAb/anti–JAM-1 in combination, as indicated. Preimmunization serum had no significant effects, whereas ICAM-1 Fab was as effective as ICAM-1 mAb (data not shown). Firmly adherent neutrophils were counted after a 5-min equilibration of flow conditions and expressed as cells/mm^2. Data are the mean ± s.d. and are representative of at least three experiments performed in triplicate. *$P < 0.05$, **$P < 0.01$. **(B)** Transendothelial chemotaxis of neutrophils across unstimulated HUVEC monolayers triggered by IL-8 (CXCL8). Experiments were performed in 5.0-µm transwell-filters with (black column) or without (white column) IL-8–stimulation. Antibody applications included neutrophils treatment with an IgG_1 isotype control, LFA-1 α_L mAb TS1/22 or β_2 integrin mAb TS1/18 and preincubation of resting HUVEC monolayers with ICAM-1 mAb, anti–JAM-1 or ICAM-1 mAb/anti–JAM-1 in combination, as indicated. Preimmunization serum had no significant effects, whereas ICAM-1 Fab was as effective as ICAM-1 mAb (data not shown). Transmigrated cells were counted by flow cytometry and expressed as the percentage of input neutrophils. Data are the mean ± s.d. and representative of at least four experiments performed in duplicate. *$P < 0.05$, **$P < 0.01$.

A significant participation of JAM-1 in neutrophil adhesion under flow, as opposed to its prominent role in LFA-1–dependent memory T cell arrest, seemed not detectable due to the involvement of Mac-1. However, chemotactic transmigration assays revealed a crucial involvement of JAM-1 in transendothelial migration of myeloid cells as demonstrated above for T lymphocytes diapedesis.

5. Discussion

5.1. Interaction of JAM-1 with the integrin subunit CD11a

The adhesion receptor lymphocyte function-associated antigen (LFA)-1 is one of the most important integrins on leukocytes. It is involved in B cell, T cell and NK cell functions and mediates firm cellular arrest on endothelial and epithelial cells within the scope of lymphocyte homing and leukocyte recruitment (Dustin *et al.*, 1989; Arnaout, 1990).

Intercellular adhesion molecules (ICAMs) and in particular ICAM-1 are the extracellular ligands of LFA-1 and mediate cellular adhesion of leukocytes (Gahmberg *et al.*, 1997). Cytoplasmic interaction partners of this integrin, on the contrary, play an important role in LFA-1–related signal transduction. For instance, the guanine nucleotide exchange factor (GEF) cytohesin-1 induces LFA-1 activation via inside-out signaling (Kolanus *et al.*, 1996), and outside-in signaling of LFA-1 can engage the transcriptional co-activator JAB1, inducing its nuclear localization and thus affecting c-Jun–driven gene transcription (Bianchi *et al.*, 2000). Both cytohesin-1 and JAB1 specifically interact with the β_2 tail of LFA-1 (CD18) and both interactions were identified by the yeast two-hybrid (YTH) system.

Specific integrin α subunits show high conservation among different species, and they mediate differential regulation of integrin function in between specific β subgroups of integrins (Hynes, 1992; Sastry *et al.*, 1993). For instance the dynamic mode of LFA-1 regulation by chemokines is specifically confered by the α_L cytoplasmic domain (Weber *et al.*, 1999a). It is conceivable that the α chain exerts regulatory function by modulating the signaling or binding properties of the associated β tail. Nevertheless, despite several indications for the importance of the α subunits in integrin function and in contrast to integrin β subunits, only few direct interactions of integrin α tails with cytoplasmic proteins have been reported to date (Hemler, 1998). One example is the α_{IIb}-binding protein CIP (Naik *et al.*, 1997) that has been identified, similarly to cytohesin-1 and JAB1, by employing the YTH system. However, none of the α subunit interaction partners were specific for the LFA-1 subunit CD11a, raising the question of the presence of further CD11a-interacting proteins. Therefore this yeast genetic-based *in vivo* assay represents a promising tool to search for novel α_L-specific binding partners of the integrin subunit CD11a.

Using the cytoplasmic part of CD11a as bait construct, one prey protein was identified as a candidate interacting protein in a YTH screen of a human leukocyte cDNA library. Isolation of the library plasmid from the candidate yeast colony and subsequent sequencing of the prey-

encoding cDNA insert revealed the full-length sequence of a gene that exhibited 75 % homology at the protein level with the previously published murine surface protein junctional adhesion molecule (JAM)-1 predominantly expressed at intercellular junctions (Martìn-Padura *et al.*, 1998). The striking high degree of homology and the utilization of a human cDNA library for the screening application predicted that the candidate prey was the human homologue of murine JAM-1. Thus, the putative human JAM-1 protein seemed a *bona fide* interaction partner for the CD11a subunit of LFA-1.

Interestingly, murine JAM-1 revealed striking structural and functional similarity with the ICAM subfamily, the counter-receptors of LFA-1, with respect to its immunoglobulin superfamily (IgSF) affiliation and its CAM function. Furthermore, it has been implicated in the transendothelial migration of monocytes and neutrophils *in vitro* and *in vivo* (Martìn-Padura *et al.*, 1998; Del Maschio *et al.*, 1999). Given the fact that JAM-1 is not expressed on murine leukocytes and thus is not available for heterotypic JAM-1/JAM-1 interactions (*i.e.* between cells of different type) this implicated a potential functional role for JAM-1 as a heterotypic binding partner of LFA-1. Moreover, the junctional location of JAM-1 was highly suggestive for an interaction with LFA-1 which plays a crucial role in transendothelial diapedesis.

To test this prediction, epithelial Chinese hamster ovary (CHO) cells were transfected with the full length JAM-1–encoding cDNA isolated from the library plasmid of the positive yeast colony. This eukaryotic cell model was particularly suited since CHO cells exhibit no preorganized tight junctions and do not express endogenous JAM-1 (Martìn-Padura *et al.*, 1998). Moreover, this adherent cell type allowed generation of confluent cell monolayers for adhesion and transmigration experiments with leukocytic cells. Specificity of a polyclonal anti–JAM-1 antibody raised by DNA-mediated immunization of mice was verified by flow cytometry and western blot analysis, where anti–JAM-1 revealed antigen binding only for CHO-JAM transfectants but not for CHO-vector transfectants or wild-type CHO cells. Gene expression of *JAM-1* in CHO-JAM cells was also confirmed at the transcriptional level by RT-PCR. Generation of the JAM-1–expressing CHO cell line and anti–JAM-1 polyclonal antibody allowed subsequent verification of the YTH results in independent experiments.

5.2. JAM-1 is expressed in human hematopoietic cells

Remarkably, JAM-1 was reported not to be expressed in hematopoietic cells of mice, with the exception of megakaryocytes (Martìn-Padura *et al.*, 1998). However, the isolation of a JAM-1–encoding nucleotide sequence from the human leukocyte cDNA library being screened was itself a strong indication that JAM-1 is indeed expressed in human leukocytes. Flow cytometry using

anti–JAM-1 established human JAM-1 expression on endothelial HUVECs and epithelial-like HeLa cells. Most interestingly, and in contrast to data published for murine JAM-1, surface expression of human JAM-1 was clearly detectable on monocytic Mono Mac 6 and THP-1 cells as well as on lymphoid Jurkat cells. Even $CD4^+CD45RO^+$ memory T cells, freshly isolated from the blood of healthy donors, revealed JAM-1 surface expression. However, consistent with previous reports, JAM-1 was barely detectable on myeloid HL-60 cells (Williams *et al.*, 1999). Together, these results confirmed that human JAM-1, as opposed to murine JAM-1, is expressed on hematopoietic cells.

These expression studies were consistent with the previous identification of human JAM-1 (Ozaki *et al.*, 1999; Williams *et al.*, 1999). The corresponding reports demonstrated a constitutive expression of human JAM-1 in circulating neutrophils, monocytes, platelets and lymphocytes. Additionally the platelet receptor F11 antigen (F11R) was shown to be identical to human JAM-1 (Sobocka *et al.*, 2000; Gupta *et al.*, 2000). With its expression on hematopoietic cells human JAM-1 seems to be strikingly different from JAM-1 in mice that exhibits a more restricted expression, detectable only in megakaryocytes, platelets and in MHC class II^+ antigen presenting cells (APCs) in lymphoid organs, but not in other hematopoietic cell types (Martìn-Padura *et al.*, 1998; Malergue *et al.*, 1998). The significance of this different expression pattern remains unclear and requires the determination of the functional role of JAM-1 in circulating blood cells.

5.3. Adhesive interaction between LFA-1 and its counter-receptor JAM-1

Functional studies using static cell adhesion assays lent support to the hypothesis which was based upon structural and functional properties, namely that the β_2 integrin LFA-1 and the IgSF member JAM-1 exert their mutual interaction by extracellular binding and thus display a receptor-ligand pair mediating cellular adhesion.

Confluent monolayers of CHO-JAM transfectants were able to firmly bind integrin-activated Jurkat T cells. Several lines of evidence revealed that this cellular interaction was specifically mediated by leukocytic LFA-1 and JAM-1 expressed on the CHO cells. i), Jurkat cell adhesion was not observed with CHO-vector transfectants or wild-type CHO cells but only with CHO-JAM cells. ii), firm arrest of Jurkat cells to CHO-JAM cell monolayers depended to a considerable extent on their pretreatment with PMA. Most integrins are normally in an inactive state when expressed on the cell surface, and they require activation to gain high affinity and

avidity. Phorbol esters like PMA are regularly used in *in vitro* cell adhesion studies (Dustin *et al.*, 1989). They are structural analogues of 1,2-diacylglycerol (DG) that is generated, besides inositol-1,4,5-triphosphate (IP_3), from phosphatidylinositol-4,5-biphosphate (PIP_2) by the activity of phospholipase C (PLC). Both second messengers have been demonstrated to lead to activation of LFA-1, e.g. DG by activation of protein kinase C (PKC) (Kolanus *et al.*, 1997; Lub *et al.*, 1995). Thus, the requirement for PMA-stimulation of Jurkat cells to induce their firm arrest to CHO-JAM cells suggested the involvement of PKC-activated integrin receptors. iii), blocking leukocytic LFA-1 with TS1/18 mAb reduced the heterotypic cell adhesion to background levels. This effect was not observed for Jurkat cells pretreated with an IgG_1 isotype control. Finally, likewise incubation of CHO-JAM cell monolayers with anti–JAM-1 reduced Jurkat cell adhesion to levels observed on CHO cell monolayers lacking JAM-1 expression. In contrast, preimmune serum did not effect cellular binding.

5.4. JAM-1 binds LFA-1 irrespective of cellular integrin surface expression

The finding that LFA-1 functions as a leukocytic adhesion receptor for JAM-1 expressed in CHO cells was further substantiated in static adhesion assays where LFA-1 protein, immobilized as an adhesion target, specifically captured CHO-JAM transfectants but not CHO-vector or wild-type CHO cells in suspension. Molecular specificity was confirmed by application of CD18 mAb and anti–JAM-1. With regards to the former adhesion assays using Jurkat cells as an LFA-1–expressing cell model, these experiments excluded the possibility that leukocyte adhesion receptors other than LFA-1 have mediated the firm arrest on JAM-1–expressing CHO cells.

The purified and immobilized LFA-1 remains in a constitutively active form as has been demonstrated elsewhere (Klickstein *et al.*, 1996). It could thus be used as a substrate for cell adhesion experiments. The composition of this LFA-1 preparation was analyzed prior to use by SDS-PAGE with subsequent western blotting using antibodies directed against CD11a and CD18 or with subsequent silver staining. Since the LFA-1 preparation was obtained from human tonsil and human spleen lysates by immunoaffinity chromatography (Klickstein *et al.*, 1996; Dustin *et al.*, 1989), the identification of JAM-1 as counter-receptor for LFA-1 raised the possibility that JAM-1 has been co-purified with LFA-1. In such a case it could not have been excluded that the arrest of CHO-JAM cells to immobilized LFA-1 could have been based, at least in part, on such a JAM-1 impurity that would be capable of homophilic interaction *in trans* (Bazzoni *et al.*, 2000a; Kostrewa *et al.*, 2001). However, the silver staining experiments and JAM-1 immunoblot analysis of the LFA-1 preparation did not reveal detectable levels of coprecipitated JAM-1, at least at concentrations used in the cell adhesion assays. The absence of LFA-1/JAM-1

copurification from organ tissue might be due to a complex cellular regulation of this heterophilic interaction that may be transient and not retained under the conditions used in purification protocols.

Static adhesion assays revealed that cell-surface expressed JAM-1 is a heterophilic ligand for LFA-1 and thus confirmed their interaction initially identified in the YTH system. The cell-protein adhesion data demonstrated here, however, were in contrast to a report where a recombinant human JAM-1–Fc chimera, ectopically expressed and secreted by insect cells, did not appear to support adhesion of lymphoid cells (Cunningham *et al.*, 2000). This may have been due to a requirement of cell surface expression for correct orientation and function of JAM-1. Differences in the post-translational modification with regards to the expression in insect cells are conceivable. In particular glycosylation can affect the adhesive properties of IgSF members as demonstrated for ICAMs. The level of ICAM-1 glycosylation affects e.g. its binding to Mac-1 that is enhanced for ICAM-1 molecules with smaller *N*-linked oligosaccharide side chains and for ICAM-1 mutants where *N*-glycosylation sites within the Mac-1 binding domain have been substituted (Diamond *et al.*, 1991). Moreover, the interaction of ICAM-2 with LFA-1 depends on a tripod-like arrangement of *N*-linked glycans in the membrane-proximal region of the Ig-like domain 2 (Casasnovas *et al.*, 1997). However, the different result is most likely due to the fact that the lymphoid cells used in their adhesion assay were unstimulated and therefore did not express activated LFA-1 integrin receptors.

5.5. Absence of redundancy for JAM-1 binding between the β_2 integrins LFA-1 and Mac-1

The IgSF member ICAM-1 is not only the principal ligand for LFA-1 (Rothlein *et al.*, 1986; Marlin *et al.*, 1987) but also a functional counter-receptor for Mac-1 (Smith *et al.*, 1989). A cooperative involvement of both β_2 integrins in adhesion of stimulated neutrophils to purified ICAM-1 has been demonstrated by the additive inhibitory effect of combinations of anti-CD11a and CD11b mAbs (Smith *et al.*, 1989). Given the structural homology between ICAM-1 and JAM-1, J-β_2.7 cells were used to investigate a potential role for Mac-1 as a JAM-1 binding receptor in addition to LFA-1.

The Jurkat T cell-derived J-β_2.7 cell line is deficient in surface expression of β_2 integrins, due to chemical mutagenesis of the gene encoding the LFA-1 α_L subunit (Weber *et al.*, 1997b) and since Mac-1 is normally not expressed in lymphoid cells (Anderson *et al.*, 1987). However, translation of the β_2 subunit-encoding mRNA in J-β_2.7 cells is unaffected (Weber *et al.*, 1997b).

This provided the possibility to reconstitute LFA-1 ($\alpha_L\beta_2$) expression or to generate heterotopic integrin expression of Mac-1 ($\alpha_M\beta_2$) in J-β_2.7 cells by transfection with integrin α_L or α_M subunit-encoding cDNA, respectively. Subsequent heterodimerization of the respective heterogenous α chain with the unaffected endogenous β_2 chain is a presupposition for integrin surface expression (Anderson *et al.*, 1987; Arnaout, 1990). The ability of a naturally expressed integrin subunit to dimerize with a recombinant counterpart subunit expressed in genetically deficient cells was shown with β_2-deficient human lymphocytes derived from LAD-I patients (see 1.5.5.5.). Hybrids generated from these cells with LFA-1–expressing murine lymphocytes showed surface expression of interspecies $\alpha_L{}^h\beta_2{}^m$ (h = human; m = murine) hybrid complexes (Marlin *et al.*, 1986). Moreover, transfection of lymphocytes from LAD-1 patients with wild-type *β_2* cDNA restored the surface expression and function of LFA-1 (Hibbs *et al.*, 1990).

Surface expression of reconstituted LFA-1 and heterotopic Mac-1 on α_L-transfected J-β_2.7/α_L and α_M-transfected J-β_2.7/α_M cells was detected by flow cytometry analysis. The J-β_2.7/α_M cells thus provided a LFA-1–deficient lymphocytic cell line expressing Mac-1 on their cell surface. Static adhesion assays on CHO cells expressing or not JAM-1 revealed that J-β_2.7/α_M cells did not bind to this IgSF protein, even though functional surface expression of Mac-1 on these cells has been demonstrated (Weber *et al.*, 1999a) and was confirmed by static adhesion assays on purified, immobilized ICAM-1. This suggested a lack of redundancy between LFA-1 and Mac-1 for JAM-1 binding that may hold true for the two other β_2 integrins p150,95 and $\alpha_D\beta_2$ as well. Furthermore, the failure of J-β_2.7 cells to adhere to CHO-JAM transfectants and the rescue of this ability by expression of LFA-1 via transfection with an α_L-encoding cDNA (J-β_2.7/α_L cells) provided additional evidence that Jurkat T cell binding to JAM-1 expressing CHO cells was specifically mediated by LFA-1.

5.6. Heterophilic nature of the molecular interaction mediating leukocyte arrest on JAM-1–expressing CHO cells

Despite indirect evidence suggesting the existence of a extracellular heterophilic binding partner (Martìn-Padura *et al.*, 1998), JAM-1 has only been described to interact in a homophilic manner both *in cis* (dimerization) and *in trans*. Such JAM-1/JAM-1 interactions appear to participate specifically in the formation and/or maintenance of intercellular junctions of endothelia and epithelia. The finding of JAM-1 expression in human hematopoietic cells, and in particular in Jurkat, J-β_2.7 and $CD4^+CD45RO^+$ T cells used within this study, raised the important issue to test whether homophilic binding between leukocytic JAM-1 and CHO cell-expressed JAM-1 was involved in the observed cell-cell adhesion phenomena.

Several lines of evidence corroborated the conclusion that such homophilic interactions *in trans* were not crucial for the firm arrest of leukocytes. i), the surface expression of JAM-1 in wild-type Jurkat cells and J-β_2.7 cells did not correlate with the marked differences in their adhesion behaviour to CHO-JAM transfectants on the one hand and CHO-vector transfectants or wild-type CHO cells on the other hand. The failure of α_L-deficient but JAM-1 expressing J-β_2.7 cells to bind to JAM-1–transfected CHO cells revealed a crucial role for heterophilic but not for homophilic JAM-1 interactions in Jurkat/CHO-JAM cell binding. Moreover, reconstitution of JAM-1 binding-properties of J-β_2.7 cells by their transfection with an α_L-encoding cDNA demonstrated the dependence on this integrin receptor. ii), leukocyte binding to CHO-JAM cells appeared to depend completely on stimulation by the phorbol ester PMA, suggesting that this cell adhesion required activated LFA-1 but not on the presence of leukocytic JAM-1 molecules. iii), preincubation of leukocytes with specific LFA-1 mAbs decreased their arrest on CHO-JAM cells to such an extent that a contribution of *trans*-homophilic JAM-1 binding to the observed cell adhesion could be convincingly excluded. iv), blocking leukocyte JAM-1 with anti–JAM-1 did not affect binding of Jurkat T cells to CHO-JAM cells nor binding of $CD4^+CD45RO^+$ memory T cells to unstimulated or cytokine-treated HUVECs, as described below. v), CHO cells with or without expression of JAM-1 showed equivalent binding to purified, immobilized LFA-1 receptor and to LFA-1–expressing Jurkat cells, respectively, and thus provided evidence against an involvement of homophilic JAM-1 interactions in the adhesive binding reported here. Notably, JAM-1 contamination of the LFA-1 preparation due to copurification was not detectable by protein analysis. vi), myeloid HL-60 cells, that did not show detectable JAM-1 surface expression in flow cytometry analysis in accordance with published data (Williams *et al.*, 1999), showed a similar LFA-1–mediated binding pattern to CHO-vector or CHO-JAM cells than JAM-1–expressing Jurkat cells. This was in contrast to a report where HL-60 cells failed to bind recombinant human JAM-1 Fc chimera (Cunningham *et al.*, 2000). However, this was most likely due to the fact that the monocytic cells were not stimulated and therefore did not express activated LFA-1. Finally, CHO-JAM transfectants in suspension failed to exert significant adhesive properties to confluent CHO-JAM cell monolayers under static conditions.

The latter finding was supported by a report demonstrating that CHO cells expressing murine JAM-1 do not aggregate in suspension (Martìn-Padura *et al.*, 1998). Possible explanations for this observation could be changes in intracellular complexes involving JAM-1 and regulatory cytoplasmic proteins, and/or alteration in the extracellular JAM-1 conformation due to the cell detachment. A similar phenomenon has been demonstrated for the adherens junction (AJ) protein VE-cadherin, which is unable to promote aggregation of detached CHO cells (Breviario *et al.*, 1995). However, this may not be relevant in this case since CHO cells in suspension expressing the homologous family member JAM-2 have been demonstrated to bind specifically to immobilized JAM-2–Fc chimera, thus identifying homophilic interactions *in trans* exerted by human JAM-2 (Cunningham *et al.*, 2000). The results demonstrated here were also in

accordance with findings that recombinant mouse as well as human JAM-1 Fc chimeras did not mediate homophilic adhesion to JAM-1 expressed by transfected COS or CHO cells in solid phase adhesion assays (Williams *et al.*, 1999; Cunningham *et al.*, 2000). Furthermore, they were consistent with the idea that a homophilic interaction of JAM-1 molecules may arise preferentially in regions of cell-cell contacts that exhibit a sufficiently high JAM-1 density, e.g. at intercellular junctions. However, the homophilic JAM-1 binding investigated under the experimental conditions of adhesion assays could be of relatively low affinity. Although there was no clear evidence for the involvement of such a type of molecular interaction in the cellular arrest of lymphoid Jurkat cells on CHO-JAM transfectants or of $CD4^+CD45RO^+$ T cells on HUVECs (as described below), it cannot be ruled out that during leukocyte recruitment JAM-1/JAM-1 interactions *in trans* may occur that are only of low stringency and therefore difficult to detect. Indeed, JAM-1–transfected CHO cell monolayers were shown to facilitate adhesion of freshly isolated human platelets (Naik *et al.*, 2001), presumably via homophilic interactions, although other heterophilic receptors on the surface of platelets have not been excluded, e.g. by blocking antibodies. Alternatively, anti–JAM-1 may not have an inhibitory effect on homophilic interactions. With regards to the blocking properties of anti–JAM-1 in LFA-1–mediated leukocyte adhesion and transmigration, the epitope targeted by this antibody is likely to be located in the LFA-1–binding membrane-proximal Ig-like domain 2 rather than in the N-terminal region that is implicated in homophilic JAM-1 interactions (Bazzoni *et al.*, 2000a; Kostrewa *et al.*, 2001).

5.7. Structural duality of JAM-1

Deletion mutagenesis revealed that the membrane-proximal Ig-like domain 2 of human JAM-1 is necessary and sufficient for LFA-1 binding, strongly suggesting that this domain bears the LFA-1 binding site. Thus, CHO cells expressing domain 2-deficient JAM-1 (CHO-$JAM^{\Delta D2}$ cells) failed to mediate adhesiveness to PMA-stimulated Jurkat T cells or to molecular LFA-1. In contrast, adhesion mediated by JAM-1 comprising only the Ig-like domain 2 (CHO-$JAM^{\Delta D1}$ cells) was equivalent to that seen with CHO-JAM transfectants. Expression of the mutated JAM-1 constructs was confirmed by RT-PCR though not verifiable at the protein level. An efficient recognition by polyclonal anti–JAM-1 appeared to require the presence of full-length JAM-1 and failed to detect the mutant proteins $JAM^{\Delta D1}$ and $JAM^{\Delta D2}$, probably due to recognition of an epitope encompassing or intervening both Ig-like domains 1 and 2. However, using CHO-$JAM^{(HA)}$, CHO-$JAM^{\Delta D1(HA)}$ and CHO-$JAM^{\Delta D2(HA)}$ cells presenting C-terminal HA-tagged JAM-1 constructs on their surface resulted in equivalent adhesion results. Flow cytometry analysis of the permeabilized CHO transfectants using anti-HA revealed that the failure of CHO-$JAM^{\Delta D2(HA)}$ cells to bind to cellular or molecular LFA-1 was not the consequence of a lack

of cell surface expression or to protein degradation of $JAM^{\Delta D2(HA)}$. It could be predicted that this was also the case for the non-tagged $JAM^{\Delta D2}$ protein expressed by CHO-$JAM^{\Delta D2}$ cells. Consistent with this prediction, with regards to the regulation of JAM-1 function by its C-terminal PDZ domain-binding motif, adhesion experiments with CHO cells expressing HA-tagged JAM-1 indicated that this C-terminal fused epitope tag did not impair the adhesiveness of these cells as compared to CHO cells expressing non-tagged JAM-1.

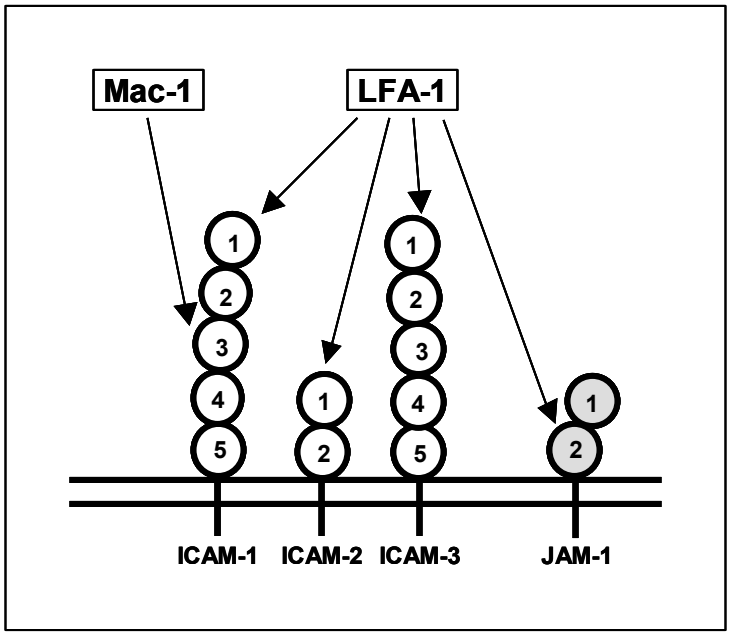

figure 27: Schematic diagram depicting the main known interactions of the β_2 integrins LFA-1 and Mac-1 with IgSF members. Notably, the interaction of LFA-1 with ICAM-1, -2, and -3 requires the N-terminal domain 1 of these IgSF members as the primary binding site, whereas the membrane-proximal domain 2 of JAM-1 appears to be sufficient to mediate the binding of LFA-1. Similarly, ICAM-1 binds Mac-1 with its Ig-like domain 3.

The ICAM proteins, vascular cell adhesion molecule (VCAM)-1 and mucosal addressin cell adhesion molecule (MAdCAM)-1 represent a subclass of the IgSF family that is able to bind integrins. They exhibit a greater amino acid sequence homology to one another than to other IgSF members (Tan *et al.*, 1998). The functionally important integrin-binding regions seem to be located mainly in their N-terminal Ig-like domain 1 (**fig. 27**) with some contribution by the second domain, as demonstrated for ICAM-1/LFA-1 (Staunton *et al.*, 1990; Stanley *et al.*, 2000), ICAM-2/LFA-1 (Springer, 1994), ICAM-3/LFA-1 (Holness *et al.*, 1995; Klickstein *et al.*, 1996), VCAM-1/VLA-4 with an additional contribution of domain 4 (Vonderheide *et al.*, 1994; Newham *et al.*, 1997) and MAdCAM/$\alpha_4\beta_7$ (Briskin *et al.*, 1996; Tan *et al.*, 1998). In this regard, the new IgSF-integrin interaction represented by JAM-1 and LFA-1 differs from the previous binding pairs in that it engages the second but not the first Ig-like domain of JAM-1 for the mutual interaction (**fig. 27**). Remarkably, ICAM-1 that binds LFA-1 with its N-terminal domain, engages its third (although not its membrane-proximal fifth) Ig-like domain to interact with

Mac-1 (**fig. 27**) (Diamond *et al.*, 1991). Similarly to ICAM-1, JAM-1 thus displays structural duality in that the membrane-distal Ig-like domain 1 appears to exert homophilic JAM-1 binding *in cis* and *in trans* (see **fig. 29**) (Bazzoni *et al.*, 2000a; Kostrewa *et al.*, 2001), whereas the membrane-proximal Ig-like domain 2 mediates heterophilic receptor binding to LFA-1. This aspect raises the possibility that lateral dimerization of endothelial JAM-1 enhances binding to leukocyte LFA-1 *in trans*, as has been demonstrated for ICAM-1 dimers (Miller *et al.*, 1995; Reilly *et al.*, 1995). Such a scenario would be reasonable given the JAM-1 redistribution from intercellular junctions to the apical cell surface of ECs under certain inflammatory conditions (Ozaki *et al.*, 1999; Shaw *et al.*, 2001c).

5.8. Validation of cellular adhesion with natural cells

The finding that the molecular interaction of JAM-1 with LFA-1 was sufficient to mediate firm cellular arrest, as determined with transfected CHO cells and leukemic Jurkat T cells, was validated in a more physiological context. i), adherent HUVECs isolated from umbilical cord veins were used as a confluent cell monolayer expressing JAM-1. Cytokine-activated HUVECs provided an model of inflamed endothelium, since they express or upregulate expression of the major adhesive ligands found on many inflamed venules, *i.e.* mainly E-selectin, P-selectin, ICAM-1 and VCAM-1 (Luscinskas *et al.*, 1995). A combined treatment with the proinflammatory cytokines TNF-α and IFN-γ was used to induce a redistribution of JAM-1 from the interendothelial junctions to the apical surface of the ECs. ii), LFA-1–bearing T lymphocytes were isolated from human venous blood. Whereas naive cells circulate predominantly through lymphoid tissues, trafficking to sites of inflammation is a characteristic property of memory $CD4^+$ T lymphocytes. Therefore only memory T cells ($CD4^+CD45RO^+$) were used and separated from naive T cell phenotypes ($CD4^+CD45RA^+$) on the basis of their differential expression of CD45R isoforms (Springer, 1994). iii), in addition to the use of phorbol ester, T lymphocytes were stimulated in a more physiological way using stromal cell-derived factor (SDF)-1α (CXCL12) immobilized and displayed on the endothelial cells (ECs). This chemokine potently attracts lymphocytes and exerts chemoattractive and activating functions upon binding to its G protein-coupled receptor CXCR4 (Campbell *et al.*, 1998; Peled *et al.*, 1999). $CD4^+CD45RO^+$ memory T cells were suitable for SDF-1α stimulation since they express CXCR4 which is crucial for their inflammatory recruitment (Nanki *et al.*, 2000). Exogenous application of SDF-1α was a prerequisite due to the fact that cultured ECs do not express lymphocyte-stimulatory chemokines normally apically presented on lymphoid or inflamed endothelia *in vivo* (Cinamon *et al.*, 2001b). VCAM-1/VLA-4 interactions have been implicated in the stable arrest of $CD4^+$ T lymphocytes on TNF-α–activated HUVECs under static and flow conditions (Luscinskas *et al.*, 1995). Blocking leukocytic VLA-4 therefore enabled the analysis of

JAM-1/LFA-1–mediated cellular arrest in the context of an induction of VCAM-1 surface expression on cytokine–stimulated HUVECs.

Antibody studies revealed that adhesion of $CD4^+CD45RO^+$ T cells on untreated or costimulated HUVECs was largely dependent on LFA-1. On resting HUVECs this interaction was only in part mediated by the main LFA-1 ligand ICAM-1, and was not affected by anti–JAM-1. However, JAM-1 significantly participated in the lymphocyte arrest on proinflammatory costimulated HUVECs. Under these specific conditions it appeared to function in conjunction with ICAM-1 as a second LFA-1 counter-receptor, since anti–JAM-1 or ICAM-1 mAb alone failed to completely inhibit LFA-1–mediated lymphocyte adhesion that was in contrast achieved by the use of both these antibodies in combination. Interestingly, blocking LFA-1 has often reported to be more effective in the inhibition of leukocyte extravasation than blocking any of its known endothelial ligands, e.g. ICAM-1 (Smith *et al.*, 1989; Weber *et al.*, 1997a). This has prompted speculation concerning the importance of additional LFA-1 ligands in transmigration. Hence, the interaction of LFA-1 with JAM-1 documented in this thesis has substantiated the hypothesis that LFA-1 may use, or even require, multiple junctional ligands during diapedesis.

The differences observed in cell adhesion on resting and costimulated HUVECs, were most likely due to the fact that ICAM-1 expression is upregulated in activated cells or inflamed tissue whereas normally it is expressed only at low levels (Nortamo *et al.*, 1991), and that an increased surface density of JAM-1 is induced under the specific conditions of a combined TNF-α/IFN-γ cytokine treatment (Ozaki *et al.*, 1999; Shaw *et al.*, 2001c). In contrast to the data described here, adhesion of monocytes to JAM-1–expressing endothelial cells was not affected by treatment with the murine JAM-1 mAb BV11 (Martìn-Padura *et al.*, 1998). This could be explained by a redundancy in adhesive receptor-ligand pairs, e.g. Mac-1/ICAM-1 and VLA-4/VCAM-1, or more likely by insufficient surface expression when JAM-1 is not redistributed from the interendothelial junctions.

In conclusion JAM-1 was confirmed as a novel counter-receptor of LFA-1 in a more physiological context. Furthermore, the results implicated a functional role for this molecular interaction in the inflammatory recruitment of memory T lymphocytes. Interestingly, endothelial expressed human JAM-2 is also able to bind T lymphocytes (Cunningham *et al.*, 2000). The receptor recognizing endothelial JAM-2 is lymphocytic JAM-3 (Arrate *et al.*, 2001; Liang *et al.*, 2002). Thus these JAM isoforms constitute mutual heterophilic interaction partners *in trans*. Notably, human JAM-2 expression is increased in tissues with chronic inflammatory disease (Liang *et al.*, 2002) and human JAM-3 expression is highly up-regulated in activated lymphocytes (Arrate *et al.*, 2001), indicating a functional role of the heterophilic JAM-2/JAM-3 interaction in inflammatory processes.

5.9. Validation under conditions of laminar flow

The process of leukocyte diapedesis through the endothelium *in vivo* occurs in the context of blood flow. To reach a site of inflammation, the cells must first marginate to the blood vessel wall and form stable adhesions before migrating into the extravascular space. Their rolling, adhesion and transmigration are thereby subjected to physiological shear (**fig. 28**).

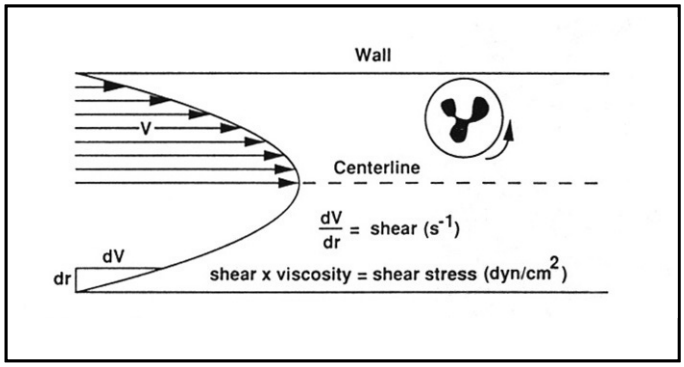

figure 28: Flow profile in a parallel plate flow chamber. Both cylindrical blood vessel and parallel-plate flow chamber (see **fig. 4**) geometries exhibit the demonstrated flow profile with parabolic increase of the flow velocity (V) from the wall toward the centerline. The shear rate describes the change in velocity (dV) per change in radial displacement (dr) and is highest at the wall. The physical forces acting on a cell under flow correlates with the shear stress, defined as product of shear rate and viscosity, that is directly proportional to the flow rate. Adapted from Lawrence *et al.*, 1991.

In vivo these external mechanical forces not only counteract initial adhesive processes by their disruptive property (Lawrence *et al.*, 1991) but they are also crucial for establishing them, e.g. by triggering mechanoresponsive elements, such as focal adhesion kinases or stretch-activated ion channels, on both migrating leukocytes and endothelial cells (Cinamon *et al.*, 2001b). Moreover, it has been demonstrated that threshold levels of fluid shear promote leukocyte adhesion through selectins (Lawrence *et al.*, 1997). Torque forces generated by shear stress may increase leukocyte contact with the EC barrier by deformation and thereby facilitate its exposure to EC-displayed CAMs (Moazzam *et al.*, 1997). Fluid shear stress also affects the endothelial lining that functions as a transducer of this biomechanical stimuli into biological responses within the vessel wall. This includes induction of nitric oxide synthase (NOS), production of prostacyclin, cytokines, growth factors, extracellular matrix components and vasoactive mediators as well as transcriptional activation of genes containing the shear stress response element (SSRE) in their promoter regions (Gimbrone, 1999).

By incorporating shear flow conditions into the adhesion assay set-up (see **fig. 4**), some of the physical constrains of force and contact time were simulated that affect leukocyte margination and cell wall attachment *in vivo*. This allowed the testing of the LFA-1/JAM-1 interaction for its

ability to form stable shear-resistant bonds and thus to verify its physiological relevance in cell adhesion and leukocyte recruitment. Flow chamber experiments were performed under a wall shear stress of 1.5 dyn/cm^2. This value is in the range estimated to exist in post-capillary and high-endothelial venules, *i.e.* approx. $1-4$ dyn/cm^2 (Lawrence *et al.*, 1991; Jones *et al.*, 1996a). Stimulation of $CD4^+CD45RO^+$ T cells with the chemokine SDF-1α was appropriate for flow chamber experiments, primarily due to its ability to induce integrin–mediated arrest of rolling T lymphocytes within subseconds even under conditions of flow (Grabovsky *et al.*, 2000; Campbell *et al.*, 1998; Constantin *et al.*, 2000). The useful characteristics of SDF-1α in this context has been previously demonstrated for $CD34^+$ progenitor cells (Peled *et al.*, 1999).

The parallel-plate flow chamber data further strengthened the results obtained in static adhesion assays. Anti–JAM-1 did not affect the LFA-1–dependent adhesion of $CD4^+CD45RO^+$ memory T cells when the endothelium was not costimulated with TNF-α/IFN-γ and JAM-1 was located in the junctions. The redistribution of JAM-1 to the surface induced by this combined cytokine treatment led to firm cellular arrest that was resistant to mechanical shear stress of 1.5 dyn/cm^2. Again, leukocyte-EC binding was reduced by anti–JAM-1 and ICAM-1 mAb alone and was diminished to background binding levels when these antibodies were combined. Their additive effect suggested that JAM-1 cooperates with ICAM-1 as an alternative IgSF ligand for the β_2 integrin LFA-1. Importantly, the shear-resistance of JAM-1/LFA-1–mediated cell arrest revealed the functional consequence of this heterophilic interaction under conditions simulating the blood circulation in post-capillary venules.

5.10. LFA-1 and JAM-1 in transendothelial extravasation of leukocytes

In contrast to tethering, rolling and firm adhesion, less is known about the molecular basis of the late steps in leukocyte recruitment controlling the cellular extravasation through tightly apposed endothelial cells (Bianchi *et al.*, 1997). It was proposed that transendothelial migration of neutrophils may involve a bypass of junctional barriers and occur at preexisting discontinuities in both their tight junctions (TJs) and adherens junctions (AJs) at tricellular corners (Burns *et al.*, 1997). This process would not require disruption or loss of junctional components. The same applies for the mechanism of transcellular extravasation observed for chemoattractant-stimulated neutrophils that traversed ECs predominantly through their cell body (Feng *et al.*, 1998). However, it appears that transmigration occurs primarily along the paracellular route, requiring a highly coordinated and reversible opening and closing of intercellular junctions in order to preserve vascular integrity (Springer, 1994; Balda *et al.*, 2000). Leukocyte diapedesis has

therefore been associated with a reversible remodeling of endothelial AJs between neighboring cells (Del Maschio *et al.*, 1996; Allport *et al.*, 2000). However, the exposure of ECs to histamine, which increases permeability and clearly induces disorganization of AJs, does not augment or substitute for chemokine-triggered leukocyte transendothelial migration (Andriopoulou *et al.*, 1999). Thus, changes in endothelial permeability *per se* do not appear to be rate-limiting for diapedesis. Nevertheless, migrating leukocytes have been found to induce a delocalization of VE-cadherin from AJs by as yet unidentified mechanisms allowing leukocytes to traverse the opened gap (Shaw *et al.*, 2001b). While gap junctions have thus far not been implicated in the process of diapedesis, the strictly occluded apical barrier of endothelial TJs must to be physically separated by extravasating leukocytes.

Localized at intercellular junctions nearby TJs and apparently involved in sealing the endothelial barrier via homophilic interactions *in trans* (Martìn-Padura *et al.*, 1998; Liu *et al.*, 2000b; Liang *et al.*, 2000), JAM-1 appeared to be ideally situated to play a functional role in leukocyte transmigration. Indeed, murine JAM-1 mAb BV11 inhibited leukocyte transmigration across endothelial cells in tissue culture assays as well as in an *in vivo* model of skin inflammation (Martìn-Padura *et al.*, 1998). Moreover, BV11 interfered with the accumulation of leukocytes in the cerebrospinal fluid in cytokine-induced meningitis (Del Maschio *et al.*, 1999). The mode of BV11 action remains unknown but could be based upon a stabilization of homophilic JAM-1 interactions between neighbouring ECs, thus inhibiting the dissociation of the junctional barrier. In this regard, the BV11 mAb was reported to specifically bind dimers but not monomers of murine rsJAM-1 *in vitro*, and not to induce dissociation of these dimers (Bazzoni *et al.*, 2000a). Alternatively, BV11 could inhibit transmigration by blocking the interaction of JAM-1 with an unidentified heterophilic receptor on leukocytes that was subsequently postulated (Martìn-Padura *et al.*, 1998).

Given the functional involvement of JAM-1/LFA-1 binding in leukocyte adhesion on ECs under inflammatory conditions, this raised the possibility that the JAM-1/LFA-1 interaction might also be involved in leukocyte diapedesis. Transmigration assays both under static and flow conditions were therefore applied to question this potential role. Extravasation of leukocytes in stasis was investigated in transwell chambers (see **fig. 3**) where chemotaxis was induced by gradients of soluble chemoattractants generated beneath endothelial monolayers. Transmigration assays were also performed in a flow system (see **fig. 4**). This was appropriate since transwell chamber assays reflect only poorly the physiological situation prevailing during diapedesis, due to the lack of a physiological mechanical context and the prolonged time scales for extravasation. Moreover, it is unclear whether leukocytes under shear flow can sense and respond to sublumenal tissue chemokines within the short time frame of their contact with the endothelium (Cinamon *et al.*, 2001a). Therefore it has been hypothesized that diapedesis across the paracellular cleft is mediated by a haptotactic gradient, *i.e.* a gradient of solid-phase–bound adhesion molecules like platelet endothelial cell adhesion molecule (PECAM)-1 and cadherins,

rather then by chemotactic migration, *i.e.* along a gradient of soluble chemokines that may predominate in subendothelial migration through extravascular tissues (Bianchi *et al.*, 1997). In this regard, it was demonstrated that $CD3^+$ T lymphocyte migration across vascular endothelium *in vitro* can be triggered solely by continuously applied physiological shear stress and apical immobilized chemokines (chemorheotaxis[2]) without the need for a chemotactic gradient (Cinamon *et al.*, 2001b; Luscinskas *et al.*, 2001). However, these data contrast markedly with previous results where neutrophils and monocytes efficiently migrated across cytokine-stimulated EC monolayers under either static or flow conditions without exogenously applied chemokines (Shaw *et al.*, 2001b).

Chemotaxis experiments under static conditions revealed that SDF-1α–triggered migration of $CD4^+CD45RO^+$ T cells across resting HUVEC monolayers was mainly LFA-1–dependent. Anti–JAM-1 significantly reduced this chemotactic emigration, which was consistent given the transmigration-blocking properties of this antibody. This finding suggested a functional role for JAM-1 in transendothelial extravasation of T lymphocytes. Experiments performed in the flow system confirmed and further strengthened these results. Blocking anti–JAM-1 reduced the LFA-1–mediated spreading or transendothelial migration of memory T cells under flow conditions. A combined blockade of JAM-1 and ICAM-1 inhibited migration additively, suggesting that both molecules display alternative ligands for LFA-1 and are required to achieve optimal diapedesis. In contrast to the failure of JAM-1 to participate under flow conditions in firm leukocyte arrest on unstimulated ECs, a dependence of JAM-1–mediated transendothelial migration under flow on TNF-α/IFN-γ–costimulation, and thus on the redistribution of JAM-1 from intercellular junctions to the apical surface, was not evident.

Besides such a redistribution, a combined treatment with these proinflammatory cytokines induces an increased paracellular permeability of endothelial monolayers (Shaw *et al.*, 2001c), indicating a decrease in paracellular barrier function. An increased junctional permeability may participate in leukocyte diapedesis by promoting accessibility to basolaterally localized JAM-1 that might guide attached T cells along the intercellular cleft in a haptotactic manner. The findings concerning the consequences of TNF-α/IFN-γ–induced endothelial permeability for leukocyte extravasation are however contradictory. Neutrophil emigration *in vitro* across costimulated endothelium was reported to be reduced in stasis (Rival *et al.*, 1996) while unaltered in flow (Shaw *et al.*, 2001c) and increased *in vivo* (Munro *et al.*, 1989), when compared to a stimulation with only TNF-α that alone does not significantly influence EC permeability (Shaw *et al.*, 2001c). These findings indirectly suggest a mutual independence in the control of endothelial permeability on one hand and transendothelial migration on the other hand. However, members of the JAM family may be directly involved in the permeability control of endothelial barriers. Thus, the expression of murine JAM-3 is restricted mainly to ECs

[2] in regard to the term “chemotaxis”; chemo: abbreviation for chemoattractant; rheo: flow; taxis: movement

of high endothelial venules (HEVs) and lymphatic vessels, two highly permeable compartments specialized in lymphocyte homing, whereas murine JAM-1 is only expressed in low amounts. At the same time murine JAM-1 is highly expressed in the vasculature of adult brain, which forms one of the tightest blood tissue barriers of the body, whereas murine JAM-3 is not expressed therein. In accordance with these findings, stable expression of JAM-1 in Madin-Darby canine kidney (MDCK) cell monolayers did not affect the paracellular permeability, whereas JAM-3 expression caused a 5-fold increase (Aurrand-Lions *et al.*, 2001b). In CHO cell monolayers murine JAM-1 even reduced the paracellular permeability (Martìn-Padura *et al.*, 1998). Murine JAM-1 and JAM-3 therefore appear to exert opposite functions at intercellular junctions. Whether their effect on permeability directly influences leukocyte transmigration remains to be tested.

5.11. JAM-1 in the extravasation of myeloid cells

As JAM-1 has been implicated in the transmigration of myeloid cells (Martìn-Padura *et al.*, 1998), the analysis of leukocyte adhesion and transmigration was extended from previously investigated T lymphocytes to isolated human neutrophils. Whereas the recruitment of memory T cells to sites of inflammation is considerably dependent on the chemokine receptor CXCR4 (Nanki *et al.*, 2000), neutrophil arrest is mainly mediated by CXCR2. Exogenous application of neutrophil stimuli was not required since TNF-α–treatment of HUVECs induces endogenous expression of the CXCR2 ligands IL-8 (CXCL8) and growth-related oncogene (GRO)-α (CXCL1) on ECs (Miller *et al.*, 1992).

In contrast to the data obtained with memory T cells, JAM-1 exerted no significant participation in CXCR2-mediated arrest of neutrophils on inflamed HUVECs under shear flow. Similar observations concerning neutrophil arrest were reported in parallel by others (Shaw *et al.*, 2001c). This result was in accordance with blocking data revealing that the JAM-1–receptor LFA-1 alone was not sufficient to meditate firm arrest of rolling neutrophils, whereas the combined blockade of both LFA-1 and Mac-1 by a β_2 mAb resulted in marked inhibition of neutrophil adhesion. These findings confirmed a report showing that both LFA-1 and Mac-1 are redundantly involved in neutrophil arrest under flow (Gopalan *et al.*, 2000), even though the relative contribution of these two β_2 integrins in neutrophil adhesion and transendothelial migration *in vivo* is still a matter of debate (Lu *et al.*, 1997; Ding *et al.*, 1999; Henderson *et al.*, 2001). The absence of an marked influence in neutrophil adhesion by JAM-1, as opposed to its prominent role in T lymphocyte arrest, thus appears to depend on the corresponding lower contribution of its receptor LFA-1 to neutrophil adhesion due to the redundant involvement of other receptor-ligand pairs, e.g. Mac-1/ICAM-1 (Gopalan *et al.*, 2000) and VLA-4/VCAM

(Henderson *et al.*, 2001). Remarkably, neutrophil adhesion was inhibited by blocking ICAM-1, which serves as a ligand for both LFA-1 and Mac-1 (Diamond *et al.*, 1991), but not by anti–JAM-1. This observation suggested that JAM-1 is a specific counter-receptor for LFA-1 but not Mac-1 and confirmed equivalent results obtained with cell adhesion assays using J-β_2.7/α_M lymphocytes and JAM-1–expressing CHO cells. Furthermore, cellular arrest was also investigated for myeloid HL-60 cells. These cells revealed LFA-1–mediated adhesion to CHO-JAM cells in a JAM-1–dependent manner.

In contrast, transendothelial chemotaxis of neutrophils, triggered by a chemotactic gradient of IL-8 (CXCL8) depended considerably on the involvement of both LFA-1 counter-receptors JAM-1 and ICAM-1. This result was in accordance with blocking data revealing that the chemotactic migration of the neutrophils, in contrast to their adhesion, was mainly LFA-1–mediated. The notion by others that human JAM-1 mAbs did not block transendothelial migration of neutrophils or monocytes in flow (Shaw *et al.*, 2001c), as opposed to murine JAM-1 mAb BV11 (Del Maschio *et al.*, 1999), is likely due to their epitope specificity. This is supported by the finding that these antibodies influence JAM-1–dependent homotypic cell-cell adhesion (Liu *et al.*, 2000b; Sobocka *et al.*, 2000), which is mediated by the membrane-distal Ig-like domain 1 (Kostrewa *et al.*, 2001; Bazzoni *et al.*, 2000a) but not the LFA-1–binding domain 2 of JAM-1. This further substantiates the functional dichotomy between both JAM-1 domains. By identifying the involvement of both LFA-1 ligands JAM-1 and ICAM-1 in myeloid cell transmigration, this adds to results that implied JAM-1 participation in chemokine-induced transmigration of monocytes and neutrophils *in vitro* and *in vivo* (Martìn-Padura *et al.*, 1998; Del Maschio *et al.*, 1999). The findings described here therefore reveal that JAM-1, although it may facilitate firm arrest of T cells but not neutrophils, may play a more prominent role in transendothelial diapedesis of myeloid cells.

5.12. The molecular zipper model

The involvement of human JAM-1 in two key aspects of leukocyte recruitment, *i.e.* adhesion and diapedesis, suggests that this IgSF protein may be particularly well suited to guide leukocyte extravasation from the apical surface across the lateral intercellular junctions. The findings described within the presented study raise the possibility that beyond a primary adhesive interaction with endothelial JAM-1, leukocytic LFA-1 may serve to intercept interendothelial JAM-1/JAM-1 interactions at cellular junctions during diapedesis of leukocytes across the endothelial barrier (see **fig. 30**).

The participation of JAM-1 in the initial arrest of leukocytes on inflamed endothelia may be enabled by partial redistribution of JAM-1 localized at intercellular junctions to the apical surface under specific inflammatory conditions (Ozaki *et al.*, 1999; Shaw *et al.*, 2001c). Subsequent LFA-1–mediated leukocyte adhesion possibly depends on or is supported by a *cis*-dimeric state of endothelial JAM-1 (Bazzoni *et al.*, 2000a), similar to what has been demonstrated for the interaction of ICAM-1 with LFA-1 (Miller *et al.*, 1995; Reilly *et al.*, 1995). Crystallographic data of recombinant soluble JAM-1 revealed that such lateral homophilic association is mediated by the N-terminal Ig-like domain 1 of both molecules, leading to a U-shaped *cis*-configuration of JAM-1 dimers on the cell surface (**fig. 29**).

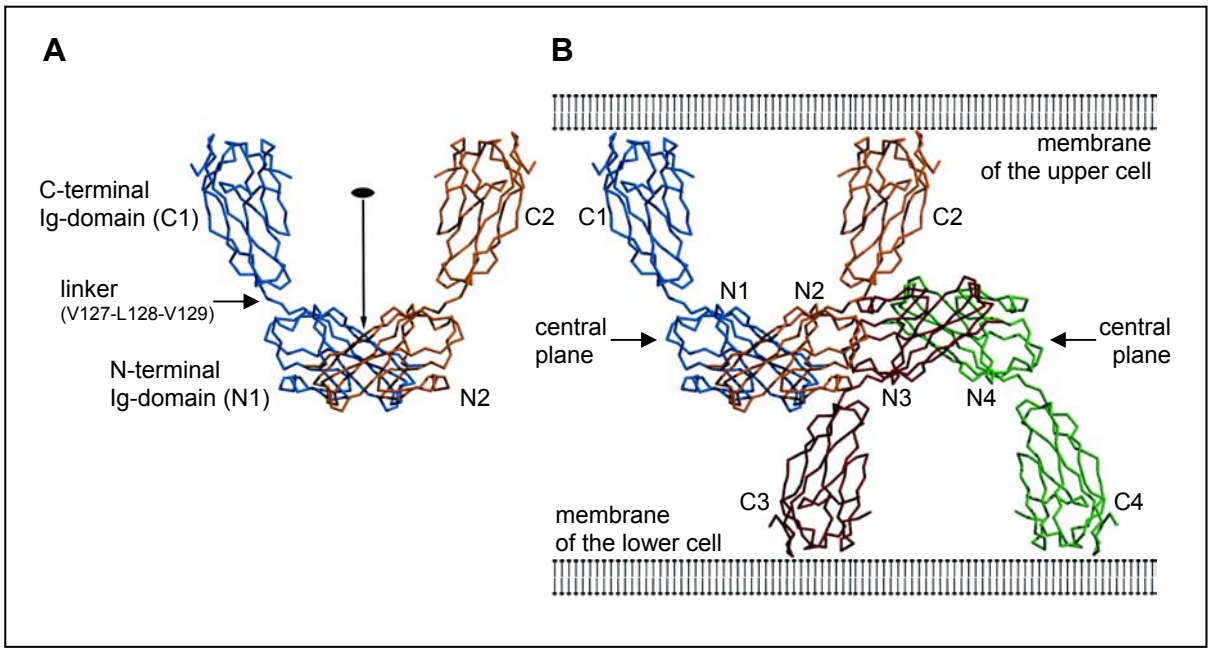

figure 29: Molecular structure of recombinant soluble murine JAM-1 (rsJAM) and its homophilic complexes *in cis* and *in trans* based on crystallographic data. **(A)** Complex of two JAM-1 molecules interacting *in cis* (lateral homophilic interaction). One molecule is coloured in blue. Its N-terminal Ig-like domain 1 is labeled N1 and its C-terminal membrane-proximal Ig-like domain 2 is labeled C1. Both domains are connected at an angle of about 125° by a short linker (Val127-Leu128-Val129). The second molecule is coloured in orange and its Ig-like domains are labeled N2 and C2, respectively. Dimerized JAM-1 molecules contact each other with their N-terminal domains (N1 and N2), leading to an U-shaped conformation. The monomers are thereby related by a crystallographic twofold rotation axis, indicated by an arrow and a dyad symbol. **(B)** Complex of two U-shaped JAM-1 dimers from opposite cell membranes interacting homophilically *in trans*. One dimer is coloured in blue and orange in the same orientation as shown in (A), the other dimer in violet (with its Ig-like domains N3 and C3) and green (with its Ig-like domains N4 and C4), respectively. The pair of *cis*-dimers contact each other at their N-terminal domains (N2 and N3) such that their C-terminal domains point pair-wise in opposite directions, representing a *trans*-interaction. The membrane-proximal Ig-like domains stick out almost perpendicular from the lipid bilayer. The predicted distance between the opposing cell surfaces is about 105-110 Å, which is comparable with the estimated distance of about 100 Å at TJs. The interacting N-terminal domains of the U-shaped *cis*-dimers lie almost parallel to the cell surfaces and contact each other in a common central plane. Repeating this structural motif over several neighbouring cells would lead to a model of a two-dimensional network of *trans*-homophilic interacting JAM-1 dimers that might participate in this way to the integrity of the junctional barrier. Adapted from Kostrewa *et al.*, 2001.

A model based on this analysis proposed a two-dimensional network of N-terminal associated JAM-1 molecules interacting *in trans* with JAM-1 dimers from the opposite cell surfaces in a common central plane (Kostrewa *et al.*, 2001). The structure analysis suggested that also this *trans*-homophilic interaction is mediated by domain 1 of JAM-1. These data support the finding

described herein, that LFA-1 binds its ligand JAM-1 at the membrane-proximal Ig-like domain 2. According to the X-ray structure this domain protrudes almost perpendicular from the cell surface (**fig. 29**). The accessibility of domain 2 for a heterophilic *trans*-interaction with opposing LFA-1 appears ensured by a steric inclination of the N-terminal domain 1 by about ~55° (Kostrewa *et al.*, 2001).

Residual junctional JAM-1 not redistributed under inflammatory conditions may guide extravasating leukocytes along the cellular cleft in a haptotactic manner. It can be speculated that leukocytic LFA-1 may sterically intercept domain 1-mediated homophilic *trans*-interactions of junctional JAM-1 by binding to domain 2, thus disrupting or intercalating their intercellular interaction and thereby unlocking cell-cell junctions in a zipper-like manner. On the other hand, it may be feasible that homotypic JAM-1 interactions on opposing ECs are replaced by an interaction of endothelial JAM-1 with JAM-1 of intruding leukocytes via the domain 1 (**fig. 30**). It is conceivable that LFA-1 may bind laterally (*in cis*) to the cytoplasmic and/or other domains of leukocytic JAM-1. For LFA-1, such an initial *cis*-binding would facilitate the recruitment of its final interaction partner, *i.e.* endothelial JAM-1, by helping to bring LFA-1 into closer proximity with domain 2 of this molecule following homotypic interactions of leukocyte and endothelial JAM-1 (**fig. 30**).

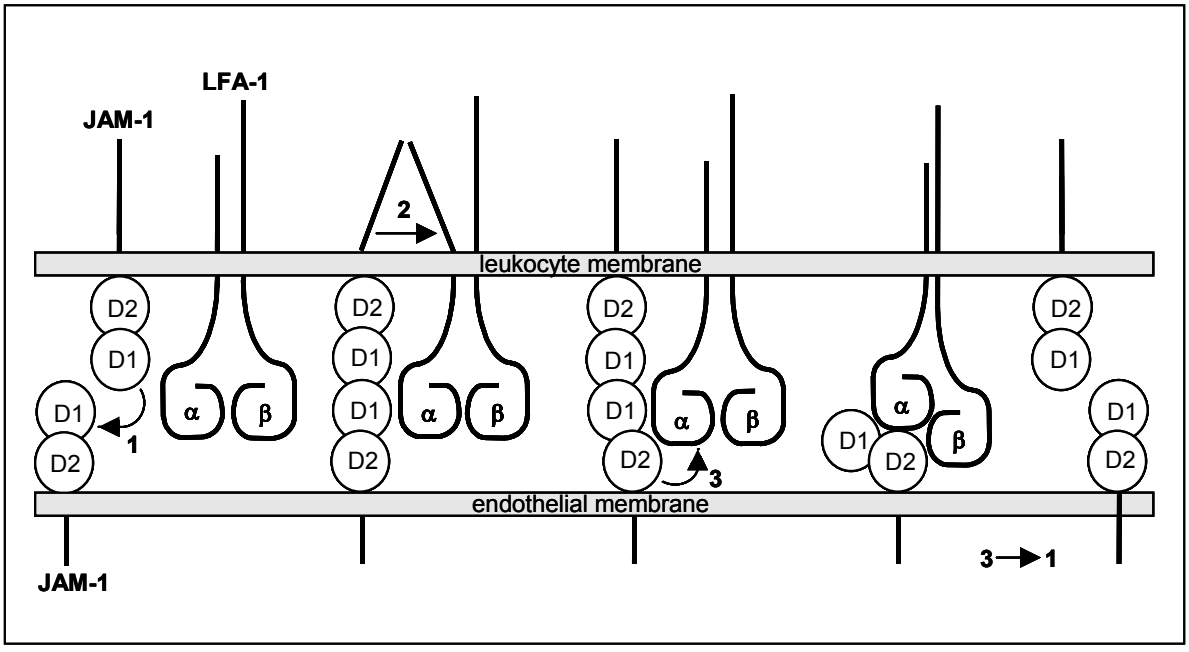

figure 30: A molecular zipper model for leukocyte diapedesis mediated by heterophilic LFA-1/JAM-1 interactions as described. **(1)** Homotypic endothelial JAM-1 interactions *in trans* intercepted by leukocytic JAM-1 result in heterotypic JAM-1 binding. **(2)** Lateral binding between LFA-1 and leukocytic JAM-1 results in close proximity to endothelial JAM-1. **(3)** LFA-1 interacts *in trans* with endothelial JAM-1 via its membrane-proximal Ig-like domain 2. **(3→1)** Further homotypic endothelial JAM-1 pairs are intercepted by leukocytic JAM-1 as described in (1) thus guiding the leukocyte across the interendothelial cleft in a zipper-like manner.

This scenario is intriguing in light of the initial findings in the YTH assay, that the interaction of LFA-1 and JAM-1 occurs via their cytoplasmic domains. This may suggest the possibility of a LFA-1/JAM-1 interaction *in cis* on leukocytes and would parallel a report showing that the IgSF member PECAM-1, which also engages in homophilic associations with other PECAM-1 molecules, functions as a *cis*-interacting ligand for the integrin $\alpha_v\beta_3$ (Wong *et al.*, 2000). Such an interaction would be indicative of a close proximity of LFA-1 and JAM-1 on leukocytes and may be highly regulated by cellular activation, so that it may not be consistently detectable in purification methods.

Altogether, the leukocytes may employ a complex interplay of homophilic JAM-1/JAM-1 and heterophilic JAM-1/LFA-1 interactions to open junctions, to migrate in a haptotactic manner along the intercellular cleft and to subsequently restore – again in a zipper-like manner – the junctional integrity (see **fig. 31**). Given its junctional localization and the redistribution under specific inflammatory conditions, JAM-1 appears ideally suited to provide such a molecular zipper for leukocyte diapedesis.

5.13. Sequential steps of leukocyte diapedesis

Emerging data provide support for the concept that junction-localized IgSF proteins, which can interact intercellularly via homophilic binding, may be particularly well suited to support transendothelial migration of leukocytes. One important example is PECAM-1 (**fig. 31**). The expression pattern and molecular structure of PECAM-1 shows a remarkable similarity to that of JAM-1, with expression at intercellular junctions (although more basolaterally localized and not associated with either TJs or AJs), as well as on circulating blood cells (Ayalon *et al.*, 1994; Johnson-Léger *et al.*, 2000). Like JAM-1, PECAM-1 can also be redistributed from cell-cell contacts by costimulation with the cytokines TNF-α and IFN-γ (Romer *et al.*, 1995). It has been implicated in two distinct steps during emigration of monocytes, neutrophils and NK cells. First, homophilic interactions of leukocytic PECAM-1 with their endothelial counterparts, mediated by the Ig-like domains 1 and 2 (Newton *et al.*, 1997), appear to contribute to diapedesis *per se*, since blockade of this step by antibodies arrests leukocytes on the apical surface of the endothelium (Muller *et al.*, 1993). Second, the domain 6 of leukocyte PECAM-1 undergoes heterophilic interactions with yet unidentified binding partners in the basement membrane, since blocking this step retains leukocytes between the basal surface of the EC and the basal lamina (Liao *et al.*, 1995). However, PECAM-1–deficient mice do not reveal a major defect in inflammatory disease models (Duncan *et al.*, 1999), indicating that the requirement for this IgSF molecule is not obligatory for leukocyte extravasation. By analogy with the redundancy displayed in the cascade of leukocyte recruitment, this suggests a crucial involvement of other junction molecules in the

process of diapedesis, e.g. JAM-1 which might collaborate with PECAM-1 in guiding the cell along the intercellular cleft.

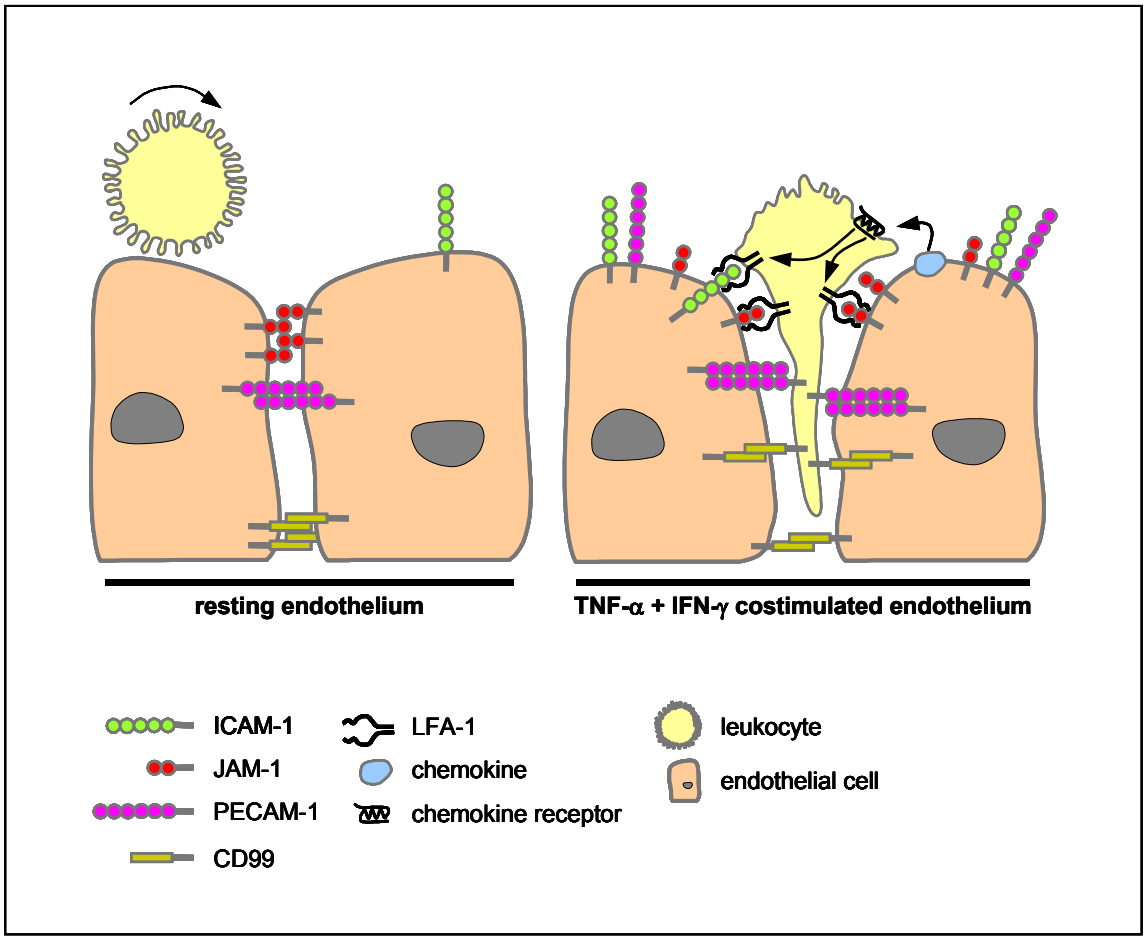

figure 31: Novel molecular mechanisms in leukocyte extravasation. **(left part)** Intercellular homophilic interactions by PECAM-1 and JAM-1 mediate, in addition to other molecules (not shown) the integrity of the junctional barrier in resting endothelium. **(right part)** Inflammatory stimulation leads to expression of ICAM-1 on the apical surface and redistribution of JAM-1 and in part PECAM-1 from the intercellular junctions to the luminal surface. After tethering and rolling, leukocytes are activated by chemokines which leads to LFA-1 engagement with vascular ICAM-1 and JAM-1 and to firm arrest of the leukocyte on the inflamed endothelium. During diapedesis, homophilic interactions of JAM-1, PECAM-1 and CD99 between opposing endothelial cells (homotypic interactions) might guide the leukocyte across the intercellular cleft, thereby being disrupted by the leukocyte and replaced by homophilic interactions of PECAM-1 and CD99 between the leukocyte and endothelial cells and by heterophilic interactions of endothelial JAM-1 with leukocytic LFA-1 (in each case heterotypic interactions) in a haptotactic and zipper-like manner. Adapted from Johnson-Léger *et al.*, 2000, and Aurrand-Lions *et al.*, 2002.

CD99, a heavily *O*-glycosylated 32-kDa type I transmembrane protein expressed on most hematopoietic cells and likewise concentrated at interendothelial junctions (**fig. 31**), has been recently shown to play an important role in the last stage of monocyte diapedesis (Schenkel *et al.*, 2002). Whereas blocking PECAM-1 arrests leukocytes on the apical surface of the endothelium, with pseudopods attempting to protrude into the junctions, blocking CD99 arrests monocytes distal to the PECAM-1–dependent step at a point where they are partially through the junction (**fig. 31**). The late arrest may be explained by a blockade of the uropod, the trailing end of the migrating cell and a membrane region that concentrates high numbers of CAMs such as ICAM-1, although it is not known whether CD99 is enriched in this region (Aurrand-Lions *et al.*,

2002). Diapedesis involves the homophilic interaction between monocytic and endothelial CD99. However, since CD99 regulates expression and affinity of the integrin LFA-1 via an unknown signal transduction pathway (Hahn *et al.*, 1997), CD99 interactions may indirectly influence leukocyte transendothelial migration, possibly by regulating the function of integrins in the uropod.

It appears that emigrating leukocytes first use heterophilic LFA-1/JAM-1 and homophilic PECAM-1 interactions to penetrate the apical entry of the junction and to initiate emigration. Homophilic CD99 interactions then allow the invading leukocyte to transmigrate through clefts in the endothelial wall and to complete emigration. Thus, diapedesis is regulated sequentially in a multi-step process by these three distinct molecules (**fig. 31**). Taken together, the recent insights into mechanisms of transendothelial migration suggest that a multi-layered molecular zipper set up by JAM-1, PECAM-1 and CD99 enables effective diapedesis of leukocytes across the endothelial barrier without a detremental leakage of the vascular endothelium.

5.14. Perspectives

This study has identified a heterophilic interaction between the β_2 integrin LFA-1 and the IgSF molecule JAM-1 and demonstrated its role in adhesion and transendothelial migration of leukocytes in the context of inflammation.

A molecular zipper model might explain the involvement of JAM-1 in leukocyte emigration. Given the redundancy of PECAM-1 illustrated in deficient mice, it remains to be determined whether the LFA-1/JAM-1 interaction cooperates with PECAM-1 and CD99 in leukocyte transendothelial migration or constitutes an alternative pathway.

Although JAM-1 is expressed in human circulating cells, its functional role in these cells remains unclear. Interestingly, initial findings within this study indicated a lateral interaction of JAM-1 and LFA-1 on the surface membrane of leukocytes. An understanding of the significance of JAM-1 expression in blood cells would be of particular interest given the highly distinctive expression pattern with abundant expression in human and lack of expression in most murine hematopoietic cells. Similarly, the striking differences which exist between the two species concerning JAM-1 expression in the brain is not understood. Whereas JAM-1 is abundantly expressed in murine brain tissues (Martìn-Padura *et al.*, 1998) it is barely detectable in human brain (Williams *et al.*, 1999; Naik *et al.*, 2001; Gupta *et al.*, 2000). This finding is tantalizing given the involvement of JAM-1 in the constitution of the blood-brain barrier (BBB) impermeability.

Although the membrane-proximal Ig-like domain 2 of JAM-1 has been characterized as the LFA-1 binding domain, it would be of special interest to further define the region or even identify critical amino acids in both LFA-1 and JAM-1 essential for their heterophilic interaction. It remains to be determined whether the I domain of the LFA-1 α chain is not only implicated in ICAM-1 but also in JAM-1 binding. Furthermore, it is remarkable that both *N*-glycosylation sites of human JAM-1 are localized within the LFA-1 binding domain 2 of JAM-1. Given the influence of glycosylation in regulation of the ICAM-1/Mac-1 and the ICAM-2/LFA-1 interactions (Diamond *et al.*, 1991; Casasnovas *et al.*, 1997) and different levels of JAM-1 glycosylation within some cell types (Liu *et al.*, 2000b; Liang *et al.*, 2000; Sobocka *et al.*, 2000), it will be important to determine whether the carbohydrate side chains of JAM-1 have any functional role in the binding of LFA-1. Moreover, it will be interest to confirm whether the lateral dimerization of JAM-1 molecules is crucial or supportive for the interaction with LFA-1, e.g. by providing a specific and functionally necessary orientation of these molecules on the cell surface. The precise stereochemical complementarity of the homophilic binding-mediating interface (see **fig. 29**) and the high affinity of rsJAM homophilic interactions *in vitro* (Bazzoni *et al.*, 2000a) suggests that JAM-1 dimers might be permanent and obligatory complexes (Jones *et al.*, 1996b) and that *cis*-dimers might occur prior to any adhesive homophilic or heterophilic *trans*-interactions of JAM-1.

An important aspect not investigated in this study is the functional role that the cytoplasmic tail of JAM-1 might play during emigration of leukocytes but also in the binding of its receptor LFA-1. Thus it should be examined whether the engagement of leukocytic LFA-1 during diapedesis induces any signal transduction by endothelial JAM-1 that may be involved in further regulation of leukocyte extravasation through the vascular wall. It would be intriguing if regulatory elements could be discovered within the cytoplasmic domain of JAM-1 that are able to participate in signal transduction. Thus JAM-1 has been shown to be phosphorylated by PKC upon platelet activation (Ozaki *et al.*, 2000). Moreover, it remains to be clarified whether the intracellular tail of leukocytic JAM-1 interacts laterally with the α tail of LFA-1.

Beside the important role of leukocyte recruitment for immune homeostasis and surveillance under physiological conditions, particular acute inflammation states such as meningitis (Del Maschio *et al.*, 1999) can lead to severe alterations in physiology and cause severe tissue damage due to excessive release of microbicidal oxygen radicals, proteases and inflammatory stimuli by emigrating leukocytes. Moreover, inflammatory processes have been implicated in human diseases such as allergic airway inflammation, rheumatic arthritis (Strieter *et al.*, 1996) and atherosclerosis (Ross, 1999; Lusis, 2000) and are implicated in allograft rejection after organ transplantation (Gerard *et al.*, 2001). The incidence of such pathological inflammation underscores the need for a more detailed understanding of the complex molecular and cellular regulation of inflammatory processes. In this regard, one principal goal is the assessment of

JAM-1 as a potential therapeutic target. At present, this is a subject of controversy. Intravenous injection of the mAb BV11 directed against murine JAM-1 into mice with bacterial meningitis caused severe complement-dependent damage in blood vessel endothelia of the brain and led consequently to central nervous system (CNS) bleeding. This could be prevented by removal of the complement-activating Fc part of the antibody but application of BV11 Fab did not show any beneficial effect to mice (Lechner *et al.*, 2000). However, in a murine model for cytokine-induced experimental meningitis, BV11 administration blocked the recruitment of neutrophils into the CNS, decreasing the permeability of the BBB and attenuating meningitis (Del Maschio *et al.*, 1999). The different mechanisms underlying leukocyte trafficking in these models should first be clarified in order to properly assess the potential of JAM-1 as a therapeutic target, in particular with respect to an improvement in the survival rate in severe pathological cases of meningitis. Moreover, the significance of JAM-1 (F11R) auto-antibodies in the circulation of patients with thrombocytopenia (Sobocka *et al.*, 2000) remains to be determined.

The functional implication of heterophilic LFA-1/JAM-1 interactions in diapedesis across inflamed endothelium was confirmed in *in vitro* assays performed under physiological conditions. Thus, the experiments were performed with cells isolated from the human vascular system, with physiological stimuli and under conditions of laminar flow simulating the microcirculation. Nevertheless, a confirmation of the results presented within this study in relevant *in vivo* models will be of compelling interest, e.g. employing intravital microscopy. Furthermore, it would be of particular interest to investigate the phenotype of JAM-1–deficient mice in terms of diapedesis during lymphocyte homing and inflammatory reactions.

6. Note added in proof

The recent identification of the interaction between the β_2 integrin LFA-1 ($\alpha_L\beta_2$) and the human IgSF protein JAM-1 constitutes a model for additional integrin-JAM binding pairs published just prior to completion of this manuscript.

Thus, the second major leukocyte β_2 integrin Mac-1 ($\alpha_M\beta_2$) is reported to bind specifically to the third member of the JAM family (JAM-3) expressed on human platelets (Santoso *et al.*, 2002). This specific interaction appears to be mediated by the I domain of Mac-1. There were also indications that JAM-3 binds to a lesser extent to p150.95 ($\alpha_X\beta_2$). An interaction with LFA-1, however, was specifically excluded. JAM-3 together with the glycoprotein (GP) Ibα (Simon *et al.*, 2000) thus serves as the major ligand on the surface of platelets for leukocyte Mac-1. Cellular interactions mediated by this binding pair may occur in the context of leukocyte attachment to and transmigration across surface-adherent platelets at sites of vascular injury under certain pathological conditions (Diacovo *et al.*, 1996).

In contrast to the other JAM proteins, human JAM-2 engages leukocyte VLA-4, a β_1 integrin ($\alpha_4\beta_1$), in cellular interactions with T lymphocytes (Cunningham *et al.*, 2002). The primary binding site for VLA-4 is the N-terminal Ig-like domain 1 of JAM-2, in contrast to the requirement for the membrane-proximal domain 2 of JAM-1 to bind to its integrin receptor LFA-1. Interestingly, an involvement of the only acidic residue in the C-D loop of this domain, namely Asp82, in binding to VLA-4 was excluded, thus JAM-2 deviates from the mechanism used by other IgSF proteins to engage integrins. Whether JAM-2 can also function as a ligand for the second α_4 integrin $\alpha_4\beta_7$, similarly to VCAM-1, remains unknown. The Mn^{2+}-dependent molecular interaction between JAM-2 and leukocytic VLA-4 , however, was reported to require prior adhesion of JAM-2 with leukocytic JAM-3 *in trans* and was not detectable in cells lacking JAM-3 expression. Such an interaction *in trans* of JAM-2 and JAM-3 between opposing cell surfaces might facilitate the subsequent JAM-2/VLA-4 binding by providing more frequent and closer contacts. This scenario resembles the hypothesis that LFA-1 might engage leukocytic JAM-1 *in cis* despite its homophilic binding to endothelial JAM-1 *in trans*, and that this lateral association may facilitate the interaction of LFA-1 with its opposite endothelial ligand JAM-1.

Whether the recently reported integrin-JAM interactions are directly involved in the diapedesis of leukocytes remains to be investigated but appears most likely. The observation that human JAM-1, JAM-2 and JAM-3 can independently function as ligands for the integrins LFA-1, VLA-4 and Mac-1, respectively, provides a completely new perspective in understanding the processes involved in inflammatory cell recruitment.

7. Summary

The recruitment of circulating leukocytes to sites of inflammation is a multi-step processes leading to their transmigration (diapedesis) through the blood vessel wall into the subvascular tissue. This process requires highly regulated cellular interactions at the molecular level to withdraw leukocytes from the blood stream and to finally enable their effective passage across the tightly connected endothelial barrier without a detremental leakage of the vessel wall. Whereas the initial steps of this process are well understood, *i.e.* leukocyte tethering, rolling on and firm adhesion to the endothelium, the molecular basis of the last step, *i.e.* the extravasation itself, remains largely unknown.

The leukocyte-specific β_2 integrin LFA-1 plays an important role in this process since it mediates firm adhesion of rolling leukocytes to the vessel wall. The cellular arrest depends thereby mainly on the molecular interaction of LFA-1 with its endothelial ligands ICAM-1 and ICAM-2, both of which are members of the IgSF family.

JAM-1, which is also an IgSF protein, is predominantly expressed at intercellular cell-cell contacts of endothelia and epithelia. Here it associates at the apical region with proteins of tight junctions (TJs) and exerts homophilic interactions *in trans* with JAM-1 molecules of opposite cells, thus participating in the arrangement of the endothelial barrier and presumably in the regulation of its paracellular permeability. JAM-1 may therefore be ideally situated to serve as a junctional gatekeeper promoting the transmigration of leukocytes.

In this study a novel candidate interaction partner of LFA-1 was identified by a yeast two-hybrid (YTH) screening of a human leukocyte cDNA library that revealed 75 % sequence homology to murine JAM-1. The identity of the candidate clone was clarified with the subsequent identification of human JAM-1 by other groups. Since LFA-1 is known to be crucial for leukocyte transmigration and given the striking structural and functional homology of JAM-1 with the main LFA-1 ligand ICAM-1 or the IgSF protein PECAM-1, it was hypothesized that JAM-1 may act as a functional ligand for LFA-1 in terms of cell adhesion and may thereby also be involved in leukocyte diapedesis.

Isolation of the full-length *JAM-1* cDNA from a YTH assay clone allowed for the generation of a JAM-1 polyclonal antibody by DNA-mediated mouse immunization and the establishment of a CHO cell line expressing heterogeneous JAM-1 (CHO-JAM cells). Specificity of anti–JAM-1 and correct surface expression of JAM-1 in CHO-JAM cells was verified by flow cytometry and immunoblot analysis. Expression studies using anti–JAM-1 revealed abundant surface

expression of JAM-1 on human hematopoietic cells which is in contrast to published expression patterns of murine JAM-1 absent on leukocytes. The significance of this finding still remains to be determined.

Static adhesion assays revealed that JAM-1 acts as a cell adhesion molecule (CAM) able to mediate LFA-1–dependent firm arrest of Jurkat T lymphocytes on JAM-1–expressing CHO cell monolayers and of CHO-JAM cells on purified, immobilized LFA-1. The specificity of this cell attachment was confirmed by the application of blocking antibodies directed against JAM-1, and by control experiments using CHO cells that lacked JAM-1 expression. Furthermore, Jurkat T cells deficient in LFA-1 expression due to chemical mutagenesis failed to bind to CHO-JAM cells but regained this ability after reconstitution of LFA-1 surface expression by cell transfection with an appropriate cDNA construct.

ICAM-1 serves as counter-receptor for both β_2 integrins LFA-1 and Mac-1. However, the failure of Mac-1–transfected but LFA-1–deficient Jurkat T cells to adhere to JAM-1 expressing CHO cells suggested a lack of redundancy for JAM-1 binding between this integrin receptors. Deletion mutagenesis revealed that the membrane-proximal Ig-like domain 2 of human JAM-1 is necessary and sufficient for LFA-1 binding. Thus CHO-JAM$^{\Delta D2}$ cells lacking this specific domain (Δ132-217) were unable to capture T lymphocytes. However, appropriate expression of mutant JAM$^{\Delta D2}$ was confirmed by RT-PCR, flow cytometry and western blot analysis. This finding suggested structural duality of JAM-1 that employs its N-terminal Ig-like domain 1 for homophilic interaction *in cis* (dimerization) and *in trans* and domain 2 as a heterophilic LFA-1 receptor binding site.

Several lines of evidence supported the conclusion that homophilic JAM-1 interactions *in trans*, implicated to occur at intercellular junctions, were not involved in the observed cellular attachment. These studies included the use of the anti–JAM-1 antibody and the JAM-1–deficient myeloid cell line HL-60. Moreover, a hypothetical contamination of the LFA-1 preparation, isolated from human organs and used in static adhesion assays, with co-purified JAM-1 was excluded by silver staining and western blot analysis.

The findings obtained with static adhesion assays were further confirmed by using memory T cells isolated from human blood and HUVECs isolated from umbilical cord veins. Firm cellular arrest of T lymphocytes to HUVEC monolayers required costimulation of the endothelial cells with the proinflammatory cytokines TNF-α and IFN-γ that induces redistribution of junctional localized JAM-1 to the apical surface. Equivalent results were obtained in experiments performed in a flow chamber system simulating the blood stream. This implicated a functional role of the LFA-1/JAM-1 interaction under inflammatory conditions. The finding that cell adhesion mediated by this receptor-ligand pair was able to resist shear stress forces induced by

laminar flow emphasized the physiological relevance of this molecular interaction. Furthermore, the use of antibodies directed against ICAM-1 and JAM-1, alone or in combination, suggested that both IgSF molecules display alternative ligands for leukocytic LFA-1.

Functional chemotaxis and flow chamber assays with physiologically relevant cell types showed that JAM-1 also plays an important role in LFA-1–dependent transendothelial migration of memory T cells under static and flow conditions. Again, a combined blockade of JAM-1 and ICAM-1 inhibited migration additively, suggesting that both molecules are required for optimal diapedesis. In contrast to lymphocyte adhesion, transmigration did not seem to be dependent on inflammatory conditions. The analysis of leukocyte adhesion and transmigration was further extended to include isolated human neutrophils. The absence of a marked influence of JAM-1 upon neutrophil adhesion, as opposed to its prominent role in T lymphocyte arrest, appeared to depend on the redundant involvement of other receptor-ligand pairs. However, diapedesis of neutrophils depended considerably on the involvement of both LFA-1 ligands JAM-1 and ICAM-1.

A molecular zipper model is proposed for the mechanisms of action of JAM-1 in leukocyte emigration at sites of inflammation. Redistribution of junctional JAM-1 under inflammatory conditions enables LFA-1–mediated leukocyte binding at the apical surface of the endothelium. Upon transmigration across the endothelial barrier, LFA-1 might repetitively intercept or intercalate junctional JAM-1 engaged in homophilic interactions *in trans*. Such sequential interactions may unlock intercellular junctions and guide the leukocyte along the basolateral site of the intercellular cleft in a zipper-like manner. These findings may explain the documented involvement of LFA-1 in leukocyte extravasation that could not be explained until now due to the absence of basolateral ICAM-1 expression which is encountered instead exclusively at the luminal surface of inflammatory endothelium.

In summary, human JAM-1 was identified as the first counter-receptor of LFA-1 that does not belong to the ICAM subgroup. The membrane-proximal Ig-like domain 2 of JAM-1 was shown to bear the LFA-1 binding site. It could be verified that the JAM-1/LFA-1 interaction is functionally implicated in lymphocyte adhesion and leukocyte transmigration under inflammatory conditions. The presented data establishes a fourth type of interaction between IgSF and integrin adhesion molecules besides the interaction of PECAM-1 with $\alpha_v\beta_3$, of VCAM-1 respective MAdCAM-1 with α_4 integrins and of ICAMs with β_2 integrins. Moreover, they constitute a general model for JAM-integrin binding pairs recently extended by the identification of the interaction partners JAM-2/VLA-4 and JAM-3/Mac-1.

8. Reference list

Allport J. R., Muller W. A., Luscinskas F. W. (2000) **Monocytes induce reversible focal changes in vascular endothelial cadherin complex during transendothelial migration under flow.** *J. Cell Biol.* 148, 1, 203-216.

Anderson D. C., Springer T. A. (1987) **Leukocyte adhesion deficiency: an inherited defect in the Mac-1, LFA-1, and p150,95 glycoproteins.** *Annu. Rev. Med.* 38, 175-194.

Anderson J. M., van Itallie C. M. (1995) **Tight junctions and the molecular basis for regulation of paracellular permeability.** *Am. J. Physiol.* 269, 4 (Pt 1), G467-G475.

Andriopoulou P., Navarro P., Zanetti A., Lampugnani M. G., Dejana E. (1999) **Histamine induces tyrosine phosphorylation of endothelial cell-to-cell adherens junctions.** *Arterioscler. Thromb. Vasc. Biol.* 19, 10, 2286-2297.

Arnaout M. A. (1990) **Structure and function of the leukocyte adhesion molecules CD11/CD18.** *Blood* 75, 5, 1037-1050.

Arrate M. P., Rodriguez J. M., Tran T. M., Brock T. A., Cunningham S. A. (2001) **Cloning of human junctional adhesion molecule 3 (JAM3) and its identification as the JAM2 counter-receptor.** *J. Biol. Chem.* 276, 49, 45826-45832.

Aurrand-Lions M., Duncan L., Du P. L., Imhof B. A. (2000) **Cloning of JAM-2 and JAM-3: an emerging junctional adhesion molecular family?** *Curr. Top. Microbiol. Immunol.* 251, 91-98.

Aurrand-Lions M., Duncan L., Ballestrem C., Imhof B. A. (2001a) **JAM-2, a novel immunoglobulin superfamily molecule, expressed by endothelial and lymphatic cells.** *J. Biol. Chem.* 276, 4, 2733-2741.

Aurrand-Lions M., Johnson-Leger C., Wong C., Du P. L., Imhof B. A. (2001b) **Heterogeneity of endothelial junctions is reflected by differential expression and specific subcellular localization of the three JAM family members.** *Blood* 98, 13, 3699-3707.

Aurrand-Lions M., Johnson-Leger C., Imhof B. A. (2002) **The last molecular fortress in leukocyte trans-endothelial migration.** *Nat. Immunol.* 3, 2, 116-118.

Ausubel F. M., Brent R., Kingston R. E., More D. D., Seidman J. G., Smith J. A., Stuhl K. (1995) **Current protocols in molecular biology.** John Wiley&Sons, New York, NY.

Ayalon O., Sabanai H., Lampugnani M. G., Dejana E., Geiger B. (1994) **Spatial and temporal relationships between cadherins and PECAM-1 in cell-cell junctions of human endothelial cells.** *J. Cell Biol.* 126, 1, 247-258.

Balda M. S., Matter K. (2000) **Transmembrane proteins of tight junctions.** *Semin. Cell Dev. Biol.* 11, 4, 281-289.

Bartel P., Chien C. T., Sternglanz R., Fields S. (1993) **Elimination of false positives that arise in using the two-hybrid system.** *BioTechniques* 14, 6, 920-924.

Barton E. S., Forrest J. C., Connolly J. L., Chappell J. D., Liu Y., Schnell F. J., Nusrat A., Parkos C. A., Dermody T. S. (2001) **Junction adhesion molecule is a receptor for reovirus.** *Cell* 104, 3, 441-451.

Bazzoni G., Martínez-Estrada O. M., Mueller F., Nelboeck P., Schmid G., Bartfai T., Dejana E., Brockhaus M. (2000a) **Homophilic interaction of junctional adhesion molecule.** *J. Biol. Chem.* 275, 40, 30970-30976.

Bazzoni G., Martínez-Estrada O. M., Orsenigo F., Cordenonsi M., Citi S., Dejana E. (2000b) **Interaction of junctional adhesion molecule with the tight junction components ZO-1, cingulin, and occludin.** *J. Biol. Chem.* 275, 27, 20520-20526.

Berlin C., Berg E. L., Briskin M. J., Andrew D. P., Kilshaw P. J., Holzmann B., Weissman I. L., Hamann A., Butcher E. C. (1993) **$\alpha_4\beta_7$ integrin mediates lymphocyte binding to the mucosal vascular addressin MAdCAM-1.** *Cell* 74, 1, 185-185.

Bianchi E., Bender J. R., Blasi F., Pardi R. (1997) **Through and beyond the wall: late steps in leukocyte transendothelial migration.** *Immunol. Today* 18, 12, 586-591.

Bianchi E., Denti S., Granata A., Bossi G., Geginat J., Villa A., Rogge L., Pardi R. (2000) **Integrin LFA-1 interacts with the transcriptional co-activator JAB1 to modulate AP-1 activity.** *Nature* 404, 6778, 617-621.

Bleijs D. A., Binnerts M. E., van Vliet S. J., Figdor C. G., van Kooyk Y. (2000) **Low-affinity LFA-1/ ICAM-3 interactions augment LFA-1/ICAM-1-mediated T cell adhesion and signaling by redistribution of LFA-1.** *J. Cell Sci.* 113 (Pt 3), 391-400.

Bork P., Holm L., Sander C. (1994) **The immunoglobulin fold: Structural classification, sequence patterns and common core.** *J. Mol. Biol.* 242, 4, 309-320.

Boudreau N. J., Jones P. L. (1999) **Extracellular matrix and integrin signalling: the shape of things to come.** *Biochem. J.* 339 (Pt 3), 481-488.

Brent R., Ptashne M. (1985) **A eukaryotic transcriptional activator bearing the DNA specificity of a prokaryotic repressor.** *Cell* 43, 3 (Pt 2), 729-736.

Breviario F., Caveda L., Corada M., Martin-Padura I., Navarro P., Golay J., Introna M., Gulino D., Lampugnani M. G., Dejana E. (1995) **Functional properties of human vascular endothelial cadherin (7B4/cadherin-5), an endothelium-specific cadherin.** *Arterioscler. Thromb. Vasc. Biol.* 15, 8, 1229-1239.

Briskin M. J., Rott L., Butcher E. C. (1996) **Structural requirements for mucosal vascular addressin binding to its lymphocyte receptor $\alpha_4\beta_7$. Common themes among integrin-Ig family interactions.** *J. Immunol.* 156, 2, 719-726.

Burns A. R., Walker D. C., Brown E. S., Thurmon L. T., Bowden R. A., Keese C. R., Simon S. I., Entman M. L., Smith C. W. (1997) **Neutrophil transendothelial migration is independent of tight junctions and occurs preferentially at tricellular corners.** *J. Immunol.* 159, 6, 2893-2903.

Butcher E. C. (1991) **Leukocyte-endothelial cell recognition: three (or more) steps to specificity and diversity.** *Cell* 67, 6, 1033-1036.

Calderwood D. A., Shattil S. J., Ginsberg M. H. (2000) **Integrins and actin filaments: reciprocal regulation of cell adhesion and signaling.** *J. Biol. Chem.* 275, 30, 22607-22610.

Campbell J. J., Hedrick J., Zlotnik A., Siani M. A., Thompson D. A., Butcher E. C. (1998) **Chemokines and the arrest of lymphocytes rolling under flow conditions.** *Science* 279, 5349, 381-384.

Casasnovas J. M., Springer T. A., Liu J. H., Harrison S. C., Wang J. H. (1997) **Crystal structure of ICAM-2 reveals a distinctive integrin recognition surface.** *Nature* 387, 6630, 312-315.

Cepek K. L., Shaw S. K., Parker C. M., Russell G. J., Morrow J. S., Rimm D. L., Brenner M. B. (1994) **Adhesion between epithelial cells and T lymphocytes mediated by E-cadherin and the $\alpha_E\beta_7$ integrin.** *Nature* 372, 6502, 190-193.

Cereijido M., Shoshani L., Contreras R. G. (2000) **Molecular physiology and pathophysiology of tight junctions. II. Biogenesis of tight junctions and epithelial polarity.** *Am. J. Physiol. Gastrointest. Liver Physiol.* 279, 3, G477-G482.

Chang D. D., Wong C., Smith H., Liu J. (1997) **ICAP-1, a novel β_1 integrin cytoplasmic domain-associated protein, binds to a conserved and functionally important NPXY sequence motif of β_1 integrin.** *J. Cell Biol.* 138, 5, 1149-1157.

Chrétien I., Marcuz A., Courtet M., Katevuo K., Vainio O., Heath J. K., White S. J., Du Pasquier L. (1998) **CTX, a *Xenopus* thymocyte receptor, defines a molecular family conserved throughout vertebrates.** *Eur. J. Immunol.* 28, 12, 4094-4104.

Cinamon G., Grabovsky V., Winter E., Franitza S., Feigelson S., Shamri R., Dwir O., Alon R. (2001a) **Novel chemokine functions in lymphocyte migration through vascular endothelium under shear flow.** *J. Leukoc. Biol.* 69, 6, 860-866.

Cinamon G., Shinder V., Alon R. (2001b) **Shear forces promote lymphocyte migration across vascular endothelium bearing apical chemokines.** *Nat. Immunol.* 2, 6, 515-522 [comment in: *Nat. Immunol.* (2001) 2, 6, 478-480].

Clemetson K. J., Clemetson J. M. (1998) **Integrins and cardiovascular disease.** *Cell. Mol. Life Sci.* 54, 6, 502-513.

Clezardin P. (1998) **Recent insights into the role of integrins in cancer metastasis.** *Cell. Mol. Life Sci.* 54, 6, 541-548.

Constantin G., Majeed M., Giagulli C., Piccio L., Kim J. Y., Butcher E. C., Laudanna C. (2000) **Chemokines trigger immediate β_2 integrin affinity and mobility changes: differential regulation and roles in lymphocyte arrest under flow.** *Immunity* 13, 6, 759-769.

Coppolino M. G., Woodside M. J., Demaurex N., Grinstein S., St-Arnaud R., Dedhar S. (1997) **Calreticulin is essential for integrin-mediated calcium signalling and cell adhesion.** *Nature* 386, 6627, 843-847.

Critchley D. R. (2000) **Focal adhesions: the cytoskeletal connection.** *Curr. Opin. Cell Biol.* 12, 1, 133-139.

Cunningham S. A., Arrate M. P., Rodriguez J. M., Bjercke R. J., Vanderslice P., Morris A. P., Brock T. A. (2000) **A novel protein with homology to the junctional adhesion molecule.** *J. Biol. Chem.* 275, 44, 34750-34756.

Cunningham S. A., Rodriguez J. M., Arrate M. P., Tran T. M., Brock T. A. (2002) **JAM2 interacts with $\alpha_4\beta_1$: facilitation by JAM3.** *J. Biol. Chem.* 277, 31, 27589-27592.

Danilenko D. M., Rossitto P. V., van der Vieren M., Le Trong H., McDonough S. P., Affolter V. K., Moore P. F. (1995) **A novel canine leukointegrin, $\alpha_D\beta_2$, is expressed by specific macrophage subpopulations in tissue and a minor $CD8^+$ lymphocyte subpopulation in peripheral blood.** *J. Immunol.* 155, 1, 35-44.

Davis H. L., Michel M. L., Whalen R. G. (1995) **Use of plasmid DNA for direct gene transfer and immunization.** *Ann. N. Y. Acad. Sci.* 772, 21-29.

de Fougerolles A. R., Springer T. A. (1992) **Intercellular adhesion molecule 3, a third adhesion counter-receptor for lymphocyte function-associated molecule 1 on resting lymphocytes.** *J. Exp. Med.* 175, 1, 185-190.

Dedhar S. (1994) **Novel functions for calreticulin: interaction with integrins and modulation of gene expression?** *Trends Biochem. Sci.* 19, 7, 269-271.

Dedhar S., Hannigan G. E. (1996) **Integrin cytoplasmic interactions and bidirectional transmembrane signalling.** *Curr. Opin. Cell Biol.* 8, 5, 657-669.

Del Maschio A., Zanetti A., Corada M., Rival Y., Ruco L., Lampugnani M. G., Dejana E. (1996) **Polymorphonuclear leukocyte adhesion triggers the disorganization of endothelial cell-to-cell adherens junctions.** *J. Cell Biol.* 135, 2, 497-510.

Del Maschio A., De Luigi A., Martìn-Padura I., Brockhaus M., Bartfai T., Fruscella P., Adorini L., Martino G., Furlan R., De Simoni M. G., Dejana E. (1999) **Leukocyte recruitment in the cerebrospinal fluid of mice with experimental meningitis is inhibited by an antibody to junctional adhesion molecule (JAM).** *J. Exp. Med.* 190, 9, 1351-1356.

Denker B. M., Nigam S. K. (1998) **Molecular structure and assembly of the tight junction.** *Am. J. Physiol.* 274, 1 (Pt 2), F1-F9.

Diacovo T. G., Roth S. J., Buccola J. M., Bainton D. F., Springer T. A. (1996) **Neutrophil rolling, arrest, and transmigration across activated, surface-adherent platelets via sequential action of P-selectin and the β_2-integrin CD11b/CD18.** *Blood* 88, 1, 146-157.

Diamond M. S., Staunton D. E., Marlin S. D., Springer T. A. (1991) **Binding of the integrin Mac-1 (CD11b/CD18) to the third immunoglobulin-like domain of ICAM-1 (CD54) and its regulation by glycosylation.** *Cell* 65, 6, 961-971.

Diamond M. S., Springer T. A. (1994) **The dynamic regulation of integrin adhesiveness.** *Curr. Biol.* 4, 6, 506-517.

Díaz-González F., Forsyth J., Steiner B., Ginsberg M. H. (1996) **Trans-dominant inhibition of integrin function.** *Mol. Biol. Cell* 7, 12, 1939-1951.

Dib K., Andersson T. (2000) **β_2 integrin signaling in leukocytes.** *Front. Biosci.* 5, D438-D451.

Dickeson S. K., Santoro S. A. (1998) **Ligand recognition by the I domain-containing integrins.** *Cell. Mol. Life Sci.* 54, 6, 556-566.

Ding Z. M., Babensee J. E., Simon S. I., Lu H., Perrard J. L., Bullard D. C., Dai X. Y., Bromley S. K., Dustin M. L., Entman M. L., Smith C. W., Ballantyne C. M. (1999) **Relative contribution of LFA-1 and Mac-1 to neutrophil adhesion and migration.** *J. Immunol.* 163, 9, 5029-5038.

Dransfield I., Hogg N. (1989) **Regulated expression of Mg^{2+} binding epitope on leukocyte integrin α subunits.** *EMBO J.* 8, 12, 3759-3765.

Duncan G. S., Andrew D. P., Takimoto H., Kaufman S. A., Yoshida H., Spellberg J., de la Pompa J. L., Elia A., Wakeham A., Karan-Tamir B., Muller W. A., Senaldi G., Zukowski M. M., Mak T. W. (1999) **Genetic evidence for functional redundancy of platelet/endothelial cell adhesion molecule-1 (PECAM-1): CD31-deficient mice reveal PECAM-1-dependent and PECAM-1-independent functions.** *J. Immunol.* 162, 5, 3022-3030.

Dunne J. L., Ballantyne C. M., Beaudet A. L., Ley K. (2002) **Control of leukocyte rolling velocity in TNF-α-induced inflammation by LFA-1 and Mac-1.** *Blood* 99, 1, 336-341.

Dustin M. L., Springer T. A. (1989) **T-cell receptor cross-linking transiently stimulates adhesiveness through LFA-1.** *Nature* 341, 6243, 619-624.

Ebnet K., Vestweber D. (1999) **Molecular mechanisms that control leukocyte extravasation: the selectins and the chemokines.** *Histochem. Cell Biol.* 112, 1, 1-23.

Ebnet K., Schulz C. U., Meyer zu Brickwedde M. K., Pendl G. G., Vestweber D. (2000) **Junctional adhesion molecule interacts with the PDZ domain-containing proteins AF-6 and ZO-1.** *J. Biol. Chem.* 275, 36, 27979-27988.

Ebnet K., Suzuki A., Horikoshi Y., Hirose T., Meyer zu Brickwedde M. K., Ohno S., Vestweber D. (2001) **The cell polarity protein ASIP/PAR-3 directly associates with junctional adhesion molecule (JAM).** *EMBO J.* 20, 14, 3738-3748.

Eigenthaler M., Hofferer L., Shattil S. J., Ginsberg M. H. (1997) **A conserved sequence motif in the integrin β_3 cytoplasmic domain is required for its specific interaction with β_3-endonexin.** *J. Biol. Chem.* 272, 12, 7693-7698.

Elices M. J., Osborn L., Takada Y., Crouse C., Luhowskyj S., Hemler M. E., Lobb R. R. (1990) **VCAM-1 on activated endothelium interacts with the leukocyte integrin VLA-4 at a site distinct from the VLA-4/fibronectin binding site.** *Cell* 60, 4, 577-584.

Etzioni A., Frydman M., Pollack S., Avidor I., Phillips M. L., Paulson J. C., Gershoni-Baruch R. (1992) **Recurrent severe infections caused by a novel leukocyte adhesion deficiency.** *N. Engl. J. Med.* 327, 25, 1789-1792.

Fanning A. S., Anderson J. M. (1999) **PDZ domains: fundamental building blocks in the organization of protein complexes at the plasma membrane.** *J. Clin. Invest.* 103, 6, 767-772.

Feng D., Nagy J. A., Pyne K., Dvorak H. F., Dvorak A. M. (1998) **Neutrophils emigrate from venules by a transendothelial cell pathway in response to FMLP.** *J. Exp. Med.* 187, 6, 903-915.

Fields S., Song O. (1989) **A novel genetic system to detect protein-protein interactions.** *Nature* 340, 6230, 245-246.

Fields S., Sternglanz R. (1994) **The two-hybrid system: an assay for protein-protein interactions.** *Trends Genet.* 10, 8, 286-292.

Furuse M., Hirase T., Itoh M., Nagafuchi A., Yonemura S., Tsukita S. (1993) **Occludin: a novel integral membrane protein localizing at tight junctions.** *J. Cell Biol.* 123, 6 (Pt 2), 1777-1788.

Gahmberg C. G., Tolvanen M., Kotovuori P. (1997) **Leukocyte adhesion: structure and function of human leukocyte β_2-integrins and their cellular ligands.** *Eur. J. Biochem.* 245, 2, 215-232.

Gahmberg C. G., Valmu L., Fagerholm S., Kotovuori P., Ihanus E., Tian L., Pessa-Morikawa T. (1998) **Leukocyte integrins and inflammation.** *Cell. Mol. Life Sci.* 54, 6, 549-555.

Geiger C., Nagel W., Boehm T., van Kooyk Y., Figdor C. G., Kremmer E., Hogg N., Zeitlmann L., Dierks H., Weber K. S., Kolanus W. (2000) **Cytohesin-1 regulates β_2 integrin-mediated adhesion through both ARF-GEF function and interaction with LFA-1.** *EMBO J.* 19, 11, 2525-2536.

Gerard C., Rollins B. J. (2001) **Chemokines and disease.** *Nat. Immunol.* 2, 2, 108-115.

Giancotti F. G. (2000) **Complexity and specificity of integrin signalling.** *Nat. Cell Biol.* 2, 1, E13-E14.

Gimbrone M. A. (1999) **Vascular endothelium, hemodynamic forces, and atherogenesis.** *Am. J. Pathol.* 155, 1, 1-5.

Girard J. P., Springer T. A. (1995) **High endothelial venules (HEVs): specialized endothelium for lymphocyte migration.** *Immunol. Today* 16, 9, 449-457.

Gopalan P. K., Burns A. R., Simon S. I., Sparks S., McIntire L. V., Smith C. W. (2000) **Preferential sites for stationary adhesion of neutrophils to cytokine-stimulated HUVEC under flow conditions.** *J. Leukoc. Biol.* 68, 1, 47-57.

Grabovsky V., Feigelson S., Chen C., Bleijs D. A., Peled A., Cinamon G., Baleux F., Arenzana-Seisdedos F., Lapidot T., van Kooyk Y., Lobb R. R., Alon R. (2000) **Subsecond induction of α_4 integrin clustering by immobilized chemokines stimulates leukocyte tethering and rolling on endothelial vascular cell adhesion molecule 1 under flow conditions.** *J. Exp. Med.* 192, 4, 495-506.

Green L. J., Mould A. P., Humphries M. J. (1998) **The integrin β subunit.** *Int. J. Biochem. Cell Biol.* 30, 2, 179-184.

Gupta S. K., Pillarisetti K., Ohlstein E. H. (2000) **Platelet agonist F11 receptor is a member of the immunoglobulin superfamily and identical with junctional adhesion molecule (JAM): regulation of expression in human endothelial cells and macrophages.** *IUBMB Life* 50, 1, 51-56.

Guthrie C., Fink G. R. (1991) **Guide to yeast genetics and molecular biology.** *Methods Enzymol.* 194, 306-307.

Hahn J. H., Kim M. K., Choi E. Y., Kim S. H., Sohn H. W., Ham D. I., Chung D. H., Kim T. J., Lee W. J., Park C. K., Ree H. J., Park S. H. (1997) **CD99 (MIC2) regulates the LFA-1/ICAM-1-mediated adhesion of lymphocytes, and its gene encodes both positive and negative regulators of cellular adhesion.** *J. Immunol.* 159, 5, 2250-2258.

Hamazaki Y., Itoh M., Sasaki H., Furuse M., Tsukita S. (2002) **Multi-PDZ Domain Protein 1 (MUPP1) is concentrated at tight junctions through its possible interaction with claudin-1 and junctional adhesion molecule.** *J. Biol. Chem.* 277, 1, 455-461.

Hannigan G. E., Leung-Hagesteijn C., Fitz-Gibbon L., Coppolino M. G., Radeva G., Filmus J., Bell J. C., Dedhar S. (1996) **Regulation of cell adhesion and anchorage-dependent growth by a new β_1-integrin-linked protein kinase.** *Nature* 379, 6560, 91-96.

Heiskala M., Peterson P. A., Yang Y. (2001) **The roles of claudin superfamily proteins in paracellular transport.** *Traffic* 2, 2, 93-98.

Hemler M. E. (1990) **VLA proteins in the integrin family: structures, functions, and their role on leukocytes.** *Annu. Rev. Immunol.* 8, 365-400.

Hemler M. E. (1998) **Integrin associated proteins.** *Curr. Opin. Cell Biol.* 10, 5, 578-585.

Henderson R. B., Lim L. H., Tessier P. A., Gavins F. N., Mathies M., Perretti M., Hogg N. (2001) **The use of lymphocyte function-associated antigen (LFA)-1-deficient mice to determine the role of LFA-1, Mac-1, and α_4 integrin in the inflammatory response of neutrophils.** *J. Exp. Med.* 194, 2, 219-226.

Hibbs M. L., Wardlaw A. J., Stacker S. A., Anderson D. C., Lee A., Roberts T. M., Springer T. A. (1990) **Transfection of cells from patients with leukocyte adhesion deficiency with an integrin β subunit (CD18) restores lymphocyte function-associated antigen-1 expression and function.** *J. Clin. Invest.* 85, 3, 674-681.

Hibbs M. L., Jakes S., Stacker S. A., Wallace R. W., Springer T. A. (1991a) **The cytoplasmic domain of the integrin lymphocyte function-associated antigen 1 β subunit: sites required for binding to intercellular adhesion molecule 1 and the phorbol ester-stimulated phosphorylation site.** *J. Exp. Med.* 174, 5, 1227-1238.

Hibbs M. L., Xu H., Stacker S. A., Springer T. A. (1991b) **Regulation of adhesion of ICAM-1 by the cytoplasmic domain of LFA-1 integrin β subunit.** *Science* 251, 5001, 1611-1613.

Holness C. L., Simmons D. L. (1994) **Structural motifs for recognition and adhesion in members of the immunoglobulin superfamily.** *J. Cell Sci.* 107 (Pt 8), 2065-2070.

Holness C. L., Bates P. A., Little A. J., Buckley C. D., McDowall A., Bossy D., Hogg N., Simmons D. L. (1995) **Analysis of the binding site on intercellular adhesion molecule 3 for the leukocyte integrin lymphocyte function-associated antigen 1.** *J. Biol. Chem.* 270, 2, 877-884.

Horton R. M., Hunt H. D., Ho S. N., Pullen J. K., Pease L. R. (1989) **Engineering hybrid genes without the use of restriction enzymes: gene splicing by overlap extension.** *Gene* 77, 1, 61-68.

Horwitz A. F. (1998) **Integrine.** *Spektrum der Wissenschaft* 1, 86-94.

Howe A., Aplin A. E., Alahari S. K., Juliano R. L. (1998) **Integrin signaling and cell growth control.** *Curr. Opin. Cell Biol.* 10, 2, 220-231.

Hughes P. E., Renshaw M. W., Pfaff M., Forsyth J., Keivens V. M., Schwartz M. A., Ginsberg M. H. (1997) **Suppression of integrin activation: a novel function of a Ras/Raf-initiated MAP kinase pathway.** *Cell* 88, 4, 521-530.

Hughes P. E., Pfaff M. (1998) **Integrin affinity modulation.** *Trends Cell Biol.* 8, 9, 359-364.

Humphries M. J. (2000) **Integrin structure.** *Biochem. Soc. Trans.* 28, 4, 311-339.

Huth J. R., Olejniczak E. T., Mendoza R., Liang H., Harris E. A., Lupher M. L., Wilson A. E., Fesik S. W., Staunton D. E. (2000) **NMR and mutagenesis evidence for an I domain allosteric site that regulates lymphocyte function-associated antigen 1 ligand binding.** *Proc. Natl. Acad. Sci. USA* 97, 10, 5231-5236.

Hynes R. O. (1992) **Integrins: versatility, modulation, and signaling in cell adhesion.** *Cell* 69, 1, 11-25.

Ingalls R. R., Golenbock D. T. (1995) **CD11c/CD18, a transmembrane signaling receptor for lipopolysaccharide.** *J. Exp. Med.* 181, 4, 1473-1479.

Ito H., Fukuda Y., Murata K., Kimura A. (1983) **Transformation of intact yeast cells treated with alkali cations.** *J. Bacteriol.* 153, 1, 163-168.

Itoh M., Sasaki H., Furuse M., Ozaki H., Kita T., Tsukita S. (2001) **Junctional adhesion molecule (JAM) binds to PAR-3: a possible mechanism for the recruitment of PAR-3 to tight junctions.** *J. Cell Biol.* 154, 3, 491-498.

Izumi Y., Hirose T., Tamai Y., Hirai S., Nagashima Y., Fujimoto T., Tabuse Y., Kemphues K. J., Ohno S. (1998) **An atypical PKC directly associates and colocalizes at the epithelial tight junction with ASIP, a mammalian homologue of *Caenorhabditis elegans* polarity protein PAR-3.** *J. Cell Biol.* 143, 1, 95-106.

Jaffe E. A., Nachman R. L., Becker C. G., Minick C. R. (1973) **Culture of human endothelial cells derived from umbilical veins. Identification by morphologic and immunologic criteria.** *J. Clin. Invest.* 52, 11, 2745-2756.

Johnson-Léger C., Aurrand-Lions M. A., Imhof B. A. (2000) **The parting of the endothelium: miracle, or simply a junctional affair?** *J. Cell Sci.* 113 (Pt 6), 921-933.

Jones D. A., Smith C. W., McIntire L. V. (1996a) **Leucocyte adhesion under flow conditions: principles important in tissue engineering.** *Biomaterials* 17, 3, 337-347.

Jones S., Thornton J. M. (1996b) **Principles of protein-protein interactions.** *Proc. Natl. Acad. Sci. USA* 93, 1, 13-20.

Jun C. D., Shimaoka M., Carman C. V., Takagi J., Springer T. A. (2001) **Dimerization and the effectiveness of ICAM-1 in mediating LFA-1-dependent adhesion.** *Proc. Natl. Acad. Sci. USA* 98, 12, 6830-6835.

Kashiwagi H., Schwartz M. A., Eigenthaler M., Davis K. A., Ginsberg M. H., Shattil S. J. (1997) **Affinity modulation of platelet integrin $\alpha_{IIb}\beta_3$ by β_3-endonexin, a selective binding partner of the β_3 integrin cytoplasmic tail.** *J. Cell Biol.* 137, 6, 1433-1443.

Keegan L., Gill G., Ptashne M. (1986) **Separation of DNA binding from the transcription-activating function of a eukaryotic regulatory protein.** *Science* 231, 4739, 699-704.

Keizer G. D., Visser W., Vliem M., Figdor C. G. (1988) **A monoclonal antibody (NKI-L16) directed against a unique epitope on the α-chain of human leukocyte function-associated antigen 1 induces homotypic cell-cell interactions.** *J. Immunol.* 140, 5, 1393-1400.

Kishimoto T. K., Larson R. S., Corbi A. L., Dustin M. L., Staunton D. E., Springer T. A. (1989) **Leukocyte integrins.** *Adv. Immunol.* 46, 149-182.

Kishore G. M., Shah D. M. (1988) **Amino acid biosynthesis inhibitors as herbicides.** *Annu. Rev. Biochem.* 57, 627-663.

Klickstein L. B., York M. R., de Fougerolles A. R., Springer T. A. (1996) **Localization of the binding site on intercellular adhesion molecule-3 (ICAM-3) for lymphocyte function-associated antigen 1 (LFA-1).** *J. Biol. Chem.* 271, 39, 23920-23927.

Kniesel U., Wolburg H. (2000) **Tight junctions of the blood-brain barrier.** *Cell. Mol. Neurobiol.* 20, 1, 57-76.

Kolanus W., Nagel W., Schiller B., Zeitlmann L., Godar S., Stockinger H., Seed B. (1996) **$\alpha_L\beta_2$ integrin/LFA-1 binding to ICAM-1 induced by cytohesin-1, a cytoplasmic regulatory molecule.** *Cell* 86, 2, 233-242.

Kolanus W., Seed B. (1997) **Integrins and inside-out signal transduction: converging signals from PKC and PIP_3.** *Curr. Opin. Cell Biol.* 9, 5, 725-731.

Kornecki E., Walkowiak B., Naik U. P., Ehrlich Y. H. (1990) **Activation of human platelets by a stimulatory monoclonal antibody.** *J. Biol. Chem.* 265, 17, 10042-10048.

Korthäuer U., Nagel W., Davis E. M., Le Beau M. M., Menon R. S., Mitchell E. O., Kozak C. A., Kolanus W., Bluestone J. A. (2000) **Anergic T lymphocytes selectively express an integrin regulatory protein of the cytohesin family.** *J. Immunol.* 164, 1, 308-318.

Kostrewa D., Brockhaus M., D'Arcy A., Dale G. E., Nelboeck P., Schmid G., Mueller F., Bazzoni G., Dejana E., Bartfai T., Winkler F. K., Hennig M. (2001) **X-ray structure of junctional adhesion molecule: structural basis for homophilic adhesion via a novel dimerization motif.** *EMBO J.* 20, 16, 4391-4398.

Lampugnani M. G., Dejana E. (1997) **Interendothelial junctions: structure, signalling and functional roles.** *Curr. Opin. Cell Biol.* 9, 5, 674-682.

Larson R. S., Corbi A. L., Berman L., Springer T. (1989) **Primary structure of the leukocyte function-associated molecule-1 α subunit: an integrin with an embedded domain defining a protein superfamily.** *J. Cell Biol.* 108, 2, 703-712.

Laudanna C., Campbell J. J., Butcher E. C. (1996) **Role of Rho in chemoattractant-activated leukocyte adhesion through integrins.** *Science* 271, 5251, 981-983.

Lawrence M. B., McIntire L. V., Eskin S. G. (1987) **Effect of flow on polymorphonuclear leukocyte/endothelial cell adhesion.** *Blood* 70, 5, 1284-1290.

Lawrence M. B., Springer T. A. (1991) **Leukocytes roll on a selectin at physiologic flow rates: distinction from and prerequisite for adhesion through integrins.** *Cell* 65, 5, 859-873.

Lawrence M. B., Kansas G. S., Kunkel E. J., Ley K. (1997) **Threshold levels of fluid shear promote leukocyte adhesion through selectins (CD62L,P,E).** *J. Cell Biol.* 136, 3, 717-727.

Lechner F., Sahrbacher U., Suter T., Frei K., Brockhaus M., Koedel U., Fontana A. (2000) **Antibodies to the junctional adhesion molecule cause disruption of endothelial cells and do not prevent leukocyte influx into the meninges after viral or bacterial infection.** *J. Infect. Dis.* 182, 3, 978-982.

Leitinger B., McDowall A., Stanley P., Hogg N. (2000) **The regulation of integrin function by Ca^{2+}.** *Biochim. Biophys. Acta* 1498, 2-3, 91-98.

Liang T. W., DeMarco R. A., Mrsny R. J., Gurney A., Gray A., Hooley J., Aaron H. L., Huang A., Klassen T., Tumas D. B., Fong S. (2000) **Characterization of huJAM: evidence for involvement in cell-cell contact and tight junction regulation.** *Am. J. Physiol. Cell Physiol.* 279, 6, C1733-C1743.

Liang T. W., Chiu H. H., Gurney A., Sidle A., Tumas D. B., Schow P., Foster J., Klassen T., Dennis K., DeMarco R. A., Pham T., Frantz G., Fong S. (2002) **Vascular endothelial-junctional adhesion molecule (VE-JAM)/JAM 2 interacts with T, NK, and dendritic cells through JAM 3.** *J. Immunol.* 168, 4, 1618-1626.

Liao F., Huynh H. K., Eiroa A., Greene T., Polizzi E., Muller W. A. (1995) **Migration of monocytes across endothelium and passage through extracellular matrix involve separate molecular domains of PECAM-1.** *J. Exp. Med.* 182, 5, 1337-1343.

Liddington R. C., Ginsberg M. H. (2002) **Integrin activation takes shape.** *J. Cell Biol.* 158, 5, 833-839.

Liliental J., Chang D. D. (1998) **Rack1, a receptor for activated protein kinase C, interacts with integrin β subunit.** *J. Biol. Chem.* 273, 4, 2379-2383.

Liu S., Thomas S. M., Woodside D. G., Rose D. M., Kiosses W. B., Pfaff M., Ginsberg M. H. (1999) **Binding of paxillin to α_4 integrins modifies integrin-dependent biological responses.** *Nature* 402, 6762, 676-681.

Liu S., Calderwood D. A., Ginsberg M. H. (2000a) **Integrin cytoplasmic domain-binding proteins.** *J. Cell Sci.* 113 (Pt 20), 3563-3571.

Liu Y., Nusrat A., Schnell F. J., Reaves T. A., Walsh S., Pochet M., Parkos C. A. (2000b) **Human junction adhesion molecule regulates tight junction resealing in epithelia.** *J. Cell Sci.* 113 (Pt 13), 2363-2374.

Longhurst C. M., Jennings L. K. (1998) **Integrin-mediated signal transduction.** *Cell. Mol. Life Sci.* 54, 6, 514-526.

Lu H., Smith C. W., Perrard J., Bullard D., Tang L., Shappell S. B., Entman M. L., Beaudet A. L., Ballantyne C. M. (1997) **LFA-1 is sufficient in mediating neutrophil emigration in Mac-1-deficient mice.** *J. Clin. Invest.* 99, 6, 1340-1350.

Lub M., van Kooyk Y., Figdor C. G. (1995) **Ins and outs of LFA-1.** *Immunol. Today* 16, 10, 479-483.

Lub M., van Kooyk Y., van Vliet S. J., Figdor C. G. (1997a) **Dual role of the actin cytoskeleton in regulating cell adhesion mediated by the integrin lymphocyte function-associated molecule-1.** *Mol. Biol. Cell* 8, 2, 341-351.

Lub M., van Vliet S. J., Oomen S. P., Pieters R. A., Robinson M., Figdor C. G., van Kooyk Y. (1997b) **Cytoplasmic tails of β_1, β_2, and β_7 integrins differentially regulate LFA-1 function in K562 cells.** *Mol. Biol. Cell* 8, 4, 719-728.

Lupher M. L., Harris E. A., Beals C. R., Sui L., Liddington R. C., Staunton D. E. (2001) **Cellular activation of leukocyte function-associated antigen-1 and its affinity are regulated at the I domain allosteric site.** *J. Immunol.* 167, 3, 1431-1439.

Luscinskas F. W., Ding H., Lichtman A. H. (1995) **P-selectin and vascular cell adhesion molecule 1 mediate rolling and arrest, respectively, of $CD4^+$ T lymphocytes on tumor necrosis factor α-activated vascular endothelium under flow.** *J. Exp. Med.* 181, 3, 1179-1186.

Luscinskas F. W., Lim Y. C., Lichtman A. H. (2001) **Wall shear stress: the missing step for T cell transmigration?** *Nat. Immunol.* 2, 6, 478-480.

Lusis A. J. (2000) **Atherosclerosis.** *Nature* 407, 6801, 233-241.

Malergue F., Galland F., Martin F., Mansuelle P., Aurrand-Lions M. A., Naquet P. (1998) **A novel immunoglobulin superfamily junctional molecule expressed by antigen presenting cells, endothelial cells and platelets.** *Mol. Immunol.* 35, 17, 1111-1119.

Marlin S. D., Morton C. C., Anderson D. C., Springer T. A. (1986) **LFA-1 immunodeficiency disease: definition of the genetic defect and chromosomal mapping of α and β subunits of the lymphocyte function-associated antigen 1 (LFA-1) by complementation in hybrid cells.** *J. Exp. Med.* 164, 3, 855-867.

Marlin S. D., Springer T. A. (1987) **Purified intercellular adhesion molecule-1 (ICAM-1) is a ligand for lymphocyte function-associated antigen 1 (LFA-1).** *Cell* 51, 5, 813-819.

Martínez-Estrada O. M., Villa A., Breviario F., Orsenigo F., Dejana E., Bazzoni G. (2001) **Association of junctional adhesion molecule with calcium/calmodulin-dependent serine protein kinase (CASK/LIN-2) in human epithelial Caco-2 cells.** *J. Biol. Chem.* 276, 12, 9291-9296.

Martìn-Padura I., Lostaglio S., Schneemann M., Williams L., Romano M., Fruscella P., Panzeri C., Stoppacciaro A., Ruco L., Villa A., Simmons D., Dejana E. (1998) **Junctional adhesion molecule, a novel member of the immunoglobulin superfamily that distributes at intercellular junctions and modulates monocyte transmigration.** *J. Cell Biol.* 142, 1, 117-127.

McEver R. P., Moore K. L., Cummings R. D. (1995) **Leukocyte trafficking mediated by selectin-carbohydrate interactions.** *J. Biol. Chem.* 270, 19, 11025-11028.

Mellado M., Rodríguez-Frade J. M., Mañes S., Martínez-A. C. (2001) **Chemokine signaling and functional responses: the role of receptor dimerization and TK pathway activation.** *Annu. Rev. Immunol.* 19, 397-421.

Meredith J. E., Fazeli B., Schwartz M. A. (1993) **The extracellular matrix as a cell survival factor.** *Mol. Biol. Cell* 4, 9, 953-961.

Miller J., Knorr R., Ferrone M., Houdei R., Carron C. P., Dustin M. L. (1995) **Intercellular adhesion molecule-1 dimerization and its consequences for adhesion mediated by lymphocyte function associated-1.** *J. Exp. Med.* 182, 5, 1231-1241.

Miller M. D., Krangel M. S. (1992) **Biology and biochemistry of the chemokines: a family of chemotactic and inflammatory cytokines.** *Crit. Rev. Immunol.* 12, 1-2, 17-46.

Miranti C. K., Brugge J. S. (2002) **Sensing the environment: a historical perspective on integrin signal transduction.** *Nat. Cell Biol.* 4, 4, E83-E90.

Moazzam F., DeLano F. A., Zweifach B. W., Schmid-Schönbein G. W. (1997) **The leukocyte response to fluid stress.** *Proc. Natl. Acad. Sci. USA* 94, 10, 5338-5343 [comment in: *Proc.Natl.Acad.Sci.USA* (1997) 94, 10, 4825-4827].

Mukai T., Iwasaki M., Gao P., Tomura M., Yashiro-Ohtani Y., Ono S., Murai M., Matsushima K., Kurimoto M., Kogo M., Matsuya T., Fujiwara H., Hamaoka T. (2001) **IL-12 plays a pivotal role in LFA-1-mediated T cell adhesiveness by up-regulation of CCR5 expression.** *J. Leukoc. Biol.* 70, 3, 422-430.

Muller W. A., Weigl S. A., Deng X., Phillips D. M. (1993) **PECAM-1 is required for transendothelial migration of leukocytes.** *J. Exp. Med.* 178, 2, 449-460.

Munro J. M., Pober J. S., Cotran R. S. (1989) **Tumor necrosis factor and interferon-γ induce distinct patterns of endothelial activation and associated leukocyte accumulation in skin of *Papio anubis*.** *Am. J. Pathol.* 135, 1, 121-133.

Nagafuchi A. (2001) **Molecular architecture of adherens junctions.** *Curr. Opin. Cell Biol.* 13, 5, 600-603.

Nagel W., Schilcher P., Zeitlmann L., Kolanus W. (1998a) **The PH domain and the polybasic c domain of cytohesin-1 cooperate specifically in plasma membrane association and cellular function.** *Mol. Biol. Cell* 9, 8, 1981-1994.

Nagel W., Zeitlmann L., Schilcher P., Geiger C., Kolanus J., Kolanus W. (1998b) **Phosphoinositide 3-OH kinase activates the β_2 integrin adhesion pathway and induces membrane recruitment of cytohesin-1.** *J. Biol. Chem.* 273, 24, 14853-14861.

Naik U. P., Ehrlich Y. H., Kornecki E. (1995) **Mechanisms of platelet activation by a stimulatory antibody: cross-linking of a novel platelet receptor for monoclonal antibody F11 with the FcγRII receptor.** *Biochem. J.* 310 (Pt 1), 155-162.

Naik U. P., Patel P. M., Parise L. V. (1997) **Identification of a novel calcium-binding protein that interacts with the integrin α_{IIb} cytoplasmic domain.** *J. Biol. Chem.* 272, 8, 4651-4654.

Naik U. P., Naik M. U., Eckfeld K., Martin-DeLeon P., Spychala J. (2001) **Characterization and chromosomal localization of JAM-1, a platelet receptor for a stimulatory monoclonal antibody.** *J. Cell Sci.* 114 (Pt 3), 539-547.

Nanki T., Hayashida K., El-Gabalawy H. S., Suson S., Shi K., Girschick H. J., Yavuz S., Lipsky P. E. (2000) **Stromal cell-derived factor-1-CXC chemokine receptor 4 interactions play a central role in $CD4^+$ T cell accumulation in rheumatoid arthritis synovium.** *J. Immunol.* 165, 11, 6590-6598.

Newham P., Craig S. E., Seddon G. N., Schofield N. R., Rees A., Edwards R. M., Jones E. Y., Humphries M. J. (1997) **α_4 integrin binding interfaces on VCAM-1 and MAdCAM-1. Integrin binding footprints identify accessory binding sites that play a role in integrin specificity.** *J. Biol. Chem.* 272, 31, 19429-19440.

Newman P. J. (1997) **The biology of PECAM-1.** *J. Clin. Invest.* 99, 1, 3-8.

Newton J. P., Buckley C. D., Jones E. Y., Simmons D. L. (1997) **Residues on both faces of the first immunoglobulin fold contribute to homophilic binding sites of PECAM-1/CD31.** *J. Biol. Chem.* 272, 33, 20555-20563.

Nortamo P., Li R., Renkonen R., Timonen T., Prieto J., Patarroyo M., Gahmberg C. G. (1991) **The expression of human intercellular adhesion molecule-2 is refractory to inflammatory cytokines.** *Eur. J. Immunol.* 21, 10, 2629-2632.

Nusrat A., Turner J. R., Madara J. L. (2000) **Molecular physiology and pathophysiology of tight junctions. IV. Regulation of tight junctions by extracellular stimuli: nutrients, cytokines, and immune cells.** *Am. J. Physiol. Gastrointest. Liver Physiol.* 279, 5, G851-G857.

Ossowski L., Aguirre-Ghiso J. A. (2000) **Urokinase receptor and integrin partnership: coordination of signaling for cell adhesion, migration and growth.** *Curr. Opin. Cell Biol.* 12, 5, 613-620.

Ozaki H., Ishii K., Horiuchi H., Arai H., Kawamoto T., Okawa K., Iwamatsu A., Kita T. (1999) **Combined treatment of TNF-α and IFN-γ causes redistribution of junctional adhesion molecule in human endothelial cells.** *J. Immunol.* 163, 2, 553-557.

Ozaki H., Ishii K., Arai H., Horiuchi H., Kawamoto T., Suzuki H., Kita T. (2000) **Junctional adhesion molecule (JAM) is phosphorylated by protein kinase C upon platelet activation.** *Biochem. Biophys. Res. Commun.* 276, 3, 873-878.

Palmeri D., van Zante A., Huang C. C., Hemmerich S., Rosen S. D. (2000) **Vascular endothelial junction-associated molecule, a novel member of the immunoglobulin superfamily, is localized to intercellular boundaries of endothelial cells.** *J. Biol. Chem.* 275, 25, 19139-19145.

Pawson T., Scott J. D. (1997) **Signaling through scaffold, anchoring, and adaptor proteins.** *Science* 278, 5346, 2075-2080.

Peled A., Grabovsky V., Habler L., Sandbank J., Arenzana-Seisdedos F., Petit I., Ben-Hur H., Lapidot T., Alon R. (1999) **The chemokine SDF-1 stimulates integrin-mediated arrest of $CD34^+$ cells on vascular endothelium under shear flow.** *J. Clin. Invest.* 104, 9, 1199-1211.

Piali L., Hammel P., Uherek C., Bachmann F., Gisler R. H., Dunon D., Imhof B. A. (1995) **CD31/PECAM-1 is a ligand for $\alpha_v\beta_3$ integrin involved in adhesion of leukocytes to endothelium.** *J. Cell Biol.* 130, 2, 451-460.

Plow E. F., Haas T. A., Zhang L., Loftus J., Smith J. W. (2000) **Ligand binding to integrins.** *J. Biol. Chem.* 275, 29, 21785-21788.

Porter J. C., Hogg N. (1998) **Integrins take partners: cross-talk between integrins and other membrane receptors.** *Trends Cell Biol.* 8, 10, 390-396.

Premack B. A., Schall T. J. (1996) **Chemokine receptors: gateways to inflammation and infection.** *Nat. Med.* 2, 11, 1174-1178.

Reilly P. L., Woska J. R., Jeanfavre D. D., McNally E., Rothlein R., Bormann B. J. (1995) **The native structure of intercellular adhesion molecule-1 (ICAM-1) is a dimer. Correlation with binding to LFA-1.** *J. Immunol.* 155, 2, 529-532.

Rietzler M., Bittner M., Kolanus W., Schuster A., Holzmann B. (1998) **The human WD repeat protein WAIT-1 specifically interacts with the cytoplasmic tails of β_7-integrins.** *J. Biol. Chem.* 273, 42, 27459-27466.

Rival Y., Del Maschio A., Rabiet M. J., Dejana E., Duperray A. (1996) **Inhibition of platelet endothelial cell adhesion molecule-1 synthesis and leukocyte transmigration in endothelial cells by the combined action of TNF-α and IFN-γ.** *J. Immunol.* 157, 3, 1233-1241.

Rojiani M. V., Finlay B. B., Gray V., Dedhar S. (1991) ***In vitro*** **interaction of a polypeptide homologous to human Ro/SS-A antigen (calreticulin) with a highly conserved amino acid sequence in the cytoplasmic domain of integrin α subunits.** *Biochemistry* 30, 41, 9859-9866.

Romer L. H., McLean N. V., Yan H. C., Daise M., Sun J., DeLisser H. M. (1995) **IFN-γ and TNF-α induce redistribution of PECAM-1 (CD31) on human endothelial cells.** *J. Immunol.* 154, 12, 6582-6592.

Ronald J. A., Ionescu C. V., Rogers K. A., Sandig M. (2001) **Differential regulation of transendothelial migration of THP-1 cells by ICAM-1/LFA-1 and VCAM-1/VLA-4.** *J. Leukoc. Biol.* 70, 4, 601-609.

Ross R. (1999) **Atherosclerosis - an inflammatory disease.** *N. Engl. J. Med.* 340, 2, 115-126.

Rothlein R., Dustin M. L., Marlin S. D., Springer T. A. (1986) **A human intercellular adhesion molecule (ICAM-1) distinct from LFA-1.** *J. Immunol.* 137, 4, 1270-1274.

Sambrook J., Fritsch E. F., Manning A. M. (1989) **Molecular cloning: a laboratory manual.** Cold Spring Harbor Laboratory Press, Cold Spring Harbor, NY.

Sánchez-Madrid F., Krensky A. M., Ware C. F., Robbins E., Strominger J. L., Burakoff S. J., Springer T. A. (1982) **Three distinct antigens associated with human T-lymphocyte-mediated cytolysis: LFA-1, LFA-2, and LFA-3.** *Proc. Natl. Acad. Sci. USA* 79, 23, 7489-7493.

Santoso S., Sachs U. J., Kroll H., Linder M., Ruf A., Preissner K. T., Chavakis T. (2002) **The junctional adhesion molecule 3 (JAM-3) on human platelets is a counterreceptor for the leukocyte integrin Mac-1.** *J. Exp. Med.* 196, 5, 679-691.

Sastry S. K., Horwitz A. F. (1993) **Integrin cytoplasmic domains: mediators of cytoskeletal linkages and extra- and intracellular initiated transmembrane signaling.** *Curr. Opin. Cell Biol.* 5, 5, 819-831.

Schenkel A. R., Mamdouh Z., Chen X., Liebman R. M., Muller W. A. (2002) **CD99 plays a major role in the migration of monocytes through endothelial junctions.** *Nat. Immunol.* 3, 2, 143-150 [comment in: *Nat. Immunol.* (2002) 3, 2, 116-118].

Schiestl R. H., Gietz R. D. (1989) **High efficiency transformation of intact yeast cells using single stranded nucleic acids as a carrier.** *Curr. Genet.* 16, 339-346.

Schneeberger E. E., Lynch R. D. (1992) **Structure, function, and regulation of cellular tight junctions.** *Am. J. Physiol.* 262, 6 (Pt 1), L647-L661.

Schoenwaelder S. M., Burridge K. (1999) **Bidirectional signaling between the cytoskeleton and integrins.** *Curr. Opin. Cell Biol.* 11, 2, 274-286.

Schwartz M. A., Lechene C., Ingber D. E. (1991) **Insoluble fibronectin activates the Na/H antiporter by clustering and immobilizing integrin $\alpha_5\beta_1$, independent of cell shape.** *Proc. Natl. Acad. Sci. USA* 88, 17, 7849-7853.

Schwartz M. A. (1993) **Spreading of human endothelial cells on fibronectin or vitronectin triggers elevation of intracellular free calcium.** *J. Cell Biol.* 120, 4, 1003-1010.

Schwartz M. A., Ginsberg M. H. (2002) **Networks and crosstalk: integrin signalling spreads.** *Nat. Cell Biol.* 4, 4, E65-E68.

Shattil S. J., Hoxie J. A., Cunningham M., Brass L. F. (1985) **Changes in the platelet membrane glycoprotein IIb-IIIa complex during platelet activation.** *J. Biol. Chem.* 260, 20, 11107-11114.

Shattil S. J., O'Toole T., Eigenthaler M., Thon V., Williams M., Babior B. M., Ginsberg M. H. (1995) **β_3-endonexin, a novel polypeptide that interacts specifically with the cytoplasmic tail of the integrin β_3 subunit.** *J. Cell Biol.* 131, 3, 807-816.

Shaw J. M., Al-Shamkhani A., Boxer L. A., Buckley C. D., Dodds A. W., Klein N., Nolan S. M., Roberts I., Roos D., Scarth S. L., Simmons D. L., Tan S. M., Law S. K. (2001a) **Characterization of four CD18 mutants in leucocyte adhesion deficient (LAD) patients with differential capacities to support expression and function of the CD11/CD18 integrins LFA-1, Mac-1 and p150,95.** *Clin. Exp. Immunol.* 126, 2, 311-318.

Shaw S. K., Bamba P. S., Perkins B. N., Luscinskas F. W. (2001b) **Real-time imaging of vascular endothelial-cadherin during leukocyte transmigration across endothelium.** *J. Immunol.* 167, 4, 2323-2330.

Shaw S. K., Perkins B. N., Lim Y. C., Liu Y., Nusrat A., Schnell F. J., Parkos C. A., Luscinskas F. W. (2001c) **Reduced expression of junctional adhesion molecule and platelet/endothelial cell adhesion molecule-1 (CD31) at human vascular endothelial junctions by cytokines tumor necrosis factor-α plus interferon-γ does not reduce leukocyte transmigration under flow.** *Am. J. Pathol.* 159, 6, 2281-2291.

Shibayama H., Anzai N., Braun S. E., Fukuda S., Mantel C., Broxmeyer H. E. (1999) **H-Ras is involved in the inside-out signaling pathway of interleukin-3-induced integrin activation.** *Blood* 93, 5, 1540-1548.

Sigal A., Bleijs D. A., Grabovsky V., van Vliet S. J., Dwir O., Figdor C. G., van Kooyk Y., Alon R. (2000) **The LFA-1 integrin supports rolling adhesions on ICAM-1 under physiological shear flow in a permissive cellular environment.** *J. Immunol.* 165, 1, 442-452.

Simmons D. L. (1995) **The role of intercellular adhesion molecules 1, 2, and 3 in cell recognition and signaling.** In: *Topics in molecular medicine: Adhesion molecules and cell signaling*. Siess W., Lorenz R., and Weber P. C. (eds.), Raven Press, New York, NY, 11-25.

Simon D. I., Chen Z., Xu H., Li C. Q., Dong J., McIntire L. V., Ballantyne C. M., Zhang L., Furman M. I., Berndt M. C., López J. A. (2000) **Platelet glycoprotein Ibα is a counterreceptor for the leukocyte integrin Mac-1 (CD11b/CD18).** *J. Exp. Med.* 192, 2, 193-204.

Smith C. W., Marlin S. D., Rothlein R., Toman C., Anderson D. C. (1989) **Cooperative interactions of LFA-1 and Mac-1 with intercellular adhesion molecule-1 in facilitating adherence and transendothelial migration of human neutrophils *in vitro*.** *J. Clin. Invest.* 83, 6, 2008-2017.

Sobocka M. B., Sobocki T., Banerjee P., Weiss C., Rushbrook J. I., Norin A. J., Hartwig J., Salifu M. O., Markell M. S., Babinska A., Ehrlich Y. H., Kornecki E. (2000) **Cloning of the human platelet F11 receptor: a cell adhesion molecule member of the immunoglobulin superfamily involved in platelet aggregation.** *Blood* 95, 8, 2600-2609.

Springer T. A. (1990) **Adhesion receptors of the immune system.** *Nature* 346, 6283, 425-434.

Springer T. A. (1994) **Traffic signals for lymphocyte recirculation and leukocyte emigration: the multistep paradigm.** *Cell* 76, 2, 301-314.

Springer T. A. (1995) **Traffic signals on endothelium for lymphocyte recirculation and leukocyte emigration.** *Annu. Rev. Physiol.* 57, 827-872.

Springer T. A. (1997) **Folding of the N-terminal, ligand-binding region of integrin α-subunits into a β-propeller domain.** *Proc. Natl. Acad. Sci. USA* 94, 1, 65-72.

Stanley P., McDowall A., Bates P. A., Brashaw J., Hogg N. (2000) **The second domain of intercellular adhesion molecule-1 (ICAM-1) maintains the structural integrity of the leucocyte function-associated antigen-1 (LFA-1) ligand-binding site in the first domain.** *Biochem. J.* 351 (Pt 1), 79-86.

Staunton D. E., Dustin M. L., Erickson H. P., Springer T. A. (1990) **The arrangement of the immunoglobulin-like domains of ICAM-1 and the binding sites for LFA-1 and rhinovirus.** *Cell* 61, 2, 243-254 [Errata: *Cell* (1990) 61, 2, 1157; *Cell* (1991) 66, 6, following 1311].

Stewart M., Thiel M., Hogg N. (1995) **Leukocyte integrins.** *Curr. Opin. Cell Biol.* 7, 5, 690-696.

Strieter R. M., Standiford T. J., Huffnagle G. B., Colletti L. M., Lukacs N. W., Kunkel S. L. (1996) **"The good, the bad, and the ugly." The role of chemokines in models of human disease.** *J. Immunol.* 156, 10, 3583-3586.

Sundberg C., Rubin K. (1996) **Stimulation of β_1 integrins on fibroblasts induces PDGF-independent tyrosine phosphorylation of PDGF β-receptors.** *J. Cell Biol.* 132, 4, 741-752.

Tan K., Casasnovas J. M., Liu J. H., Briskin M. J., Springer T. A., Wang J. H. (1998) **The structure of immunoglobulin superfamily domains 1 and 2 of MAdCAM-1 reveals novel features important for integrin recognition.** *Structure* 6, 6, 793-801.

Tsukita S., Furuse M., Itoh M. (1999) **Structural and signalling molecules come together at tight junctions.** *Curr. Opin. Cell Biol.* 11, 5, 628-633.

van der Vieren M., Le Trong H., Wood C. L., Moore P. F., St John T., Staunton D. E., Gallatin W. M. (1995) **A novel leukointegrin, $\alpha_D\beta_2$, binds preferentially to ICAM-3.** *Immunity* 3, 6, 683-690.

van Kooyk Y., Weder P., Hogervorst F., Verhoeven A. J., van Seventer G., te Velde A. A., Borst J., Keizer G. D., Figdor C. G. (1991) **Activation of LFA-1 through a Ca^{2+}-dependent epitope stimulates lymphocyte adhesion.** *J. Cell Biol.* 112, 2, 345-354.

van Kooyk Y., van Vliet S. J., Figdor C. G. (1999) **The actin cytoskeleton regulates LFA-1 ligand binding through avidity rather than affinity changes.** *J. Biol. Chem.* 274, 38, 26869-26877.

van Kooyk Y., Figdor C. G. (2000) **Avidity regulation of integrins: the driving force in leukocyte adhesion.** *Curr. Opin. Cell Biol.* 12, 5, 542-547.

Vaughn D. E., Bjorkman P. J. (1996) **The (Greek) key to structures of neural adhesion molecules.** *Neuron* 16, 2, 261-273.

Vonderheide R. H., Tedder T. F., Springer T. A., Staunton D. E. (1994) **Residues within a conserved amino acid motif of domains 1 and 4 of VCAM-1 are required for binding to VLA-4.** *J. Cell Biol.* 125, 1, 215-222.

Vuori K., Ruoslahti E. (1993) **Activation of protein kinase C precedes $\alpha_5\beta_1$ integrin-mediated cell spreading on fibronectin.** *J. Biol. Chem.* 268, 29, 21459-21462.

Ward S. G., Westwick J. (1998) **Chemokines: understanding their role in T-lymphocyte biology.** *Biochem. J.* 333 (Pt 3), 457-470.

Weber C., Alon R., Moser B., Springer T. A. (1996) **Sequential regulation of $\alpha_4\beta_1$ and $\alpha_5\beta_1$ integrin avidity by CC chemokines in monocytes: implications for transendothelial chemotaxis.** *J. Cell Biol.* 134, 4, 1063-1073.

Weber C., Lu C. F., Casasnovas J. M., Springer T. A. (1997a) **Role of $\alpha_L\beta_2$ integrin avidity in transendothelial chemotaxis of mononuclear cells.** *J. Immunol.* 159, 8, 3968-3975.

Weber C., Springer T. A. (1998) **Interaction of very late antigen-4 with VCAM-1 supports transendothelial chemotaxis of monocytes by facilitating lateral migration.** *J. Immunol.* 161, 12, 6825-6834.

Weber K. S., York M. R., Springer T. A., Klickstein L. B. (1997b) **Characterization of lymphocyte function-associated antigen 1 (LFA-1)-deficient T cell lines: the $\alpha_L\beta_2$ subunits are interdependent for cell surface expression.** *J. Immunol.* 158, 1, 273-279.

Weber K. S., Klickstein L. B., Weber C. (1999a) **Specific activation of leukocyte β_2 integrins lymphocyte function-associated antigen-1 and Mac-1 by chemokines mediated by distinct pathways via the α subunit cytoplasmic domains.** *Mol. Biol. Cell* 10, 4, 861-873.

Weber K. S., von Hundelshausen P., Clark-Lewis I., Weber P. C., Weber C. (1999b) **Differential immobilization and hierarchical involvement of chemokines in monocyte arrest and transmigration on inflamed endothelium in shear flow.** *Eur. J. Immunol.* 29, 2, 700-712.

Weber K. S., Ostermann G., Zernecke A., Schröder A., Klickstein L. B., Weber C. (2001a) **Dual role of H-Ras in regulation of lymphocyte function antigen-1 activity by stromal cell-derived factor-1α: implications for leukocyte transmigration.** *Mol. Biol. Cell* 12, 10, 3074-3086.

Weber K. S., Weber C., Ostermann G., Dierks H., Nagel W., Kolanus W. (2001b) **Cytohesin-1 is a dynamic regulator of distinct LFA-1 functions in leukocyte arrest and transmigration triggered by chemokines.** *Curr. Biol.* 11, 24, 1969-1974.

Williams A. F., Barclay A. N. (1988) **The immunoglobulin superfamily: domains for cell surface recognition.** *Annu. Rev. Immunol.* 6, 381-405.

Williams L. A., Martìn-Padura I., Dejana E., Hogg N., Simmons D. L. (1999) **Identification and characterisation of human junctional adhesion molecule (JAM).** *Mol. Immunol.* 36, 17, 1175-1188.

Williams M. J., Hughes P. E., O'Toole T. E., Ginsberg M. H. (1994) **The inner world of cell adhesion: integrin cytoplasmic domains.** *Trends Cell Biol.* 4, 109-112.

Wong C. W., Wiedle G., Ballestrem C., Wehrle-Haller B., Etteldorf S., Bruckner M., Engelhardt B., Gisler R. H., Imhof B. A. (2000) **PECAM-1/CD31 trans-homophilic binding at the intercellular junctions is independent of its cytoplasmic domain; evidence for heterophilic interaction with integrin $\alpha_v\beta_3$ in *cis*.** *Mol. Biol. Cell* 11, 9, 3109-3121.

Xiong J. P., Stehle T., Diefenbach B., Zhang R., Dunker R., Scott D. L., Joachimiak A., Goodman S. L., Arnaout M. A. (2001) **Crystal structure of the extracellular segment of integrin $\alpha_V\beta_3$.** *Science* 294, 5541, 339-345.

Yamamoto T., Harada N., Kano K., Taya S., Canaani E., Matsuura Y., Mizoguchi A., Ide C., Kaibuchi K. (1997) **The Ras target AF-6 interacts with ZO-1 and serves as a peripheral component of tight junctions in epithelial cells.** *J. Cell Biol.* 139, 3, 785-795.

Yap A. S., Brieher W. M., Gumbiner B. M. (1997) **Molecular and functional analysis of cadherin-based adherens junctions.** *Annu. Rev. Cell Dev. Biol.* 13, 119-146.

Zhang Z., Vuori K., Wang H., Reed J. C., Ruoslahti E. (1996) **Integrin activation by R-ras.** *Cell* 85, 1, 61-69.

Zlotnik A., Yoshie O. (2000) **Chemokines: a new classification system and their role in immunity.** *Immunity* 12, 2, 121-127.

9. Curriculum vitae

Personal data

Name	• Georg Ostermann
Date and place of birth	• May 17th, 1968 in Cochem/Mosel

Education

1974 - 1978	• Grundschule Kurfürst-Balduin-Schule Kaisersesch
1978 - 1979	• Hauptschule Kurfürst-Balduin-Schule Kaisersesch
1979 - 1981	• Staatliche Realschule Mayen
1981 - 1988	• Staatliches Gymnasium Mayen Graduation: General high school graduation (Abitur)

Military service

07/1988 - 09/1989	• Military service in Diez and Koblenz

Higher education

10/1989 - 03/1998	• Study of chemistry Rheinische Friedrich-Wilhelms-Universität Bonn Degree: Master of science in chemistry (Diplom-Chemiker)

Studies abroad

10/1995 - 12/1995	• Practical research training in the lab of Prof. Dr. P. Chambon Institut de Génétique et de Biologie Moléculaire et Cellulaire (IGBMC), Strasbourg/France
03/1997 - 03/1998	• Diploma thesis in the lab of Prof. Dr. J.-L. Mandel IGBMC, Strasbourg/France Subject: *"Search for the substrate of PHEX involved in human X-linked hypophosphatemic rickets"*

Scientific background

08/1998 - 12/2001	• Scientific employee and doctoral thesis in the lab of Prof. Dr. C. Weber Institute for Prevention of Cardiovascular Disease, University Hospital, Ludwig-Maximilians-Universität, Munich
since 01/2002	• Department of Molecular Cardiovascular Research, University Hospital, Aachen

Award

10/2002	• Award of the Society for Microcirculation and Vascular Biology (GfMVB), Cologne

10. List of personal publications

Filisetti D., Ostermann G., von Bredow M., Strom T., Filler G., Ehrich J., Pannetier S., Garnier J. M., Rowe P., Francis F., Julienne A., Hanauer A., Econs M. J., Oudet C. (1999) **Non-random distribution of mutations in the PHEX gene, and under-detected missense mutations at non-conserved residues.** *Eur. J. Hum. Genet.* 7, 5, 615-619.

Neuzil J., Weber T., Schröder A., Lu M., Ostermann G., Gellert N., Mayne G. C., Olejnicka B., Nègre-Salvayre A., Stícha M., Coffey R. J., Weber C. (2001) **Induction of cancer cell apoptosis by α-tocopheryl succinate: molecular pathways and structural requirements.** *FASEB J.* 15, 2, 403-415.

Weber K. S., Ostermann G., Zernecke A., Schröder A., Klickstein L. B., Weber C. (2001) **Dual role of H-Ras in regulation of lymphocyte function antigen-1 activity by stromal cell-derived factor-1α: implications for leukocyte transmigration.** *Mol. Biol. Cell* 12, 10, 3074-3086.

Weber K. S., Weber C., Ostermann G., Dierks H., Nagel W., Kolanus W. (2001) **Cytohesin-1 is a dynamic regulator of distinct LFA-1 functions in leukocyte arrest and transmigration triggered by chemokines.** *Curr. Biol.* 11, 24, 1969-1974.

Ostermann G., Weber K. S., Zernecke A., Schröder A., Weber C. (2002) **JAM-1 is a ligand of the β_2 integrin LFA-1 involved in transendothelial migration of leukocytes.** *Nature Immunol.* 3, 2, 151-158.

Neuzil J., Zhao M., Ostermann G., Sticha M., Gellert N., Weber C., Eaton J. W., Brunk U. T. (2002) **α-Tocopheryl succinate, an agent with *in vivo* anti-tumour activity, induces apoptosis by causing lysosomal instability.** *Biochem. J.* 362 (Pt 3), 709-71.